MASTER OF SCIENCE BY RESEARCH

Research into the Potential of Variable Aerodynamic Properties to Modify Ground Vehicle Behaviour

Atkinson, James

Award date:
2015

Awarding institution:
Coventry University

COVENTRY UNIVERSITY

Research into the Potential of Variable Aerodynamic Properties to Modify Ground Vehicle Behaviour

MSc by Research

James Atkinson

SID: 2191500

Original Submission - September 2013

Amended Submission – August 2014

Director of Studies: Dr David Trepess

Secondary Supervisor: Dr Gary Wood

James Edward Atkinson 2191500

Declaration

A thesis submitted in partial fulfilment of the University's requirements for the Master of Research award.

This project is all my own work and has not been copied in part or in whole from any other source except where duly acknowledged. As such, all use of previously published work (from books, journals, magazines, internet, etc…) has been acknowledged within the main report to an item in the References or Bibliography lists.

I also agree that an electronic copy of this project may be stored and used for the purposes of plagiarism prevention and detection.

Copyright Acknowledgement

Signed: _____

Original Thesis Submission Date: 01st September 2013

Amended Thesis Submission Date: 01st August 2014

Abstract

This report investigates the possibility of using a variable aerodynamic device to improve a vehicle's dynamic behaviour during a side wind scenario often experienced on open roads. In order to understand the effect of using a stability device, a literature review was undertaken, from which information was able to be extracted to create a mathematical model to demonstrate how vehicle characteristics are changed. Using the mathematical model, a range of concepts were able to be generated, with the variable stability fin being selected and developed further. The design was manufactured and tested using both wind tunnel testing and CFD simulations to determine how the forces and moments that act on the vehicle change with yaw angle and fin deployment stages. From the research that was carried out it can be said that the side force and yaw moment are affected by the inclusion of a stability fin, particularly at greater yaw angles. The investigations have also provided a number of key areas where future work could be undertaken to further understand the effect of a side wind gust on a vehicle's behaviour.

Acknowledgements

I would like to thank the following individuals for their help and advice towards the completion of this research project: Firstly, Dr David Trepess, Dr Gary Wood and Damian Harty who allowed me to explore a vast and interesting subject of automotive engineering, and who were always available to discuss details with. I would also like to thank Remus Cirstea for his assistance in organising the wind tunnel model and assisting me with the understanding of the aerodynamic data. Further acknowledgements go to Terry Beale and Ian Wilson who aided me with the manufacture of the stability devices and Phillip Garner for the running of the wind tunnel test program and providing me with key information which was integral to the research undertaken.

James Atkinson

Contents

Figure List

Tables List

Nomenclature

Abbreviations

2 DoF	*Two Degrees of Freedom*
CAD	*Computer Aided Design*
CFD	*Computational Fluid Dynamics*
CofG	*Centre of Gravity*
CofP	*Centre of Pressure*
CNC	*Computer Numerically Controlled*
DRS	*Drag Reduction System*
DTM	*Deutsche Tourenwagen Masters*
FIA	*Federation Internationale de l-Automobile*
NASCAR	*National Association for Stock Car Auto Racing*

Symbols

a	*Front Axle to CofG Location Distance*	*m*
A	*Projected Frontal Area*	m^2
b	*Rear Axle to CofG Location Distance*	*m*
C_d	*Drag Force Coefficient*	*No Units*
C_y	Side Force Coefficient	No Units
$C_{\alpha f}$	*Front Cornering Stiffness*	*N/rad*
$C_{\alpha r}$	*Rear Cornering Stiffness*	*N/rad*
F_{wind}	*Wind Force*	*N*
F_y	Force (y direction)	N
F_{yf}	Front Lateral Force	N
F_{yr}	Rear Lateral Force	N
G	Acceleration due to gravity	m/s^2
I_{zz}	*Moment of Inertia about the z axis*	*kg* m^2
kph	*Kilometres per Hour*	
L	*Wheelbase*	*m*
m	*Mass*	*kg*
mph	*miles per hour*	
r	*Yaw Rate*	*Rad/s & Deg/s*
$\dot{r}$	Yaw Rate Gain	Rad/s^2 & Deg/s^2

V_{Res}	*Resultant Velocity*	*m/s*
V_w	*Wind Velocity*	*m/s*
V_x	*Vehicle Forward Velocity*	*m/s*
V_y	*Vehicle Lateral Velocity*	*m/2*
y	*Side Force*	*N*
ρ	*Density*	*kg/m^3*
θ	*Wind Approach Angle*	°
β	*Vehicle Yaw/Sideslip Angle*	°
$\dot{\beta}$	Change in Vehicle Yaw/Sideslip Angle	°
δ	*Steering Angle*	°
α_f	*Front Slip Angle*	°
α_r	*Rear Slip Angle*	°

1 Introduction

The field of vehicle dynamics encompasses a vast array of subjects. From defining the perceived handling characteristics to reducing the effect of the noise, vibration and harshness of the vehicle, the subject matter is wide and varied. It can be said that this extensive topic can be considered to be governed by two key characteristics; Isolation and Control (Blundell 2004:3). Isolation is defined as the vehicle being designed as such to reduce the effect(s) of internal and external excitation disturbances; whether this be the vibrations caused by the engine or the vehicle travelling over a rough road surface (Blundell 2004:3). Within dynamics, the control of a vehicle is defined as how a vehicle controls the outcome(s) of these disturbances to ensure that the vehicle remains within the recoverable bounds of the driver (Harty 2012). These definitions are further identified and expanded upon in Figure 1.

Figure 1 - Vehicle Dynamics Section Interactions

(Blundell and Harty 2004:3)

One of the main components which acts upon a vehicle and can dramatically affect its performance is aerodynamics. As can be seen in Figure 1, the aerodynamic profile of a vehicle can be considered to affect both the isolation and control aspects of the vehicle dynamics field, thus further understanding of this subject is imperative.

When a vehicle is travelling along a given path, aerodynamic forces and moments constantly act upon the vehicle body with these having a great effect on the vehicle performance. The forces and moments that are generated can be used to increase the control boundary through the use of negative lift, otherwise known as downforce, allowing for a greater

cornering ability of the vehicle. The use of negative lift for control will inherently induce drag upon the vehicle. This drag force will limit the maximum velocity and thus limit the performance of a particular vehicle. There are, however, cases whereby the vehicle is required to isolate the driver from external disturbances, with one such case being side winds or gusts that act at an angle to the vehicle's direction of travel. Side winds cause an increase in the side force and increase the lateral force component acting on the vehicle. The ability of the vehicle to isolate and control the effects of a side force in order to reduce the corrective input required of the driver and assist in maintaining the vehicle in a linear state is of great importance to both the safety of the occupants but also other road users. In order to reduce the effects of disturbances, aerodynamic devices can be used to modify the flow structure around a body. This practice has been common place within the aerospace industry ever since the inception of the first aircraft through the use of ailerons and control surfaces. The technology has only been beneficially incorporated on ground vehicles within the last fifty years via the use of vortex generators, spoilers and additional stability devices (Barnard 2009:138). Altering the air flow around a vehicle through the use of the devices named above can have a major impact on a vehicle's dynamic capabilities through both the isolation and control paths (Barnard 2009).

This report will focus on identifying the possibilities of using a variable aerodynamic device(s) to enable greater isolation and control to be achieved when a vehicle is being acted on by aerodynamically induced forces and moments. Key disturbances will be highlighted and solutions researched to identify how the implementation of a variable device would affect how a vehicle would behave. The research will involve both theoretical and practical based investigation through the creation of a mathematical dynamics model, CFD simulations and physical wind tunnel experimentation.

2 Project Aims and Objectives

To further understand the main aspects of the research project, a number of key aims and objectives have been established to ensure the project contains a relevant contribution to real world issues. The agreed aims and objectives can be seen below.

2.1 Aims & Objectives

- To establish the effect of variable aerodynamic devices through research and to discuss how this can be implemented in a given scenario.
- To derive, from research, a device with the ability to modify vehicle behaviour and offer a dynamic advantage.
- Investigate active aerodynamics using simulation techniques including CFD and wind tunnel testing.
- Write a detailed report indicating the findings with relevant justification.

2.2 Relevance to Professional or Academic Field

- Active aerodynamics that change the behaviour of ground vehicles are not common place within the automotive industry, with only a small number of examples, particularly on high performance vehicles, being available. These include the air brake system used on the McLaren Mercedes SLR, MP4-12C and Bugatti Veyron, and within the motorsport sector, the Drag Reduction System (DRS) and adjustable front wing elements used within various Formula categories.
- Through research in this area, it will be able to be established whether active aerodynamic devices would offer a sufficient improvement in dynamic behaviour.
- If found suitable, then this research could be applied to relevant ground vehicles.

2.3 Research Approach and Methodology

- Produce a project plan, plotting key milestones in the research and targets for simulations and practical experimentation (see Appendix A).
- To produce an initial literature review into the field of interest.
- In order to manufacture the models for use in the wind tunnel, CAD Software, CNC Machines and Laser Cutting tools will be utilised.
- Data obtained from the wind tunnel tests and CFD simulations will then be analysed to establish the effect, positive or negative, that a variable aerodynamic device can have on the vehicle's behaviour.
- Once analysed, the data will be explained and displayed in a detailed report.

3 Literature Review

In order to understand the overall effect of aerodynamics on a vehicle's behaviour an extensive literature review was undertaken, encompassing obtaining material from published articles, technical papers, books and the internet. The key areas were then able to be evaluated to establish how the use of a variable aerodynamic device could improve vehicle behaviour. These findings are presented below.

3.1 Variable Aerodynamics

The use of variable aerodynamic devices to control the airflow around a vehicle has been ever present within the aerospace industry and is currently being implemented successfully within the automotive sector. The following section identifies a number of variable aerodynamic devices that have been implemented within the aerospace and automotive industry, highlighting the resulting vehicular behaviour characteristics.

3.1.1 Aerospace Industry

The aerospace industry is at the forefront of the implementation of variable aerodynamic devices, with numerous control surfaces utilised during all phases of flight. Control surfaces are defined as generators of forces and moments that are required to allow for equilibrium flight, to allow the aircraft to respond to the pilot's commands and to offer stability during disturbances (Stengel 2004:214). The use of these devices allows an aircraft to manoeuvre when in flight by generating rolling, pitching or yawing moments as well as allowing for the effect of lift, side and drag forces to act on the aircraft.

There are a number of control surfaces that are installed on an aircraft in order to control these forces and moments, ranging from wing flaps and ailerons to rudders and stabilisers, all of which are demonstrated in Figure 2 below.

This image has been removed

Figure 2 - Aircraft Control Surfaces

(Airliners.net 2007)

As can be seen in Figure 2 the devices can be divided into two distinct categories, Primary Flight Controls and Slats and Aero Flaps. The primary control devices consist of both wing and tail components and are defined as a variable surface that pivots about a point on the wing/tail sections. The aileron control surfaces are designed to produce the rolling moments required to manoeuvre the aircraft at all flying speeds. The location of the ailerons is critical as poor placement could lead to an opposing rolling moment being generated thus reducing the control available to the pilots (Stengel 2004:217). Using a combination of devices can lead to an increase in efficiency and effectiveness and this is shown by the slats that are used on the leading edge of a wing providing a more suitable flow to the ailerons to further control the rolling moments (Stengel 2004:217). The secondary elements such as the arrangement of slots and flaps on the wing section of an aircraft provide a number of advantages when the control of the airflow to the ailerons is considered. The slats that are located at the leading edge of the wing are designed to control the boundary layer of the fluid (air) while also increasing the camber of the wing. The flaps are often only used during take-off and landing and are designed to control lift and drag with a limited variability compared to the primary control surfaces (Stengel 2004:3).

The boundary layer is the layer of fluid that is in close proximity to the surface over which it is travelling. As the fluid approaches the surface, the fluid velocity decreases to a point whereby the fluid in direct contact with the surface has a velocity of zero, thus creating the boundary layer 'slope' that can be seen in Figure 3. As the fluid travels over a surface, the boundary layer increases in depth and is therefore required to be controlled in order to

provide the most suitable airflow over the surface. Through the use of a slot on the leading edge of the wing the boundary layer can be controlled and reduced while also assisting in the directing of the airflow over the upper wing surface at high angles of attack, thus delaying the stalling of the leading edge (Milliken Milliken 1995:512-513).

This image has been removed

Figure 3 - Boundary Layer Formation
(Milliken Milliken 1995:512)

A further advantage of the slot and aero flap configuration is the increase in camber of the wing. The camber of the wing is defined as the curvature of the wing and it is said that increasing this curvature moves the stagnation point of the airflow rearwards and increases the flow over the wing profile (Milliken Milliken 1995:512-513).

As can be seen, the aerodynamic design of an aircraft is of particular importance when taking into account the form and function of the vehicle. Through the amendment of the various aerodynamic devices, the dynamic behaviour of the aircraft can be changed to offer the most suitable force and moment configurations for the pilot's chosen task.

3.1.1.1 'The Flying Wing'

The majority of aircraft, as shown in Figure 2, use a vertical fin, to which the steering rudder is connected, to stabilise the aircraft and to produce a yawing moment, however, one such aircraft, the Northrop-Grumman B-2 bomber, otherwise known as the 'The Flying Wing' does not have a tail section, as can be seen in Figure 4.

This image has been removed

Figure 4 - Northrop-Grumman B2 Military Aircraft

(Bibliotecapleyades 2005)

The B-2 bomber is a stealth aircraft and thus, the profile of the fuselage is of key importance to reduce its radar visibility. By not having a tail section, radar visibility is reduced, however, an alternative method of negating the yawing moment of the aircraft by controlling the side force is required. To achieve this a range of spoilers and ailerons are positioned on the 'wing' of the B-2 with the interaction between these and an arrangement of yaw flaps positioned at the wing tips controlling the side force and therefore yawing moment of the aircraft (Stengel 2004:217).

3.1.2 Ground Vehicles

The use of variable aerodynamic devices within the automotive industry has also become more pronounced in recent times, with motorsport leading the way. There are a number of devices that are currently used, from air brakes to control flaps, all of which have a great impact of the performance of the vehicle, whether this be from a safety aspect or with a view to improving and amending the vehicles performance and dynamics during a particular manoeuvre or task. The following sections demonstrate how the change in aerodynamic properties that these devices provide can affect the vehicles behaviour in certain scenarios.

3.1.2.1 Air Brakes

The first documented use of air brakes on sports vehicles occurred during the 1955 Le Mans event in which the Mercedes-Benz 330SL entries both tested a driver deployable panel situated behind the driver (Aird 2009). When the car was approaching a corner which required high braking, such as at the end of Le Mans' Mulsanne Straight, the driver would deploy the rear bodywork which acted as an air brake and thus produce a significant deceleration of between 0.12g at 100mph and 0.34g at maximum velocity (Aird 2009: 60). The air brake on the Mercedes-Benz 330SL was situated at the rear of the vehicle and as such, when deployed, would reduce the forward pitching moment of the vehicle as the weight transfer from rear to front would not be so great, offering preferable dynamic properties, see Figure 5.

Figure 5 - Mercedes 300SL Air Brake (Left: Closed, Right: Deployed)

(Modern Mechanix 2012)

The principal of the air brake was to decrease the stopping distances of the vehicles in order to decrease the overall circuit lap time. It can be said that in order to slow a vehicle using aerodynamics, the vehicle's drag force is required to increase. The two simplest methods to increase the drag force of a vehicle are to increase the drag coefficient and/or increase the frontal area of the vehicle, which is demonstrated in Equation 1 (Aird 2009: 59).

$$Drag\ Force = \frac{1}{2}\rho C_D A V^2$$

Equation 1 - Drag Force

Further evidence of this can be seen in Figure 6 which shows how the drag force increases when the frontal area and drag coefficient are increased. The increase in drag force can be seen to be linear in both instances when travelling at a constant velocity and constant fluid density.

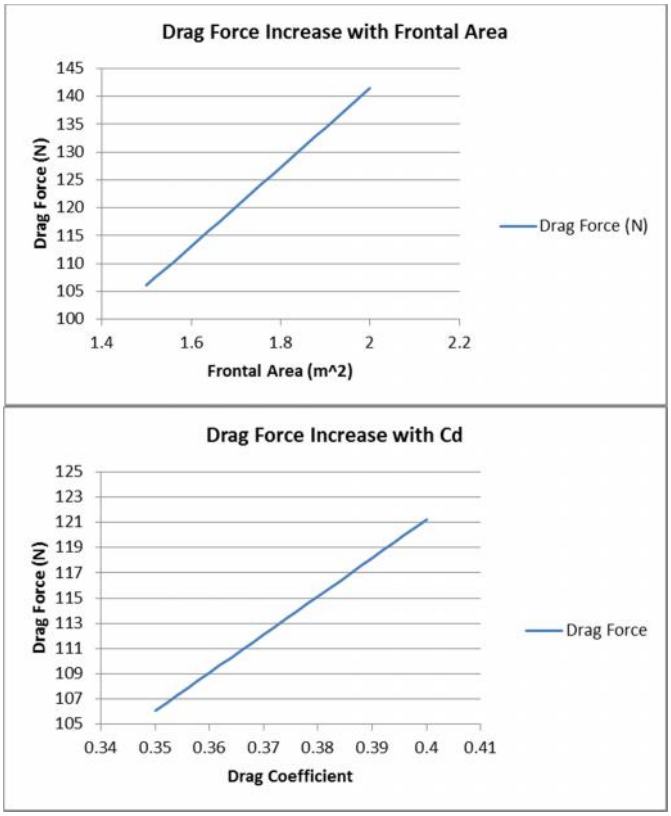

Figure 6 - Drag Force Comparison

The installation of air brakes has continued to this day, particularly when considering high performance vehicles, such as the Bugatti Veyron and the McLaren Mercedes SLR. However, as the understanding of aerodynamics has increased, so too has the effectiveness of these air brakes with the Bugatti Veyron able to generate a deceleration of up to 0.6g with an angle of attack of 5.5° (Aird 2009:60).

3.1.2.2 NASCAR Roof Flaps

Air brakes remain in active use within motorsport, with one of the main examples being in NASCAR. Research undertaken by Nelson et al. shows that at high speeds, when travelling at a high yaw angle, commonly after an accident on the circuit, the design of the vehicle creates a high lift force, thus causing the vehicle to become airborne. It was found that when a NASCAR vehicle was subject to yaw angles between -70° to -150°, an area of low pressure would be present on the horizontal surfaces such as the roof, bonnet and boot area (Nelson et al 1994). This area of low pressure was great enough to cause the vehicle to generate lift that could cause a vehicle with an approximate mass of 1,600kg to become airborne (Nelson et al 1994).

The roof flaps are engineered to be a passive variable device, thus not relying on driver input to be actuated during an accident. When the vehicle is at the prescribed yaw angle whereby there are areas of low pressure on the roof, bonnet and boot, the air contained under the roof flap wants to diffuse from a higher pressure region to a lower pressure region, thus causing the flap to open slightly. Once the roof flaps have begun to open, the force of the air passing over the vehicle causes the flaps to open fully and therefore cause the dissipation of the area of low pressure, reducing the lift force acting on the vehicle.

The image below shows the location of the air brake flaps. One of the flaps was positioned along the longitudinal plane of the vehicle, with the second flap being situated at an angle of 140°, with this yaw angle being found, through experimentation and real world scenario analysis, to provide the highest lift force (McBeath 2011:80).

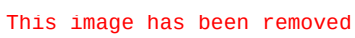

Figure 7 - NASCAR Roof Flap Placement

(Nelson et al. 1994)

Through the introduction of the roof flaps, the lift force that is generated by a NASCAR vehicle when travelling at extreme yaw angles is said to have been decreased significantly. This can be seen in Figure 8, which compares the lift at the rear and on the right hand side of the vehicle over a range of yaw angles between 130° and 160°. From this it can be seen that through the use of the anti-lift devices (roof flap arrangement and a splitter located along the right-hand side top surface of the vehicle), the lift generated on the right hand side is reduced considerably between 130° and 160° by up 57 percent (Nelson et al. 1994).

This image has been rermoved

Figure 8 - Lift vs. Yaw of NASCAR Roof Flaps

(Nelson et al. 1994)

It is to be noted that since the introduction of the roof flap devices, the frequency of aerodynamic lift-off incidents has reduced dramatically, indicating that variable devices can allow for an increase in safety through the generation of downforce or the reduction in lift (McBeath 2011:79-80).

3.1.2.3 Drag Reduction Devices

Within the automotive industry large amounts of research is undertaken in order to identify methods of reducing the drag generated by a vehicle to improve characteristics such as maximum velocity, longitudinal acceleration and fuel economy. In recent years motorsport series have implemented drag reduction systems in the regulations to increase overtaking by reducing the drag of a vehicle in key 'zones' of a circuit. The following section describes the drag reduction devices utilised.

3.1.2.3.1 F-Duct & Drag Reduction System (DRS)

The Drag Reduction System was introduced to the 2011 FIA Formula One Technical Regulations to promote overtaking within races through increasing the size of the slot between the rear wing main element and upper aerofoil element and has since been adopted by other racing categories including Formula Renault 3.5 and DTM. DRS replaced the excluded 'F-Duct' system whereby, air would flow into a duct, and through the chassis. At the drivers discretion a secondary duct could be covered by the driver's hand or knee, which redirected the airflow to the rear wing, causing the wing to stall and reduce drag and downforce and therefore a greater maximum velocity would be obtainable (Rendle 2011). "Stall is described as the condition where an aerofoil does not generate a lift or drag force" (Nasri 2012). As the 'F-Duct' would only be deployed on a circuit's straights, downforce would not be required. Figure 9 shows the F-Duct configuration of the Red Bull Racing RB6. Note the two pipes, the lower pipe providing air to stall the main beam and the upper pipe supplying the air to stall the secondary smaller element (Rendle 2011). Due to safety concerns the development of F-Ducts was outlawed from the start of the 2011 season and replaced by a moveable rear wing section, referred to as DRS.

This image has been removed

Figure 9 - Red Bull RB6 F-Duct Configuration

(Autosprint 2010)

The Drag Reduction System consists of the secondary (upper) wing element being allowed to pivot about its trailing edge allowing a slot of up to 50mm to be created between the main and upper wing elements. The aim of the DRS was to offer the chasing competitor a speed advantage of approximately 4 to 5kph over the car ahead in a designated zone on the circuit and therefore provide the opportunity for an overtaking manoeuvre to occur (Lis 2010:38), however it has been seen since the inception of the concept that differences in speed between a car with DRS in operation and one that does not have it active can be in excess of 10 kph (ScarbsF1 2011).

When the driver in the following car is within a second of the car in front, when in a relevant detection zone, the DRS will be activated. This is achieved through the driver pressing a button on the steering wheel or in the cockpit which then allows the hydraulic actuators that are located in the actuator housing to be activated and thus move the pivoting upper element into its 'open' position. When the brakes are applied, the system automatically returns the upper element to its original position to provide the downforce required to navigate the upcoming corner. Figure 10 shows the DRS in operation on the rear wing of the 2013 Ferrari F138.

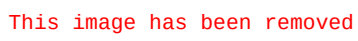

Figure 10 - DRS in Operation on the Ferrari F138

(Formula 1 2013)

3.1.2.4 Driver-Adjustable Front Wing

A further adjustable device that was implemented on Formula One cars for the 2009 and 2010 seasons was the introduction of a driver adjustable front wing. The aim of this adjustable flap on the front wing was to promote overtaking by allowing a car in the wake of the car in-front to run a greater wing angle to compensate for the reduction in downforce associated with following another car. When a car follows another car, the turbulent wake, commonly known in Formula One as 'dirty' air, causes the car behind to lose downforce as the air is approaching the car in a highly turbulent fashion. With the increase in front wing angle, the loss of downforce would be significantly less, therefore, allowing the following car to remain closer through the corners, presenting an overtaking opportunity on the circuit's straights.

The use of this device did not promote as much overtaking as intended due to the fact that "as a following car crosses the wake of a leading car, the balance goes and the wing setting is not right," (Lis 2010:41). In fact teams used the movable device to reduce the drag of the vehicle when on a straight section of track by reducing the angle and thus reducing the frontal area of the vehicle.

Figure 11 - Driver Adjustable Front Wing Flap Mechanism

(Rendle 2011)

Studies have been conducted into the effect of increasing the angle of attack of both the front and rear wings. From these studies it can be said that the lift coefficient of the vehicle can be changed by up to 2.6%, with a transfer of pressure of 2.4% towards the front axle (Skinner, Clifford, Martins 1996). Figure 12 shows the schematic of the actuator setup for both front and rear wings.

This image has been removed

Figure 12 – Schematic of Front & Rear Wind Adjustment Mechanisms
(Skinner, Clifford, Martins 1996)

3.1.2.5 Dynamic Control Surfaces

Aerodynamics have become an integral component of hypercars in recent years, and non-more so than on the 2012 Pagani Huayra. The Huayra utilises four control surfaces that are situated at the four corners of the vehicle that are used to achieve a neutral behaviour under all conditions (Pagani 2012). These result in a vehicle with controlled pitching, yawing and rolling moments under braking, acceleration and cornering. The flaps are actuated electronically through information obtained and computed by the ECU to deliver the optimum control flap angle, with the information concerning the vehicle's velocity, yaw angle, lateral acceleration, steering angle and throttle position (Pagani 2012).

Following the lead of the Pagani Huayra, the recently announced LaFerrari also uses an arrangement of variable control surfaces in order to offer a highly stable vehicle capable of using aerodynamics to improve its overall performance (Ferrari 2013).

3.2 Crosswind Stability

3.2.1 Stability Devices

When developing a vehicle, particularly commercial vehicles with high exposed side surfaces, the effect of crosswinds needs to be considered. There have been a number of studies that have been undertaken to determine the effect of crosswinds, from which it can be said that the lateral and yawing response of a vehicle are the main causes of sensitivity of the vehicle, which could affect the ability of the driver to maintain the vehicles course (Singh et al 2009). These studies such as the ones undertaken by Mayer et al. and Schroeck et al. concern the investigation of vehicles in steady and unsteady flows in an attempt to simulate real-world conditions through inducing an asymmetric flow structure to simulate a 'gust' of wind at various yaw angles.

Reducing the effect of crosswinds on vehicles has become a key aspect within the motorsport sector, with a number of device profiles being utilised. The main device that has been used through various categories of motor racing, from Le Mans to Formula One and IndyCar, is the vertical stability fin.

The aerodynamic stability of a vehicle when subject to a crosswind is described as when a vehicle 'generates a counteracting yawing moment to the direction of the resulting oncoming wind, and thus reducing the overall yawing moment of the vehicle' (Hucho 1998:247). When the yawing moment produced by the side wind increases the overall disturbance of the vehicle, it is said that the vehicle is aerodynamically unstable (Hucho 1998:247). When the air flow over the vehicle is attached around the front and rear of the vehicle, a large yawing moment is generated, which as stated, would cause a substantial reduction in the stability of the vehicle. It is known that causing a flow separation at the rear of the vehicle would cause a reduction in the yawing moment and as such allow the vehicle to offer greater stability under crosswind conditions (Hucho 1998:247).

In order to cause a flow separation at the rear, a device has to be used to create a higher rear side force, with a stability fin being the preferred option, particularly within the motorsport sector. The stability fin also provides additional benefits within certain applications such as Formula One where rear wings and spoilers are utilised. The vertical fin provides a control surface whereby the airflow from the front section, air box and roll-over crash structure of the Formula One car can be aligned and presented to the rear wing in a

more structured and less turbulent fashion, thus allowing the rear wing to function more effectively and produce a greater level of negative lift.

Figure 13 shows the stability fin installed on the Red Bull RB6 Formula One car that contested the 2010 Formula One season. Here it can be seen that the airflow is designed to be attached along the length of the vehicle body to produce the greatest amount of downforce possible. This attached flow could lead to a reduction in stability when subject to crosswind conditions if a stability fin was not utilised.

Figure 13 - Stability 'Shark' Fin on the Red Bull RB6

(Red Bull Haynes Manual 2011:51)

The benefits of crosswind stability devices such as fins have been the subject of a number of investigations concentrated on the forces and moments produced. From these studies it can be assumed that the addition of a fin increases the overall side force that acts on the vehicle, moving the Centre of Pressure rearwards (Schroeck et al 2011). By moving of the Centre of Pressure rearwards, the yawing moment is decreased (Mayer et al 2007). While this information is public knowledge, the use of a variable device that could be deployed either manually or passively to reduce the risk of instability during crosswinds has not yet been investigated.

3.2.2 Vehicle Dynamic Characteristics in Crosswinds

The vehicle's dynamic characteristics, when subject to a crosswind, are based upon the location of the vehicle's Centre of Pressure relative to the Centre of Gravity. The Centre of Pressure is the location on the vehicle where the sum of the aerodynamic forces and moments act, and as such is dependent on the shape and design of the vehicle (Rendle 2011:51). The Centre of Gravity is also an important parameter to consider when engineering a vehicle for stability in both the lateral and longitudinal planes. The distance between the Centre of Gravity and the Centre of Pressure is known as the 'Static Margin' (Katz 2006:175).

The principals of vehicle stability due to crosswinds can be seen in the following Figures. Figure 14 shows a plan view of a vehicle when the Centre of Pressure is located at a position forward of the Centre of Gravity. When under these conditions, the front of the vehicle will be forced in the direction of the crosswind, thus increasing the yawing moment of the vehicle, reducing its stability (Katz 2006:177). This is due to the increase in induced lateral acceleration turning the vehicle away from the wind direction (Gillespie 1992:108).

Figure 14 - Centre of Pressure forward of the Centre of Gravity

(Katz 2006:177)

When the Centre of Pressure is located behind that of the Centre of Gravity, shown in Figure 15, the vehicle is considered to be stable. This is due to the fact that the higher rear side force would cause the vehicle to yaw into the direction of the crosswind and therefore lead to a reduction in the driver correction inputs required to maintain the vehicles path.

These images have been removed

Figure 15 - Centre of Pressure aft the Centre of Gravity Position

(Katz 2006: 177)

During these scenarios, the driver would have to apply a steering input to ensure that the vehicle would continue to travel along its desired path. Figure 16 shows that there is a significant difference in the required driver input for the vehicle to maintain its course when comparing a Centre of Pressure point before and after the Centre of Gravity. Here it can be seen that when the Centre of Pressure is behind the Centre of Gravity the curve is dramatically reduced in comparison and is well damped, providing a more stable vehicle at speed. When the Centre of Pressure is ahead of the Centre of Gravity the sideslip of the vehicle tends to oscillate and reduce at a lesser rate, indicating an underdamped and less stable vehicle.

Figure 16 - Side-Slip of a Vehicle Subject to a Side Force

(Katz 2006:178)

As identified above, when the Centre of Pressure is located behind that of the Centre of Gravity the stability of the vehicle is greater under crosswinds conditions than when compared to the forward position. To achieve this, the side force acting on the rear is required to be greater, allowing the Centre of Pressure position to transfer rearwards, which can be achieved through the use of a device such as the stability fin described above.

3.2.3 CFD Analysis of the Cross Wind Situation

The effects of crosswind disturbance have also been investigated through the use of CFD within the industry, with a number of studies being undertaken into the force coefficients at varying vehicle and wind velocities. Singh et al (2009), through the use of CFD, were able to establish the effect of crosswind angle on drag, lift and yaw coefficients. The following graphs show that at a crosswind approach angle of 15°, the drag coefficient can be seen to be at its lowest value, this is due "to the overall flow distributed over the vehicle with a relatively higher spread and slightly higher velocity in the rear wake compared to the baseline and other crosswind angle cases" (Singh et al 2009:5). This can be shown in Figure 17 where the fluid velocity in the wake of the vehicle is considerably greater than at the other displayed yaw angles. Once the yaw angle increases past 15°, it can be said that the drag coefficient increases in a relatively linear manor.

Figure 17 - Drag Coefficient vs Crosswind Angle & Velocity Distribution

(Singh et al. 2009)

The linear increase is also exhibited in Figure 18 which show the lift and yaw coefficients, here it can be seen that as the crosswind angle increases, so too does the coefficient. It can be said that with a fixed crosswind angle, a vehicle with a lower velocity would exhibit greater handling difficulty (Singh et al. 2009:6).

This image has been removed

Figure 18 - Lift Coefficient vs Crosswind Angle & Yaw Moment vs Crosswind Angle

(Singh et al. 2009)

Each of these scenarios demonstrates that there is potential for a variable aerodynamic device to positively affect the vehicles dynamic ability, when acted on by a crosswind, at various approach angles.

3.3 Literature Review Conclusions

From the literature that has been reviewed, it can be said that aerodynamics have a great effect on the performance of a vehicle, both concerning longitudinal and lateral aspects. It can also be said that there are a number of devices used for aerodynamic gain, whether these be static or variable, such as the range of ailerons and elevators or the DRS system that is currently being utilised by a number of motorsport categories.

Furthermore, using the information that has been obtained from literature, there is scope for further research to be undertaken into understanding how a vehicle reacts to a side wind disturbance. It was decided that the implementation of a variable device to modify the effect of a side wind disturbance would prove beneficial and further expand on the current knowledge of this field of interest. To achieve this, as outlined in the project plan, a range of tasks will be completed including the mathematical analysis of a vehicle and the completion of physical and virtual simulations to assess the use of variable devices.

The following section identifies how aerodynamic forces affect a vehicle's dynamic behaviour using a mathematical model, concerning the front and rear lateral forces and slip angles to analyse the corrective steering angle required to maintain linearity.

4 Vehicle Dynamics Mathematical Model

4.1 Mathematical Model & Justification

4.1.1 The Bicycle Model

To fully understand the effects of a crosswind gust on the dynamic behaviour of a vehicle a mathematical model can be utilised. The model will be based on a 2 DoF single track theory model, otherwise known as the Bicycle Model. The Bicycle model is a suitable method of analysing the lateral motion of a vehicle for the application of the research as it can supply the required information without the addition of further degrees of freedom. In order to utilise the Bicycle model, a number of assumptions are required to be made, including; the vehicle is considered to be travelling on a level surface, the vehicle's suspension is rigid and the steering angle is constant (Dukkipati et al: 361). Furthermore, in preparing the model, the tyres of each axle are deemed to be a single tyre, hence the 'Bicycle' term. Figure 19 below shows the bicycle model and the relevant parameters.

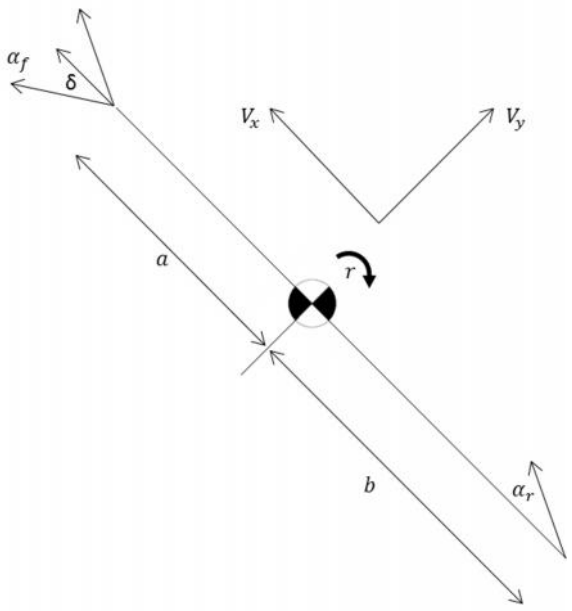

Figure 19 - Bicycle Model Schematic

(Adapted from Dukkipati et al 2008: 361)

The following sections demonstrate how the bicycle model can be used in order to determine how an aerodynamic side force caused by a side wind gust, can affect the dynamic characteristics of a vehicle with set parameters.

4.1.2 Modelling Assumptions

As stated above, to enable the Bicycle model to function and produce suitable results, there are a number of key assumptions and parameters that have to be in place, which concern both the vehicle and the driving environment;

(a) '*The vehicle is considered to be travelling on a level surface*.'
(b) *'The vehicle's suspension is rigid*.'

These two assumptions allow the vehicle to be analysed when the vehicle body is parallel to the ground plane and thus the analysis of the external forces and moments acting on the vehicle can be considered in isolation. It is therefore not required to separate the forces and moments induced by a crosswind disturbance from those generated by the surface that the vehicle is travelling along, ensuring the model remains a 2DOF system, thus reducing complexity.

(c) '*The steering angle is constant.*'
(d) '*The tyres on each axle are joined to make one single tyre, hence the 'bicycle' model.*'

In order to fully understand the lateral forces and moments that are acting on the vehicle, it is required that the model does not induce any additional lateral components, as this would increase the complexity of the model. It is for this reason that the steering angle is considered to be constant throughout the initial analysis of the vehicle. To enable the model to be considered a bicycle model, the tyres on each axle can be considered to be joined, and hence create a bicycle model. The joining of the tyres allows for the forces acting at the tyres to be analysed at a central point along each axle.

By using these assumptions the model remains a 2DOF system and allows for suitable analysis of the lateral components to be achieved. If these assumptions had not been used, the complexity of the model would increase significantly, as the displacement of the sprung mass of the vehicle body would have to be taken into consideration when the vehicle is travelling along a chosen path, as this would alter the aerodynamic properties of the vehicle. Also, the lateral forces and moments acting on the vehicle body, caused by external elements such as crosswinds, would have to be separated from those induced by the driver if the steering angle is not constant. Through the use of the above assumptions, the model can be used to analyse, in isolation, the behaviour of the vehicle when acted on by a crosswind.

4.2 Vehicle Characteristics

4.2.1 Yaw Rate

Yaw rate is defined as the velocity at which a vehicle rotates around the yaw axis, commonly said to be the z axis (Blundell 2004: 501).

For the purpose of this mathematical model, it was decided that the vehicle would have a constant forward velocity of 20 m/s, which equates to 45mph. From research, it was able to be established that a typical vehicle travelling at this velocity has a maximum yaw rate of approximately 25 deg/sec, as can be seen in Figure 20, it was therefore decided that for the lateral calculations, this yaw rate would be used. For the mathematical model, care had to be taken to ensure the unit outcomes were correct, therefore a yaw rate with units of rad/sec was used.

This image has been removed

Figure 20 - Yaw Rate of a Typical Vehicle

(Blundell 2004: 402)

4.2.2 Vehicle Variables

To enable the mathematical model to be created, a number of vehicle characteristics are required to be known, with the values shown in Table 1 obtained through research.

Vehicle Characteristics		
Vehicle Parameter	Value	Units
Vehicle Mass, M	1,200	kg
Moment of Inertia, Izz	1,350	kgm^2
Wheelbase, L	3	m
Distance of front axle to C of G, a	1.25	m
Distance of rear axle to C of G, b	1.75	m
Front Cornering Stiffness, CαF	-100,000	N/rad
Rear Cornering Stiffness, CαR	-100,000	N/rad
Forward Velocity, Vx	20	m/s
Steering Angle, δ	0	Degrees

Table 1 - Vehicle Variable Characteristics

4.3 Lateral Components & Analysis

Through researching literature, a method of analysing the effect of side wind gusts on vehicle behaviour was able to be established, and is explored below. Also described is the resulting graphical output from the mathematical model that utilises these numerical methods.

4.3.1 Side Wind and the Resultant Vehicle Yaw Angle

The behaviour of a vehicle in the lateral plane is of great importance when the vehicle is acted upon by a side wind force as a disturbance of this nature can cause the vehicle to become less stable and lead to a loss of control by the driver. As described in the literature review, the translation of the centre of pressure from in front of the centre of gravity position to after it can cause the vehicle to remain within the driver's recoverable bounds.

To enable further evaluation into whether a variable device could improve the vehicle's behavioural characteristics in such a situation, the mathematical model described below, can be interrogated to offer an appropriate analysis of the scenario.

The first process that is required is to calculate the resultant velocity of the wind element when taking into account the forward velocity of the vehicle. It can be assumed that the driving velocity of the vehicle can also be expressed as the air velocity approaching a stationary vehicle, allowing the road velocity to become a positive vector. The side wind velocity can also be expressed as a vector, as can be seen in Figure 21, whereby the side wind approach angle is defined as θ, which for this analysis remains constant.

This image has been removed

Figure 21 - Resultant Velocity Vector Addition

(Barnard 2009: 217)

The vector connecting the drive velocity and side wind velocity can be said to be the wind resultant velocity approaching the vehicle, which is calculated through using Equation 2.

This image has been removed

Equation 2 - Resultant Vehicle Velocity

(Hucho 1998: 266)

The angle formed between the vehicle longitudinal heading axis and the resultant velocity can be described as the yaw/sideslip angle of the vehicle, β (Dukkipati et al 2008: 361). This can be calculated using the Sine Rule, where the angle opposite the resultant velocity vector is 180° minus the side wind approach angle, highlighted in Figure 21.

The graphs that are obtained through the implementation of these equations can be seen below. Figure 22 demonstrates the change in resultant air velocity approaching the vehicle as the side wind velocity increases. It can be seen that as the side wind velocity increases the resultant velocity increases in a linear manor. This is to be expected as if the side wind is acting at 0°, hence a head-wind, the resultant velocity would be the addition of the 'driving' air velocity and the side wind velocity.

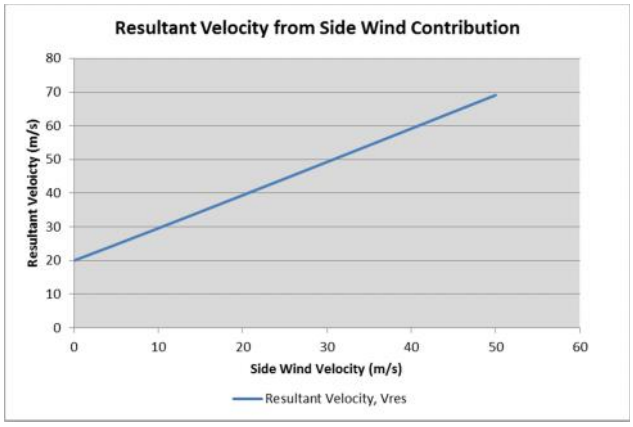

Figure 22 - Resultant Side Wind Velocity

It can also be seen that there is an increase in yaw/sideslip angle as the side wind angle increases, as is demonstrated in Figure 23. This can be explained through the addition of vectors causing the sideslip angle to increase.

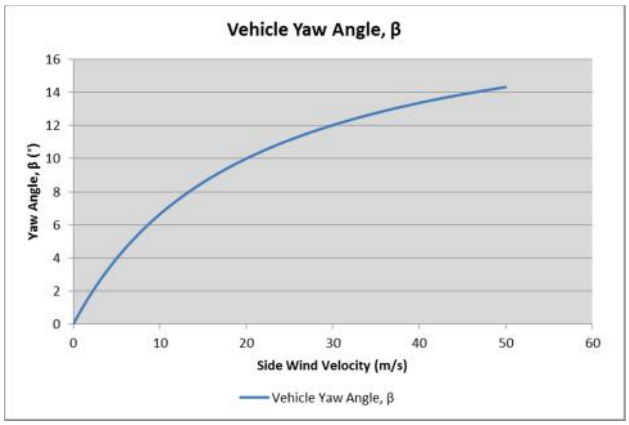

Figure 23 – Change in Vehicle Yaw/Sideslip Angle

4.3.2 Introducing an Aerodynamic Side Force

To have the ability to calculate the total lateral force acting on the vehicle, it is required that the aerodynamic side force is defined. In order to determine the force acting on the vehicle at a constant side wind approach angle and varying velocity, the aerodynamic equation shown below is used.

$$Side\ Force, y = \frac{1}{2}\rho C_y A V^2$$

Equation 3 - Aerodynamic Side Force

With the use of Equation 3 it is required that a number of constants are known, which are; the side force coefficient of the vehicle which is obtained through CFD analysis and/or wind tunnel testing, the air density, for which the value used as the constant air density with Star CCM+ has been used, and the projected frontal area of the vehicle. The values that have been used for these parameters can be seen below in Table 2.

Parameters	Value	Units
Side Force Coefficient, Cy	0.2	No Units
Air Density, ρ	1.18415	kg/m^3
Vehicle Projected Frontal Area, A	1.8	m^2

Table 2 - Vehicle Aerodynamic Parameters

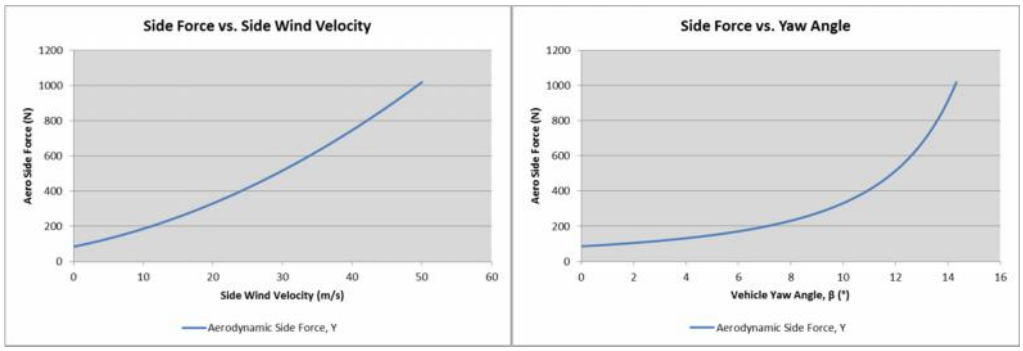

Figure 24 - Aerodynamic Side Force against Velocity & Yaw Angle

Figure 24 shows the resulting aerodynamic side force that acts on the vehicle described in Table 2, when compared to the velocity of the side wind and the yaw angle of the vehicle. It can be said that there is a relatively linear relationship between the side wind velocity and the aerodynamic side force, with the force increasing as side wind velocity increases. It is displayed from Figure 24(b), that the side force initially increases by a comparatively small amount as yaw angle increases from 0° to 8°, however as the yaw angle increases further, in this case up to approximately 14°, the aerodynamic side force increases at a greater rate, thus signifying that as a greater proportion of the vehicle's side profile is being acted on by the side wind, the greater the side force, which is to be expected.

Furthermore, as the mass of the vehicle is known, it is possible to determine the lateral acceleration of the vehicle as a result of the side gust, which is shown below in Figure 25. The acceleration acts in a similar fashion to that of the aerodynamic force, whereby the lateral acceleration increases as the side wind velocity increases. The lateral acceleration also increases greatly as the yaw angle increases to that of beyond approximately 8°.

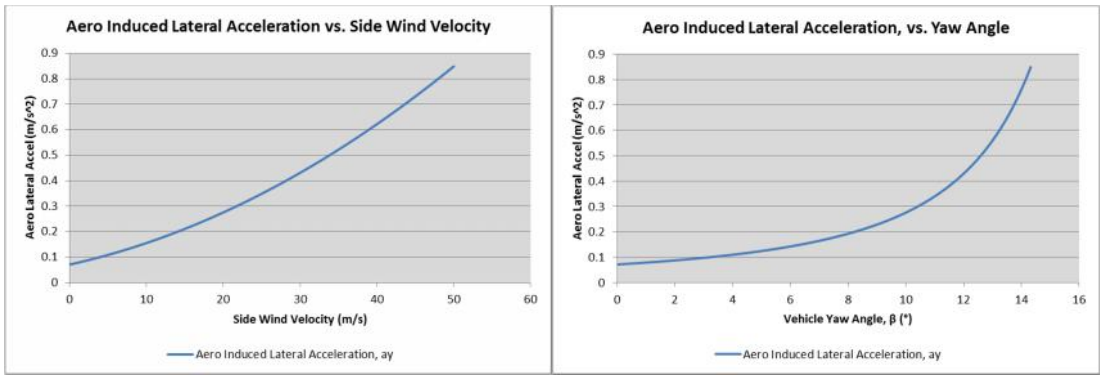

Figure 25 - Aerodynamically Induced Acceleration against Side Wind Velocity and Yaw Angle

4.3.3 Lateral Axle Forces

4.3.3.1 Front & Rear Slip Angles

Considering the bicycle model described in Figure 19, the sum of the lateral forces that act upon the vehicle can be determined, and are shown in Equation 4.

$$\sum F_y = C_{\alpha f}.\alpha_f + C_{\alpha r}.\alpha_r + F_{Wind}$$

Equation 4 - Sum of Lateral Forces acting on the Vehicle

Equation 4 can be split into a number of different sections concerning the front and rear axle, and are shown below.

$$\alpha_f$$

These images have been removed

Equation 6 - Rear Axle Force

(Dukkipati et al 2008: 362)

Equation 5 and Equation 6 demonstrate that the lateral force that acts on each axle is a function of the cornering stiffness of the tyre and the slip angle generated at the tyre. The slip angle, Figure 26, is defined as the "*angle between the direction of wheel heading and the direction of travel*" (Gillespie 1992:198).

This image has been removed

Figure 26 - Slip Angle Schematic

(Gillespie 1992:198)

It can also be seen that the slip angle is a function of the sideslip angle of the vehicle and yaw rate at a constant velocity as is highlighted in the equations above. For the vehicle

analysed through the mathematical model, the difference in slip angle of the front and rear axle has been calculated and can be seen in Figure 27.

Figure 27 - Front & Rear Slip Angle Comparison

It can be seen that the front and rear slip angles change by a different amount when acted on by a side wind. From Figure 27, the change in front slip angle is greater than that of the rear, which is due to the centre of gravity being positioned further forward. This, as discussed, causes the front of the vehicle to be forced from the path of travel at a greater angle. To reduce this effect, the centre of pressure location is required to be translated rearward of the centre of gravity.

4.3.3.2 Change in Sideslip and Yaw Rate Gain

Using the information that has been obtained throughout the mathematical analysis, the change in the vehicle's sideslip angle can be calculated, and is achieved through inputting the relevant values into Equation 7, including the aerodynamically induced side force acting on the vehicle. Furthermore, the change in yaw rate, otherwise known as yaw rate gain, can be found through the use of Equation 8 which utilises the moment created by the aerodynamic side force acting a distance 'i' from the centre of gravity position.

.

These have been removed

.

Equation 8 - Change in Yaw Rate with respect to Aerodynamic Moment

(Dukkipati et al 2008: 365)

With these being calculated, the equations can be developed so as to allow the required steering angle to maintain the vehicle on its designated path to be found. During such an event it is ideal that the corrective steering angle remains as small as possible as this would lead to a reduced input from the driver. The equations that are derived are shown below. It is to be noted that for this theoretical model the longitudinal force acting on the front axle, F_{xf}, of the vehicle is deemed to be negligible in comparison to the front cornering stiffness, $C_{\alpha f}$.

$$\dot{\beta} = -\left(\frac{C_r + C_f}{mV_x}\right).\beta + \left(\frac{C_f.b - C_r.a}{mV_x^2} - l\right).r + \left(\frac{C_f + F_{xf}}{mV_x}\right).\delta$$

Rearranged

$$\delta = \dot{\beta} + \left(\frac{C_r + C_f}{mV_x}\right).\beta - \left(\frac{C_f.b - C_r.a}{mV_x^2} - l\right).r/(\frac{C_f + F_{xf}}{mV_x})$$

Equation 9 – Steering angle with respect to Sideslip Gain

These have been removed

Equation 10 - Steering Angle with Respect to Yaw Rate Gain

(Dukkipati et al 2008: 363)

For this analysis, Equation 10 can be used as it offers the yawing moment of the vehicle to be analysed, which as previously discussed, is the most critical moment acting on the vehicle when subject to side wind conditions. In order to understand the effect of the centre of pressure location on vehicle stability and the amount of steering angle required to correct the vehicle when acted on by a side wind, three scenarios have been simulated. For these scenarios, the centre of pressure will be located before, after and in an identical position to the centre of gravity. The results of these various scenarios can be seen below in Figure 28.

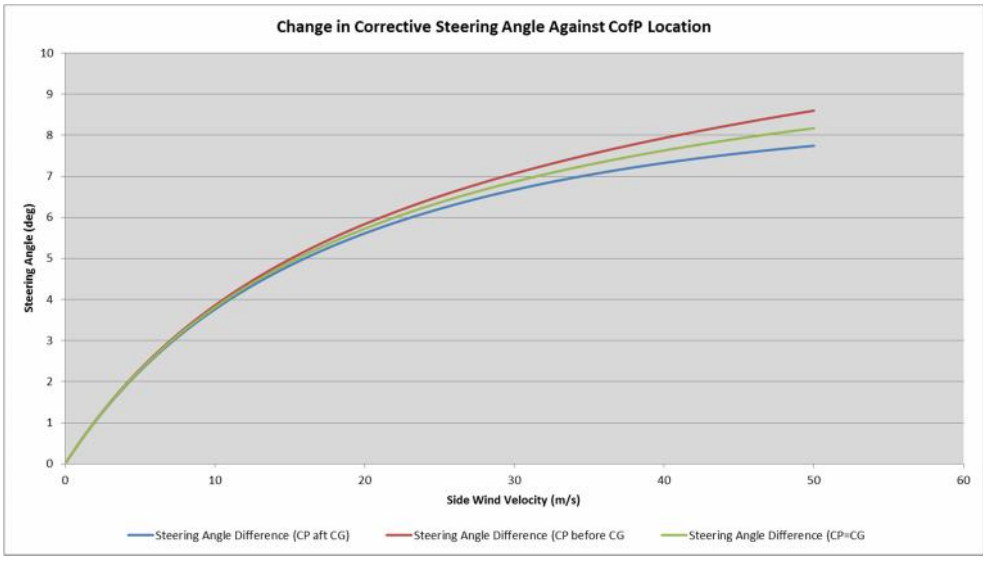

Figure 28 – Steering Angle Change with Respect to CofP Location

Figure 28 shows the difference in steering angle required to be input by the driver when the vehicle is subject to a side wind gust. The application of the steering angle is calculated to be the angle required to maintain the vehicle on a linear trajectory, and it can be seen there are distinct differences between the plots. Firstly, it can be seen that a greater steering angle is required when the CofP is located ahead of the CofG, which, as discussed in this report, is to be expected. Also, when the CofP is located after the CofG the steering angle is reduced. While the difference in required angles are considered small, the steering ratio between the 'hand wheel' and the front wheels does mean that there is a noticeable difference between

the vehicle configurations. Furthermore, it is to be noted that the vehicle characteristics chosen for this analysis represent a relatively stable vehicle, and reducing the cornering stiffness's would lead to a significant increase in required steering angle.

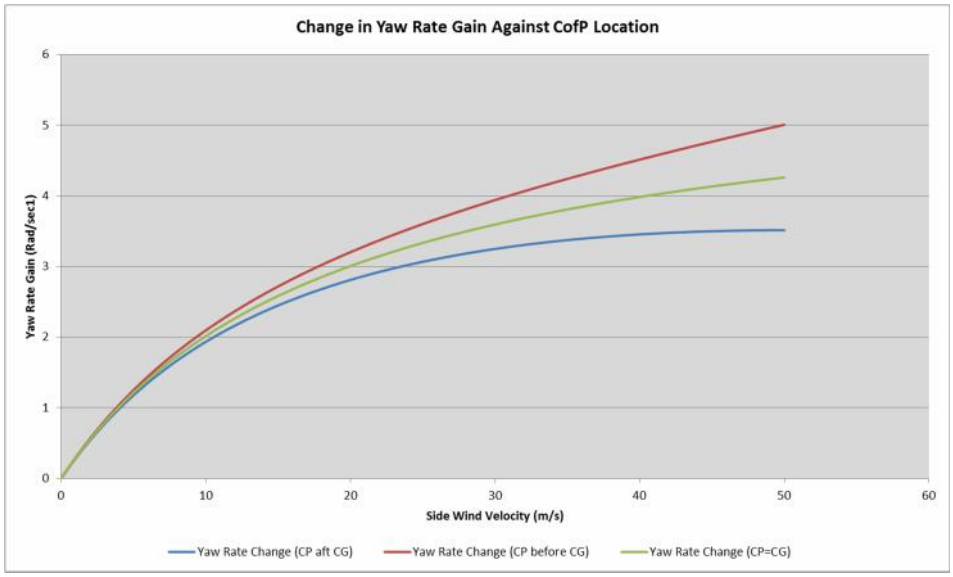

Figure 29 - Yaw Rate Gain with Respect to CofP Location

The rate at which the vehicle rotates around its yawing axis is of key importance, as a vehicle with a high yaw rate gain could prove difficult to control. Figure 29 shows a comparison between the three scenarios identified previously, and displays a number of interesting results. As with the steering angle, the greatest acceleration about the yaw axis occurs when the CofP location is forward of the CofG location, with signifies that a greater yaw rate gain is attributed to a vehicle with reduced stability. Also it can be seen that when the side wind velocity is between 0 and 10 m/s, the yaw rate gain for each scenario increases linearly at a comparable rate, however, as the velocity increases, yaw rate gain for the CofP forward of CofG vehicle increases at a greater rate than the CofP after the CofG vehicle, with this vehicle even providing a constant yaw rate gain of the wind velocity range of 30 – 50 m/s offering more stable and predictable vehicle handling characteristics.

The results shown in this section are, as described, for set vehicle characteristics, however, amendments to these characteristics can be made in the spreadsheet on the accompanying CD.

4.3.3.3 Driver in the Loop

One aspect that has not been included in the vehicle model is that of 'Driver-in-the-Loop'. Driver-in-the-Loop is the term used to identify a human aspect to the control of the vehicle. In order to maintain the simplicity of the model, it was decided that the driver would be removed from the system, however, as this could have a significant impact on the vehicles behaviour, the theory behind this topic is shown below.

A number of studies have been undertaken to understand the effect of having a driver in the loop, when the control of the vehicle is of key importance. Wagner and Wiedemann describe the involvement of a driver using the driver-vehicle schematic shown in Figure 30. Here it can be seen that when a vehicle is acted upon by an excitation force, both the vehicle and the driver react. These reactions, when input into a vehicle model, can potentially make a vehicle that is not sensitive to crosswinds unstable. This is due to the inputs, and reactions of the driver (Wagner, Wiedemann 2002:4).

Figure 30 - Driver & Vehicle Inputs and Output

(Wagner, Wiedemann 2004:4)

This instability can be caused by the vehicle reacting to reduce the effect of the crosswind, and then, with a delay due to a human reaction time, the driver then trying to compensate for the crosswind and 'over-correcting' the vehicle. This could lead to a greater input having to be applied by the driver, or at worst, the vehicle being removed from the range of the drivers recoverable bounds, and a loss of control.

One of the main variables with the inclusion of a driver is the reaction time. The time it takes for a human to acknowledge that an input is required to the time it takes for this input to be actioned varies significantly. It would therefore be decided that if a driver in the loop was to be included within the mathematical model then an average reaction time from input required to input actioned would have to be used. Such responses could be modelled using software such as MATLAB Simulink, and is proposed as a future work action.

4.3.3.4 Mathematical Analysis Discussion

It can be seen in the mathematical model that when the centre of pressure position of the vehicle is ahead of the centre of gravity, a greater corrective steering angle is required to maintain the vehicle on a straight path. It has also been proven that by translating the centre of pressure to a location behind that of the centre of gravity, along the vehicle's longitudinal axis, the corrective steering angle is reduced and therefore offers a vehicle that can be controlled to a greater effect during a crosswind event, this can be seen in Figure 31. This theory, as previously discussed, is widely accepted, however, the use of a variable aerodynamic device to adjust the centre of pressure location during a side gust has yet to be fully understood. The following sections of the report propose concepts that could be utilised to translate the centre of pressure rearwards using a variable device, with the most suitable solution being analysed through CFD simulations and wind tunnel analysis.

Figure 31 - Crosswind Lateral Acceleration Response with Variation in CP Location

(Gillespie 1992:108)

The ideal device will produce a greater side force at the rear of the vehicle thus translating the centre of pressure rearwards, with the benefit of reducing the yawing moment of the vehicle and therefore resulting in a vehicle that is more stable under side wind and gust conditions.

5 Device Conceptual Design

5.1 Initial Ideas

Through interrogating the mathematical model, it was able to be identified that the use of a device to translate the centre of pressure rearwards will create a more stable vehicle. The introduction of a device that could achieve this centre of pressure movement would reduce the required steering angle input when acted on by a side wind, therefore allowing the vehicle to remain as linear as possible for as long as possible.

The following pages show a number of initial ideas that could potentially make the centre of pressure rearward bias, leading to greater stability. The initial concepts are designed so as to be able to be installed on a range of vehicles.

5.1.1 Aerodynamic Fins

One of the simplest methods of moving the Centre of Pressure rearwards is through the use of an aerodynamic fin at the rear of the vehicle. When a side wind acts on the vehicle, the presence of the fin increases the side area of the vehicle and causes a greater force to act on the fin, thus moving the Centre of Pressure towards the rear. An example of an aerodynamic fin can be seen in Figure 32.

This image has been removed

Figure 32 - JCB DieselMax Record Car with Rear Fin

(Alpha Coders n.d)

It is to be noted that the fin on the vehicle in Figure 32 is reasonably small in area. This is because a greater fin area will cause a greater yaw tendency into the wind direction which is not desirable (Barnard 2009:219). The concepts below show how a deployable fin could be integrated onto a vehicle, with more detailed concepts being available in Appendix A.

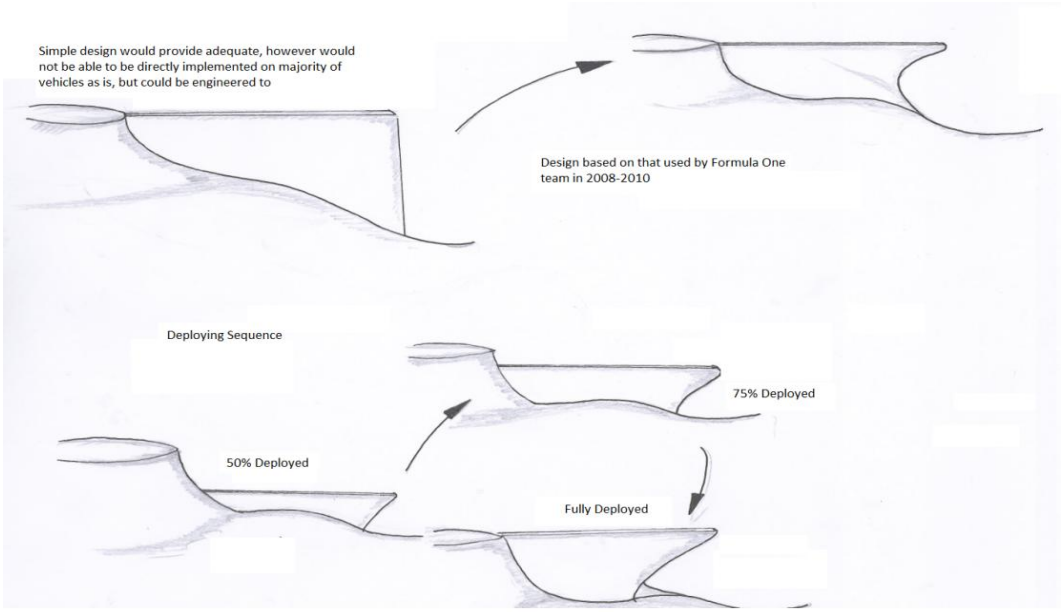

Figure 33 - Stability Fin Initial Concepts

5.1.2 Deployable Wings

As has been highlighted through the literature review, there are a number of deployable wings and spoilers that offer a degree of variability, however, the majority of such devices concern the longitudinal aspects of vehicle performance; maximum velocity and braking. When these devices are deployed there could be a possibility of introducing a range of side panels that have the potential to increase the side force acting on the vehicle. A range of concepts demonstrating this idea can be seen below, with a detailed image being available in Appendix A.

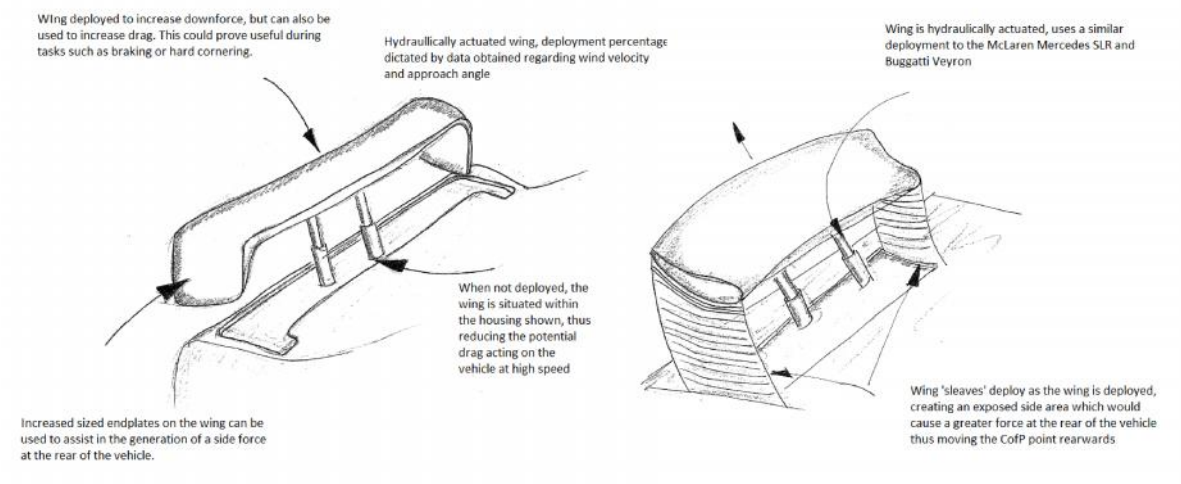

Figure 34 - Deployable Wing Initial Concepts

5.1.3 Controllable Surfaces

The use of controllable surfaces, much like those currently utilised on the Pagani Huayra, is becoming increasingly widespread throughout automotive engineering, with inspiration coming in the form of aircraft and the variable slats, slots and ailerons used to control the yaw, pitch and roll moments. Figure 35 shows a number of control surface concepts that could be used to reduce the effect of a side wind gust on a vehicle.

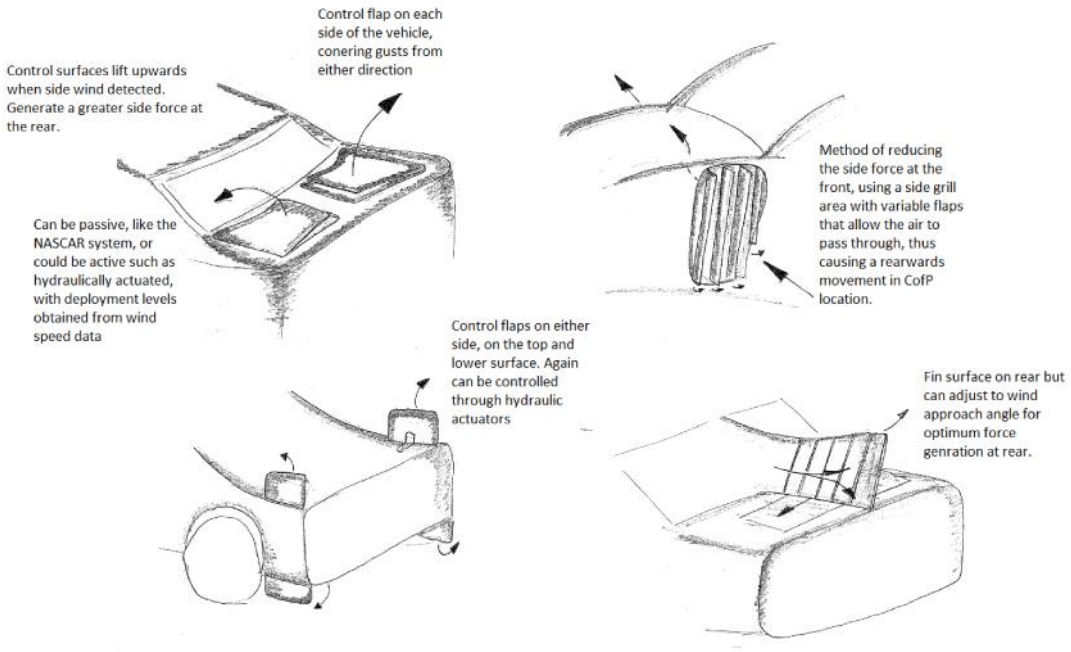

Figure 35 - Controllable Surfaces Initial Concepts

5.1.4 Concept Selection

The concepts that have been created would produce an increase in the side force that acts on the vehicle during a side wind, however, to what extent is not currently known. For the analysis concerned within this report it was decided that the concept of using a deployable stability fin would be developed to understand the effect on vehicle behaviour. This was chosen because, as is outlined in the literature review, it would be possible to confirm the effects of a fully deployed fin and compare these results against the ones from a deployable fin. The following section describes how the initial idea of using a variable stability fin has been developed and manufactured through to a stage where physical and virtual testing can be conducted on it.

5.2 Developed Ideas

5.2.1 Vehicle Selection

Before developing a range of aerodynamic fins, the carrier model had to be identified as this would form the basis around which the fins would be developed. Consideration was made towards manufacturing a complete model incorporating fins at numerous stages of deployment, however, it was determined that while this would be beneficial for controlling the fin deployment, it could pose issues with ensuring that the air flow remained attached along the length of the vehicle, so as to offer representative results over the section of interest, namely the rear section of the vehicle. It was therefore decided that an existing model which offered the air flow to be attached up to the leading edge of the rear section of the vehicle would be a suitable choice.

The model that was selected for this investigation was the 'Lynne Turner' model, which is formed of a body section with detachable diffuser and rear notchback sections, as can be seen in Figure 36.

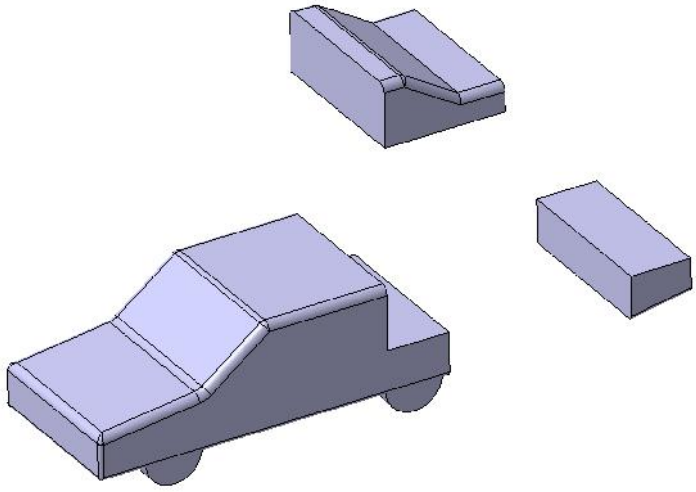

Figure 36 - Lynne Turner Model with Detachable Sections

Due to the nature of the model, there was a possibility of testing a range of different rear sections and diffuser profiles to modify the airflow around the vehicle. It was decided that due to the fact that the investigation centred around the possibility of a stability fin positioned at the rear of the vehicle, the diffuser section would remain constant with a 0° incline, however, a range of different rear sections with various notch angles would be analysed as this would offer a greater insight into how such a device would affect the behaviour of a range of vehicles. The rear section notch angles that were selected for analysis were the 25°, 32° and 43° rear sections, which were selected as they were readily available, while also providing a stable platform on which to develop the fin concepts.

5.2.2 Fin & Base Design

5.2.2.1 Fin Base Manufacture

Once the vehicle had been selected, the stability fin concepts were able to be developed to ensure they could be attached to each of the rear sections of the Lynne Turner model while also performing the intended function. Figure 37 below demonstrates the development of the stability fins, including the fixing method. Larger images can be seen in Appendix A.

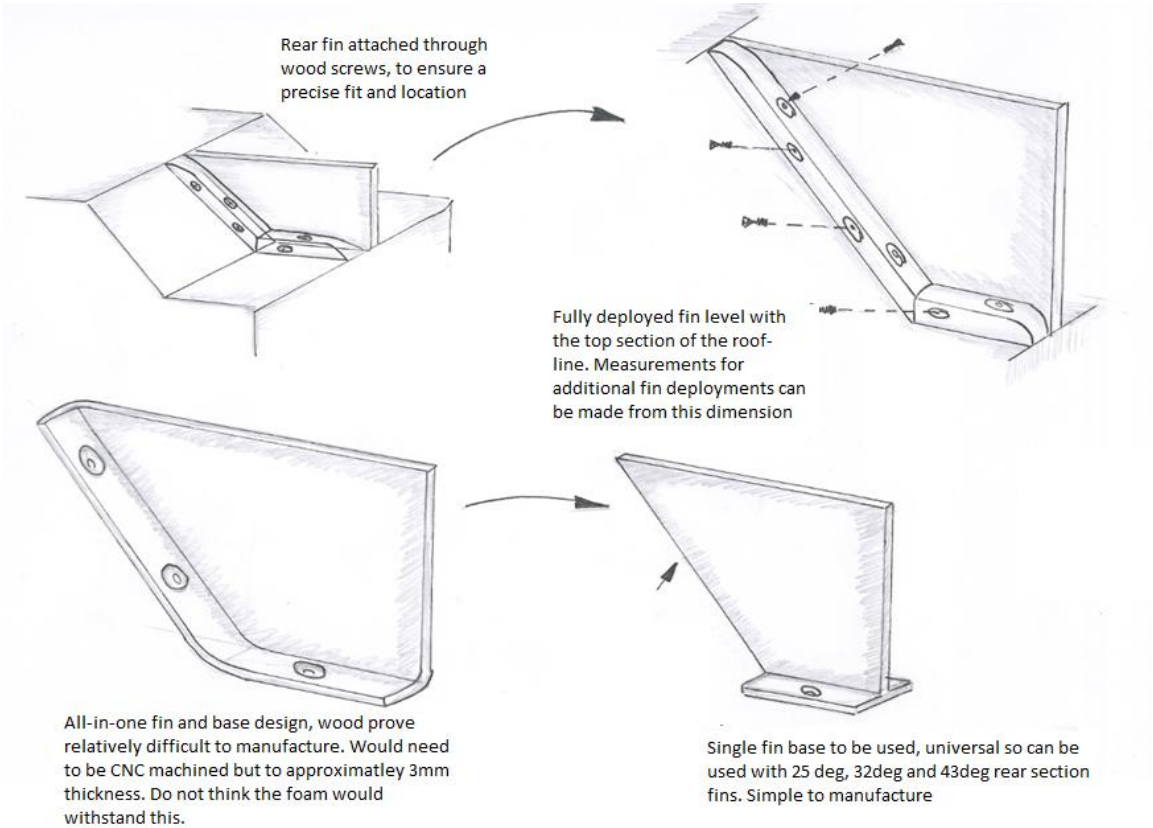

Figure 37 - Developed Stability Device & Fixing Bases

As is shown in Figure 37, the fin design that has been chosen is relatively simple, however, still relevant for this investigatory study, with the overall height of the fin controlled by the dimensions of each rear section of the Lynne Turner model. To enable the fins to be positioned in the centre of the rear sections of the Lynne Turner model, a base was designed that allowed for universal use with each rear section and permitted quick and simple fitting of the range of fins that were to be tested. Furthermore, the base would have to offer a stable platform which could be securely attached and limit the movement of the fin when deployed. The fixing method proved to be somewhat problematic as care needed to be taken to ensure that the base plate would not heavily interfere with the air flow over the vehicle as this would lead to correlation issues between the virtual simulations and the wind tunnel results. It can be seen that through the development of the fin and base design, a minimal interaction between the base and air flow has been achieved. The design of which can be seen below in Figure 38.

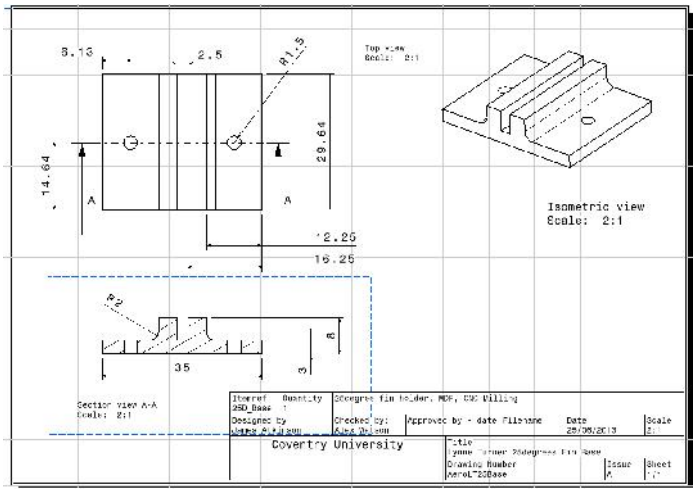

Figure 38 - Lynne Turner Fin Attachment Base Design

To maintain accuracy, the base section was manufactured using a Tooltec CNC Milling Machine. The material that was chosen for this was a high density polymer that would offer adequate support while also being simple to manufacture. An image of the final machined component can be seen in Figure 39. It is to be noted that the method that will be used to fix the base to the Lynne Turner rear sections will be through the use of two wood screws.

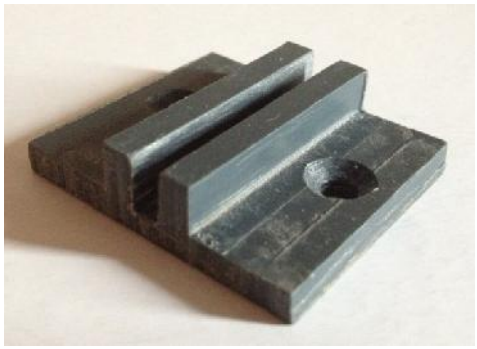

Figure 39 - Manufactured Stability Base Design

5.2.2.2 Fin Manufacturing

It was decided that the fins would be manufactured in acrylic using a CNC milling machine, as this would provide a suitable level of accuracy and allow the fins to be manufactured in a short time scale. Figure 40 shows the CNC machining of one set of the aerodynamic fins.

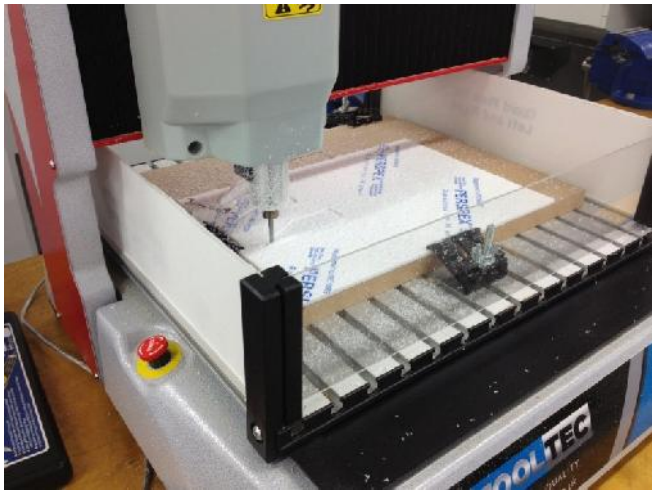

Figure 40 - CNC Machining of Aerodynamic Fin Profiles

Each of the fins were manufactured from 3mm Acrylic sheet as it was decided that the use of such thickness would not cause a great effect on the air flow over the rear section of the model, but would also be able to withstand the forces produced by the air over the fin and not deform, leading to anomalies within the results.

5.2.3 Assembly Design

Through the development of the stability fins and base, the design was able to be represented using a CAD software package, thus allowing the components to be able to be manufactured using a combination of CNC machining and laser cutting. This can be seen in Figure 41.

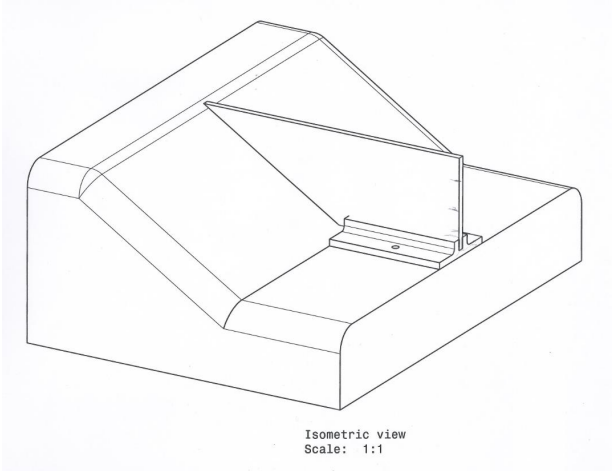

Figure 41 - Stability Fin & Rear Section Assembly

Once manufactured, the final outcome of the fins and base can be seen below in Figure 42. The base is universal and is thus used for each of the Lynne Turner rear sections; 25°, 32° and 43°, and each of the fin deployment stages; 25%, 50%, 75% and 100%.

Figure 42 - Manufactured Fin & Base

6 Simulation & Data Analysis

To understand the effects of the inclusion of a variable aerodynamic device such as a deployable stability fin, and how the use of such a device can alter the behaviour of a vehicle, a range of tests were completed. The investigation that has been conducted concerns the use of CFD simulations and a wind tunnel testing programme. Each of the tests are described in the following sections, including why each technique was utilised, how the simulations were defined and the discussed results concerning the aerodynamic forces and moments that are acting on the vehicle. The investigations were conducted simultaneously with the results from each scenario being compared against one another and against published literature to determine correlation and enable a complete analysis of how a vehicle's dynamic behaviour is affected through the inclusion of a variable stability fin.

6.1 CFD Analysis

6.1.1 Uses of CFD

The use of Computational Fluid Dynamics has become widespread within the automotive and aerospace industries in recent years, providing the ability for engineers to simulate and analyse the fluid flow around a body in a virtual capacity. This proves beneficial as a range of useful data can be obtained concerning every aspect and component of a vehicle and the forces and moments that act up on it. CFD software uses a combination of the fluid mechanics governing equations and the approximations to these equations in order to process a solution (Tu 2008:5-6). "The equations are the Navier-Stokes equations which provide the relationship between the pressure, momentum and viscous forces within the 3D space" (Barnard 2009:256-257). There are a number of advantages of the use of CFD, with one particular benefit being the cost effective nature of performing a simulation in comparison to generating a physical model and wind tunnel running costs (Tu 2008:5). A further advantage is the ability of CFD to allow for visualisation of the fluid flow around a body, while enabling numerous data fields to be analysed with ease (Tu 2008:5). It can be said that the use of CFD through the increase in computing ability is becoming ever more imperative for engineers with discrepancies of as low as 2 percent being achieved (Barnard 2009:265). The software package that has been used for the CFD investigation and analysis of the stability fin configuration of the Lynne Turner model for this project was CD-Adapco's STAR CCM+.

6.1.2 Meshing Models

The process of running a CFD simulation initially involved importing the base geometry and creating a test area, otherwise known as a virtual wind tunnel. Once this had been achieved, a mesh was defined and generated. The mesh on the body is of great importance as it is said that “the accuracy of a CFD solution is governed by the number of cells in the mesh within the component domain” (Tu 2008:36). This indicates that the greater number of cells and therefore a finer mesh, the greater accuracy in the output solution, leading to closer correlation between a CFD simulation and a wind tunnel test. In order to generate the mesh, the meshing models are required to be defined within the software. The meshing models that have been selected for this investigation are; Surface Remesher, Polyhedral Mesher and Prism Layer Mesher. The surface remesher model is a requirement of the software due to the fact that the simulation is being conducted on imported CAD geometry (CD-Adapco 2012:319). Furthermore, the use of the surface remesher model allows for the surface mesh to be optimised before a volume mesh is generated, which is how the main solution is developed (CD-Adapco 2012:1871-1872). The use of a Polyhedral meshing model is beneficial for the simulations that have been undertaken for this report as it permits the use of various mesh sizes on each region of the Lynne Turner model, such as the rear section which is of great interest (CD-Adapco 2012:319). The analysis of the boundary layer is of key importance due to the fact that the air flow velocity reduces to zero as it approaches the body surface, therefore it is required that additional cells are present within the mesh to provide suitable data. To achieve this, the Prism Layer mesh model is used as it provides user-defined cell rows in close proximity to the vehicle surface (CD-Adapco 2012:319).

6.1.3 Physics Models

6.1.3.1 CFD Physics Model

A further stage required to setup a CFD simulation is to select the Physics models and therefore define the physical properties of the fluid, such as velocity, turbulence intensity and fluid state. Defining and inputting the physics conditions allows the selected fluid equations to be solved. The physics models that have been selected for the investigation outlined in this report can be seen in Table 3.

Physics Models			
Selection Field	Model Selected		Resulting Models
Space	Three Dimensional		Three Dimensional
Time	Steady		Steady
Material	Gas		Gas
Flow	Segregated		Segretated Flow
Equation of State	Constant Density		Constant Density
Viscous Regime	Turbulent		Turbulent
Reynolds-Averaged Turbulence	K-Epsilon Turbulence		K-Epsilon Turbulence
Optional Models	Cell Quality Remediation		Cell Quality Remediation
			Realisable K-Epsilon Two-Layer
			Reynolds-Averaged Navier Stokes
			Two-Layer All Y+ Wall Treatment

Table 3 - Selected Physics Models

The turbulence model that has been used for the investigations is the K-Epsilon Turbulence model which has been chosen as it offers the default turbulence model and that it would closely match the wind tunnel model. K-Epsilon is the most widely used approach within industry and can be used with either a Low Reynolds Number solver or a Two-Layer solver (CD-Adapco 2012:3073). This allows the Y+ Wall treatment to be optimised and the boundary layer analysed with greater accuracy. The two-layer Y+ wall treatment uses the 'All Y+' approach which is a hybrid treatment that is designed to allow the use of both coarse and finer meshes (Cirstea 2013).

The additional physics models that have been selected for the analysis define the fluid and its flow characteristics, such as turbulence and compressibility. By maintaining simplicity through the use of these models the ability of the stability fins will be able to be established.

6.1.3.2 Physics Modelling of Temperature & Humidity

As discussed, the pressure of the air that passes over a bluff body, such as a vehicle, is of key importance, and can have a great effect on the forces and moments that act on a vehicle. This air pressure can be affected by a number of factors, such as the temperature and the humidity of the air.

The effect of the absolute temperature can be explained through the use of fundamental fluid mechanics. As explained by Barnard (2009:2), the density of air is "inversely proportional to the absolute temperature of the air". This statement is key when it is considered that the aerodynamic forces and moments that act on a vehicle are indeed directly proportional to the density, as can be seen on the below equation.

$$Aerodynamic\ Force = \frac{1}{2}\rho C_{Aero} A V^2$$

Equation 11 - Aerodynamic Force proportional to Fluid Density

Furthermore, humidity can have a substantial impact on the density of a fluid such as air. Humidity is defined as the "measurement of water vapour in a defined amount of air" (MetOffice 2014). When the humidity is low the air density decreases, and when high, the density of the air increases. This has a minor impact on the aerodynamic forces and moments due to the need to for density to be used to calculate these forces and moments. Considerations for the temperature, pressure, humidity and density have to be taken into account when setting up the CFD fluid physics models.

6.1.4 Y+ Wall Independency

As discussed above, the Y+ wall treatment is a key parameter when analysing the near-wall area of the vehicle. The treatment is particularly critical when considering the boundary layer of the flow. The Y+ treatment is divided into three specific regions; Viscous Sublayer, Buffer Layer and the Log-Law Layer (CFD-Online 2011).

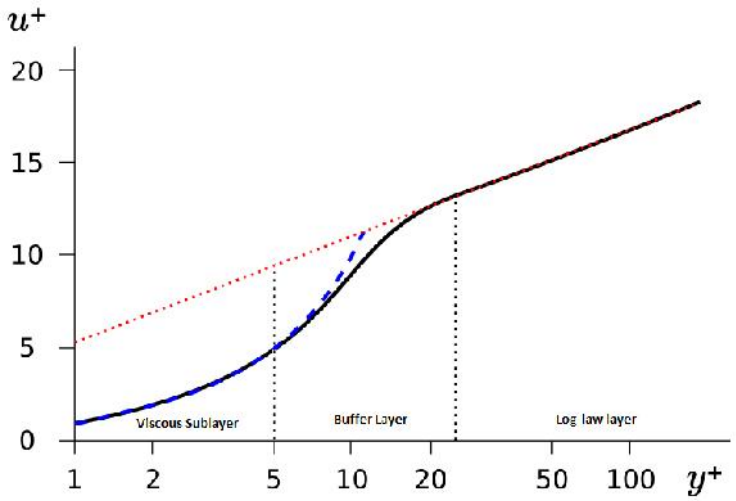

Figure 43 - Boundary Layer Regions

(Watson 2013)

Adapted from (CFD-Online 2011)

From Figure 43, it can be seen that ideally the wall y+ values would be positioned within the Viscous Sublayer or the Log-Law Layer, with preference towards the later for this scenario. This is due to these two areas being of a linear fashion, with the buffer layer being non-linear. To achieve a wall y+ value within the Log-Law region the mesh properties outlined in Table 4 and Table 5 were used.

Mesh Properties		
Continua Values		
Field	Value	Additional Information
Base Size	100mm	n/a
Number of Prism Layers	5	n/a
Prism Layer Stretching	1.3	na/
Prism Layer Thickness	5% of base (5mm)	Relative to base
Surface Size	25% of base (25mm)	Relative Minimum Size
	100% of base (100mm)	Relative Target Size
Body Region		
Field	Value	Additional Information
Number of Prism Layers	5	n/a
Prism Layer Stretching	1.3	n/a
Prism Layer Thickness	10% of base (10mm)	Relative to base
Surface Size	0.15% of base (0.15mm)	Relative Minimum Size
	1% of base (1mm)	Relative Target Size
Diffuser Region		
Field	Value	Additional Information
Number of Prism Layers	5	n/a
Prism Layer Stretching	1.15	n/a
Prism Layer Thickness	10% of base (10mm)	Relative to base
Surface Size	0.15% of base (0.15mm)	Relative to base
	1% of base (1mm)	Relative Target Size
Notch Region		
Field	Value	Additional Information
Number of Prism Layers	4	n/a
Prism Layer Stretching	1.25	n/a
Prism Layer Thickness	10% of base (10mm)	Relative to base
Surface Size	0.15% of base (0.15mm)	Relative Minimum Size
	1% of base (1mm)	Relative Target Size

Table 4 - Defined Mesh Properties

Virtual Wind Tunnel & Control Definitions			
Wind Tunnel			
	x-coordinates	y-coordinates	z-coordinates
Corner 1	-1.5	-0.75	-0.032
Corner 2	3.5	0.75	1
Volumetric Controls			
VC1 - Near Wake	x-coordinates	y-coordinates	z-coordinates
Corner 1	-0.3	-0.25	-0.035
Corner 2	1.2	0.25	0.3
VC2 - Far Wake	x-coordinates	y-coordinates	z-coordinates
Corner 1	-0.8	-0.3	-0.035
Corner 2	1.8	0.3	0.4

Table 5 - Wind Tunnel & Control Definitions

Through the use of these properties, the wall y+ distribution of the Lynne Turner model, shown below, was able to be achieved.

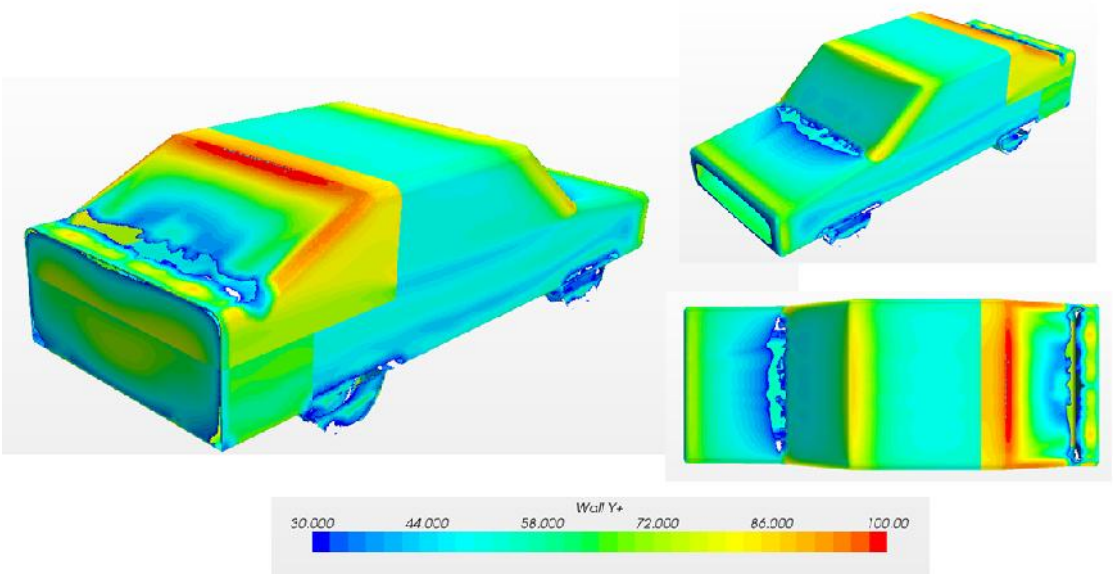

Figure 44 - Finalised Y+ Distribution

Figure 44 shows the wall y+ distribution over the Lynne Turner model when cropped to be located within the Log-Law region, 30 to 100, as see on the scalar bar. It can be seen that there are a number of areas where the y+ distribution is not as desired, particularly at the front bumper and the angle between the bonnet and the windscreen. As the area of greatest importance for the research that is being carried out, is the rear notch area, these sections of low y+ can be tolerated. With regard to the rear notch section, it can be seen that there is a small section of low y+ across the rear window and boot angle, however, if an

attempt was to be made to increase this area, the value of the roof trailing edge would become too great and thus the computation of this section would be negatively affected due to the fact that the y+ would be situated beyond that of the Log-Law region.

In order to determine the mesh criteria a y+ independency study was conducted, with the results of this study being available within Appendix B.

6.1.5 Simulation Testing Plan

6.1.5.1 Wind Velocity

Once the physics conditions have been established, the velocity of the air at the inlet can be inserted into the physics values. In order to determine the velocity that the vehicle will be subject to, research was undertaken to identify measured wind velocities. From this research a number of wind velocities and their resulting actions on the environment were able to be established. It was found that vehicle's begin to become effected by winds of a velocity of approximately 20m/s, with higher velocities having a greater effect on the vehicle (Windfinder n.d). Detailed wind velocities can be obtained through investigating wind speeds that are found on open transport links including bridges such as the Forth Bridge in Scotland, from which it can be said that cars are permitted to travel when the wind gusts in excess of 65mph (29m/s), however, as wind gusts approach 80mph (35m/s) travelling is restricted (Forth Road Bridge 2013).

It was therefore decided that the simulations will be completed with a physical wind inlet velocity of 30m/s as this will provide a near worst case scenario and therefore provide the conditions at which the stability fins would be deployed at.

6.1.5.2 Deployment Levels & Yaw Angle

In order to determine the effect of inserting a deployable aerodynamic device on a vehicle, it is necessary for the device to be tested at a range of deployment stages to offer a greater understanding of the scenario. For the tests that have been conducted, the fins on the model were static, as this would reduce the variables within the test process. As the CFD simulations would mainly support the findings from the wind tunnel data, it was deemed that the tests could be conducted for a reduced number of fin deployment stages and yaw angles, therefore the following fin deployments and yaw angles were chosen for the simulation analysis. A full yaw angle sweep would be conducted on the fin when at 0% deployment, 50% deployment and 100% deployment. The yaw sweep that would be conducted for the CFD simulations were 0°, 10°, 30°, 60° and 90° as this would offer a suitable range of results to compared against the data obtained from the wind tunnel.

6.2.1 Simulation Results

By running the CFD simulations described above, the following results were able to be obtained for the Lynne Turner model in a range of configurations. It was identified that when the vehicle was fitted with the 25°, 32° and 43° rear sections the results followed a similar trend and thus the results discussed below concern the tests conducted on the 43° rear section with various stability fin deployment stages.

6.2.1.1 Side Force & Coefficient Comparison

When the stability of a vehicle is of concern when subject to a side wind gust, the force and moments that have the greatest influence on the vehicle behaviour are the side force and the yawing moment (Barnard 2009: 218). Figure 45 below shows the side force that is acting on the vehicle with respect to the yaw angle. It can be seen that as the yaw angle increases from 0° to 30° the side force increases linearly, and for each instance, peaks at a 30° yaw angle. This can be explained through literature with identifies an approximate yaw angle of 40° being attributed to generating the greatest side force. Figure 45 demonstrates that the inclusion of a stability fin assists in creating a greater side force, with a 30% increase in side force with a fully deployed fin and a 24.5% increase for a 75% fin at the 30° yaw.

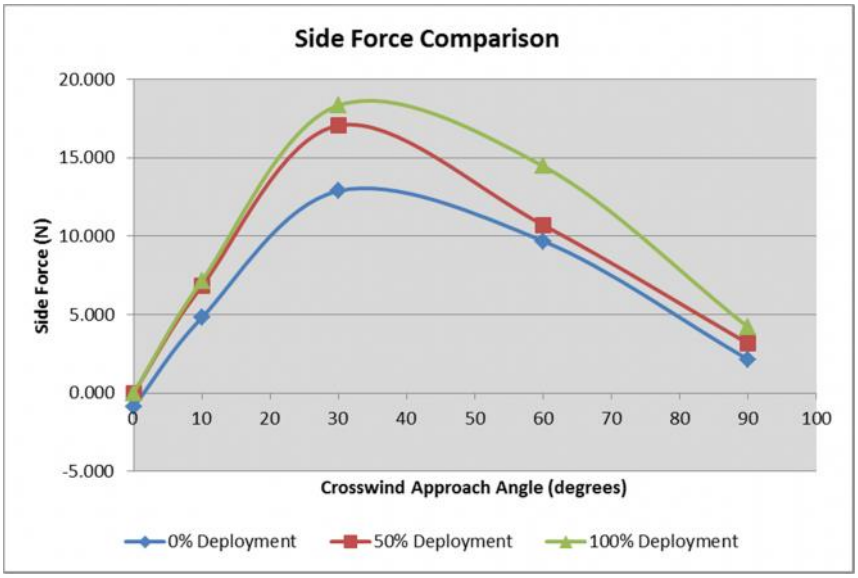

Figure 45 - Side Force Comparison (CFD)

As the yaw angle increases, there is a sharp decrease in the side force that is acting on the vehicle. This can also be seen in Figure 46 which demonstrates that as the yaw angle reaches 30° the coefficient, and therefore, the force stabilises until an angle of 50° is achieved, where the coefficient decrease.

This image has been removed

Figure 46 - Force Coefficient Expectant Results

(Katz 2006: 206)

When a stability fin is introduced to the vehicle, it can be seen that there is an increase in the side force acting on the vehicle. As the side wind approach angle increases between 0° and 20° it can be seen that the side force increases in a linear and similar fashion for the vehicle that is fitted with a stability fin of 50% and 100% deployment, however, as the side wind angle increases to 30° there is a difference of approximately 2N between the two levels of fin deployment. It can also be stated that as the approach angle increases further, much like the vehicle with no fin, the side force decreases, however, it is to be noted that the vehicle with a fully deployed fin generates a greater side force for the duration of the test, whereas the 50% deployed fin correlates well to the base vehicle between 60° and 90° side wind angle.

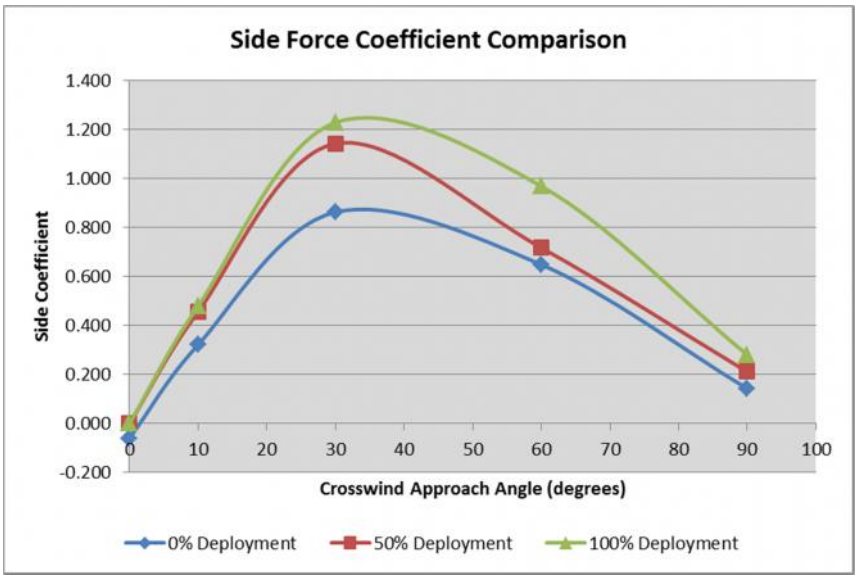

Figure 47 - Side Coefficient Comparison (CFD)

A similar trend for each of the vehicle configurations can be seen when viewing the side force coefficients, which can be seen in Figure 47. Furthermore, the linear increase and side coefficient peak is confirmed through literature which indicates that the linear response occurs up to 35°, a 5° increase on the acquired CFD data, and peaks at approximately 45°, which can be said to be an approximately 10° increase on the CFD data. This shows that while the results do not replicate the literature exactly, a high degree of correlation is visible, thus verifying the results.

This image has been removed

Figure 48 - Side Force Coefficient against Side Wind Approach Angle

(Katz 2006: 174)

6.2.1.2 Yaw Moment & Yaw Moment Coefficient Comparison

Figure 49 shows the yawing moment that is experience by the vehicle when under the outlined side wind conditions. It can be seen that when the vehicle is in its standard configuration, the yawing moment is negative. This is not apparent on the Lynne Tuner model when the rear section has a 32° angle, as is seen in Figure 50 hence it is assumed that this negative yaw moment is an anomaly, possibly due to the yawing axis that the vehicle is positioned on within the CFD software. With regard to the vehicle with the fins installed, it can be seen that the yawing moment decreases as the fin deployment increases. This is ideal as reducing the yawing moment reduces the tendency of the vehicle to yaw, and as described by Barnard "the ideal yawing response would be no response; that is, the vehicle would simply continue on its path (2009: 218)."

As the vehicle enters the yaw angle range of 70° to 90° it is seen that the yawing moment becomes negative. This is assumed to signal that the vehicle's yaw tendency direction is changing at high yaw angles.

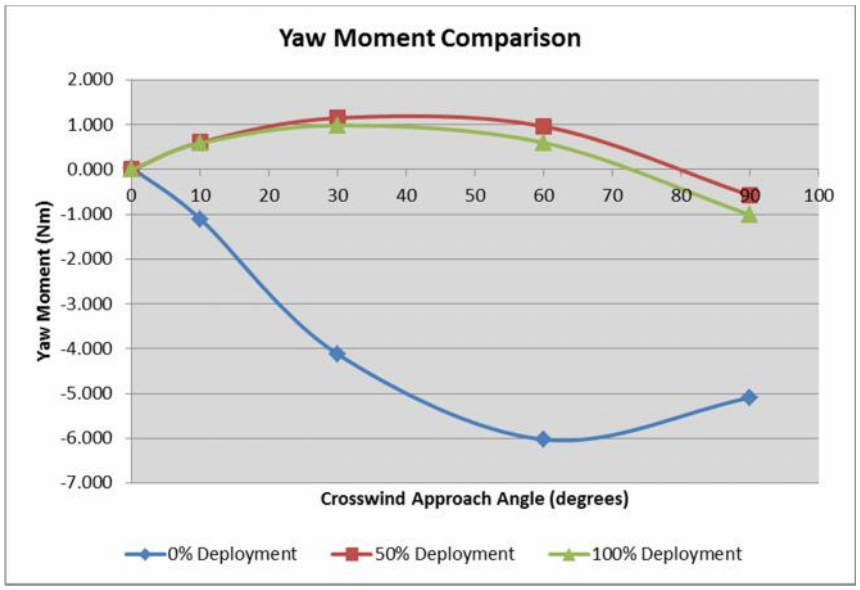

Figure 49 - Yaw Moment Comparison

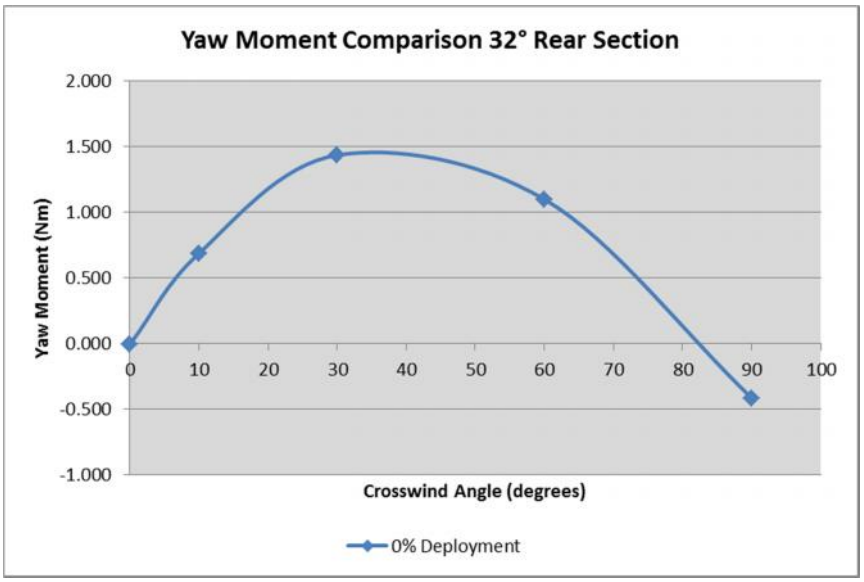

Figure 50 - Yaw Moment of 32 degree Rear Section

Due to the fact that the Yawing Moment Coefficient is a function of the yawing moment, the plots follow a similar profile and show how the introduction of a stability fin does reduce the yawing moment acting on the vehicle. It can also be said that increasing the deployment of the stability fin also reduces the yawing moment, which as previously described, is ideal. The yawing moment coefficient can be seen below in Figure 51.

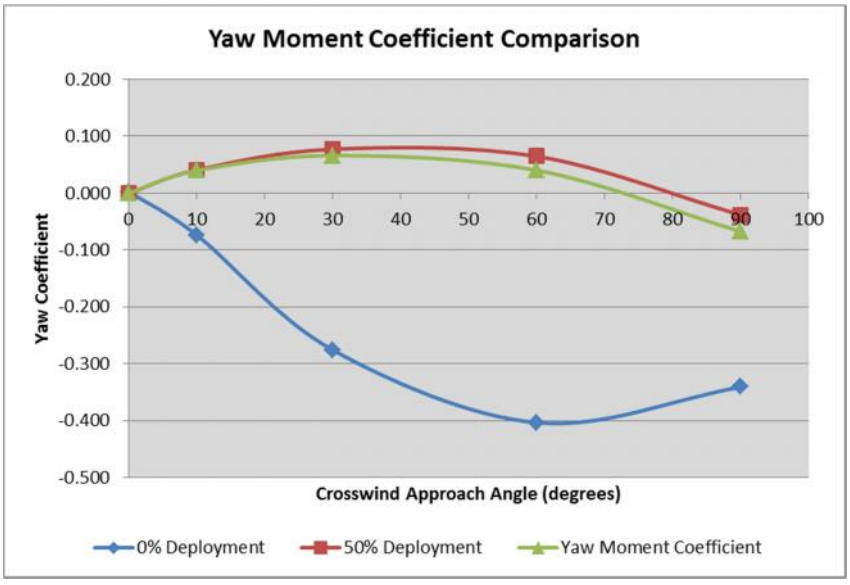

Figure 51 - Yaw Coefficient Comparison (CFD)

6.2.1.3 Additional Forces, Moments & Coefficients Results

While the most critical forces and moments when concerning the effects of side winds on vehicles are side forces, yaw moments and the corresponding coefficients, the findings were not limited to these, with the complete range of forces and moments being measured. Through the implementation of the stability fins, the advantages and disadvantages of using such a device are able to be established and are highlighted below.

6.2.1.3.1 Drag Force & Coefficient Results

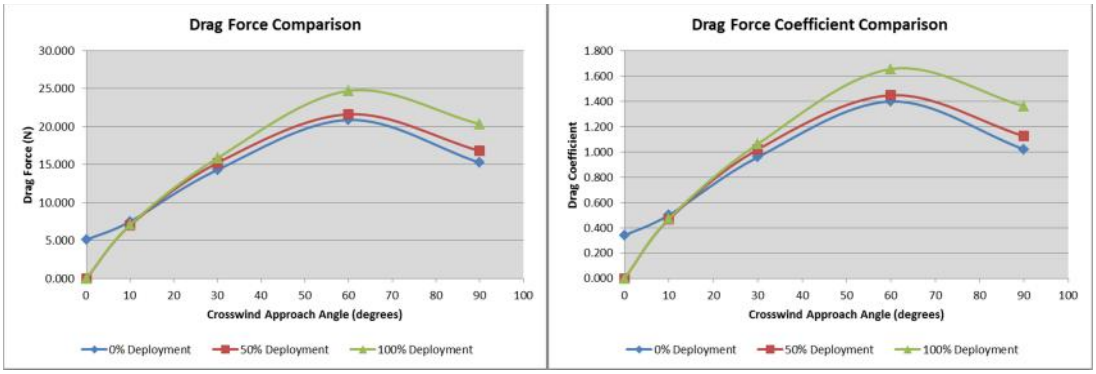

Figure 52 - Drag Force & Coefficient Comparison

Figure 52 (a) shows the change in drag force that acts on the vehicle as the side wind approach angle increases. This highlights that as the wind approach angle increase from 0° to 60° the drag force increases at a linear rate for all fin deployment stages. From Figure 52 it can be said that there is a minor difference in the forces and coefficients of the vehicle in its standard configuration than when the fin is 50% deployed, however, when the fin is 100% deployed the drag force and coefficient has increased, particularly between the yaw angles of 30° to 90°, which is as to be expected as the fin effectively increases the projected area that the side wind acts on.

6.2.1.3.2 Lift Force & Coefficient Results

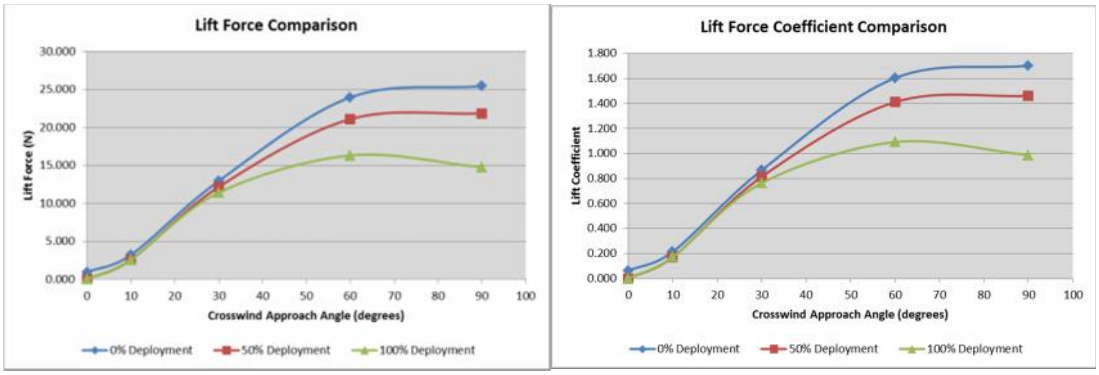

Figure 53 - Lift Force & Coefficient Comparison

The graphs shown above in Figure 53 show the effect of using a stability device on the rear section of the Lynne Turner aerodynamic model. This demonstrated that as the stability fin was being deployed there was a decrease in the lift force of approximately 40% when the side wind approached at an angle of 90°. This decrease in force would also assist in keeping the lift coefficient below 1.1 for approach angles above 30°. This reduction in lift could be due to the disturbance caused by the fin not allowing the flow to travel over the full rear section of the vehicle.

6.2.1.3.3 Roll Moment & Coefficient Results

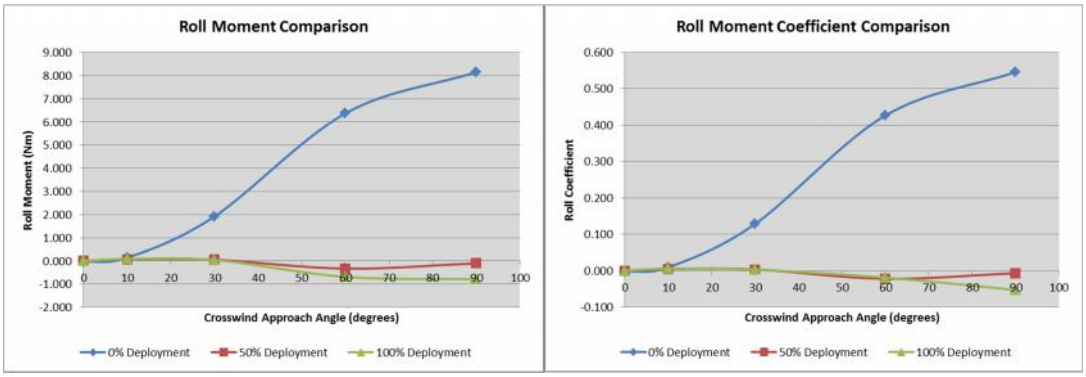

Figure 54 - Roll Moment & Coefficient Comparison

The roll moment of the vehicle about the vehicles longitudinal axis is shown above in Figure 54. It can be seen that there is a large effect on the roll moment when the stability fin is at both 50% and 100% deployment. For a vehicle in a standard setup with no fin attached, the roll moment increases greatly from 10° onwards, peaking at 8Nm, whereas when the fins are deployed the roll moment remains between approximately 0Nm and -0.8Nm. This is further demonstrated in the graph displaying the roll moment coefficient that the inclusion of a stability fin reduces the rolling moment drastically along the entire side wind angle approach range.

6.2.1.3.4 Pitch Moment & Coefficient Results

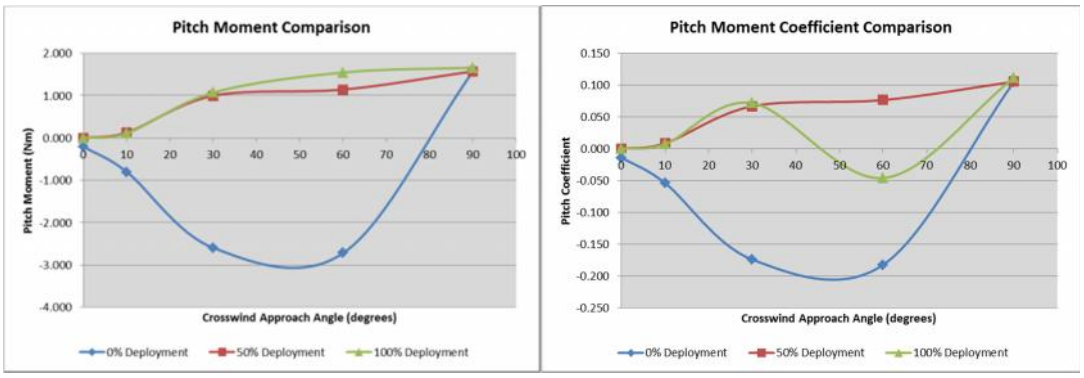

Figure 55 - Pitch Moment & Coefficient Comparison

It can be seen from Figure 55 that there is a significant change in the vehicle's pitching moment when the stability fin is deployed than when compared to the baseline vehicle. The graphs show that as the yaw angle increases, the pitch moment becomes negative and peaks at a value of approximately -3Nm at an angle of 50°, however, the moment does increase sharply between 60° and 90° yaw whereby the pitch moment increases from -2.7Nm to 1.5Nm, this could be caused by possible misalignment of the pitch axis on the vehicle during simulation setup. When the stability fin is deployed, the pitching moment can be said to be positive for duration of the test, with small differences between the fully deployed and 50% deployed fin, particularly in the range of 30° to 85°. The second graph shows the pitch moment coefficient, and while the standard vehicle and the 50% deployed fin act as expected, when the fin is fully deployed and the side wind is approaching at 60° to the vehicle, there is a distinct decrease in the pitch coefficient from 0.075 to -0.050, which then recovers up to a value of 0.10 at 90° approach angle. Due to the nature of the curve, it is assumed that this fluctuation is caused through an error within the axis system of the vehicle.

6.2.2 CFD Simulation Summary

Following the completion of the CFD simulations, it can be seen that the use of stability device, in this case, in the form of a stability fin, can significantly affect the forces and moments that act upon a vehicle during a crosswind. The results shown that the stability fin does increase the side force, and thus causes the centre of pressure location to move rearwards, as required to improve stability, while also reducing the yawing moment of the vehicle to assist in maintaining the vehicle within the drivers recoverable bounds, leading to reduced corrective inputs from the driver.

From undertaking the CFD simulations outlined above, a number of interesting results were able to be obtained. Firstly, it can be seen that the forces and moments are affected when comparing the base model to the fully deployed fin results. This is the case when studying the two key forces and moments; side force and yaw moment, where it can be said that the side force increases by approximately 30% at high yaw angles, with the yaw moment decreasing significantly across the range of yaw angles as fin deployment increased. This, as the literature suggests, is the ideal response, as to allow the vehicle to be stable with the side force at the rear increasing, causing the CofP to move rearwards and hence reduce the yawing moment. It can also be seen that the other forces and moments are affected by the deployment of the fin as yaw angle increases, most notably, whereby the positive lift force actually reduces at the rear.

While these results do offer an insight into the ability for a variable stability fin to modify a vehicles behaviour, it must be highlighted that these results are applicable to the Lynne Turner model, and therefore can only be used as a reference for further research.

6.3 Wind Tunnel Testing

In order to validate the CFD results and to provide an extensive data set, a wind tunnel test was conducted on the Lynne Turner model with a range of removable rear sections tested with the complete set of stability fins and deployments analysed to further understand whether a device of a variable nature could be used on road vehicles to maintain a linear response when being subject to a side force defined as a side wind gust.

6.3.1 The Wind Tunnel

The wind tunnel that was used for the testing of the deployable stability fins was the Coventry University Mercedes AMG PETRONAS 20% Scale Wind Tunnel. The wind tunnel is of a closed return, open-jet test section configuration, a schematic of which can be seen below.

Figure 56 - Coventry University Mercedes AMG PETRONAS Scale Model Wind Tunnel

(Mercedes AMG PETRONAS F1 Team)

The use of a wind tunnel is advantageous when conducting aerodynamic tests on a vehicle, due to the fact that it is not an approximation like CFD. Also the wind tunnel does not require a fine mesh to be generated, as all force and moment measurements are calculated from data obtained through the aerodynamic balance. One limitation of the wind tunnel, particularly when considering the subject of this report is that, “the wind tunnel offers a steady state simulation of a highly transient condition, such as a side gust, and can therefore only be used as an indicator” (Cirstea 2013).

6.3.2 Model Setup

Figure 57 and Figure 58 shown below indicate how the model was tested in the wind tunnel. It was decided that due to the nature of the project, with the main emphasis on the rear section and how a deployable fin could affect the aerodynamic forces and moments and thus, the vehicles dynamic behaviour, that the model be tested upside down. The model was inverted so as to allow the rear section and fin attachment zone to have as laminar air flow as possible by moving the strut and securing attachment to the underside of the vehicle. Also it was decided that a ground board to simulate the road would not be required as the main area of investigate was the fin rear section.

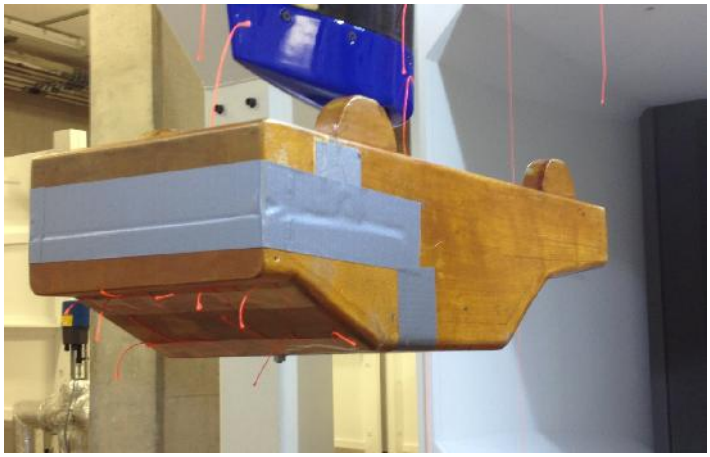

Figure 57 - Lynne Turner Baseline Configuration

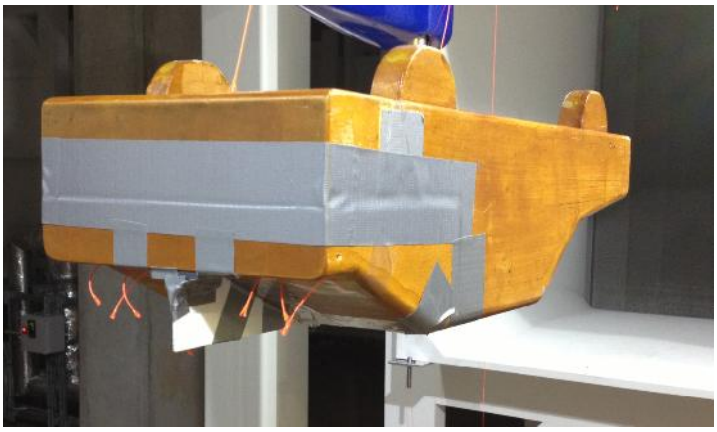

Figure 58 - Lynne Turner Fully Deployed Fin with Base Plate Configuration

6.3.3 Wind Tunnel Test Plan

To ensure that a complete set of results was collected during the wind tunnel test day, a testing plan was created. This was created based on the CFD physics models and from the data that was required in order to research how a variable device could affect the vehicle's behaviour during a side wind gust. As a result of this, the testing plan outlined below was used for the duration of the wind tunnel test day.

Wind Tunnel Testing Plan	
Test Number: 1	
Model: Lynne Turner Model	
Rear Section: 43 degrees	
The following tests are to be completed in the wind tunnel for the 43 degrees rear section:	
Baseline	0° yaw with no fin attached
	Yaw variation at 15m/s & 30m/s for the following yaw angles: 0°, 5°, 10°, 20°, 30°, 40°, 50°, 60°, 70°, 80°, 90°
The test will then be repeated for the rear section when the fin is at 25%, 50%, 75% and 100% deployment	
Wind Tunnel Testing Plan	
Test Number: 2	
Model: Lynne Turner Model	
Rear Section: 32 degrees	
The following tests are to be completed in the wind tunnel for the 32 degrees rear section:	
Baseline	0° yaw with no fin attached
	Yaw variation at 15m/s & 30m/s for the following yaw angles: 0°, 5°, 10°, 20°, 30°, 40°, 50°, 60°, 70°, 80°, 90°
The test will then be repeated for the rear section when the fin is at 25%, 50%, 75% and 100% deployment	
Wind Tunnel Testing Plan	
Test Number: 3	
Model: Lynne Turner Model	
Rear Section: 25 degrees	
The following tests are to be completed in the wind tunnel for the 25 degrees rear section:	
Baseline	0° yaw with no fin attached
	Yaw variation at 15m/s & 30m/s for the following yaw angles: 0°, 5°, 10°, 20°, 30°, 40°, 50°, 60°, 70°, 80°, 90°
The test will then be repeated for the rear section when the fin is at 25%, 50%, 75% and 100% deployment	

Table 6 - Wind Tunnel Test Plan

6.3.4 Wind Tunnel Results

The data that was obtained from the wind tunnel was then analysed to determine the effect of the use of the variable stability fin on ground vehicle behaviour. As previously discussed, the side force and yawing moment are the critical components when stability under crosswind conditions is being analysed. The following pages define and discuss these results, as well as the remaining forces and moments. The analysis that has been conducted on the Lynne Turner model wind tunnel data concerns the aerodynamic forces and moments that act on the model when under test conditions. The forces and moments were chosen to be analysed as the analysis of the force and moment coefficients would prove inaccurate due to the fact that the frontal area of the vehicle changed significantly as the yaw angle increased, and thus introduce an additional variable. This would in turn affect the results concerning the effect of the use of a stability fin, which is the main focus of this project.

6.3.4.1 Side Force Comparison

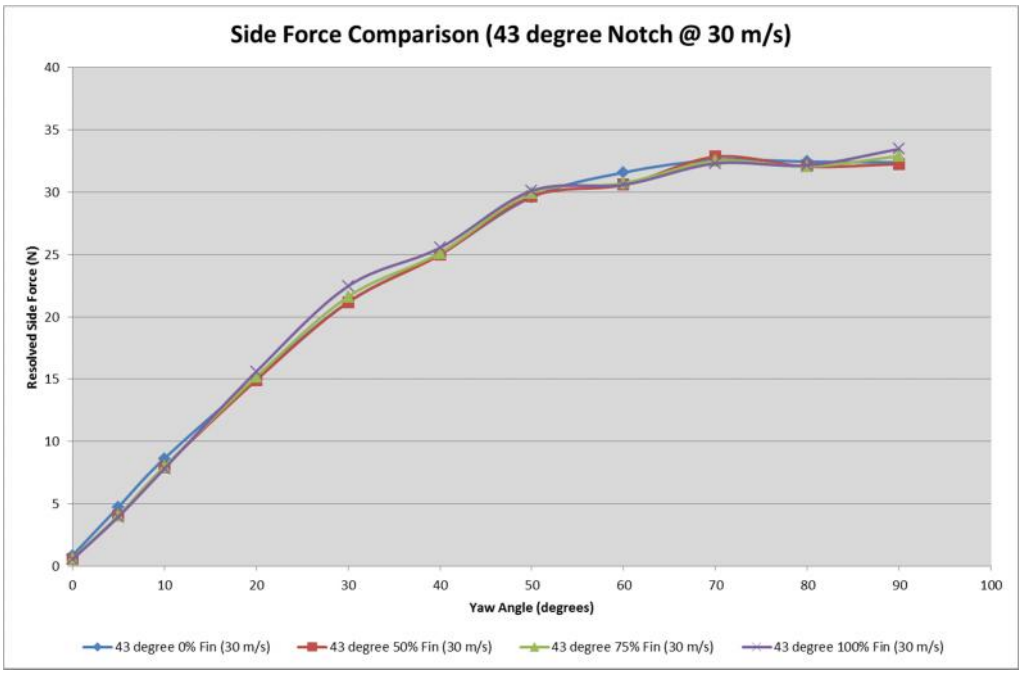

Figure 59 - Side Force Comparison

Figure 59 shows the comparison of the side force against yaw angle for when the vehicle has a stability fin at a range of different deployment stages. It is seen that the side force that acts on the vehicle increases linearly with yaw angle up to approximately 35°. This can be confirmed through literature which states that the side force coefficient, which is a function of the side force, increases at a linear rate up to a yaw angle of 40° (Cirstea 2013). The linear

relationship is further demonstrated in Figure 60 which shows how the side force coefficient of a Rover 800 changes with yaw angle.

This image has been removed

Figure 60 - Side Coefficient Variation with Yaw Angle

(Barnard 2009:215)

It can also be said that the maximum side force remains relatively constant from 65° yaw upwards, furthermore, this finding is confirmed by the general assumption that the maximum side force value occurs when the vehicle is at a yaw angle of 60° (Cirstea 2013). As Figure 59 shows the comparison between the different vehicle setups, the ability of the stability fins can also be analysed. It can be seen that initially the side force at low yaw angles, between 0° and 15°, for the baseline vehicle is marginally greater than that of the vehicle with the fins, which can be explained due to the configuration of the wind tunnel and the possible variation of exact wind speed and air density. As the yaw angle increases the vehicles with a stability fin can be seen to generate a slightly higher side force, particularly as the yaw angle approached 90°. This is expected due to the greater projected frontal area that is created through the addition of a vertical stability fin. While the deployment of a stability fin does increase the side force acting on the vehicle, from the wind tunnel tests undertaken, it can be said that this increase is not as large as what was expected.

6.3.4.2 Yawing Moment Comparison

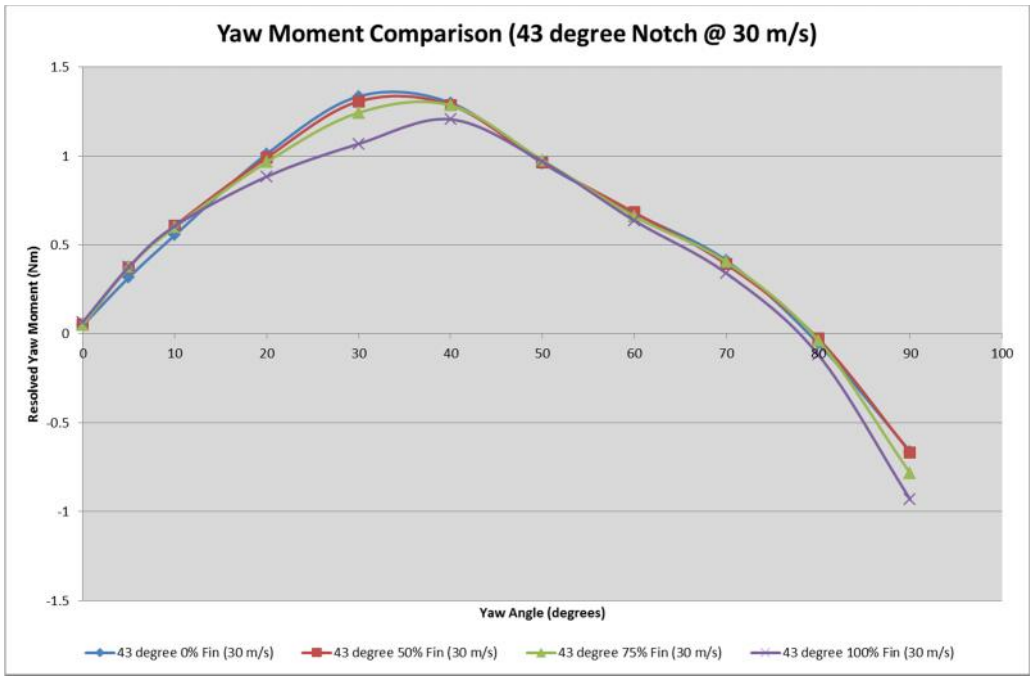

Figure 61 - Yaw Moment Comparison

The yawing moment of the Lynne Turner model shows a number of interesting results and is shown above in Figure 61. Firstly, it can be stated that at smaller yaw angles, within the range of 0° to 10°, the vehicle in all configurations follows a linear path, with each setup returning a similar value. As the yaw angle increases beyond 10° it can be seen that the baseline vehicle with no stability fin has a greater yawing moment peaking at 1.35Nm. As the fin deployment increases, as the graph shows, the yawing moment within the 20° to 45° range decreases, which is desirable for yaw stability under crosswind conditions, as a neutral yawing response is the ideal scenario (Barnard 2009:218). The peak in yawing moment for each of the vehicle configurations can be seen to be between 30° and 40°, which is confirmed through literature which states that the maximum yawing moment coefficient, and therefore yawing moment occurs at a yaw angle of 30° (Cirstea 2013). This further validates the results that have been obtained for this study.

As the yaw angle increases further, it can be seen that the yaw moment decreases significantly, with the vehicle's with a stability fin displaying a reduced yawing moment, however, as the yaw angle approaches 90° it is shown that the yawing moment becomes negative which demonstrates that the vehicle's yawing tendency direction has changed. This could possibly indicate a translation of the centre of pressure point causing a change in the yawing direction.

6.3.4.3 Drag Force Comparison

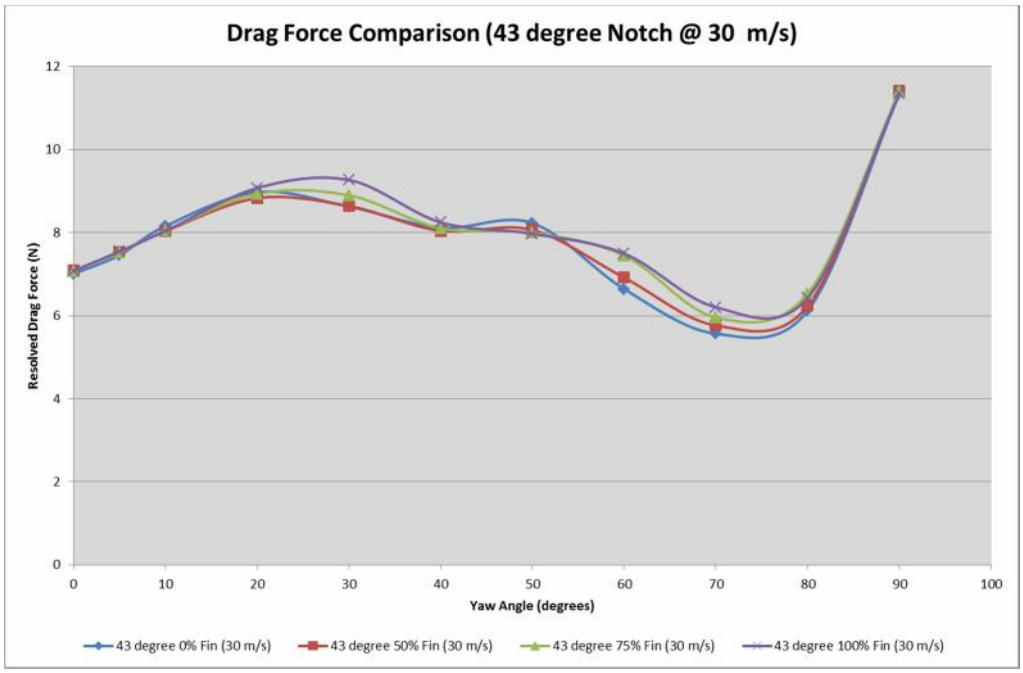

Figure 62 - Drag Force Comparison

As previously discussed, there are four additional aerodynamic forces and moments that act on the vehicle, with each one having an effect on the vehicle's behaviour, whether it be with regard to the maximum velocity of the vehicle, or the lift that is exhibited that could cause handling issues. The following pages display the results for these forces and moments acting on the Lynne Turner vehicle when subject to the described wind tunnel test.

The drag force that acts on the model can be viewed in Figure 62, from which it can be said that in the yaw angle range of 0° to 20°, each of the vehicle configurations display a linear increase in drag force of approximately 3N on the scale model. As the yaw angle increases beyond 20° there is a departure of drag force of the baseline and 50% and 75% deployed fins, however, the fully deployed fin shows an increase in drag at 30° before reaching its minimum value of 6N at a 75° yaw angle. Moreover, it can be seen that as the yaw angle increases to 70°, each of the vehicle configurations display a reduction in drag force before increasing to a peak value of 11.5N at 90°. The vehicle is expected to show this large increase in drag force at these yaw angles due to the major change in projected frontal area of the vehicle.

6.3.4.4 Lift Force Comparison

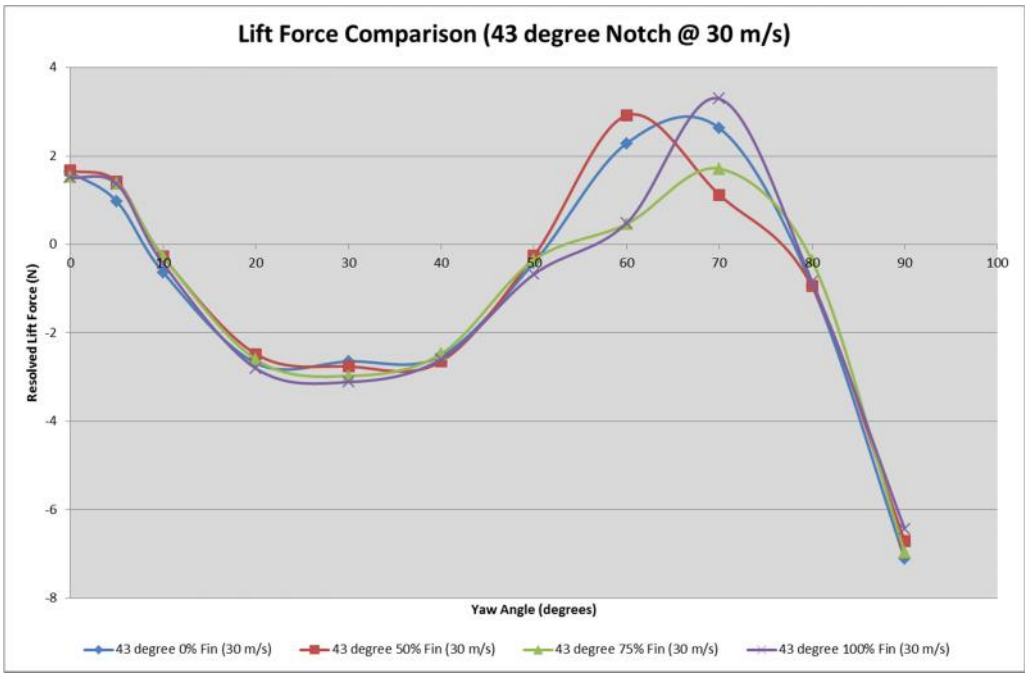

Figure 63 - Lift Force Comparison

While there are small fluctuations in the drag force acting on the vehicle when comparing each configuration, the lift force, as displayed in Figure 63, demonstrates a number of interesting traits. Between the yaw angles of 0° and 50° each of the model configurations follows a similar path, however, interestingly the vehicle produces up to 3N of negative lift, otherwise known as downforce between 20° and 40° yaw. As the yaw angle increases beyond 40°, the downforce decreases and positive lift is generated. It is at this stage that the influence of a stability fin begins to become apparent. As yaw increases, the baseline lift force peaks at a value of 3N and then steadily decreases until 7N of downforce is generated at 90° yaw, however, when a 50% fin is used, the peak lift force is delayed by 8°. A fully deployed fin causes an even greater lift force of 3.2N at 70° yaw. Interestingly, when analysing the 75% deployed fin, it can be seen that it produced the least lift over the 50° to 80° yaw range, with a peak value of 1.8N at 70°. This difference in lift could cause a vehicle to be perceived to have reduced stability and a reduction in handling ability.

6.3.4.5 Roll Moment Comparison

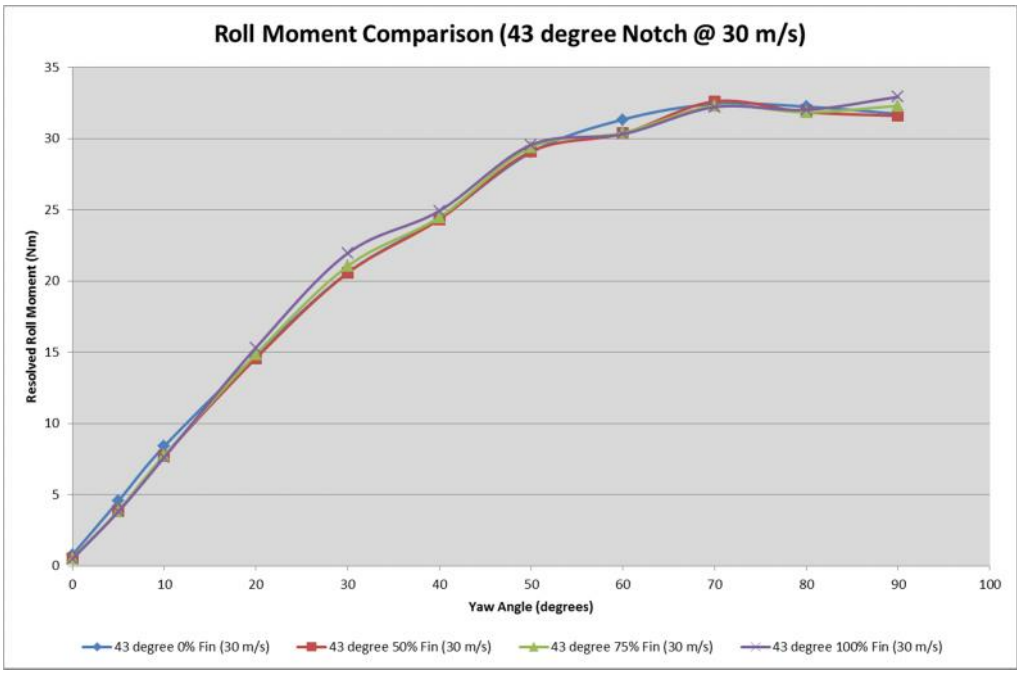

Figure 64 - Roll Moment Comparison

The roll moment that acted on the Lynne Turner model during the wind tunnel tests can be seen above in Figure 64. Here it is seen, much like the side force, that initially as the yaw angle increases, the rolling moment increases in a linear manor up to 35° yaw. From this point onwards the roll moment tends to stabilise at 32.5Nm, reaching a peak at approximately 70°. From the graph it can be said that utilising a variable stability device such as a fin, does not have a great effect on the rolling moment that has been measured through the wind tunnel balance. This is due to the similarity in the results that have been obtained, with only minimal differences between each of the fin deployment stages.

6.3.4.6 Pitch Moment Comparison

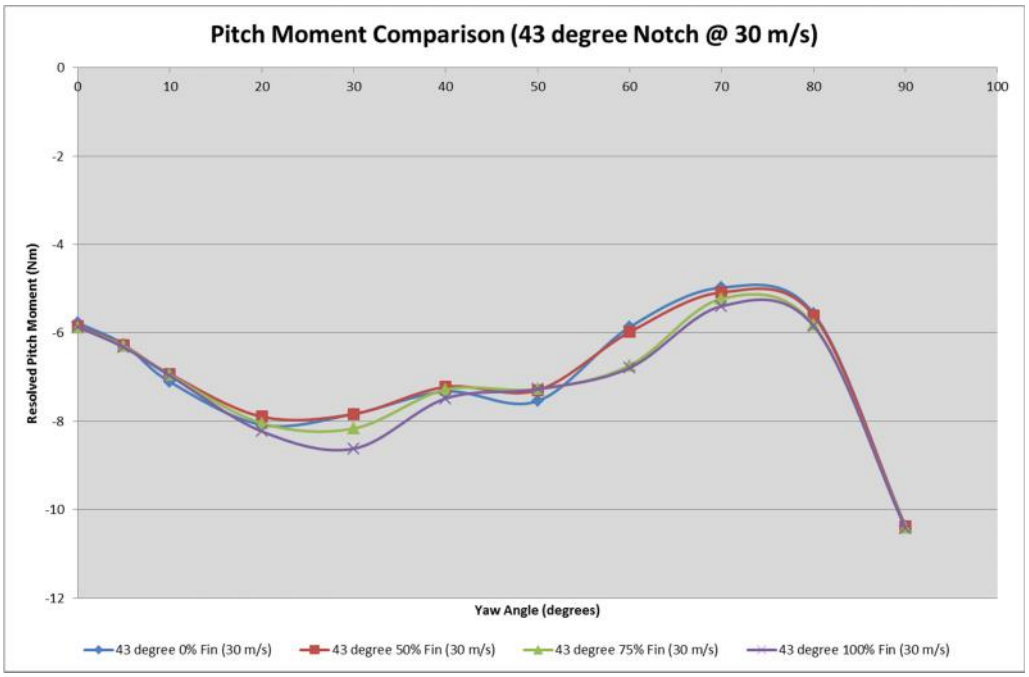

Figure 65 - Pitch Moment Comparison

The pitching moment output, shown above in Figure 65 indicates several interesting traits. When the vehicle is yawed up to 20° the pitching moment can be seen to become more negative linearly from -6Nm to -8.2Nm. When the yaw angle increases further, the vehicle baseline setup pitching moment can be seen to increase up to 40° yaw. This is shown for the plots of the 50% and 75% deployed fin, however, it can be seen that the introduction of a fully deployed fin causes the pitching moment to increase further to a value of -8.7Nm before increasing at 40°. Once again, as the yaw angle increase further, the pitching moment of each configuration is seen to become less negative with a peak value of between -5Nm and -5.5Nm occurring at 70°, before increasing the moment's negativity with a value of -10.5Nm being indicated at 90° yaw.

6.4 Wind Tunnel Data Issues

The following section of the report concerns the correlation between the data obtained through CFD and wind tunnel testing. Correlation is a key parameter between the two simulation sources, as results from an individual source may not be representative of the problem that is being investigated.

6.4.1 Resolved Force Correlation Issues

There were a number of issues that became apparent when analysing the data that had been obtained from the wind tunnel. These mainly concerned the lack of perceived correlation between the measured forces and the resolved forces. This was particularly evident when analysing the drag and side forces that were acting on the vehicle. The issue that was identified was that for the tests, the wind tunnel resolver, selected on the wind tunnel controller, was appointed to the vehicle and the balance, thus meaning that when the vehicle was yawed throughout the range of 0° to 90°, the resolved drag (x) and side force (y) axes would rotate with the vehicle. This resulted in each of the resolved forces containing both drag and lift components, and thus provided the correlation issues. Figure 66 shows a schematic of the resolved and actual force components when related to the vehicle and the wind tunnel.

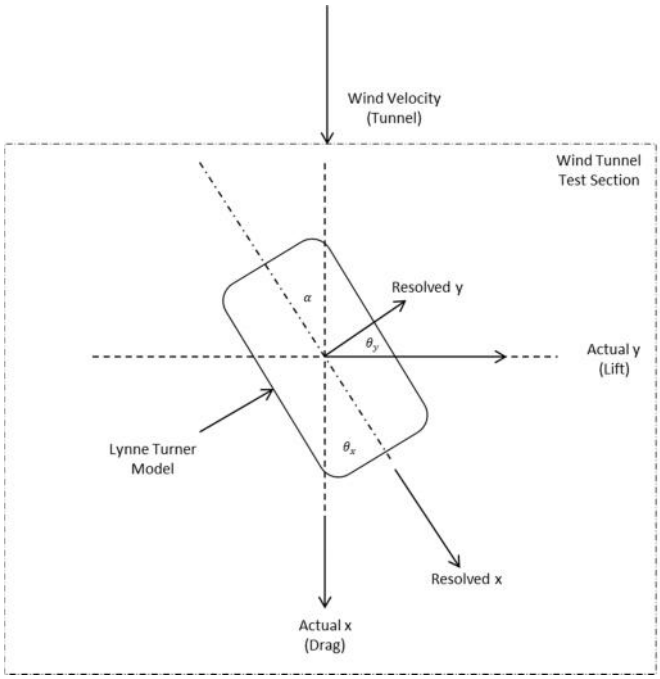

Figure 66 - Aerodynamic Forces with Respect to the Wind Tunnel Resolver

6.4.2 Wind Tunnel Strut

In order for the wind tunnel tests to be completed, it was required that the Lynne Turner model be attached to the balance which is used to measure the aerodynamic forces and moments that act on the vehicle. To achieve this, the aerodynamic strut was used as this would provide a method of connecting the model to the balance while having minimal effect of the aerodynamic data output. This was not modelled in the CFD simulations to maximise the free-stream air flow over the top of the vehicle and towards the rear section and stability fin, as this is the main area of investigation of this project. The exclusion of this in the results, however small, could cause minor correlation issues between the CFD and wind tunnel test data. The aerodynamic strut and balance are shown below in Figure 67.

Figure 67 - Wind Tunnel Aerodynamic Strut

6.4.3 Surface Roughness

One of the main differences between a physical model and a virtual model designed for CFD investigation is the surface finish on the model. The surface of the virtual model was chosen to be smooth, whereas, the physical model, manufactured from wood had a rougher surface. This would produce different results due to the skin friction of the air on the surface of both the physical and virtual models.

6.4.4 Stability Fin Base Attachment

In order to secure the fins to the rear sections of the Lynne Turner model, as previously described, a base plate was manufactured into which the fin could be placed and secured using tape. While this attachment had little effect on the projected frontal area of the model, due to the nature of its design, it can be said that it could affect the results when compared to them of the CFD simulations where it was not a required component of these investigations.

6.5 Wind Tunnel Testing Summary

The results that have been obtained through the wind tunnel analysis do not show major differences between a zero deployed fin and a fully deployed fin, as can be seen on the above pages. However, when considering the yawing moment, it can be seen that stability fin does assist in reducing the yawing moment of the vehicle, when compared to a zero deployed fin, particularly over the 20°-45° yaw angle range. The anomalies within these results when compared to those of the CFD analysis, as explained above, could be due to a number of correlation issues generated by the wind tunnel balance solver, dimensional accuracy of the model surface, and the aerodynamic strut used in the wind tunnel not being simulated with the CFD analysis.

Repeating these wind tunnel tests would be beneficial to the research as it would allow for an additional data set to be obtained, which would then be able to be analysed to assess the correlation between the two wind tunnel data sets and the data obtained through the CFD testing. By repeating the tests, the anomalies that have been described above would be able to be firmly identified.

7 Discussion

Throughout the duration of the research that is shown within this report there have been a number of challenges that have had to be overcome in order to progress the research and to propose the additional knowledge gained of the subject area.

Firstly, the subject of the research had to be defined so as to be able to expand on the knowledge that has already been established regarding the effect of aerodynamics on vehicle behaviour. This required in an extensive literature review, designed to define the areas where additional research would be beneficial. The main challenge of this proved to be obtaining significant numerical and graphical data to establish a baseline when comparing a vehicle with and without a fin, as this would be required to correlate the experimental data with that of the literature. Through reading a number of different sources, a theoretical overview of the effect of a fin was able to be established, with this data then being expanded on through the use of the mathematical modelling.

The mathematical modelling of the 2DOF system proved to be one of the most involved sections of the project, with the effect of a crosswind on the vehicle being shown as forces at each axle, which is then translated into the corrective steering angle required to maintain the vehicle along a linear path. This dynamic analysis of the vehicle behaviour identifies the theory and then interrogates the model against a set of pre-defined vehicle characteristics to produce the results, with this analysis providing a new approach to how aerodynamics affects vehicle behaviour.

The simulation aspects of the research, namely the CFD and wind tunnel testing, also caused a number of difficulties, particularly concerning the correlation between each data set and the data that had been obtained through the literature review. This can be attributed to a number of key aspects; While interpreting the data that was obtained through the CFD and wind tunnel simulations, one of the key challenges was the alignment of the axis and balance system, which were used to calculate the forces and moments acting on the vehicle. This proved especially challenging with the wind tunnel data, due to the resolver axis being aligned to the vehicle axis and not that of the wind tunnel, thus providing a force and moment consisting of a combination of two or more elements, which then had to be separated in order to conduct the analysis. However, the separation of these elements, through calculation, could result in minor errors with the forces and moments being carried

into the results data. As described, on the following pages, the correlation between the wind tunnel, CFD and previously published data would provide a substantial future work action.

The most significant issue with using the CFD and the wind tunnel as defined was the fact that the analysis provides the results of a steady state simulation, whereby, a crosswind is a highly transient flow scenario. It was decided that for the basis of this research that the steady state analysis would provide a suitable indication as to whether a variable stability fin would assist in maintaining the vehicle within a drivers recoverable bounds, with potential future work of simulating a highly transient scenario being proposed.

Through this research project, it can be said that numerous issues and challenges had to be solved in order to progress and expand on the knowledge already known through published literature concerning the subject of how a variable stability fin can affect the behaviour of vehicle when acted on by a crosswind.

8 Conclusion

The research that has been conducted for this project has provided a number of interesting traits and developed the understanding of the subject area, from which the following can be concluded;

- It can be concluded through the use of the mathematical model, that by utilising a stability fin, using pre-defined vehicle characteristics, the corrective steering angle required to be input by the driver, reduces significantly as the deployment of the stability fin increases, maintaining the vehicle within the drivers recoverable bounds.

- The maintaining of the vehicle within a drivers recoverable bounds is also shown when comparing the gathered data. This is shown when comparing the CFD and wind tunnel data for a vehicle with no fin against a vehicle where the fin is fully deployed, whereby the side force increases and the yawing moment decreases, thus correlating with previously published literature.

- Implementing a variable stability fin does affect a vehicles dynamic behaviour when acted on by a crosswind, however, from the research it can be seen that the stability effect is reduced at lower yaw/crosswind approach angles of between 0°and 20°. Once the yaw angle increases beyond 20° the differences between a vehicle with no fin, one with a 50% deployed fin and a fully deployed fin does become apparent. Therefore it can be said that as the yaw angle increase, the use of a variable stability fin becomes more beneficial and the vehicle stability is positively affected.

- While the CFD and wind tunnel data provides an indication on how a crosswind would affect a vehicles behaviour, the simulations do not fully represent the highly transient nature of a crosswind, therefore, the data that has been obtained for this investigation can only be used as an indication.

- It can be seen from studying the data obtained from the CFD and wind tunnel simulations that there are a number of correlation issues. These issues were mainly attributed to the wind tunnel resolver balance, with the potential for future work to be conducted to fully configure the wind tunnel.

9 Future Work

While the project provided an indication that the use of a variable aerodynamic device to alter a vehicle's behaviour would be suitable, there are a number of recommendations of future work that could be undertaken to further confirm the use of a stability device to amend vehicle behaviour. Initially as the tests were only carried out on the Lynne Turner model, and thus only the effect on this vehicle is known, the simulation of an additional model would be beneficial. A proposed solution would be to test a set of stability fins on the Mercedes AMG PETRONAS Formula One Blob model located in the Coventry University wind tunnel. Evaluating the vehicles, with each one having a theoretical different centre of pressure location, will provide an expansive data set that would be able to be evaluated. Figure 68 shows the rear cowling attached to the Mercedes AMG PETRONAS model that has been designed to accommodate the inclusion of a stability fin, with the original design being displayed below it.

Figure 68 - Rear Cowling Redesign for Wind Tunnel Testing

As stated within the report, within the mathematical model, the vehicle was simulated without the inclusion of a driver. An activity that could be beneficial to understanding how such an open-loop and variable scenario would alter the output of the vehicle behaviour would be interesting to model. To simulate this, a function could be created within a software package such as Simulink and then inserted into the Excel based model as an equation. This function would provide a random and transient input function for the crosswind and would then link to a reactive response from a driver.

With regards to the CFD simulations, as number of parameters could be evaluated in the future, which could lead to further experimentation being required into the effects. Such tasks as increasing the approach angle of the crosswind on the vehicle and allowing the crosswind to act from 90° to 180° yaw approach angle. This would identify the structure of the flow and the forces and moments that act on the vehicle at higher yaw angles.

Also with regards to the CFD simulations, further progress on the Y+ Wall distribution could be made in the future to optimise the mesh for the given scenario. The optimisation of the Y+ values would lead to a greater accuracy of results if the values were to be situated in the Log-Law Layer. With regard to the fin, the mesh for this component could be engineered to ensure that it remains in the Viscous Sub-Layer. This is required as the fin element has a relatively small thickness in comparison to the boundary layer. Further to the Y+, the physics models could be altered to provide an unsteady flow, simulating a gust of wind to a greater effect. Furthermore, correlation issues could be improved by measuring and then modelling the roughness of the surface of the Lynne Turner model, and also running a simulation on a secondary CFD software to ensure that the results that were being obtained from STAR CCM+ were representative. This repetition of the simulations could also, as stated, be incorporated into the wind tunnel testing to confirm the validity of the data obtained.

Experimentation with alternative devices would be recommended to fully understand the ability of such devices in a side wind scenario. The devices could range from variable control surfaces to a deployable spoiler assembly, however, exploration into fin design and the possibility of a variable deployable and rotating fin could prove interesting.

From the research that has been carried out, the effect on the aerodynamic forces and moments, particularly the side force and yawing moment of the vehicle with the inclusion of a variable device have been able to be established, however, the full effect of a side wind on a vehicle, from this information, can only be estimated. Therefore, a full vehicle behaviour analysis would provide a greater understanding of the effect of a side wind on the vehicle behaviour. To achieve this, a vehicle model is required be built using a multibody software such as MSC ADAMS or Simpack, with a program being written to enable the multibody and CFD software's to simultaneously communicate. This will allow a 'live' data feed of the aerodynamic forces and moments acting on the vehicle to be input into the multibody

simulation and thus a complete analysis of the vehicle's behaviour would be able to be established.

The recommendations that are outlined above would enable the change in behaviour of a vehicle when installed with a variable aerodynamic device, active during a side wind, to be further and fully investigated to evaluate the possibilities of such a device being utilised on road-going vehicles.

10 References

Aird. F (2009) '*Brake Dancing'*. Racecar Engineering 19 (12), 55-60

Airliners.net (2007) *Aviation Forums – Aircraft Control Surfaces* [online] available from <http://www.airliners.net/aviation-forums/tech_ops/read.main/191925/> [13th May 2013]

Alpha Coders (n.d) *JCB DieselMax Speed Record Car* [online] available from <http://wall.alphacoders.com/big.php?i=282939> [01st August 2013]

Autosprint (2010) *Red Bull RB6 F-Duct Uncovered* [online] available from <http://www.auto.it/images/auto/69/C_3_Media_1062369_immagine_fullw.jpg> [13th May 2013]

Barnard. R.H (2009) *Road Vehicle Aerodynamic Design: An Introduction* 3rd Edition: MechAero Publishing: St Albans

Bibliotecapleyades (2005) *'Northrop-Grumman B-2 Tailless Bomber'* [online] available from <http://www.bibliotecapleyades.net/ciencia/ciencia_antigravity.htm> [13th May 2013]

Blundell. M, Harty. D (2004) *The Multibody Systems Approach to Vehicle Dynamics* 1st Edition: Butterworth Heinemann: Oxford

CFD-Online (2011) *Law of the Wall* [online] available from <http://www.cfd-online.com/Wiki/Law_of_the_wall> [27th August 2013]

Cirstea. R (2013) *CFD Theory Lecture M59MAE Ground Vehicle Aerodynamics* Coventry University: Coventry

Cirstea. R (2013) *Vehicle Stability Lecture M59MAE Ground Vehicle Aerodynamics* Coventry University: Coventry

Dukkipati R.V et al (2008*) Road Vehicle Dynamics*
1st Edition: Society of Automotive Engineers: Warrendale

Ferrari (2013) *Ferrari LaFerrari Press Release: Aerodynamics* [online] available from <http://www.laferrari.com/en/aerodynamics/> [12th June 2013]

Formula 1 (2013) *'Ferrari Targeting Perfection Following Bahrain Woes'* [online] available from <http://www.formula1.com/news/headlines/2013/4/14506.html> [13th May 2013]

Forth Road Bridge (2013) *Weather Status Updates* [online] available from <http://www.forthroadbridge.org/weather-and-status-updates> [30th May 2013]

Gillespie. T.D (1992) *Fundamentals of Vehicle Dynamics*
1st Edition: Society of Automotive Engineers: Warrendale

Harty. D (2012) '*Vehicle Dynamics: The Big Picture*. [online Lecture] available from <http://moodle.coventry.ac.uk/ec/course/view.php?id=4878> [25th February 2013]

Hucho. W.H (1998) *Aerodynamics of Road Vehicles*
4th Edition: Society of Automotive Engineers: Warrendale

Katz. J (2006) *Race Car Aerodynamics: Designing for Speed*
2nd Edition: Bentley Publishers: Cambridge MA

Lis. A (2010) *'Bringing up the Rear*'. Racecar Engineering 20 (10), 37-41

Mayer, J. Schrelf, M. Demuth, R. (2007) '*On Various Aspects of the Unsteady Aerodynamic Effects on Cars Under Crosswind Conditions'*. Paper No. 2007-01-1548. Society of Automotive Engineers

McBeath. S (2011) *Competition Car Aerodynamics*
2nd Edition: Haynes Publishing: Sparkford

Mercedes AMG PETRONAS F1 Team (2012) *Wind-Tunnel Specification Summary Sheet* Coventry University: Coventry

MetOffice (2014) *Temperature and Humidity* [online] available from <http://www.metoffice.gov.uk/learning/learn-about-the-weather/weather-phenomena/humidity> [14th June 2014]

Milliken. W.F, Milliken. D.L (1995) *Race Car Vehicle Dynamics* 1st Edition: Society of Automotive Engineers: Warrendale

Modern Mechanix (2012) *Mercedes-Benz Air Brake: Oct 1955* [online] available from <http://blog.modernmechanix.com/mercedes-benz-air-brake/> [14th June 2013]

Nasri. N.M (2012) *Investigation on Effect of Drag Reduction System (DRS) on an Open Wheel Race Car:* 1st Edition: Coventry University: Coventry

Nelson. G, Roush. J, Eaker. G, Wallis. S (n.d.) *'The Development and Manufacture of a Roof Mounted Aero Flap System for Race Car Applications.'* Paper no. 942522: Society of Automotive Engineers

Pagani (2012) *The Pagani Huayra: English Press Release* [online] available from <http://www.pagani.com/en/huayra/default.aspx> [25th February 2013]

Rendle. S (2011) *Red Bull Racing F1 Car 2010 (RB6): Owner's Workshop Manual* 1st Edition: Haynes Publishing: Sparkford

Ryan. A, Dominy. R.G (1998) *'The Aerodynamic Forces Induced on the Passenger Vehicle in Response to a Transient Cross-Wind Gust at a Relative Incidence of 30°.'* Paper no. 980392: Society of Automotive Engineers

ScarbsF1 (2011) *DRS: Optical Illusion why some wings appear to open appear* [online] available from <http://scarbsf1.com/blog1/2011/05/20/drs-optical-illusion-why-some-wings-appear-to-open-wider/> [12th June 2013]

Schroeck, D. Krantz, W. Widdecke, N. Wiedemann, J. (2011) *'Unsteady Aerodynamic Properties of a Vehicle Model and their Effect on Driver and Vehicle under Side Wind Conditions*'. Paper No. 2011-01-0154. Society of Automotive Engineers

Singh. G, Nagpurwala. Q.H, Nassar. A, Shankapal. S.R (2009) '*Numerical Investigations on Crosswind Aerodynamics and its Effect on the Stability of a Passenger Car*.' Paper no. 2009-26-059: Society of Automotive Engineers

Skinner. P.J, Clifford. A.T, Martins. J.C.F (1996) *'Effects of Wing Adjustment Mechanisms on the Aerodynamics of an Open Wheel Racing Car Model.'* Paper no. 962520: Society of Automotive Engineers

Stengel. R.F (2004) *Flight Dynamics*
1st Edition: Princeton University Press: Princeton and Oxford

Tu. J, Yeoh. G.H, Liu. C (2008) *Computational Fluid Dynamics: A Practical Approach*
1st Edition: Butterworth-Heinemann: Oxford

Wagner. A, Wiedemann, J (2002) '*Crosswind Behavior in the Driver's Perspective*.' Paper no. 2002-01-0086: Society of Automotive Engineers

Watson. A.B. (2013) *Aerodynamic Benchmarking of a Mercedes F1 Vehicle*
Coventry University: Coventry

Windfinder (n.d) *Wind Speeds* [online] available from
<http://www.windfinder.com/wind/windspeed.htm)> [30th June 2013]

Wood. G (2013) *M26MAE Coursework 1: Eigenvalue Analysis Definition*
Coventry University: Coventry

11 Bibliography

Abdelhady. M.B.A (2002) *'Aerodynamic Effects on Ride Comfort and Road Holding of Actively Suspended Vehicles.'* Paper no. 2002-01-2205: Society of Automotive Engineers

Aschwanden. P, Muller. J, Travaglio. G.C, Schoning. T (2008) *'The Influence of Motion Aerodynamics on the Simulation of Vehicle Dynamics.'* Paper no. 2008-01-0657: Society of Automotive Engineers

Bolitho. M, Jacob. J (2008) *'Active Vortex Generators Using Jet Vectoring Plasma Actuators.'* Paper no. 2008-01-2234: Society of Automotive Engineers

Dominy. R.G, Richardson. S (2004) '*The Aerodynamic Characteristics of a WRC Rally Car at High Slip Angles.'* Paper no. 2004-01-3508: Society of Automotive Engineers

Gadola. M, Candelpergher. A, Adami. R (2002) *'The Impact of Non-Linear Aerodynamics on Racecar Behaviour and Lap Time Simulation.'* Paper no. 2002-01-3332 Society of Automotive Engineers

Gajendra Singh. M, Nagpurwala. Q.H, Nassar. A, Shankapal. S.R (2009) *'Numerical Investigations on Crosswind Aerodynamics and its Effect on the Stability of a Passenger Car.'* Paper no. 2009-26-059: Society of Automotive Engineers

Ghosh. S, Deb. A, Mahala. M, Tanbakuchi. M, Makowski. M (2012) *'Active Yaw Control of a Vehicle using a Fuzzy Logic Algorithm.'* Paper no. 2012-01-0229 Society of Automotive Engineers

Gogel. D, Sakurai. H (2006) '*The Effects of End Plates on Downforce in Yaw.'* Paper no. 2006-01-3647 Society of Automotive Engineers

Guilmineau, E. Chometon, F. (2007) *'Experimental and Numerical Analysis of the Effect of Side Wind on a Simplified Car Model'*. Paper No. 2007-01-0108. Society of Automotive Engineers

Gullberg. P, Lofdahl. L (2008) *'The Role of Aerodynamics in the 1955 Le Mans Crash.'* Paper no. 2008-01-2996: Society of Automotive Engineers

Hac. A, Simpson. M.D (2000) *'Estimation of Vehicle Side Slip Angle and Yaw Rate.*' Paper no. 2000-01-0696: Society of Automotive Engineers

Harty. D (2003) *'Brand-by-Wire – A Possibility?'* Paper no. 2003-01-0097: Society of Automotive Engineers

Huminic. A, Huminic. G (2008) *'On the Aerodynamics of the Racing Cars.'* Paper no. 2008-01-0099: Society of Automotive Engineers

Katz. J, Garcia. D, Sluder. R (2004) *'Aerodynamics of Race Car Liftoff.'* Paper no 2004-01-3506: Society of Automotive Engineers

Kermode. AC., Barnard. R.H, Philpott. D.R (2006) *Mechanics of Flight* 11th Edition: Person Prentice Hill: Harlow

Lowe. A.J. (2000) Quality Function Deployment: The House of Quality [online] available from <http://www.webducate.net/qfd/qfd.html> [19th August 2013]

Mankowski. O, Sims-Williams. D, Dominy. R, Duncan. B, Gargoloff. J (2011) *'The Bandwidth of Transient Yaw Effects on Vehicle Aerodynamics.'* Paper no. 2011-01-0160 Society of Automotive Engineers

McBeath. S (2010) 'How Low Can You Go'. Racecar Engineering 20 (10), 12-19

Mckay. N.J, Gopalarathnam. A (2002) *'The Effects of Wing Aerodynamics on Race Vehicle Performance.'* Paper no. 2002-01-3294: Society of Automotive Engineers

Okada. Y, Nouzawa. T, Okamoto. S, Fujita. T, Kamioka. T, Tsubokura. M (2012) *'Unsteady Vehicle Aerodynamics during a Dynamic Steering Action: 1st Report, On-Road Analysis.'* Paper no. 2012-01-0446: Society of Automotive Engineers

Sahoo. R.K, Mishra. J.N (1999) *'Flow Characteristics of a Van during Cross-Wind and Overtaking Process.'* Paper no.990022: Society of Automotive Engineers

Scibor-Rylski. A.J (1984) *Road Vehicle Aerodynamics* 2nd Edition: Pentech Press: London

Tsubokura. M, Ikawa. Y, Nakashima. T, Okada. Y, Kamioka. T, Nouzawa. T (2012) *'Unsteady Vehicle Aerodynamics during a Dynamic Steering Action: 2nd Report, Numerical Analysis.'* Paper no. 2012-01-0448: Society of Automotive Engineers

12 Appendix A

Documents contained within Appendix A

1) Project Plan
2) Variable Device Concepts

12.1 Project Plan

The project will be completed over a 12 month period between September 2012 and September 2013. During this time period, there are a number of different tasks that are required to be competed such as the initial literature review to identify key areas where variable aerodynamic properties could be implemented to maintain or improve the dynamic characteristics of a vehicle. From this initial investigation, a research area will be established that will form the basis of the project. In order to manage the project, a research plan has been created which highlights key milestones and dates by which tasks are too be completed. This method of time management will ensure the completion of the research project to a high standard and by a pre-determined date. The project plan will also be reviewed and revised throughout the duration of the project to ensure that key deliverables are met. Figure 69, below, shows the revised project plan with the key milestones, a full page version of which can be seen in Appendix A.

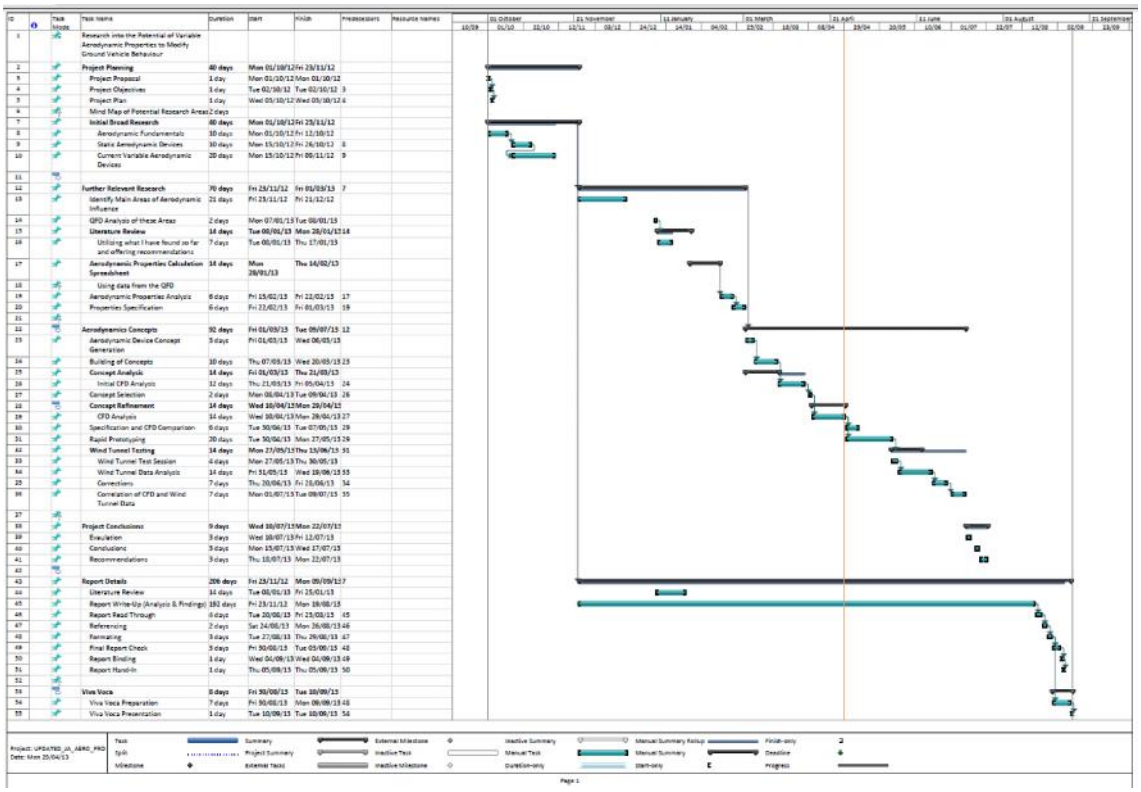

Figure 69 - Revised Research Project Plan

12.2 Project Plan

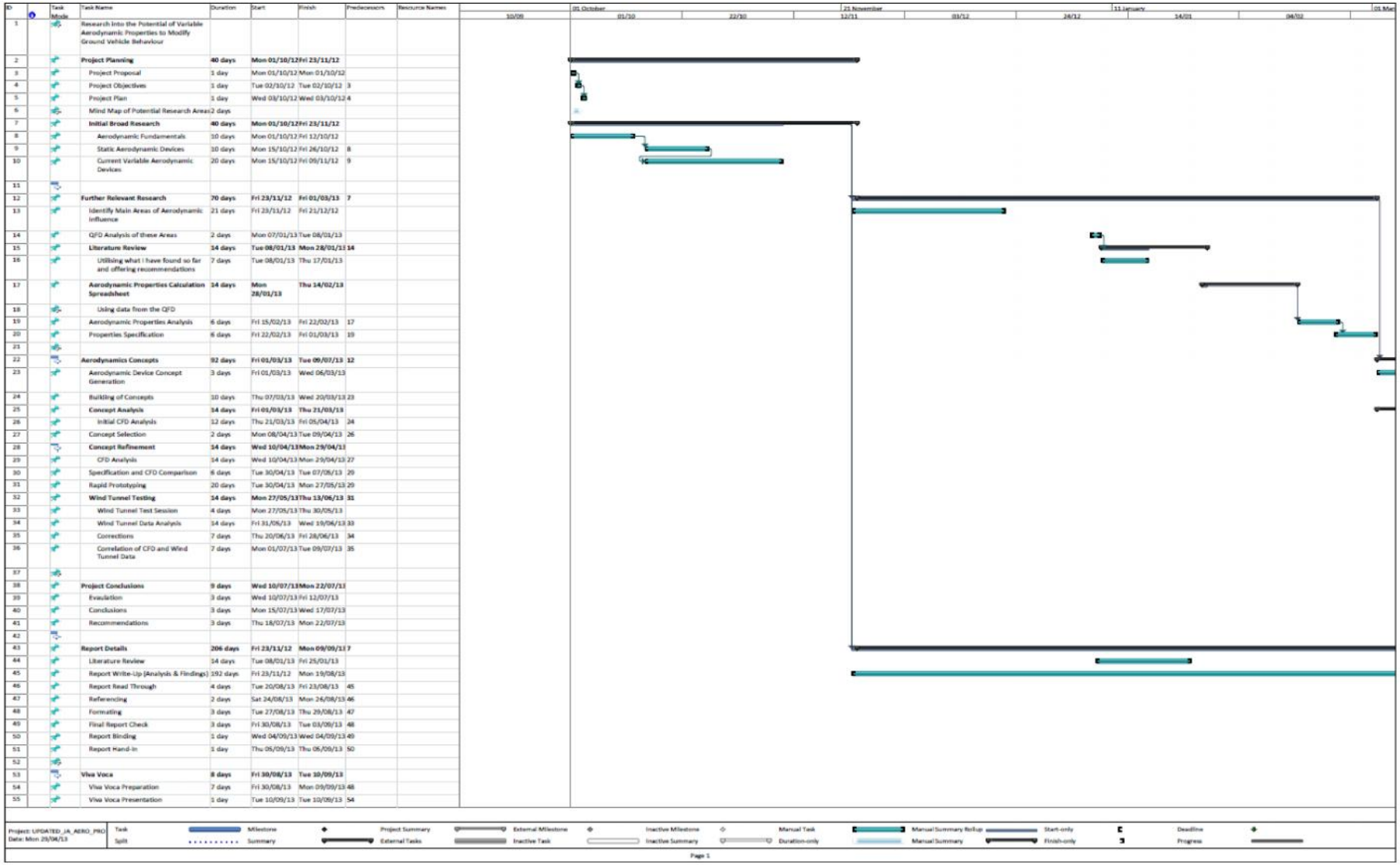

ID	Task Mode	Task Name	Duration	Start	Finish	Predecessors	Resource Names
1		Research Into the Potential of Variable Aerodynamic Properties to Modify Ground Vehicle Behaviour					
2		**Project Planning**	**40 days**	**Mon 01/10/12**	**Fri 23/11/12**		
3		Project Proposal	1 day	Mon 01/10/12	Mon 01/10/12		
4		Project Objectives	1 day	Tue 02/10/12	Tue 02/10/12	3	
5		Project Plan	1 day	Wed 03/10/12	Wed 03/10/12	4	
6		Mind Map of Potential Research Areas	2 days				
7		**Initial Broad Research**	**40 days**	**Mon 01/10/12**	**Fri 23/11/12**		
8		Aerodynamic Fundamentals	10 days	Mon 01/10/12	Fri 12/10/12		
9		Static Aerodynamic Devices	10 days	Mon 15/10/12	Fri 26/10/12	8	
10		Current Variable Aerodynamic Devices	20 days	Mon 15/10/12	Fri 09/11/12	9	
11							
12		**Further Relevant Research**	**70 days**	**Fri 23/11/12**	**Fri 01/03/13**	7	
13		Identify Main Areas of Aerodynamic Influence	21 days	Fri 23/11/12	Fri 21/12/12		
14		QFD Analysis of these Areas	2 days	Mon 07/01/13	Tue 08/01/13		
15		**Literature Review**	**14 days**	**Tue 08/01/13**	**Mon 28/01/13**	14	
16		Utilising what I have found so far and offering recommendations	7 days	Tue 08/01/13	Thu 17/01/13		
17		**Aerodynamic Properties Calculation Spreadsheet**	**14 days**	**Mon 28/01/13**	**Thu 14/02/13**		
18		Using data from the QFD					
19		Aerodynamic Properties Analysis	6 days	Fri 15/02/13	Fri 22/02/13	17	
20		Properties Specification	6 days	Fri 22/02/13	Fri 01/03/13	19	
21							
22		**Aerodynamics Concepts**	**92 days**	**Fri 01/03/13**	**Tue 09/07/13**	12	
23		Aerodynamic Device Concept Generation	3 days	Fri 01/03/13	Wed 06/03/13		
24		Building of Concepts	10 days	Thu 07/03/13	Wed 20/03/13	23	
25		**Concept Analysis**	**14 days**	**Fri 01/03/13**	**Thu 21/03/13**		
26		Initial CFD Analysis	12 days	Thu 21/03/13	Fri 05/04/13	24	
27		Concept Selection	2 days	Mon 08/04/13	Tue 09/04/13	26	
28		**Concept Refinement**	**14 days**	**Wed 10/04/13**	**Mon 29/04/13**		
29		CFD Analysis	14 days	Wed 10/04/13	Mon 29/04/13	27	
30		Specification and CFD Comparison	6 days	Tue 30/04/13	Tue 07/05/13	29	
31		Rapid Prototyping	20 days	Tue 30/04/13	Mon 27/05/13	29	
32		**Wind Tunnel Testing**	**14 days**	**Mon 27/05/13**	**Thu 13/06/13**	31	
33		Wind Tunnel Test Session	4 days	Mon 27/05/13	Thu 30/05/13		
34		Wind Tunnel Data Analysis	14 days	Fri 31/05/13	Wed 19/06/13	33	
35		Corrections	7 days	Thu 20/06/13	Fri 28/06/13	34	
36		Correlation of CFD and Wind Tunnel Data	7 days	Mon 01/07/13	Tue 09/07/13	35	
37							
38		**Project Conclusions**	**9 days**	**Wed 10/07/13**	**Mon 22/07/13**		
39		Evaulation	3 days	Wed 10/07/13	Fri 12/07/13		
40		Conclusions	3 days	Mon 15/07/13	Wed 17/07/13		
41		Recommendations	3 days	Thu 18/07/13	Mon 22/07/13		
42							
43		**Report Details**	**206 days**	**Fri 23/11/12**	**Mon 09/09/13**	7	
44		Literature Review	14 days	Tue 08/01/13	Fri 25/01/13		
45		Report Write-Up (Analysis & Findings)	192 days	Fri 23/11/12	Mon 19/08/13		
46		Report Read Through	4 days	Tue 20/08/13	Fri 23/08/13	45	
47		Referencing	2 days	Sat 24/08/13	Mon 26/08/13	46	
48		Formating	3 days	Tue 27/08/13	Thu 29/08/13	47	
49		Final Report Check	3 days	Fri 30/08/13	Tue 03/09/13	48	
50		Report Binding	1 day	Wed 04/09/13	Wed 04/09/13	49	
51		Report Hand-in	1 day	Thu 05/09/13	Thu 05/09/13	50	
52							
53		**Viva Voca**	**8 days**	**Fri 30/08/13**	**Tue 10/09/13**		
54		Viva Voca Preparation	7 days	Fri 30/08/13	Mon 09/09/13	48	
55		Viva Voca Presentation	1 day	Tue 10/09/13	Tue 10/09/13	54	

12.3 Initial Concepts

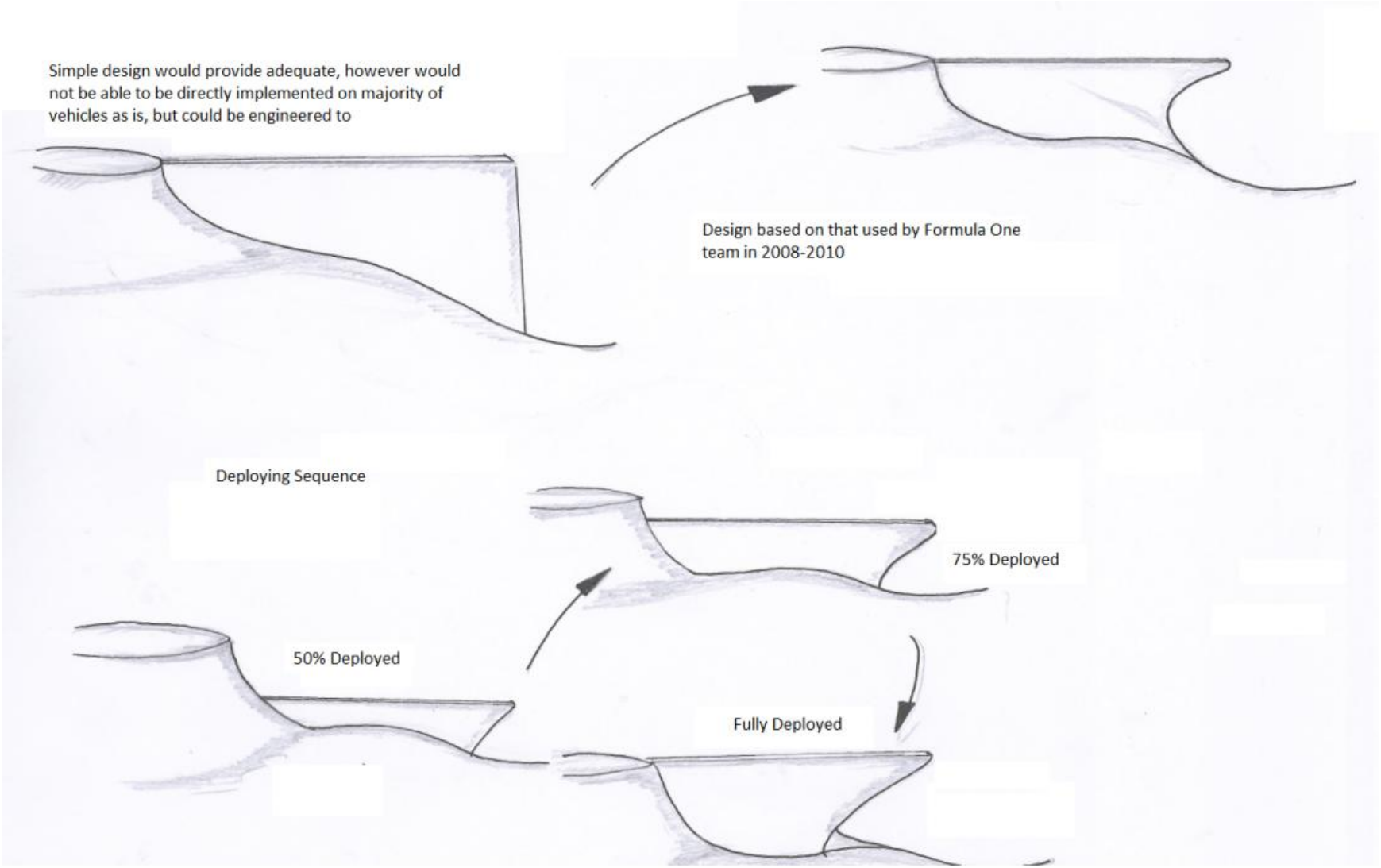

12.4 Initial Concepts

Control flap on each side of the vehicle, conering gusts from either direction

Control surfaces lift upwards when side wind detected. Generate a greater side force at the rear.

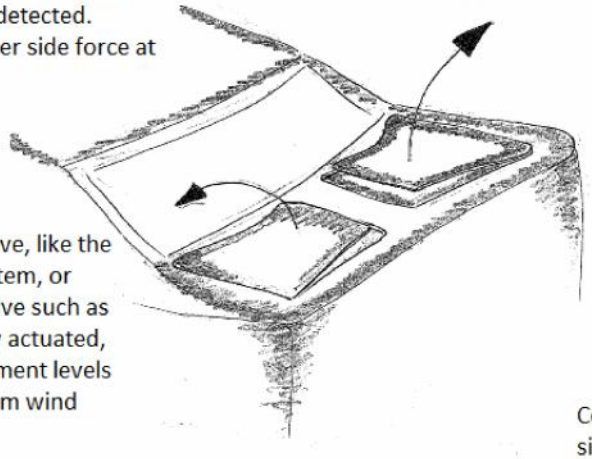

Can be passive, like the NASCAR system, or could be active such as hydraulically actuated, with deployment levels obtained from wind speed data

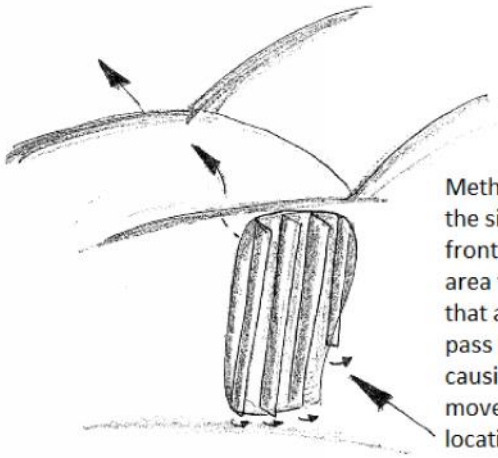

Method of reducing the side force at the front, using a side grill area with variable flaps that allow the air to pass through, thus causing a rearwards movement in CofP location.

Control flaps on either side, on the top and lower surface. Again can be controlled through hydraulic actuators

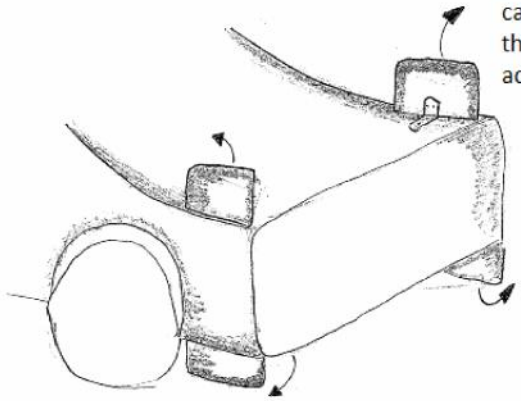

Fin surface on rear but can adjust to wind approach angle for optimum force genration at rear.

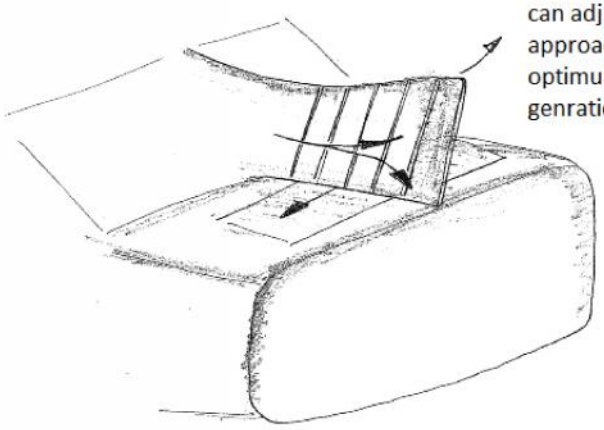

12.5 Initial Concepts

WIng deployed to increase downforce, but can also be used to increase drag. This could prove useful during tasks such as braking or hard cornering.

Hydraullically actuated wing, deployment percentage dictated by data obtained regarding wind velocity and approach angle

Wing is hydraulically actuated, uses a similar deployment to the McLaren Mercedes SLR and Buggatti Veyron

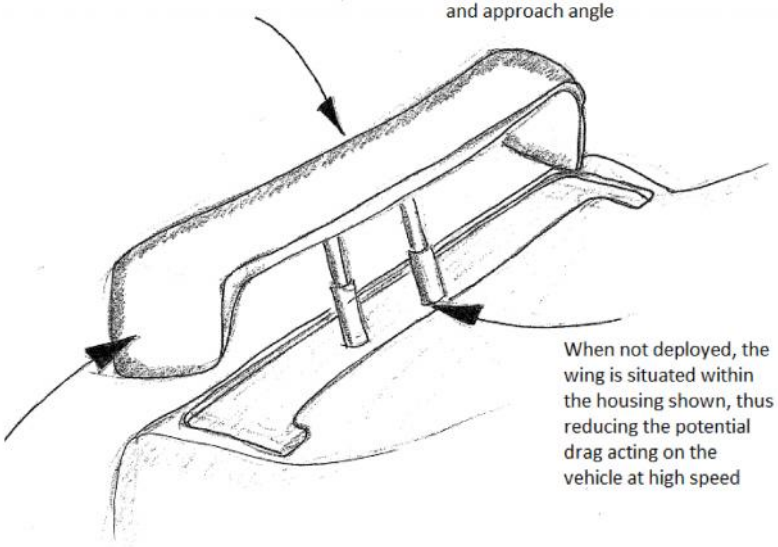

When not deployed, the wing is situated within the housing shown, thus reducing the potential drag acting on the vehicle at high speed

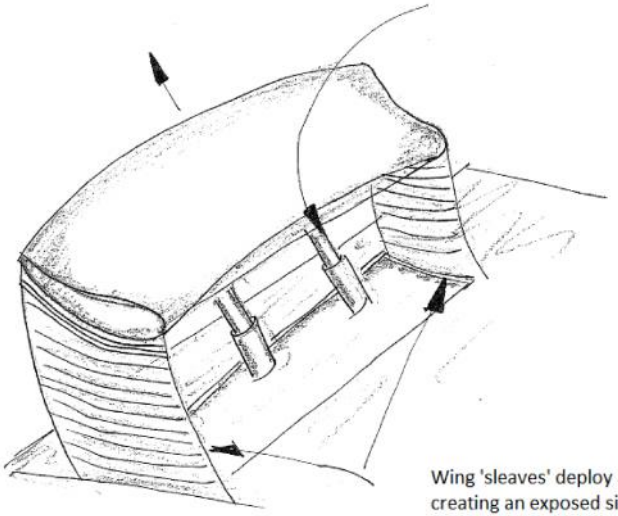

Increased sized endplates on the wing can be used to assist in the generation of a side force at the rear of the vehicle.

Wing 'sleaves' deploy as the wing is deployed, creating an exposed side area which would cause a greater force at the rear of the vehicle thus moving the CofP point rearwards

12.6 Developed Concepts

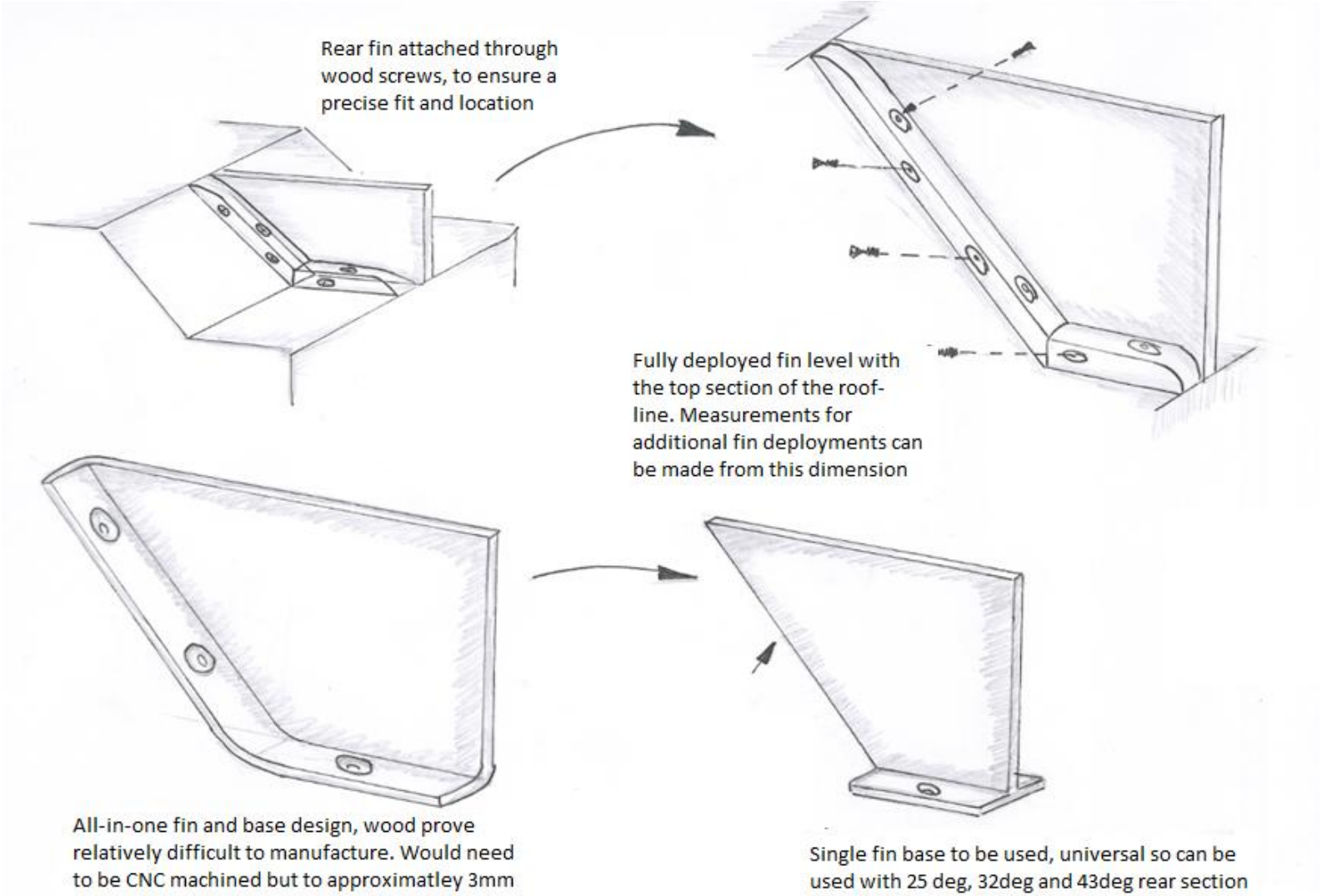

12.7 Developed Concepts

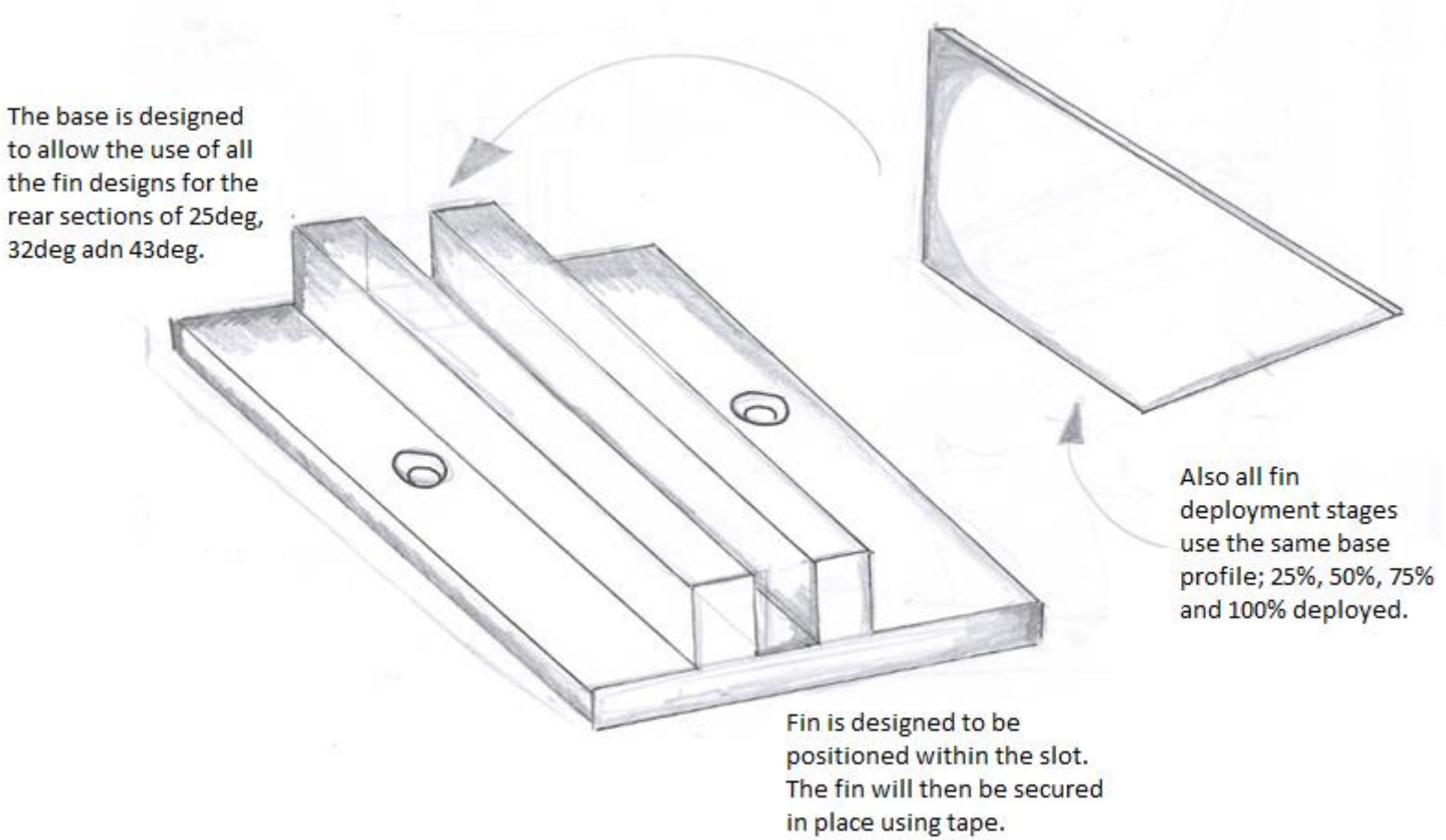

12.8 Developed Concepts

Final Assembly of the rear section of the Lynne Turner model with fully deployed fin and base attachment.

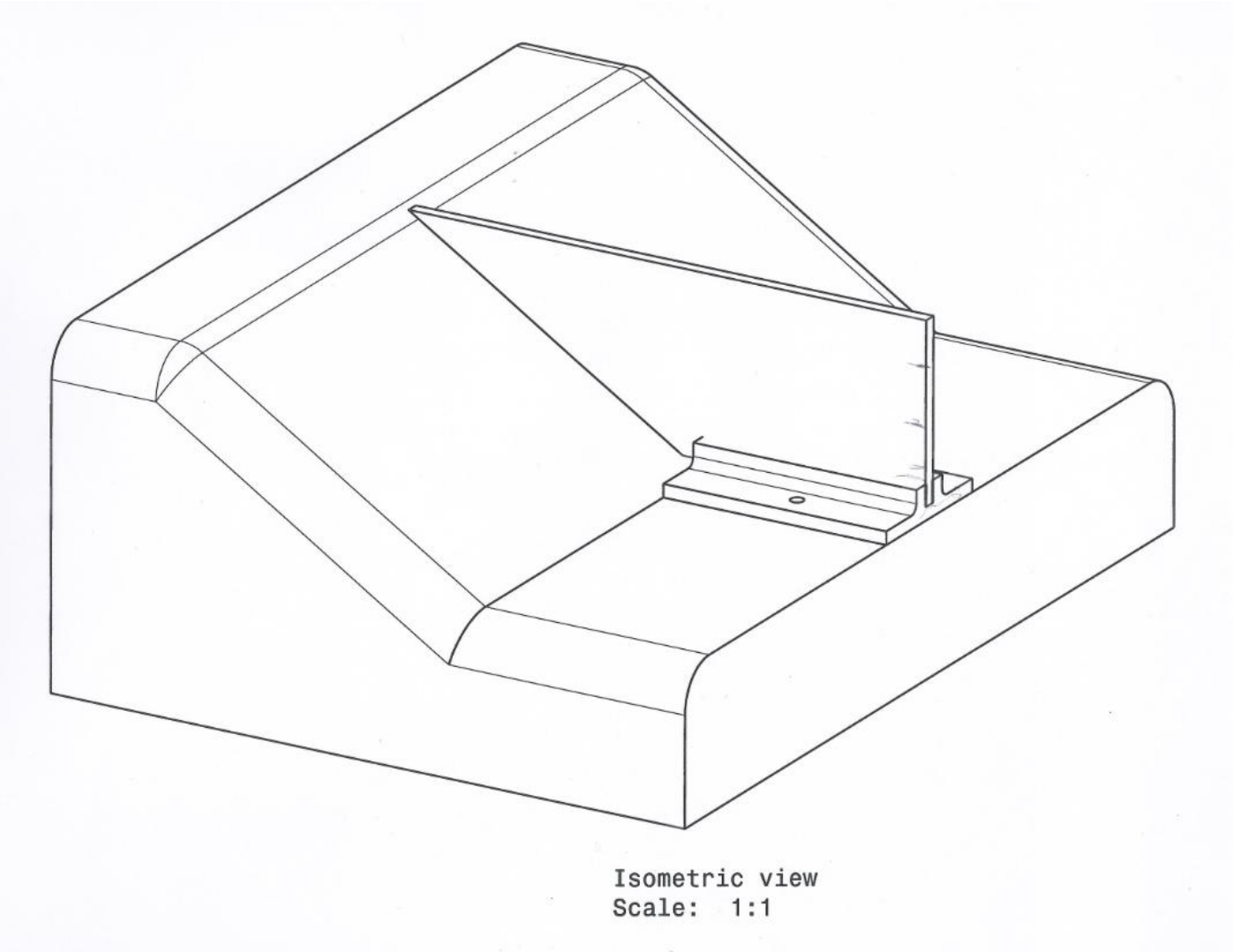

13 Appendix B

Appendix B contains information regarding the y+ wall initial analysis which is used to ensure that the vehicle remains within the Log-Law region of the y+ distribution.

13.1 Wall y+ Distribution

13.1.1 Initial Mesh

An initial exploratory simulation was run to understand how the y+ distribution would perform under default condition. The result of this test and the mesh properties used can be seen below.

File Name: 02_07_13_25deg_complete.

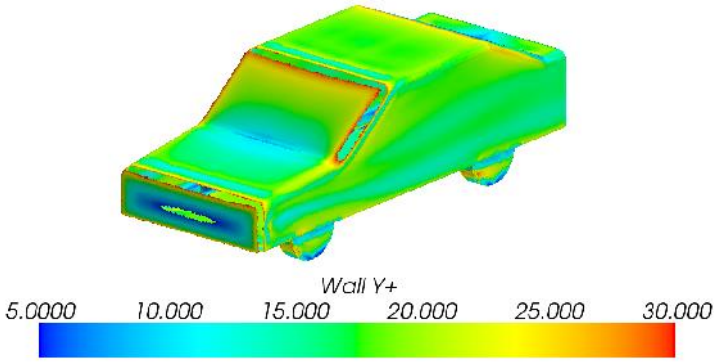

Figure 70 - Initial y+ Wall Distribution Scalar Scene

Mesh Properties		
Continua Values		
Field	Value	Additional Information
Base Size	50mm	n/a
Number of Prism Layers	5	n/a
Prism Layer Stretching	1.5	n/a
Prism Layer Thickness	10% of base (5mm)	Relative to base
VC1	10% of base (5mm)	Relative to Base
VC2	20% of base (10mm)	Relative to Base
Body Region		
Field	Value	Additional Information
Surface Size	1% of base (0.5mm)	Relative Minimum Size
	5% of base (2.5mm)	Relative Target Size
Diffuser Region		
Surface Size	1% of base (0.5mm)	Relative Minimum Size
	5% of base (2.5mm)	Relative Target Size
Notch Region		
Surface Size	1% of base (0.5mm)	Relative Minimum Size
	5% of base (2.5mm)	Relative Target Size

Table 7 - Initial Mesh Properties

It can be seen that the majority of the vehicle is contained between the y+ values of 5 and 30, indicating that the y+ distribution is within the 'Buffer Layer'. This is not ideal as there is no set equation for solving the fluid flow in close proximity to the boundary layer within this region. It is therefore required that the mesh values be amended to move the vehicle from this region to either the viscous sub-layer or to the log-law region.

13.1.2 Prism Layer Stretching Mesh

File name: 25deg_comparison_dec_pl_stretching_complete.

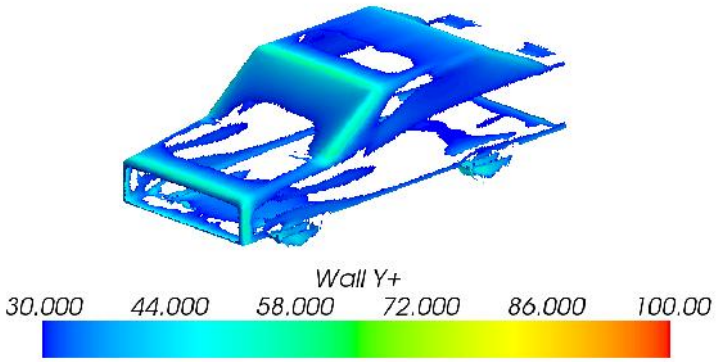

Figure 71 – Second Attempt y+ Wall Distribution

Mesh Properties		
Continua Values		
Field	Value	Additional Information
Base Size	50mm	n/a
Number of Prism Layers	5	n/a
Prism Layer Stretching	1.2	n/a
Prism Layer Thickness	10% of base (5mm)	Relative to base
VC1	10% of base (5mm)	Relative to Base
VC2	20% of base (10mm)	Relative to Base
Body Region		
Field	Value	Additional Information
Surface Size	1% of base (0.5mm)	Relative Minimum Size
	5% of base (2.5mm)	Relative Target Size
Diffuser Region		
Surface Size	1% of base (0.5mm)	Relative Minimum Size
	5% of base (2.5mm)	Relative Target Size
Notch Region		
Surface Size	1% of base (0.5mm)	Relative Minimum Size
	5% of base (2.5mm)	Relative Target Size

Table 8 - Secondary Mesh Properties

The number of prism layers and the prism layer thickness can be altered in order to increase the y+ value. For this simulation the prism layer stretching has been decreased from 1.5 to 1.2 and the effect of this is shown in Figure 71. It can be seen that a proportion of the vehicle is contained within the log-law region, however, substantial sections remain within the viscous sub-layer, which is not desirable. It was decided that for future simulations that the base size would be increased and separate meshes would be generated for each component of the vehicle.

13.1.3 Prism Layer Mesh

File Name: 25deg_comparison_inc_prism_layer_ready_complete

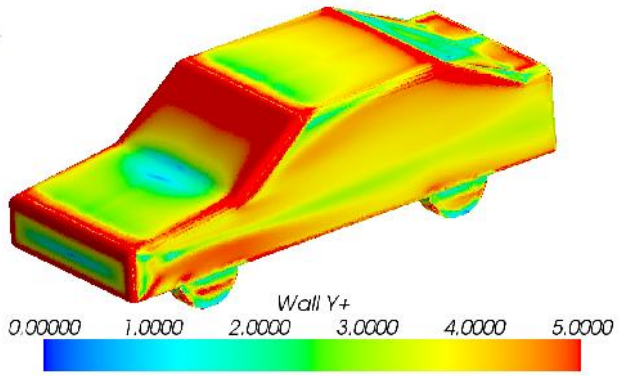

Figure 72 - Third Attempt y+ Wall Distribution

Mesh Properties		
Continua Values		
Field	Value	Additional Information
Base Size	50mm	n/a
Number of Prism Layers	8	n/a
Prism Layer Stretching	1.5	n/a
Prism Layer Thickness	10% of base (5mm)	Relative to base
VC1	10% of base (5mm)	Relative to Base
VC2	20% of base (10mm)	Relative to Base
Body Region		
Field	Value	Additional Information
Surface Size	1% of base (0.5mm)	Relative Minimum Size
	5% of base (2.5mm)	Relative Target Size
Diffuser Region		
Surface Size	1% of base (0.5mm)	Relative Minimum Size
	5% of base (2.5mm)	Relative Target Size
Notch Region		
Surface Size	1% of base (0.5mm)	Relative Minimum Size
	5% of base (2.5mm)	Relative Target Size

Table 9 - Third Attempt Mesh Properties

Figure 72 indicates that increasing the number of prism layers from 5 to 8 decreases the y+ values significantly. Whereas the default mesh properties returned a vehicle solely contained within the 'buffer layer', the increase in prism layers causes the whole vehicle to be situated within the 'viscous sub-layer'. This scenario is ideal, however, further studies were undertaken in an attempt to return a vehicle within the 'log-law' region.

The solution that has been chosen for the CFD analysis that has been undertaken for this project is detailed within the CFD section of the report.

14 Appendix C

Appendix C contains the numerical data that has been obtained through the completion of the CFD simulations and the Wind Tunnel Test programme. This tabulated data can be seen on the following pages.

14.1 CFD Simulation Data Tables

The data shown on the following pages concerns the 43° Notch on the Lynne Turner Model

0% Deployment	Yaw				
Force, Moments & Coefficients	0	10	30	60	90
Drag Force (N)	5.076	7.484	14.308	20.886	15.242
Drag Force Coefficient	0.340	0.501	0.958	1.399	1.021
Lift Force (N)	0.943	3.192	12.923	23.940	25.420
Lift Force Coefficient	0.063	0.214	0.865	1.603	1.702
Side Force (N)	-0.897	4.804	12.881	9.680	2.125
Side Force Coefficient	-0.060	0.322	0.863	0.648	0.142
Roll Moment (Nm)	-0.033	0.141	1.923	6.371	8.152
Roll Moment Coefficient	-0.002	0.009	0.129	0.427	0.546
Pitch Moment (Nm)	-0.208	-0.805	-2.598	-2.721	1.572
Pitch Moment Coefficient	-0.014	-0.054	-0.174	-0.182	0.105
Yaw Moment (Nm)	0.034	-1.110	-4.124	-6.027	-5.090
Yaw Moment Coefficient	0.002	-0.074	-0.276	-0.404	-0.341
Reference Pressure (Pa)	3.33271	3.74525	6.56809	10.85789	7.50184
Frontal Area (m^2)	0.02802	0.02802	0.02802	0.02802	0.02802

50% Deployment	Yaw				
Force, Moments & Coefficients	0	10	30	60	90
Drag Force (N)	N/A	6.965	15.214	21.622	16.788
Drag Force Coefficient	N/A	0.466	1.019	1.448	1.124
Lift Force (N)	N/A	2.550	12.142	21.067	21.830
Lift Force Coefficient	N/A	0.171	0.813	1.411	1.462
Side Force (N)	N/A	6.814	17.054	10.704	3.149
Side Force Coefficient	N/A	0.456	1.142	0.717	0.211
Roll Moment (Nm)	N/A	0.070	0.054	-0.330	-0.100
Roll Moment Coefficient	N/A	0.005	0.004	-0.022	-0.007
Pitch Moment (Nm)	N/A	0.129	0.997	1.142	1.572
Pitch Moment Coefficient	N/A	0.009	0.067	0.076	0.105
Yaw Moment (Nm)	N/A	0.606	1.151	0.965	-0.576
Yaw Moment Coefficient	N/A	0.041	0.077	0.065	-0.039
Reference Pressure (Pa)	N/A	4.59961	10.13401	14.84611	11.32190
Frontal Area (m^2)	0.02802	0.02802	0.02802	0.02802	0.02802

100% Deployment	Yaw				
Force, Moments & Coefficients	0	10	30	60	90
Drag Force (N)	N/A	7.050	15.853	24.715	20.338
Drag Force Coefficient	N/A	0.472	1.062	1.655	1.362
Lift Force (N)	N/A	2.573	11.396	16.293	14.737
Lift Force Coefficient	N/A	0.172	0.763	1.091	0.987
Side Force (N)	N/A	7.150	18.338	14.458	4.183
Side Force Coefficient	N/A	0.479	1.228	0.968	0.280
Roll Moment (Nm)	N/A	0.085	0.043	-0.686	-0.786
Roll Moment Coefficient	N/A	0.006	0.003	-0.019	-0.053
Pitch Moment (Nm)	N/A	0.109	1.071	1.545	1.659
Pitch Moment Coefficient	N/A	0.007	0.072	-0.046	0.111
Yaw Moment (Nm)	N/A	0.591	0.985	0.598	-1.012
Yaw Moment Coefficient	N/A	0.040	0.066	0.040	-0.068
Reference Pressure (Pa)	N/A	4.659	10.805	16.707	14.035
Frontal Area (m^2)	0.028	0.028	0.028	0.028	0.028

Comparison @ 10° Yaw	Fin Deployment Stage		
Force, Moments & Coefficients	0	50	100
Drag Force (N)	7.484	6.965	7.050
Drag Force Coefficient	0.501	0.466	0.472
Lift Force (N)	3.192	2.550	2.573
Lift Force Coefficient	0.214	0.171	0.172
Side Force (N)	4.804	6.814	7.150
Side Force Coefficient	0.322	0.456	0.479
Roll Moment (Nm)	0.141	0.070	0.085
Roll Moment Coefficient	0.009	0.005	0.006
Pitch Moment (Nm)	-0.805	0.129	0.109
Pitch Moment Coefficient	-0.054	0.009	0.007
Yaw Moment (Nm)	-1.110	0.606	0.591
Yaw Moment Coefficient	-0.074	0.041	0.040
Reference Pressure (Pa)	3.745	4.600	4.659
Frontal Area (m^2)	0.028	0.028	0.028

Comparison @ 30° Yaw	Fin Deployment Stage		
Force, Moments & Coefficients	0	50	100
Drag Force (N)	14.308	15.214	15.853
Drag Force Coefficient	0.958	1.019	1.062
Lift Force (N)	12.923	12.142	11.396
Lift Force Coefficient	0.865	0.813	0.763
Side Force (N)	12.881	17.054	18.338
Side Force Coefficient	0.863	1.142	1.228
Roll Moment (Nm)	1.923	0.054	0.043
Roll Moment Coefficient	0.129	0.004	0.003
Pitch Moment (Nm)	-2.598	0.997	1.071
Pitch Moment Coefficient	-0.174	0.067	0.072
Yaw Moment (Nm)	-4.124	1.151	0.985
Yaw Moment Coefficient	-0.276	0.077	0.066
Reference Pressure (Pa)	6.568	10.134	10.805
Frontal Area (m^2)	0.028	0.028	0.028

Comparison @ 60° Yaw	Fin Deployment Stage		
Force, Moments & Coefficients	0	50	100
Drag Force (N)	20.886	21.622	24.715
Drag Force Coefficient	1.399	1.448	1.655
Lift Force (N)	23.940	21.067	16.293
Lift Force Coefficient	1.603	1.411	1.091
Side Force (N)	9.680	10.704	14.458
Side Force Coefficient	0.648	0.717	0.968
Roll Moment (Nm)	6.371	-0.330	-0.686
Roll Moment Coefficient	0.427	-0.022	-0.019
Pitch Moment (Nm)	-2.721	1.142	1.545
Pitch Moment Coefficient	-0.182	0.076	-0.046
Yaw Moment (Nm)	-6.027	0.965	0.598
Yaw Moment Coefficient	-0.404	0.065	0.040
Reference Pressure (Pa)	10.858	14.846	16.707
Frontal Area (m^2)	0.028	0.028	0.028

Comparison @ 90° Yaw	Fin Deployment Stage		
Force, Moments & Coefficients	0	50	100
Drag Force (N)	15.242	16.788	20.338
Drag Force Coefficient	1.021	1.124	1.362
Lift Force (N)	25.420	21.830	14.737
Lift Force Coefficient	1.702	1.462	0.987
Side Force (N)	2.125	3.149	4.183
Side Force Coefficient	0.142	0.211	0.280
Roll Moment (Nm)	8.152	-0.100	-0.786
Roll Moment Coefficient	0.546	-0.007	-0.053
Pitch Moment (Nm)	1.572	1.572	1.659
Pitch Moment Coefficient	0.105	0.105	0.111
Yaw Moment (Nm)	-5.090	-0.576	-1.012
Yaw Moment Coefficient	-0.341	-0.039	-0.068
Reference Pressure (Pa)	7.502	11.322	14.035
Frontal Area (m^2)	0.028	0.028	0.028

14.2 Wind Tunnel Test Data

The wind tunnel test data shown is for the 43° Notch of the Lynne Turner Model at 30 m/s wind velocity.

	Test 9b - 43 degree Notch 0% Fin Deployment (30 m/s)											
	43 degree 0% Fin (30 m/s)											
	Data Section	1	1	1	1	1	1	1	1	1	1	1
	Data Section Time (sec)	825.8	825.8	825.8	825.8	825.8	825.8	825.8	825.8	825.8	825.8	825.8
	Begin Sample	470.6	506.3	535.7	563.7	595.9	648.4	679.4	708.2	737.4	765.5	799.5
	Data Section	1	1	1	1	1	1	1	1	1	1	1
	Data Section Time (sec)	825.8	825.8	825.8	825.8	825.8	825.8	825.8	825.8	825.8	825.8	825.8
	End Sample	491.3	527.4	556.3	584.8	632.7	671.1	700.6	730	759.5	789.7	820.4
	Drag Coef (user defined)	-2.1525	-2.04213	-1.89443	-1.58224	-1.14509	-0.64662	-0.20321	0.213559	0.422723	0.452982	0.453392772
	Drag Force (N)	**11.34552**	**6.123354**	**5.565557**	**6.640125**	**8.228029**	**8.116071**	**8.625411**	**8.973649**	**8.154738**	**7.453177**	**7.006595805**
	Lift Coef (user defined)	0.471763	0.062892	-0.17184	-0.15114	0.026856	0.167461	0.17351	0.17668	0.038917	-0.06175	-0.104267187
	Lift Force (N)	**-7.10589**	**-0.92705**	**2.631298**	**2.286971**	**-0.41069**	**-2.52382**	**-2.64741**	**-2.68674**	**-0.63163**	**0.974317**	**1.634633632**
	Side Coef (user defined)	-0.75652	-0.77255	-1.08178	-1.42142	-1.66887	-1.60004	-1.4822	-1.12569	-0.64179	-0.34687	-0.053429972
	Side Force (N)	**32.39179**	**32.44011**	**32.57677**	**31.57553**	**29.59471**	**25.03424**	**21.17744**	**15.10898**	**8.625296**	**4.738597**	**0.839617863**
	Roll Coef (user defined)	-0.06724	-0.09613	-0.14955	-0.19665	-0.23385	-0.21532	-0.20042	-0.15679	-0.08592	-0.04214	-0.005990116
	Roll Moment (Nm)	**31.73023**	**32.2455**	**32.42817**	**31.33773**	**29.03945**	**24.40472**	**20.59002**	**14.78239**	**8.399021**	**4.553261**	**0.781447876**
	Pitch Coef (user defined)	0.332652	0.350807	0.336006	0.288925	0.20141	0.126571	0.061544	0.01007	-0.00974	-0.00398	8.23932E-05
	Pitch Moment (Nm)	**-10.3767**	**-5.56078**	**-4.9779**	**-5.87246**	**-7.54355**	**-7.32766**	**-7.83612**	**-8.08273**	**-7.10999**	**-6.264**	**-5.776545174**
	Yaw Coef (user defined)	-0.04401	-0.00361	0.02715	0.04463	0.063178	0.085181	0.087314	0.065821	0.035879	0.020467	0.003112342
	Yaw Moment (Nm)	**-0.66237**	**-0.05496**	**0.411726**	**0.678573**	**0.95923**	**1.29868**	**1.334665**	**1.010937**	**0.554398**	**0.316559**	**0.047883755**
	Resolved Force X (N)	-32.3915	-30.8848	-28.7117	-24.0267	-17.3819	-9.87481	-3.12127	3.265568	6.533843	7.012209	7.005702935
	Resolved Force Y (N)	-11.3472	-11.6674	-16.3703	-21.538	-25.3268	-24.3942	-22.652	-17.2668	-9.90883	-5.36878	-0.8390642
	Resolved Force Z (N)	7.105888	0.927053	-2.6313	-2.28697	0.410686	2.523816	2.647411	2.686737	0.631628	-0.97432	-1.634633632
	Resolved Moment Pitch (Nm)	5.00733	5.309641	5.085355	4.381905	3.056548	1.926898	0.935766	0.154018	-0.15327	-0.05841	0.00361145
	Resolved Moment Roll (Nm)	-1.01727	-1.45292	-2.26197	-2.98488	-3.55058	-3.28039	-3.06148	-2.41023	-1.3305	-0.65187	-0.089033862
	Resolved Moment Yaw (Nm)	-0.66237	-0.05496	0.411726	0.678573	0.95923	1.29868	1.334665	1.010937	0.554398	0.316559	0.047883755
	Pitch Angle Actual (°)	0	0	0	0	0	0	0	0	0	0	0
	Yaw Angle Actual (°)	**89.99654**	**80.00023**	**70.00039**	**60.00026**	**50.0005**	**40.0003**	**30.00042**	**20.00073**	**10.00022**	**5.000434**	**0.000463288**
	Wind Speed Syn (m/s)	**29.66757**	**29.72868**	**29.70718**	**29.72146**	**29.73562**	**29.83071**	**29.89162**	**29.96803**	**30.02981**	**30.03039**	**29.99229897**
	Wind Speed Pitot (m/s)	29.53277	29.59391	29.58674	29.61283	29.64336	29.75146	29.81864	29.90061	29.9632	29.9596	29.9227828
	Fan Speed (rpm)	685.6132	685.6056	685.6064	685.5918	685.6061	685.595	685.6101	685.5958	685.6218	685.6298	685.6267908
	Pressure Ambient Tunnel Hall (mbar)	996.4977	996.5246	996.5126	996.5002	996.5098	996.4886	996.482	996.4821	996.4635	996.4439	996.4491703
	Temperature Ambient Tunnel Hall (°C)	22.32174	22.28242	22.27046	22.24541	22.20882	22.1481	22.13082	22.12347	22.09656	22.07751	22.05981945
	Temperature Tunnel Air Temp (°C)	21.55342	21.36845	20.73218	20.35702	20.57999	21.15641	21.54285	21.61346	21.04901	20.56267	20.48251442
	Sample Number (user defined)	11.99727	12.99732	13.99726	14.99732	15.99846	16.99751	17.99733	18.99741	19.99744	20.99767	21.99729665
	Air Density (kg/m3)	**1.177968**	**1.17874**	**1.181278**	**1.182773**	**1.181887**	**1.179547**	**1.177992**	**1.17771**	**1.179948**	**1.181878**	**1.182206839**
Calculations	Drag Force Coefficient (x) 30 m/s	0.753517	0.404749	0.367621	0.437624	0.542166	0.532439	0.564293	0.584225	0.527726	0.481519	0.453691012
	Lift Force Coefficient (z) 30 m/s	-0.90758	-0.11784	0.33424	0.289856	-0.05204	-0.3184	-0.33308	-0.33638	-0.07861	0.121051	0.203549574
	Side Force Coefficient (y) 30 m/s	2.151313	2.144269	2.151787	2.081015	1.950071	1.642321	1.385474	0.983664	0.558177	0.306141	0.054366926
	Rolling Moment Coefficient 30 m/s	4.052644	4.098856	4.119176	3.971811	3.679776	3.07889	2.590468	1.850771	1.045258	0.565706	0.097308277
	Pitching Moment Coefficient 30 m/s	-1.32534	-0.70685	-0.63232	-0.74429	-0.95589	-0.92446	-0.98588	-1.01197	-0.88484	-0.77825	-0.719313052
	Yawing Moment Coefficient 30 m/s	-0.0846	-0.00699	0.052299	0.086004	0.12155	0.163841	0.167917	0.12657	0.068995	0.03933	0.005962632

	Test 10b - 43 degree Notch 50% Fin Deployment (30 m/s)											
	43 degree 50% Fin (30 m/s)											
	Data Section	1	1	1	1	1	1	1	1	1	1	1
	Data Section Time (sec)	794	794	794	794	794	794	794	794	794	794	794
	Begin Sample	475.5	506	534.7	566.3	595.4	625.1	654.2	683.8	713.1	741.5	770.1
	Data Section	1	1	1	1	1	1	1	1	1	1	1
	Data Section Time (sec)	794	794	794	794	794	794	794	794	794	794	794
	End Sample	496.7	527.3	558.3	588.7	617.5	646.7	676.2	705.6	735	763.3	791.8
	Drag Coef (user defined)	-2.15494	-2.02585	-1.91388	-1.5229	-1.1595	-0.65391	-0.20367	0.211386	0.424081	0.464917	0.460211
	Drag Force (N)	**11.41817**	**6.238175**	**5.763959**	**6.914954**	**8.06215**	**8.041799**	**8.639847**	**8.827551**	**8.032396**	**7.526417**	**7.083591**
	Lift Coef (user defined)	0.449061	0.066119	-0.07219	-0.1917	0.018046	0.174266	0.181041	0.165115	0.018413	-0.09196	-0.10857
	Lift Force (N)	**-6.71199**	**-0.94865**	**1.122309**	**2.917402**	**-0.25907**	**-2.64558**	**-2.76214**	**-2.48056**	**-0.27932**	**1.415783**	**1.670552**
	Side Coef (user defined)	-0.76453	-0.78129	-1.10973	-1.4111	-1.67167	-1.60326	-1.48878	-1.11703	-0.60139	-0.30416	-0.03773
	Side Force (N)	**32.25321**	**32.04699**	**32.83565**	**30.58529**	**29.65522**	**24.97752**	**21.15202**	**14.91313**	**7.954695**	**4.041708**	**0.57821**
	Roll Coef (user defined)	-0.06425	-0.09276	-0.14641	-0.18606	-0.23	-0.21324	-0.20063	-0.15488	-0.07862	-0.03483	-0.0025
	Roll Moment (Nm)	**31.59721**	**31.85397**	**32.6086**	**30.35461**	**29.09236**	**24.33358**	**20.56734**	**14.5833**	**7.728418**	**3.861273**	**0.516091**
	Pitch Coef (user defined)	0.332703	0.349308	0.337293	0.284866	0.207574	0.12806	0.061779	0.013248	-0.00667	-0.00208	-0.00051
	Pitch Moment (Nm)	**-10.3858**	**-5.60752**	**-5.08677**	**-5.98493**	**-7.299**	**-7.22323**	**-7.83867**	**-7.89948**	**-6.93259**	**-6.28847**	**-5.85215**
	Yaw Coef (user defined)	-0.04456	-0.00187	0.026121	0.045232	0.063928	0.084759	0.085982	0.064976	0.039584	0.02428	0.003356
	Yaw Moment (Nm)	**-0.66794**	**-0.02799**	**0.391119**	**0.681401**	**0.964047**	**1.28599**	**1.306528**	**0.990361**	**0.607135**	**0.373346**	**0.05176**
	Resolved Force X (N)	-32.2515	-30.4771	-28.8873	-23.0276	-17.5355	-9.89482	-3.09225	3.19534	6.530335	7.144323	7.083356
	Resolved Force Y (N)	-11.4187	-11.7111	-16.6431	-21.2815	-25.2382	-24.3037	-22.637	-17.0343	-9.2268	-4.68245	-0.57679
	Resolved Force Z (N)	6.71199	0.948647	-1.12231	-2.9174	0.259069	2.645582	2.762135	2.480559	0.279325	-1.41578	-1.67055
	Resolved Moment Pitch (Nm)	4.988303	5.252414	5.073023	4.295663	3.127721	1.944799	0.942943	0.200698	-0.09865	-0.03323	-0.00831
	Resolved Moment Roll (Nm)	-0.96681	-1.39433	-2.19975	-2.80368	-3.4702	-3.23292	-3.05472	-2.35271	-1.20141	-0.5317	-0.03954
	Resolved Moment Yaw (Nm)	-0.66794	-0.02799	0.391119	0.681401	0.964047	1.28599	1.306528	0.990361	0.607135	0.373346	0.05176
	Pitch Angle Actual (°)	0	0	0	0	0	0	0	0	0	0	0
	Yaw Angle Actual (°)	**89.99661**	**80.00027**	**70.00035**	**60.00039**	**50.00039**	**40.00034**	**30.00043**	**20.00073**	**10.00022**	**5.000452**	**0.000426**
	Wind Speed Syn (m/s)	**29.58967**	**29.64515**	**29.62251**	**29.63962**	**29.65224**	**29.73217**	**29.79287**	**29.85264**	**29.94629**	**29.96347**	**29.94807**
	Wind Speed Pitot (m/s)	29.45106	29.50713	29.49541	29.52474	29.5538	29.64741	29.71605	29.77847	29.86892	29.88896	29.87316
	Fan Speed (rpm)	684.5329	684.5628	684.528	684.5087	684.5359	684.5275	684.5322	684.5416	684.5241	684.4993	684.539
	Pressure Ambient Tunnel Hall (mbar)	996.2173	996.2279	996.2097	996.2426	996.2072	996.2175	996.1905	996.1653	996.1663	996.1777	996.1849
	Temperature Ambient Tunnel Hall (°C)	22.01284	22.0111	21.99892	21.9845	21.95606	21.93218	21.91899	21.89411	21.89074	21.88413	21.86576
	Temperature Tunnel Air Temp (°C)	21.58824	21.48123	20.81384	20.37197	20.44559	20.79966	21.16933	21.54558	21.62042	21.07375	20.57912
	Sample Number (user defined)	11.99733	12.99735	13.99761	14.99748	15.99744	16.99738	17.99743	18.99741	19.99742	20.99741	21.9974
	Air Density (kg/m3)	**1.177498**	**1.177938**	**1.180591**	**1.182407**	**1.182068**	**1.180657**	**1.179142**	**1.177607**	**1.177309**	**1.17951**	**1.181505**
Calculations	Drag Force Coefficient (x) 30 m/s	0.762645	0.414948	0.383128	0.458398	0.534145	0.53057	0.568436	0.579216	0.523884	0.489405	0.460306
	Lift Force Coefficient (z) 30 m/s	-0.44831	-0.0631	0.074599	0.193397	-0.01716	-0.17455	-0.18173	-0.16276	-0.01822	0.092061	0.108556
	Side Force Coefficient (y) 30 m/s	2.154264	2.131688	2.182572	2.027526	1.964761	1.647929	1.391641	0.978519	0.518816	0.262812	0.037573
	Rolling Moment Coefficient 30 m/s	4.058554	4.074708	4.168231	3.869681	3.706673	3.087393	2.602257	1.840149	0.969342	0.482845	0.064494
	Pitching Moment Coefficient 30 m/s	-1.33402	-0.71731	-0.65022	-0.76297	-0.92997	-0.91647	-0.99178	-0.99677	-0.86952	-0.78636	-0.73132
	Yawing Moment Coefficient 30 m/s	-0.08579	-0.00358	0.049995	0.086867	0.12283	0.163164	0.165307	0.124966	0.07615	0.046686	0.006468

	Test 11b - 43 degree Notch 75% Fin Deployment (30 m/s)											
	43 degree 75% Fin (30 m/s)											
	Data Section	1	1	1	1	1	1	1	1	1	1	1
	Data Section Time (sec)	776.05	776.05	776.05	776.05	776.05	776.05	776.05	776.05	776.05	776.05	776.05
	Begin Sample	451.4	482	512.9	543.1	571.9	605.5	634.4	663	691.6	720.1	749.2
	Data Section	1	1	1	1	1	1	1	1	1	1	1
	Data Section Time (sec)	776.05	776.05	776.05	776.05	776.05	776.05	776.05	776.05	776.05	776.05	776.05
	End Sample	473.4	503.4	533.8	564.8	594.7	627.4	656.2	685.3	713.3	742.8	771.5
	Drag Coef (user defined)	-2.18128	-2.02088	-1.88963	-1.50428	-1.17138	-0.64997	-0.20379	0.208784	0.424953	0.464235	0.457572
	Drag Force (N)	**11.39819**	**6.534661**	**5.956203**	**7.446837**	**7.992662**	**8.102564**	**8.896801**	**8.930821**	**8.04396**	**7.521926**	**7.078913**
	Lift Coef (user defined)	0.46374	0.022572	-0.11386	-0.03006	0.021652	0.163538	0.194794	0.17155	0.017627	-0.08846	-0.10024
	Lift Force (N)	**-6.97255**	**-0.36569**	**1.71277**	**0.462028**	**-0.3538**	**-2.47301**	**-2.97601**	**-2.60362**	**-0.27094**	**1.365445**	**1.529569**
	Side Coef (user defined)	-0.75243	-0.79844	-1.10793	-1.43765	-1.66864	-1.60326	-1.51603	-1.13001	-0.60072	-0.30277	-0.03795
	Side Force (N)	**32.89307**	**32.05889**	**32.49996**	**30.72011**	**29.95763**	**25.12169**	**21.60666**	**15.18128**	**7.963884**	**4.029902**	**0.585795**
	Roll Coef (user defined)	-0.06639	-0.09006	-0.14385	-0.2009	-0.23213	-0.21414	-0.20903	-0.1586	-0.07928	-0.03506	-0.00315
	Roll Moment (Nm)	**32.29937**	**31.84509**	**32.28817**	**30.40759**	**29.39612**	**24.48345**	**21.04815**	**14.86562**	**7.753224**	**3.855744**	**0.533265**
	Pitch Coef (user defined)	0.342662	0.347938	0.334342	0.269394	0.206827	0.128451	0.058346	0.010826	-0.00682	-0.00333	-0.0021
	Pitch Moment (Nm)	**-10.4048**	**-5.81912**	**-5.22954**	**-6.74111**	**-7.27508**	**-7.28596**	**-8.16535**	**-8.04458**	**-6.95141**	**-6.3047**	**-5.87464**
	Yaw Coef (user defined)	-0.05194	-0.00257	0.026747	0.043476	0.064168	0.084119	0.081247	0.062973	0.038869	0.024309	0.003157
	Yaw Moment (Nm)	**-0.78475**	**-0.03775**	**0.4039**	**0.65953**	**0.976116**	**1.284037**	**1.242919**	**0.965328**	**0.598492**	**0.374525**	**0.049033**
	Resolved Force X (N)	-32.8934	-30.4338	-28.4947	-22.8828	-17.8072	-9.93901	-3.09922	3.199283	6.538493	7.143194	7.079342
	Resolved Force Y (N)	-11.396	-12.0033	-16.7137	-21.8119	-25.3781	-24.4531	-23.1612	-17.3192	-9.23998	-4.66959	-0.58541
	Resolved Force Z (N)	6.972546	0.365687	-1.71277	-0.46203	0.353796	2.473014	2.976007	2.603621	0.270942	-1.36545	-1.52957
	Resolved Moment Pitch (Nm)	5.161675	5.241004	5.039016	4.086118	3.149009	1.955113	0.897071	0.164561	-0.105	-0.05224	-0.03442
	Resolved Moment Roll (Nm)	-1.00165	-1.35961	-2.16982	-3.04896	-3.53188	-3.26504	-3.20346	-2.43193	-1.21951	-0.53784	-0.05028
	Resolved Moment Yaw (Nm)	-0.78475	-0.03775	0.4039	0.65953	0.976116	1.284037	1.242919	0.965328	0.598492	0.374525	0.049033
	Pitch Angle Actual (°)	0	0	0	0	0	0	0	0	0	0	0
	Yaw Angle Actual (°)	**89.99678**	**80.00021**	**70.00036**	**60.00037**	**50.00054**	**40.00037**	**30.00043**	**20.0007**	**10.00018**	**5.000467**	**0.000408**
	Wind Speed Syn (m/s)	**29.65938**	**29.67634**	**29.70055**	**29.76711**	**29.77072**	**29.81128**	**29.87088**	**29.92407**	**29.99151**	**30.02845**	**30.06341**
	Wind Speed Pitot (m/s)	29.52157	29.54093	29.57164	29.66042	29.67897	29.73188	29.79216	29.85245	29.91839	29.95573	29.9893
	Fan Speed (rpm)	685.6	685.6097	685.6059	685.6026	685.614	685.6422	685.6491	685.6192	685.6137	685.5971	685.5997
	Pressure Ambient Tunnel Hall (mbar)	996.1076	996.0892	996.0641	996.0267	996.0544	996.0853	996.0881	996.0689	996.0491	996.04	996.0231
	Temperature Ambient Tunnel Hall (°C)	21.94738	21.93373	21.93196	21.91936	21.89514	21.88069	21.86485	21.83316	21.81283	21.80527	21.80483
	Temperature Tunnel Air Temp (°C)	20.91386	21.47567	21.63792	21.00585	20.49058	20.40075	20.72096	21.08873	21.47186	21.68038	21.23132
	Sample Number (user defined)	11.99743	12.99736	13.9973	14.9974	15.99752	16.99742	17.99741	18.99747	19.9974	20.99751	21.99747
	Air Density (kg/m3)	**1.180068**	**1.177796**	**1.177118**	**1.179603**	**1.181706**	**1.182104**	**1.18082**	**1.179321**	**1.177764**	**1.17692**	**1.178696**
Calculations	Drag Force Coefficient (x) 30 m/s	0.756085	0.433809	0.39499	0.490601	0.525496	0.531094	0.581461	0.58235	0.522855	0.48807	0.457567
	Lift Force Coefficient (z) 30 m/s	-0.46252	-0.02428	0.113584	0.030439	-0.02326	-0.1621	-0.1945	-0.16977	-0.01761	0.088599	0.098868
	Side Force Coefficient (y) 30 m/s	2.181922	2.128255	2.155261	2.023855	1.969634	1.646637	1.412128	0.989923	0.51765	0.261486	0.037865
	Rolling Moment Coefficient 30 m/s	4.120269	4.065504	4.117723	3.852436	3.716761	3.086159	2.645435	1.864114	0.969148	0.481125	0.066287
	Pitching Moment Coefficient 30 m/s	-1.32728	-0.7429	-0.66692	-0.85405	-0.91984	-0.9184	-1.02626	-1.00877	-0.86892	-0.78671	-0.73024
	Yawing Moment Coefficient 30 m/s	-0.10011	-0.00482	0.05151	0.083558	0.123417	0.161854	0.156216	0.12105	0.074811	0.046734	0.006095

	Test 12b - 43 Degree Notch 100% Fin Deployment (30 m/s)											
	43 degree 100% Fin (30 m/s)											
	Data Section	1	1	1	1	1	1	1	1	1	1	1
	Data Section Time (sec)	763.7	763.7	763.7	763.7	763.7	763.7	763.7	763.7	763.7	763.7	763.7
	Begin Sample	424.2	457.4	490.4	523.6	554.5	583.8	612.7	641.8	671.9	703.9	733.1
	Data Section	1	1	1	1	1	1	1	1	1	1	1
	Data Section Time (sec)	763.7	763.7	763.7	763.7	763.7	763.7	763.7	763.7	763.7	763.7	763.7
	End Sample	446.5	483	512.1	545	576.4	605.9	634.1	663.7	693.9	726.7	755.5
	Drag Coef (user defined)	-2.21865	-2.02372	-1.86653	-1.49562	-1.18072	-0.66	-0.20804	0.208642	0.425523	0.463547	0.457771
	Drag Force (N)	**11.34521**	**6.432174**	**6.201715**	**7.494741**	**7.969996**	**8.246375**	**9.266192**	**9.069974**	**8.035752**	**7.544547**	**7.075835**
	Lift Coef (user defined)	0.425917	0.053609	-0.21602	-0.03155	0.044225	0.170849	0.206085	0.184791	0.027148	-0.08714	-0.09772
	Lift Force (N)	**-6.43788**	**-0.83785**	**3.29682**	**0.48198**	**-0.67576**	**-2.59759**	**-3.11579**	**-2.80628**	**-0.43543**	**1.364485**	**1.516438**
	Side Coef (user defined)	-0.75116	-0.79269	-1.1193	-1.4331	-1.67461	-1.63013	-1.5747	-1.15643	-0.5916	-0.2974	-0.03458
	Side Force (N)	**33.45775**	**32.15483**	**32.29852**	**30.5855**	**30.10634**	**25.53564**	**22.45049**	**15.5938**	**7.814109**	**3.957881**	**0.531593**
	Roll Coef (user defined)	-0.07062	-0.09793	-0.14324	-0.20217	-0.23464	-0.22264	-0.22614	-0.16745	-0.07844	-0.03598	-0.00422
	Roll Moment (Nm)	**32.92697**	**32.01829**	**32.20973**	**30.30711**	**29.55577**	**24.92962**	**21.95057**	**15.31847**	**7.617833**	**3.813199**	**0.502841**
	Pitch Coef (user defined)	0.352981	0.352027	0.339688	0.269648	0.208057	0.128641	0.056521	0.008695	-0.00863	-0.00389	-0.00195
	Pitch Moment (Nm)	**-10.4219**	**-5.84389**	**-5.397**	**-6.79469**	**-7.27578**	**-7.48594**	**-8.62223**	**-8.23063**	**-6.96929**	**-6.33131**	**-5.8686**
	Yaw Coef (user defined)	-0.06171	-0.00783	0.022656	0.041898	0.063698	0.07904	0.069839	0.057657	0.039328	0.024278	0.004286
	Yaw Moment (Nm)	**-0.93191**	**-0.11809**	**0.340222**	**0.635889**	**0.968098**	**1.205375**	**1.067954**	**0.883421**	**0.605508**	**0.376077**	**0.066365**
	Resolved Force X (N)	-33.4608	-30.5492	-28.2294	-22.7419	-17.9407	-10.0969	-3.2002	3.187964	6.55618	7.170662	7.076359
	Resolved Force Y (N)	-11.3469	-11.9196	-16.8753	-21.7834	-25.4574	-24.8607	-24.0747	-17.755	-9.09472	-4.59972	-0.5322
	Resolved Force Z (N)	6.437881	0.837852	-3.29682	-0.48198	0.675758	2.597592	3.115789	2.806277	0.435426	-1.36449	-1.51644
	Resolved Moment Pitch (Nm)	5.322807	5.313534	5.130993	4.088614	3.163475	1.960028	0.867818	0.13651	-0.13103	-0.0589	-0.03088
	Resolved Moment Roll (Nm)	-1.0625	-1.48251	-2.16674	-3.06646	-3.56903	-3.398	-3.45861	-2.56205	-1.21211	-0.55524	-0.06425
	Resolved Moment Yaw (Nm)	-0.93191	-0.11809	0.340222	0.635889	0.968098	1.205375	1.067954	0.883421	0.605508	0.376077	0.066365
	Pitch Angle Actual (°)	0	0	0	0	0	0	0	0	0	0	0
	Yaw Angle Actual (°)	**89.99671**	**80.00029**	**70.00034**	**60.00033**	**50.00054**	**40.00034**	**30.00045**	**20.00075**	**10.0002**	**5.000434**	**0.000408**
	Wind Speed Syn (m/s)	**29.67532**	**29.69618**	**29.71046**	**29.76369**	**29.76686**	**29.83462**	**29.87891**	**29.93913**	**30.01832**	**30.05041**	**30.03565**
	Wind Speed Pitot (m/s)	29.53944	29.56019	29.5855	29.65468	29.6749	29.75287	29.80357	29.86857	29.94009	29.97601	29.95896
	Fan Speed (rpm)	685.6203	685.6117	685.607	685.6052	685.6045	685.6087	685.6188	685.6222	685.6154	685.6077	685.5974
	Pressure Ambient Tunnel Hall (mbar)	995.9284	995.921	995.9436	995.944	995.917	995.94	995.9378	995.9374	995.9233	995.9133	995.936
	Temperature Ambient Tunnel Hall (°C)	21.93299	21.9275	21.91784	21.89576	21.88404	21.86633	21.85482	21.82384	21.80497	21.80521	21.79075
	Temperature Tunnel Air Temp (°C)	20.98091	21.24828	21.32155	20.87544	20.59113	20.78179	21.07736	21.47314	21.66925	21.08386	20.56376
	Sample Number (user defined)	11.99747	12.99779	13.9974	14.99736	15.99742	16.99744	17.99736	18.99742	19.99743	20.99752	21.99748
	Air Density (kg/m3)	**1.179587**	**1.178507**	**1.17824**	**1.180029**	**1.181139**	**1.1804**	**1.179211**	**1.177627**	**1.176827**	**1.179157**	**1.181271**
Calculations	Drag Force Coefficient (x) 30 m/s	0.75207	0.426178	0.410606	0.493693	0.524394	0.540454	0.606103	0.591679	0.521804	0.487896	0.457215
	Lift Force Coefficient (z) 30 m/s	-0.42676	-0.05551	0.218277	0.031749	-0.04446	-0.17024	-0.2038	-0.18307	-0.02827	0.088239	0.097987
	Side Force Coefficient (y) 30 m/s	2.2179	2.130488	2.138435	2.014725	1.980876	1.673566	1.468489	1.01726	0.507411	0.255951	0.03435
	Rolling Moment Coefficient 30 m/s	4.19753	4.079695	4.101069	3.839204	3.739713	3.142015	2.761132	1.921728	0.951281	0.47422	0.062484
	Pitching Moment Coefficient 30 m/s	-1.32858	-0.74461	-0.68717	-0.86073	-0.92061	-0.94349	-1.08458	-1.03255	-0.87029	-0.78738	-0.72925
	Yawing Moment Coefficient 30 m/s	-0.1188	-0.01505	0.043318	0.080552	0.122494	0.15192	0.134336	0.110827	0.075613	0.04677	0.008247

COVENTRY UNIVERSITY

Research into the Potential of Variable Aerodynamic Properties to Modify Ground Vehicle Behaviour

Summary of Amendments

James Atkinson

SID: 2191500

01/08/2014

Contents

1 Summary of Changes

The following pages describe the amendments that have been made to the thesis titled 'Research into the Potential of Variable Aerodynamic Properties to Modify Ground Vehicle Behaviour' which was submitted as an MSc by Research project. These amendments were advised by the chosen examiners from the Viva Voca conducted on 2nd April 2014 at Coventry University.

1.1 Requested Amendments

1) Provide more detail about the assumptions made in the modelling and a short description about the effects these assumptions would have on the results

2) What about temperature & humidity effects on the vehicle aerodynamic behaviour. Include a section explaining this.

3) How would repeating the wind tunnel experimental tests influence the results? A short explanation would suffice.

4) The simulated results do not include a driver. Explain the significance of the results, having included the driver.

5) Equation List: completely remove the equation list.

6) Project plan: it should not be a separate chapter. Could integrate this into the methodology section and include the plan in the appendixes.

7) Nomenclature: rewrite and provide more details, i.e. units' beside each symbol. No need to have separate section for units.

8) Literature review:
    a. Continue the sections (4.1, 4.1.1 and so on…) following chapter 4 in the same page; remove the blank section
    b. What about similar CFD work conducted by other researchers? No mentioning of this on the literature review.

9) The Bicycle Model: why include this? Does it add value to your research?

10) Device Reasoning: I don't think this should be in here, and not really a chapter in itself. Integrate this into another chapter or completely remove.

11) Design Evaluation & Simulation: should this chapter be in here?

12) CFD Analysis: you should include a summary section at the end of this chapter.

13) Wind Tunnel Testing: you should include a summary section at the end of this chapter.

14) Chapters: reduce the number of chapters

15) Chapter Numbers: you go from chapter 13 to chapter 15?

16) Chapter 15: this should be titled 'Discussion'. You should include a discussion section in the thesis. In here you would outline the challenges you faced, the challenges of software simulations, the limitations of the software, the capability of the software, the accuracy of the data, what about experimental setup and measurement…and so on…a lot more to be said.

17) Conclusion & Future Work
    a. Separate the future work from the conclusion, place future work section following conclusion. Also include the other factors that you did not consider in your research; vehicle with driver, higher yaw angle, repeating experimental tests, measuring surface roughness, using other simulation software for comparison and correlation.
    b. Conclusion should be rewritten, and include your findings in bullet points, 5-6 points should surface. As a guide no more than 1 page.

1.2 Explanation of Amendments

The details of the changes to the research project can be seen below, with a brief description of the amendments that have been made and the referenced page number of these changes.

1) An explanation detailing the assumptions that were used in the mathematical model is shown on pages 24. This section of the report states that the assumptions used within the mathematical model are;
    a. The vehicle is considered to be travelling on a level surface.
    b. The vehicles suspension is rigid.
    c. The initial steering angle of the vehicle is constant.
    d. A single tyre on each axle is modelled, leading to the 'Bicycle Model'.

2) Section 6.1.3.2 has been added to the report to identify the effect of humidity and temperature, and how these parameters affect the CFD and wind tunnel simulation setup.

3) A short description of how repeating the wind tunnel test is included in the section 6.5 Wind Tunnel Testing Summary. Also a potential future work action to complete the CFD testing for greater yaw angles past 90° is proposed within the future work section.

4) The inclusion of a driver-in-the-loop is described in section 4.3.3.3, and states how this could potentially be incorporated into the vehicle mathematical model.

5) The equation list has been removed as requested.

6) A statement on the project plan has now been added to Section 2.3 Research Approach & Methodology, with a copy of the Project Plan being made available in Appendix A, pages 91-92.

7) The Nomenclature, pages xii - xiii, has been updated and the units added where necessary.

8) Literature Review;
    a. The headings for the Literature Review, Section 3, have been reformatted so that the section headings are now in succession.
    b. A section concerning published CFD work on the subject of crosswind stability has been added, and can be seen on pages 20-21. The references that have been used in this section have also been added to the References section.

9) The reasoning for using the Bicycle Model within this research has been integrated into the report, and can be seen on page 23.

10) The Device Reasoning chapter has been removed and incorporated into the Device Conceptual Design chapter.

11) The Design Evaluation & Simulation chapter has been removed and replaced by a single chapter with explains the CFD and wind tunnel investigations, now named Simulation & Data Analysis.

12) A summary detailing the results of the CFD simulations has now been added to the CFD section (page 62).

13) A summary detailing the results of the Wind Tunnel testing has been added to the Wind Tunnel section (page 76).

14) As requested, the number of chapters has been reduced, with the contents updated accordingly.

15) The chapter and section numbering has been revised and formatted, as requested.

16) The Discussion, section 7 (page 77-78), has been rewritten as requested.

17) The Conclusion and Future Work sections have been separated, with the conclusion being placed first, as section 8, page 79.
    a. The Conclusion has been rewritten into 5 bullet points, detailing the main findings of the research.
    b. The Future Work section has been moved to section 9, and details on additional work that could be done has been highlighted.

The above amendments have been made to the document 'Research into the Potential of Variable Aerodynamic Properties to Modify Ground Vehicle Behaviour' by the author for assessment, as a requirement of a MSc by Research qualification.

James Atkinson

Variable Aerodynamics Research Project
Yaw Rate Change

Vehicle Characteristics

Vehicle Parameters	Value	Units
Vehicle Mass, m	1200	kg
Moment of Inertia, Izz	1250	kgm^2
Wheelbase, l	3	m
Distance from Front Axle to CofG, a	1.25	m
Distance from Rear Axle to CofG, b	1.75	m
Front Cornering Stiffness, CαF	-100,000	N/rad
Rear Cornering Stiffness, CαR	-100,000	N/rad
Vehicle Forward Velocity, Vx	20	m/s
Steering Angle, δ	0	degrees
Longitudinal Front Axle Force, Fxf	0	N
Vehicle Yaw Rate, r	0.436332313	Rad/Sec
CofP Position from CofG, (forward +ve)	0	m
CofP Position from CofG, (forward +ve)	-0.5	m
CofP Position from CofG, (forward +ve)	0.5	m

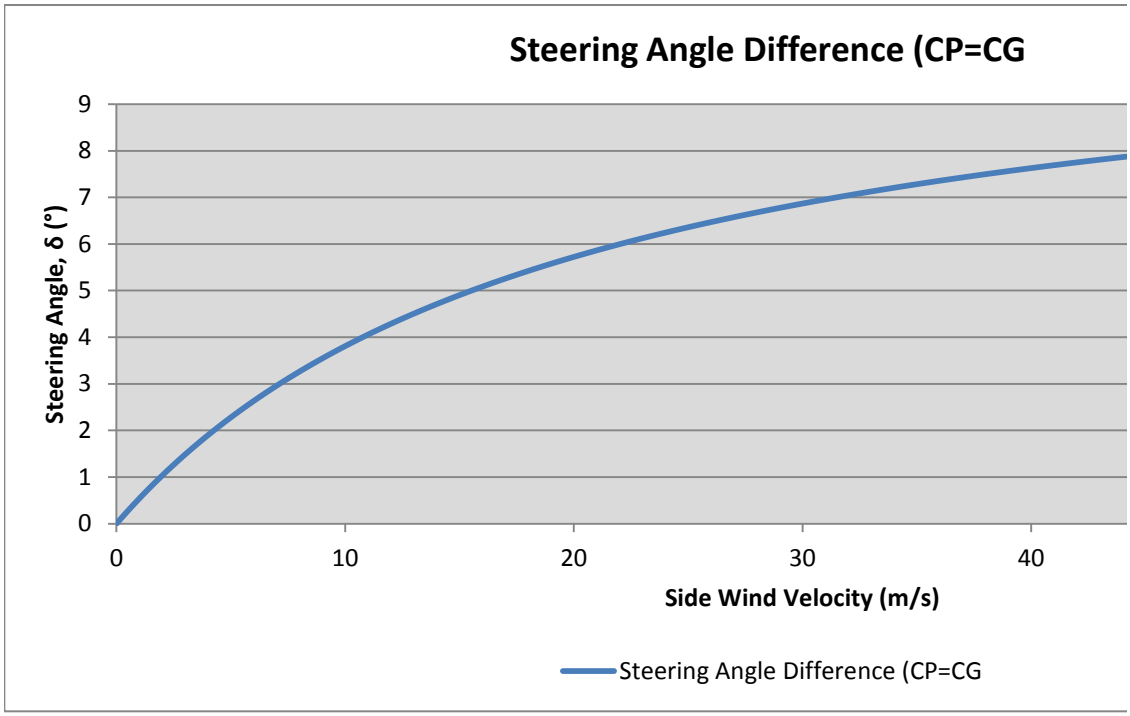

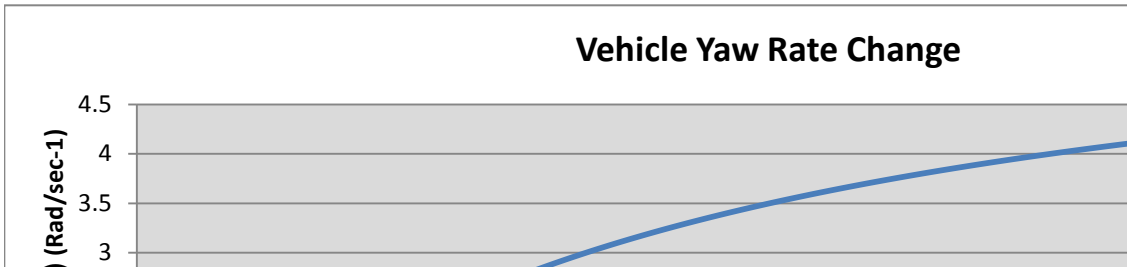

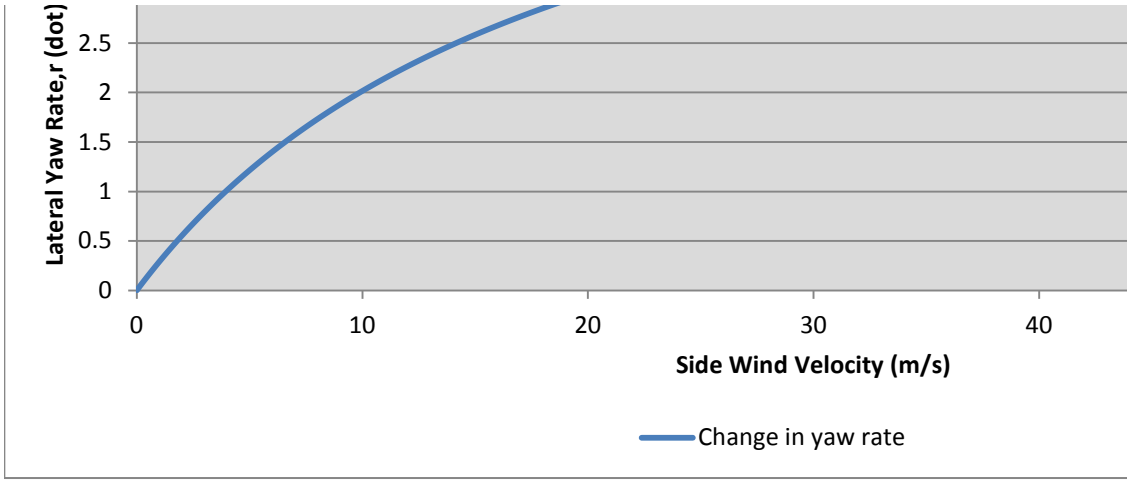
Lateral Yaw Rate,r (dot)
2.5
2
1.5
1
0.5
0
0
10
20
30
40
Side Wind Velocity (m/s)
Change in yaw rate

Side Wind Velocity m/s	Resultant Velocity m/s	Yaw Angle, β degrees	Yaw Angle in Radians Radians
0	20	0	0
0.1	20.09399837	0.09752325	0.001702102
0.2	20.18805441	0.194138056	0.003388348
0.3	20.28216733	0.289856513	0.005058951
0.4	20.37633632	0.384690509	0.006714116
0.5	20.47056063	0.478651734	0.008354049
0.6	20.56483948	0.571751682	0.009978949
0.7	20.65917214	0.664001659	0.011589015
0.8	20.75355786	0.755412777	0.01318444
0.9	20.84799593	0.845995969	0.014765415
1	20.94248564	0.935761985	0.016332128
1.1	21.03702629	1.024721398	0.017884762
1.2	21.13161721	1.112884609	0.019423501
1.3	21.22625771	1.200261847	0.020948521
1.4	21.32094714	1.286863176	0.022459999
1.5	21.41568484	1.372698492	0.023958108
1.6	21.51047019	1.457777536	0.025443018
1.7	21.60530255	1.542109889	0.026914895
1.8	21.70018131	1.625704975	0.028373904
	21.79510585	1.708572071	0.029820208
	21.8900756	1.790720302	0.031253965
	21.98508995	1.87215865	0.032675333
	22.08014834	1.95289595	0.034084464
	22.17525019	2.0329409	0.035481512
	22.27039496	2.112302059	0.036866626
	22.36558209	2.190987852	0.038239952
	22.46081104	2.26900657	0.039601635
	22.55608129	2.346366373	0.040951819
	22.65139231	2.423075297	0.042290642
	22.74674359	2.499141249	0.043618243
	22.84213463	2.574572016	0.044934759
	22.93756493	2.649375261	0.046240321
	23.033034	2.723558531	0.047535064
	23.12854137	2.797129256	0.048819115
	23.22408656	2.870094753	0.050092603
	23.3196691	2.942462226	0.051355654
	23.41528854	3.014238767	0.052608391
	23.51094443	3.085431364	0.053850936
3.8	23.60663632	3.156046897	0.05508341
	23.70236378	3.226092141	0.05630593
	23.79812638	3.29557377	0.057518613
	23.8939237	3.364498358	0.058721574
	23.98975532	3.432872379	0.059914926
	24.08562083	3.500702213	0.06109878
	24.18151983	3.567994141	0.062273245
	24.27745192	3.634754354	0.063438431

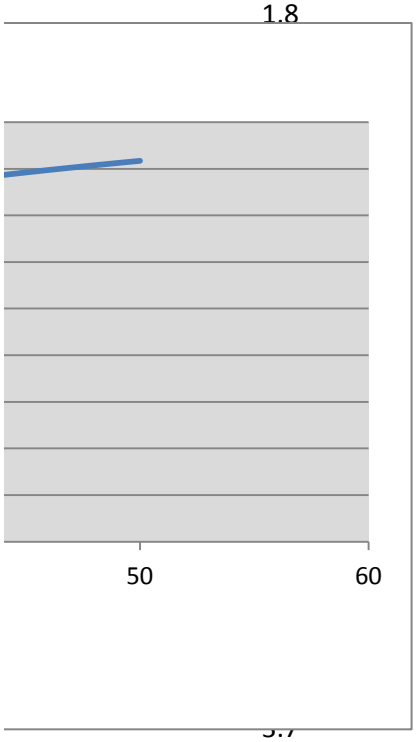

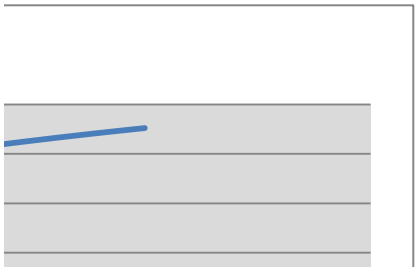

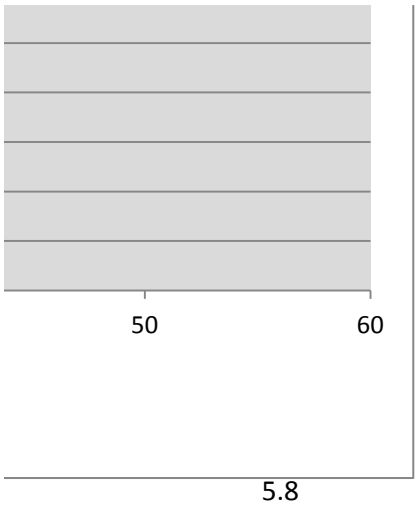

	24.37341671	3.700988951	0.064594443
	24.46941382	3.766703938	0.065741386
	24.56544287	3.831905236	0.066879363
	24.66150348	3.896598678	0.068008477
	24.75759528	3.960790011	0.069128827
	24.85371792	4.024484899	0.070240512
	24.94987104	4.087688923	0.071343631
	25.04605429	4.150407584	0.072438278
	25.14226732	4.212646302	0.073524548
	25.23850979	4.274410421	0.074602535
	25.33478137	4.335705206	0.075672331
	25.43108172	4.396535848	0.076734026
5.8	25.52741052	4.456907463	0.07778771
5.9	25.62376745	4.516825096	0.07883347
6	25.7201522	4.576293718	0.079871393
6.1	25.81656444	4.63531823	0.080901565
6.2	25.91300388	4.693903465	0.08192407
6.3	26.00947021	4.752054189	0.082938992
6.4	26.10596313	4.809775098	0.083946412
6.5	26.20248235	4.867070824	0.084946411
6.6	26.29902758	4.923945935	0.085939069
6.7	26.39559854	4.980404934	0.086924464
6.8	26.49219494	5.036452264	0.087902675
6.9	26.58881651	5.092092303	0.088873777
7	26.68546297	5.147329373	0.089837845
7.1	26.78213405	5.202167733	0.090794955
7.2	26.87882949	5.256611585	0.09174518
7.3	26.97554903	5.310665074	0.092688591
7.4	27.0722924	5.364332288	0.093625261
7.5	27.16905936	5.41761726	0.094555259
7.6	27.26584964	5.470523968	0.095478655
7.7	27.36266301	5.523056336	0.096395518
7.8	27.45949922	5.575218235	0.097305915
7.9	27.55635804	5.627013486	0.098209912
8	27.65323921	5.678445857	0.099107577
8.1	27.75014251	5.729519065	0.099998972
8.2	27.8470677	5.78023678	0.100884163
8.3	27.94401457	5.830602622	0.101763213
8.4	28.04098287	5.880620163	0.102636184
8.5	28.13797241	5.930292928	0.103503137
8.6	28.23498294	5.979624396	0.104364134
8.7	28.33201426	6.028618	0.105219233
8.8	28.42906616	6.077277128	0.106068495
8.9	28.52613842	6.125605123	0.106911978
9	28.62323084	6.173605288	0.107749739
9.1	28.72034321	6.221280879	0.108581835
9.2	28.81747533	6.268635112	0.109408322
9.3	28.91462701	6.315671161	0.110229256
9.4	29.01179804	6.36239216	0.111044691
9.5	29.10898823	6.408801202	0.111854682

9.6	29.2061974	6.454901341	0.112659281
9.7	29.30342534	6.500695591	0.113458542
9.8	29.40067189	6.54618693	0.114252515
9.9	29.49793684	6.591378295	0.115041253
10	29.59522002	6.636272588	0.115824807
10.1	29.69252126	6.680872676	0.116603225
10.2	29.78984037	6.725181385	0.117376558
10.3	29.88717718	6.769201511	0.118144854
10.4	29.98453152	6.812935812	0.118908162
10.5	30.08190321	6.856387012	0.119666528
10.6	30.17929209	6.899557802	0.120420001
10.7	30.276698	6.942450839	0.121168625
10.8	30.37412076	6.985068747	0.121912448
10.9	30.47156023	7.027414119	0.122651514
11	30.56901623	7.069489513	0.123385868
11.1	30.66648861	7.11129746	0.124115555
11.2	30.76397722	7.152840456	0.124840617
11.3	30.86148189	7.19412097	0.125561098
11.4	30.95900249	7.235141438	0.12627704
11.5	31.05653885	7.275904269	0.126988486
11.6	31.15409084	7.316411841	0.127695476
11.7	31.2516583	7.356666505	0.128398052
11.8	31.34924109	7.396670581	0.129096255
11.9	31.44683907	7.436426365	0.129790125
12	31.5444521	7.475936122	0.1304797
12.1	31.64208003	7.515202092	0.13116502
12.2	31.73972273	7.554226489	0.131846125
12.3	31.83738007	7.593011497	0.132523051
12.4	31.9350519	7.63155928	0.133195836
12.5	32.0327381	7.669871971	0.133864519
12.6	32.13043854	7.70795168	0.134529135
12.7	32.22815309	7.745800494	0.135189722
12.8	32.32588161	7.783420473	0.135846314
12.9	32.42362399	7.820813654	0.136498948
13	32.52138009	7.85798205	0.137147659
13.1	32.61914979	7.894927651	0.137792482
13.2	32.71693298	7.931652424	0.13843345
13.3	32.81472953	7.968158313	0.139070598
13.4	32.91253932	8.00444724	0.139703959
13.5	33.01036224	8.040521104	0.140333567
13.6	33.10819816	8.076381782	0.140959454
13.7	33.20604698	8.112031133	0.141581652
13.8	33.30390858	8.147470989	0.142200194
13.9	33.40178284	8.182703167	0.142815112
14	33.49966966	8.217729459	0.143426436
14.1	33.59756893	8.252551639	0.144034198
14.2	33.69548054	8.287171461	0.144638428
14.3	33.79340437	8.321590659	0.145239156
14.4	33.89134033	8.355810946	0.145836413
14.5	33.98928831	8.389834018	0.146430227

14.6	34.08724821	8.423661551	0.147020629
14.7	34.18521992	8.457295202	0.147607647
14.8	34.28320334	8.490736611	0.14819131
14.9	34.38119838	8.523987398	0.148771645
15	34.47920493	8.557049167	0.149348682
15.1	34.57722289	8.589923502	0.149922448
15.2	34.67525218	8.622611973	0.150492969
15.3	34.77329268	8.655116129	0.151060274
15.4	34.87134432	8.687437504	0.151624388
15.5	34.96940699	8.719577615	0.152185339
15.6	35.0674806	8.751537963	0.152743152
15.7	35.16556506	8.783320033	0.153297854
15.8	35.26366028	8.814925291	0.15384947
15.9	35.36176617	8.846355191	0.154398025
16	35.45988265	8.877611169	0.154943545
16.1	35.55800962	8.908694646	0.155486054
16.2	35.65614699	8.939607029	0.156025576
16.3	35.75429469	8.970349707	0.156562137
16.4	35.85245263	9.000924058	0.157095761
16.5	35.95062071	9.031331443	0.15762647
16.6	36.04879887	9.061573209	0.158154288
16.7	36.14698702	9.091650687	0.158679239
16.8	36.24518508	9.121565198	0.159201346
16.9	36.34339296	9.151318046	0.159720631
17	36.44161059	9.180910522	0.160237117
17.1	36.53983788	9.210343903	0.160750826
17.2	36.63807477	9.239619453	0.161261781
17.3	36.73632118	9.268738424	0.161770003
17.4	36.83457702	9.297702054	0.162275514
17.5	36.93284222	9.326511567	0.162778335
17.6	37.03111671	9.355168175	0.163278487
17.7	37.12940042	9.383673079	0.163775991
17.8	37.22769327	9.412027467	0.164270869
17.9	37.32599518	9.440232512	0.164763139
18	37.4243061	9.46828938	0.165252824
18.1	37.52262594	9.49619922	0.165739943
18.2	37.62095464	9.523963172	0.166224515
18.3	37.71929213	9.551582365	0.166706561
18.4	37.81763833	9.579057915	0.1671861
18.5	37.91599319	9.606390927	0.167663151
18.6	38.01435663	9.633582495	0.168137733
18.7	38.11272859	9.660633701	0.168609866
18.8	38.211109	9.687545619	0.169079567
18.9	38.3094978	9.714319309	0.169546857
19	38.40789491	9.740955821	0.170011751
19.1	38.50630029	9.767456197	0.17047427
19.2	38.60471387	9.793821465	0.170934431
19.3	38.70313557	9.820052646	0.171392251
19.4	38.80156535	9.846150748	0.171847749
19.5	38.90000314	9.872116772	0.172300942

19.6	38.99844888	9.897951706	0.172751846
19.7	39.0969025	9.92365653	0.17320048
19.8	39.19536396	9.949232215	0.17364686
19.9	39.29383318	9.974679721	0.174091003
20	39.39231012	10	0.174532925
20.1	39.49079471	10.02519399	0.174972643
20.2	39.5892869	10.05026263	0.175410174
20.3	39.68778664	10.07520684	0.175845532
20.4	39.78629385	10.10002754	0.176278735
20.5	39.8848085	10.12472563	0.176709798
20.6	39.98333052	10.149302	0.177138737
20.7	40.08185986	10.17375756	0.177565567
20.8	40.18039647	10.19809317	0.177990303
20.9	40.27894029	10.22230971	0.178412962
21	40.37749127	10.24640804	0.178833557
21.1	40.47604936	10.27038901	0.179252104
21.2	40.57461451	10.29425349	0.179668617
21.3	40.67318666	10.31800229	0.180083112
21.4	40.77176576	10.34163625	0.180495603
21.5	40.87035177	10.36515621	0.180906103
21.6	40.96894463	10.38856296	0.181314628
21.7	41.0675443	10.41185732	0.181721191
21.8	41.16615072	10.43504009	0.182125807
21.9	41.26476385	10.45811206	0.182528489
22	41.36338364	10.48107402	0.182929251
22.1	41.46201004	10.50392674	0.183328106
22.2	41.56064301	10.52667099	0.183725068
22.3	41.65928249	10.54930755	0.18412015
22.4	41.75792845	10.57183715	0.184513366
22.5	41.85658083	10.59426056	0.184904729
22.6	41.95523959	10.61657851	0.18529425
22.7	42.05390469	10.63879175	0.185681944
22.8	42.15257608	10.66090099	0.186067824
22.9	42.25125372	10.68290697	0.1864519
23	42.34993756	10.70481039	0.186834187
23.1	42.44862756	10.72661196	0.187214696
23.2	42.54732368	10.7483124	0.18759344
23.3	42.64602587	10.76991239	0.187970431
23.4	42.7447341	10.79141262	0.188345681
23.5	42.84344832	10.81281378	0.188719202
23.6	42.94216848	10.83411654	0.189091005
23.7	43.04089456	10.85532158	0.189461103
23.8	43.1396265	10.87642956	0.189829507
23.9	43.23836428	10.89744113	0.190196228
24	43.33710784	10.91835697	0.190561278
24.1	43.43585715	10.9391777	0.190924668
24.2	43.53461217	10.95990397	0.19128641
24.3	43.63337286	10.98053643	0.191646514
24.4	43.73213919	11.00107569	0.192004992
24.5	43.83091111	11.02152238	0.192361854

24.6	43.92968858	11.04187713	0.192717111
24.7	44.02847158	11.06214054	0.193070775
24.8	44.12726005	11.08231323	0.193422855
24.9	44.22605398	11.10239579	0.193773361
25	44.32485331	11.12238883	0.194122306
25.1	44.42365801	11.14229294	0.194469698
25.2	44.52246806	11.1621087	0.194815548
25.3	44.6212834	11.1818367	0.195159867
25.4	44.72010401	11.20147751	0.195502664
25.5	44.81892985	11.22103171	0.195843949
25.6	44.91776089	11.24049986	0.196183732
25.7	45.0165971	11.25988253	0.196522024
25.8	45.11543843	11.27918027	0.196858833
25.9	45.21428486	11.29839364	0.197194169
26	45.31313635	11.31752318	0.197528043
26.1	45.41199287	11.33656944	0.197860463
26.2	45.51085438	11.35553295	0.198191438
26.3	45.60972086	11.37441425	0.198520979
26.4	45.70859227	11.39321387	0.198849094
26.5	45.80746858	11.41193233	0.199175793
26.6	45.90634976	11.43057016	0.199501085
26.7	46.00523578	11.44912786	0.199824978
26.8	46.1041266	11.46760596	0.200147481
26.9	46.2030222	11.48600496	0.200468604
27	46.30192254	11.50432536	0.200788356
27.1	46.40082759	11.52256766	0.201106744
27.2	46.49973733	11.54073235	0.201423778
27.3	46.59865172	11.55881993	0.201739465
27.4	46.69757073	11.57683088	0.202053816
27.5	46.79649434	11.59476569	0.202366837
27.6	46.89542252	11.61262483	0.202678538
27.7	46.99435523	11.63040878	0.202988927
27.8	47.09329246	11.648118	0.203298011
27.9	47.19223416	11.66575297	0.203605799
28	47.29118031	11.68331415	0.203912299
28.1	47.39013089	11.70080199	0.20421752
28.2	47.48908586	11.71821696	0.204521468
28.3	47.58804521	11.7355595	0.204824153
28.4	47.68700889	11.75283006	0.205125581
28.5	47.78597689	11.77002908	0.20542576
28.6	47.88494918	11.78715701	0.205724699
28.7	47.98392573	11.80421428	0.206022405
28.8	48.08290652	11.82120132	0.206318885
28.9	48.18189151	11.83811857	0.206614146
29	48.28088069	11.85496645	0.206908197
29.1	48.37987402	11.87174539	0.207201045
29.2	48.47887149	11.8884558	0.207492697
29.3	48.57787307	11.90509809	0.20778316
29.4	48.67687872	11.9216727	0.208072441
29.5	48.77588843	11.93818001	0.208360548

29.6	48.87490218	11.95462044	0.208647488
29.7	48.97391993	11.9709944	0.208933267
29.8	49.07294167	11.98730227	0.209217893
29.9	49.17196736	12.00354446	0.209501373
30	49.270997	12.01972137	0.209783713
30.1	49.37003054	12.03583337	0.210064921
30.2	49.46906797	12.05188086	0.210345002
30.3	49.56810927	12.06786423	0.210623964
30.4	49.66715441	12.08378385	0.210901814
30.5	49.76620336	12.0996401	0.211178558
30.6	49.86525612	12.11543336	0.211454202
30.7	49.96431265	12.131164	0.211728754
30.8	50.06337293	12.14683238	0.212002219
30.9	50.16243694	12.16243889	0.212274604
31	50.26150465	12.17798387	0.212545915
31.1	50.36057605	12.19346769	0.212816158
31.2	50.45965112	12.20889071	0.213085341
31.3	50.55872982	12.22425328	0.213353468
31.4	50.65781215	12.23955576	0.213620547
31.5	50.75689807	12.25479849	0.213886583
31.6	50.85598758	12.26998182	0.214151582
31.7	50.95508064	12.2851061	0.21441555
31.8	51.05417724	12.30017167	0.214678494
31.9	51.15327735	12.31517887	0.214940419
32	51.25238097	12.33012803	0.215201331
32.1	51.35148805	12.34501949	0.215461236
32.2	51.45059859	12.35985358	0.21572014
32.3	51.54971257	12.37463062	0.215978048
32.4	51.64882996	12.38935095	0.216234966
32.5	51.74795075	12.40401489	0.2164909
32.6	51.84707492	12.41862276	0.216745856
32.7	51.94620244	12.43317488	0.216999838
32.8	52.0453333	12.44767157	0.217252853
32.9	52.14446748	12.46211313	0.217504906
33	52.24360496	12.47649989	0.217756002
33.1	52.34274572	12.49083215	0.218006147
33.2	52.44188975	12.50511022	0.218255347
33.3	52.54103702	12.51933441	0.218503606
33.4	52.64018751	12.53350501	0.218750929
33.5	52.73934122	12.54762232	0.218997323
33.6	52.83849811	12.56168666	0.219242792
33.7	52.93765817	12.5756983	0.219487341
33.8	53.03682139	12.58965755	0.219730976
33.9	53.13598775	12.6035647	0.219973702
34	53.23515722	12.61742004	0.220215523
34.1	53.3343298	12.63122384	0.220456445
34.2	53.43350546	12.64497641	0.220696472
34.3	53.53268418	12.65867802	0.22093561
34.4	53.63186596	12.67232896	0.221173864
34.5	53.73105077	12.6859295	0.221411238

34.6	53.83023859	12.69947991	0.221647738
34.7	53.92942942	12.71298049	0.221883367
34.8	54.02862323	12.72643149	0.222118131
34.9	54.12782001	12.73983319	0.222352035
35	54.22701973	12.75318585	0.222585083
35.1	54.32622239	12.76648976	0.22281728
35.2	54.42542797	12.77974516	0.223048631
35.3	54.52463645	12.79295233	0.223279139
35.4	54.62384782	12.80611152	0.22350881
35.5	54.72306206	12.819223	0.223737649
35.6	54.82227916	12.83228702	0.223965659
35.7	54.92149909	12.84530384	0.224192845
35.8	55.02072185	12.85827371	0.224419212
35.9	55.11994742	12.87119688	0.224644764
36	55.21917578	12.88407361	0.224869506
36.1	55.31840692	12.89690415	0.225093441
36.2	55.41764083	12.90968873	0.225316574
36.3	55.51687748	12.92242761	0.225538909
36.4	55.61611687	12.93512103	0.225760451
36.5	55.71535898	12.94776923	0.225981204
36.6	55.8146038	12.96037245	0.226201172
36.7	55.9138513	12.97293093	0.226420358
36.8	56.01310148	12.98544491	0.226638768
36.9	56.11235433	12.99791461	0.226856406
37	56.21160982	13.01034028	0.227073275
37.1	56.31086795	13.02272215	0.227289379
37.2	56.4101287	13.03506044	0.227504723
37.3	56.50939205	13.04735538	0.22771931
37.4	56.608658	13.05960721	0.227933145
37.5	56.70792653	13.07181614	0.228146231
37.6	56.80719762	13.0839824	0.228358572
37.7	56.90647127	13.09610622	0.228570173
37.8	57.00574745	13.10818781	0.228781036
37.9	57.10502616	13.12022739	0.228991166
38	57.20430739	13.13222518	0.229200567
38.1	57.30359111	13.14418139	0.229409243
38.2	57.40287732	13.15609625	0.229617196
38.3	57.502166	13.16796996	0.229824432
38.4	57.60145715	13.17980273	0.230030952
38.5	57.70075074	13.19159479	0.230236763
38.6	57.80004677	13.20334632	0.230441866
38.7	57.89934522	13.21505755	0.230646265
38.8	57.99864608	13.22672868	0.230849965
38.9	58.09794934	13.23835991	0.231052968
39	58.19725499	13.24995145	0.231255278
39.1	58.29656301	13.26150349	0.2314569
39.2	58.39587339	13.27301624	0.231657835
39.3	58.49518613	13.28448991	0.231858088
39.4	58.5945012	13.29592467	0.232057663
39.5	58.69381859	13.30732074	0.232256562

39.6	58.7931383	13.31867831	0.232454789
39.7	58.89246031	13.32999757	0.232652347
39.8	58.99178462	13.34127871	0.23284924
39.9	59.0911112	13.35252193	0.233045471
40	59.19044005	13.36372741	0.233241044
40.1	59.28977116	13.37489535	0.233435961
40.2	59.38910451	13.38602593	0.233630226
40.3	59.48844009	13.39711934	0.233823843
40.4	59.5877779	13.40817576	0.234016814
40.5	59.68711792	13.41919537	0.234209142
40.6	59.78646014	13.43017837	0.234400832
40.7	59.88580455	13.44112493	0.234591885
40.8	59.98515114	13.45203523	0.234782306
40.9	60.08449989	13.46290945	0.234972097
41	60.18385081	13.47374777	0.235161261
41.1	60.28320387	13.48455036	0.235349802
41.2	60.38255906	13.4953174	0.235537722
41.3	60.48191638	13.50604907	0.235725025
41.4	60.58127582	13.51674554	0.235911714
41.5	60.68063736	13.52740698	0.236097791
41.6	60.780001	13.53803355	0.23628326
41.7	60.87936671	13.54862545	0.236468123
41.8	60.97873451	13.55918282	0.236652384
41.9	61.07810436	13.56970584	0.236836045
42	61.17747627	13.58019467	0.23701911
42.1	61.27685022	13.59064948	0.237201581
42.2	61.37622621	13.60107044	0.237383461
42.3	61.47560422	13.61145771	0.237564753
42.4	61.57498425	13.62181145	0.23774546
42.5	61.67436627	13.63213182	0.237925584
42.6	61.7737503	13.64241898	0.238105129
42.7	61.87313631	13.6526731	0.238284097
42.8	61.97252429	13.66289433	0.238462491
42.9	62.07191424	13.67308282	0.238640314
43	62.17130614	13.68323874	0.238817568
43.1	62.2707	13.69336224	0.238994257
43.2	62.37009579	13.70345347	0.239170382
43.3	62.46949351	13.71351259	0.239345947
43.4	62.56889315	13.72353974	0.239520954
43.5	62.6682947	13.73353509	0.239695405
43.6	62.76769815	13.74349878	0.239869305
43.7	62.86710349	13.75343096	0.240042654
43.8	62.96651071	13.76333179	0.240215456
43.9	63.06591981	13.7732014	0.240387713
44	63.16533078	13.78303994	0.240559428
44.1	63.2647436	13.79284756	0.240730603
44.2	63.36415827	13.80262441	0.240901241
44.3	63.46357478	13.81237063	0.241071345
44.4	63.56299312	13.82208636	0.241240916
44.5	63.66241328	13.83177174	0.241409958

44.6	63.76183526	13.84142692	0.241578473
44.7	63.86125904	13.85105204	0.241746463
44.8	63.96068462	13.86064724	0.241913931
44.9	64.06011198	13.87021264	0.242080879
45	64.15954113	13.8797484	0.242247309
45.1	64.25897204	13.88925466	0.242413224
45.2	64.35840472	13.89873153	0.242578627
45.3	64.45783916	13.90817917	0.24274352
45.4	64.55727534	13.91759771	0.242907904
45.5	64.65671326	13.92698727	0.243071783
45.6	64.75615291	13.936348	0.243235158
45.7	64.85559429	13.94568003	0.243398033
45.8	64.95503738	13.95498348	0.243560409
45.9	65.05448218	13.96425848	0.243722288
46	65.15392868	13.97350518	0.243883673
46.1	65.25337687	13.98272369	0.244044567
46.2	65.35282674	13.99191414	0.24420497
46.3	65.45227829	14.00107667	0.244364887
46.4	65.55173151	14.01021139	0.244524318
46.5	65.65118639	14.01931844	0.244683266
46.6	65.75064293	14.02839793	0.244841733
46.7	65.85010111	14.03745	0.244999721
46.8	65.94956092	14.04647477	0.245157233
46.9	66.04902237	14.05547235	0.24531427
47	66.14848545	14.06444288	0.245470836
47.1	66.24795014	14.07338647	0.245626931
47.2	66.34741644	14.08230325	0.245782558
47.3	66.44688434	14.09119333	0.245937719
47.4	66.54635384	14.10005683	0.246092416
47.5	66.64582492	14.10889388	0.246246652
47.6	66.74529759	14.11770458	0.246400428
47.7	66.84477183	14.12648907	0.246553746
47.8	66.94424763	14.13524744	0.246706608
47.9	67.043725	14.14397983	0.246859017
48	67.14320391	14.15268634	0.247010975
48.1	67.24268438	14.16136709	0.247162482
48.2	67.34216638	14.17002219	0.247313542
48.3	67.44164992	14.17865176	0.247464157
48.4	67.54113498	14.1872559	0.247614327
48.5	67.64062155	14.19583474	0.247764056
48.6	67.74010965	14.20438838	0.247913345
48.7	67.83959924	14.21291693	0.248062197
48.8	67.93909034	14.2214205	0.248210612
48.9	68.03858292	14.2298992	0.248358593
49	68.138077	14.23835314	0.248506142
49.1	68.23757255	14.24678243	0.248653261
49.2	68.33706957	14.25518717	0.248799952
49.3	68.43656806	14.26356747	0.248946215
49.4	68.53606801	14.27192344	0.249092055
49.5	68.63556942	14.28025519	0.249237471

49.6	68.73507227	14.28856281	0.249382466
49.7	68.83457656	14.29684641	0.249527042
49.8	68.93408229	14.3051061	0.249671201
49.9	69.03358944	14.31334198	0.249814944
50	69.13309802	14.32155414	0.249958274

Aerodynamic Side Force	Change in Yaw Rate		
N	a21	a22	Section A
85.2588	40	18.5	0
86.06210212	40	18.41345825	0.068084072
86.86966718	40	18.32767004	0.135533931
87.68149519	40	18.24262635	0.20235802
88.49758613	40	18.15831826	0.268564639
89.31794001	40	18.07473702	0.334161949
90.14255683	40	17.99187396	0.399157975
90.9714366	40	17.90972056	0.463560607
91.8045793	40	17.82826841	0.527377607
92.64198494	40	17.74750922	0.590616605
93.48365352	40	17.66743482	0.653285106
94.32958504	40	17.58803715	0.715390493
95.17977951	40	17.50930827	0.776940025
96.03423691	40	17.43124036	0.837940845
96.89295725	40	17.35382568	0.898399977
97.75594053	40	17.27705664	0.958324333
98.62318675	40	17.20092572	1.017720711
99.49469592	40	17.12542554	1.076595799
100.370468	40	17.05054879	1.134956179
101.2505031	40	16.97628828	1.192808326
102.134801	40	16.90263692	1.25015861
103.023362	40	16.82958773	1.307013302
103.9161858	40	16.7571338	1.363378571
104.8132726	40	16.68526834	1.419260488
105.7146224	40	16.61398465	1.474665029
106.6202351	40	16.54327612	1.529598076
107.5301107	40	16.47313623	1.584065416
108.4442492	40	16.40355855	1.638072747
109.3626507	40	16.33453675	1.691625678
110.2853152	40	16.26606457	1.744729731
111.2122426	40	16.19813586	1.79739034
112.1434329	40	16.13074453	1.849612857
113.0788861	40	16.06388459	1.901402549
114.0186024	40	15.99755013	1.952764605
114.9625815	40	15.93173532	2.003704132
115.9108236	40	15.8664344	2.054226158
116.8633286	40	15.80164171	2.104335637
117.8200966	40	15.73735165	2.154037446
118.7811275	40	15.6735587	2.203336388
119.7464213	40	15.61025742	2.252237193
120.7159781	40	15.54744244	2.300744521
121.6897978	40	15.48510846	2.348862961
122.6678805	40	15.42325026	2.396597033
123.6502261	40	15.36186269	2.44395119
124.6368346	40	15.30094066	2.490929818
125.6277061	40	15.24047916	2.537537239

126.6228405	40	15.18047323	2.583777711
127.6222379	40	15.120918	2.629655427
128.6258982	40	15.06180866	2.67517452
129.6338214	40	15.00314044	2.720339062
130.6460076	40	14.94490865	2.765153067
131.6624567	40	14.88710869	2.809620487
132.6831688	40	14.82973597	2.85374522
133.7081438	40	14.77278599	2.897531106
134.7373817	40	14.71625432	2.940981928
135.7708826	40	14.66013655	2.984101417
136.8086464	40	14.60442838	3.02689325
137.8506732	40	14.54912552	3.069361049
138.8969629	40	14.49422375	3.111508388
139.9475155	40	14.43971893	3.153338786
141.0023311	40	14.38560694	3.194855716
142.0614097	40	14.33188374	3.2360626
143.1247511	40	14.27854531	3.27696281
144.1923555	40	14.22558772	3.317559673
145.2642229	40	14.17300707	3.357856469
146.3403531	40	14.12079951	3.397856432
147.4207464	40	14.06896125	3.43756275
148.5054025	40	14.01748854	3.476978567
149.5943216	40	13.96637767	3.516106985
150.6875037	40	13.91562501	3.55495106
151.7849487	40	13.86522694	3.59351381
152.8866566	40	13.8151799	3.631798207
153.9926274	40	13.76548038	3.669807186
155.1028612	40	13.71612491	3.707543641
156.217358	40	13.66711007	3.745010424
157.3361177	40	13.61843247	3.782210352
158.4591403	40	13.57008877	3.819146202
159.5864258	40	13.52207568	3.855820713
160.7179743	40	13.47438994	3.892236589
161.8537858	40	13.42702833	3.928396495
162.9938602	40	13.37998768	3.964303064
164.1381975	40	13.33326486	3.99995889
165.2867978	40	13.28685677	4.035366535
166.439661	40	13.24076035	4.070528525
167.5967871	40	13.19497257	4.105447356
168.7581762	40	13.14949047	4.140125488
169.9238282	40	13.10431109	4.17456535
171.0937432	40	13.05943152	4.208769338
172.2679211	40	13.01484889	4.242739817
173.4463619	40	12.97056035	4.276479123
174.6290657	40	12.92656312	4.30998956
175.8160324	40	12.8828544	4.343273401
177.0072621	40	12.83943148	4.376332892
178.2027547	40	12.79629165	4.409170249
179.4025102	40	12.75343222	4.44178766
180.6065287	40	12.71085058	4.474187283

181.8148101	40	12.66854411	4.506371252
183.0273545	40	12.62651023	4.538341669
184.2441618	40	12.58474641	4.570100615
185.465232	40	12.54325013	4.60165014
186.6905652	40	12.5020189	4.632992269
187.9201613	40	12.46105027	4.664129004
189.1540204	40	12.42034181	4.695062319
190.3921424	40	12.37989114	4.725794164
191.6345273	40	12.33969588	4.756326466
192.8811752	40	12.29975369	4.786661126
194.1320861	40	12.26006226	4.816800023
195.3872598	40	12.2206193	4.846745012
196.6466965	40	12.18142256	4.876497925
197.9103962	40	12.14246981	4.906060571
199.1783587	40	12.10375883	4.935434738
200.4505843	40	12.06528744	4.964622191
201.7270727	40	12.02705351	4.993624673
203.0078241	40	11.98905488	5.022443909
204.2928385	40	11.95128946	5.051081598
205.5821157	40	11.91375516	5.079539422
206.875656	40	11.87644993	5.107819043
208.1734591	40	11.83937174	5.135922099
209.4755252	40	11.80251857	5.163850213
210.7818543	40	11.76588843	5.191604986
212.0924463	40	11.72947937	5.219188
213.4073012	40	11.69328943	5.246600819
214.726419	40	11.65731671	5.273844987
216.0497998	40	11.62155929	5.300922031
217.3774436	40	11.5860153	5.32783346
218.7093503	40	11.55068289	5.354580764
220.0455199	40	11.51556022	5.381165416
221.3859525	40	11.48064548	5.407588873
222.730648	40	11.44593686	5.433852573
224.0796064	40	11.41143261	5.459957938
225.4328278	40	11.37713095	5.485906374
226.7903121	40	11.34303016	5.511699269
228.1520594	40	11.30912852	5.537337997
229.5180696	40	11.27542434	5.562823916
230.8883427	40	11.24191593	5.588158366
232.2628788	40	11.20860163	5.613342673
233.6416778	40	11.17547981	5.63837815
235.0247398	40	11.14254883	5.663266091
236.4120647	40	11.1098071	5.688007779
237.8036525	40	11.07725302	5.712604479
239.1995033	40	11.04488503	5.737057444
240.599617	40	11.01270157	5.761367912
242.0039937	40	10.98070109	5.785537107
243.4126333	40	10.94888209	5.80956624
244.8255358	40	10.91724306	5.833456507
246.2427013	40	10.8857825	5.857209092

247.6641297	40	10.85449895	5.880825165
249.0898211	40	10.82339095	5.904305883
250.5197754	40	10.79245706	5.927652391
251.9539926	40	10.76169585	5.95086582
253.3924728	40	10.73110592	5.973947289
254.8352159	40	10.70068586	5.996897904
256.282222	40	10.67043429	6.019718762
257.733491	40	10.64034986	6.042410943
259.189023	40	10.61043121	6.06497552
260.6488178	40	10.58067699	6.087413551
262.1128757	40	10.5510859	6.109726083
263.5811964	40	10.52165661	6.131914153
265.0537801	40	10.49238783	6.153978786
266.5306268	40	10.46327828	6.175920995
268.0117363	40	10.43432669	6.197741784
269.4971089	40	10.40553181	6.219442145
270.9867443	40	10.37689238	6.241023059
272.4806427	40	10.34840718	6.262485498
273.9788041	40	10.320075	6.283830422
275.4812284	40	10.29189462	6.305058781
276.9879156	40	10.26386486	6.326171516
278.4988657	40	10.23598453	6.347169557
280.0140788	40	10.20825247	6.368053826
281.5335549	40	10.18066751	6.388825232
283.0572939	40	10.15322852	6.409484678
284.5852958	40	10.12593436	6.430033054
286.1175607	40	10.09878391	6.450471244
287.6540885	40	10.07177606	6.47080012
289.1948792	40	10.0449097	6.491020548
290.7399329	40	10.01818376	6.511133382
292.2892495	40	9.991597144	6.531139469
293.8428291	40	9.965148799	6.551039647
295.4006716	40	9.938837664	6.570834743
296.962777	40	9.912662695	6.59052558
298.5291454	40	9.886622855	6.610112968
300.0997767	40	9.86071712	6.629597712
301.674671	40	9.834944476	6.648980608
303.2538282	40	9.809303917	6.668262442
304.8372483	40	9.78379445	6.687443994
306.4249314	40	9.758415088	6.706526036
308.0168774	40	9.733164857	6.725509332
309.6130864	40	9.708042791	6.744394637
311.2135583	40	9.683047933	6.763182699
312.8182931	40	9.658179337	6.781874261
314.4272909	40	9.633436064	6.800470055
316.0405516	40	9.608817185	6.818970807
317.6580753	40	9.584321782	6.837377237
319.2798619	40	9.559948942	6.855690056
320.9059114	40	9.535697765	6.873909968
322.5362239	40	9.511567356	6.892037672

324.1707993	40	9.48755683	6.910073859
325.8096377	40	9.463665312	6.928019212
327.452739	40	9.439891932	6.945874408
329.1001033	40	9.416235832	6.963640119
330.7517304	40	9.39269616	6.981317008
332.4076206	40	9.369272072	6.998905733
334.0677736	40	9.345962732	7.016406945
335.7321896	40	9.322767314	7.03382129
337.4008686	40	9.299684996	7.051149405
339.0738104	40	9.276714968	7.068391923
340.7510153	40	9.253856424	7.08554947
342.432483	40	9.231108568	7.102622667
344.1182137	40	9.20847061	7.119612128
345.8082074	40	9.185941768	7.136518462
347.502464	40	9.163521267	7.15334227
349.2009835	40	9.14120834	7.17008415
350.9037659	40	9.119002226	7.186744694
352.6108113	40	9.096902171	7.203324486
354.3221197	40	9.074907429	7.219824107
356.037691	40	9.05301726	7.236244131
357.7575252	40	9.031230931	7.252585127
359.4816224	40	9.009547717	7.26884766
361.2099825	40	8.987966898	7.285032286
362.9426055	40	8.96648776	7.301139561
364.6794915	40	8.945109598	7.317170031
366.4206404	40	8.923831711	7.33312424
368.1660523	40	8.902653405	7.349002725
369.9157271	40	8.881573994	7.36480602
371.6696648	40	8.860592797	7.380534652
373.4278655	40	8.839709137	7.396189144
375.1903291	40	8.818922347	7.411770015
376.9570557	40	8.798231763	7.427277778
378.7280452	40	8.777636729	7.442712941
380.5032976	40	8.757136592	7.45807601
382.282813	40	8.736730709	7.473367482
384.0665913	40	8.71641844	7.488587854
385.8546326	40	8.69619915	7.503737615
387.6469368	40	8.676072212	7.518817251
389.4435039	40	8.656037002	7.533827244
391.244334	40	8.636092905	7.548768072
393.049427	40	8.616239307	7.563640206
394.858783	40	8.596475603	7.578444115
396.6724019	40	8.576801191	7.593180264
398.4902837	40	8.557215477	7.607849114
400.3124285	40	8.537717869	7.622451119
402.1388362	40	8.518307782	7.636986732
403.9695069	40	8.498984636	7.651456401
405.8044405	40	8.479747856	7.665860571
407.643637	40	8.460596872	7.68019968
409.4870965	40	8.441531117	7.694474165

411.334819	40	8.422550033	7.708684459
413.1868043	40	8.403653063	7.72283099
415.0430526	40	8.384839656	7.736914182
416.9035639	40	8.366109267	7.750934457
418.768338	40	8.347461354	7.764892232
420.6373752	40	8.32889538	7.77878792
422.5106752	40	8.310410814	7.792621931
424.3882382	40	8.292007128	7.806394673
426.2700642	40	8.273683798	7.820106547
428.1561531	40	8.255440306	7.833757953
430.0465049	40	8.237276138	7.847349287
431.9411196	40	8.219190784	7.860880942
433.8399973	40	8.201183738	7.874353307
435.743138	40	8.1832545	7.887766768
437.6505416	40	8.16540257	7.901121706
439.5622081	40	8.147627458	7.914418502
441.4781375	40	8.129928674	7.927657531
443.39833	40	8.112305732	7.940839166
445.3227853	40	8.094758154	7.953963776
447.2515036	40	8.077285461	7.967031728
449.1844848	40	8.059887181	7.980043386
451.121729	40	8.042562846	7.992999109
453.0632361	40	8.02531199	8.005899255
455.0090061	40	8.008134153	8.018744177
456.9590391	40	7.991028876	8.031534228
458.913335	40	7.973995707	8.044269756
460.8718939	40	7.957034196	8.056951104
462.8347157	40	7.940143896	8.069578618
464.8018004	40	7.923324366	8.082152634
466.7731481	40	7.906575165	8.094673492
468.7487587	40	7.88989586	8.107141524
470.7286323	40	7.873286018	8.119557061
472.7127688	40	7.856745212	8.131920433
474.7011682	40	7.840273015	8.144231965
476.6938306	40	7.823869008	8.156491979
478.6907559	40	7.807532772	8.168700797
480.6919442	40	7.791263893	8.180858736
482.6973954	40	7.775061959	8.192966112
484.7071095	40	7.758926563	8.205023236
486.7210866	40	7.742857299	8.217030419
488.7393266	40	7.726853768	8.228987968
490.7618296	40	7.710915569	8.240896188
492.7885955	40	7.695042309	8.252755383
494.8196243	40	7.679233596	8.264565851
496.8549161	40	7.66348904	8.276327891
498.8944709	40	7.647808256	8.288041798
500.9382885	40	7.632190862	8.299707864
502.9863691	40	7.616636478	8.311326381
505.0387127	40	7.601144727	8.322897636
507.0953191	40	7.585715235	8.334421915

509.1561886	40	7.570347633	8.345899502
511.2213209	40	7.555041551	8.357330678
513.2907162	40	7.539796626	8.368715722
515.3643745	40	7.524612494	8.380054911
517.4422957	40	7.509488798	8.39134852
519.5244798	40	7.49442518	8.402596821
521.6109268	40	7.479421286	8.413800084
523.7016368	40	7.464476767	8.424958579
525.7966098	40	7.449591273	8.43607257
527.8958457	40	7.434764458	8.447142322
529.9993445	40	7.419995981	8.458168096
532.1071062	40	7.405285501	8.469150154
534.2191309	40	7.39063268	8.480088751
536.3354186	40	7.376037183	8.490984146
538.4559692	40	7.361498677	8.50183659
540.5807827	40	7.347016834	8.512646336
542.7098592	40	7.332591324	8.523413634
544.8431986	40	7.318221824	8.534138733
546.9808009	40	7.303908012	8.544821877
549.1226662	40	7.289649566	8.555463311
551.2687944	40	7.275446169	8.566063278
553.4191856	40	7.261297506	8.576622018
555.5738397	40	7.247203265	8.58713977
557.7327567	40	7.233163135	8.597616769
559.8959367	40	7.219176808	8.608053252
562.0633796	40	7.205243977	8.618449452
564.2350855	40	7.19136434	8.628805599
566.4110543	40	7.177537595	8.639121923
568.591286	40	7.163763444	8.649398653
570.7757807	40	7.150041589	8.659636014
572.9645383	40	7.136371735	8.669834232
575.1575589	40	7.122753592	8.679993528
577.3548424	40	7.109186867	8.690114123
579.5563888	40	7.095671274	8.700196238
581.7621982	40	7.082206526	8.71024009
583.9722705	40	7.068792339	8.720245895
586.1866058	40	7.055428433	8.730213868
588.405204	40	7.042114526	8.740144222
590.6280651	40	7.028850342	8.750037167
592.8551892	40	7.015635605	8.759892914
595.0865762	40	7.002470041	8.769711671
597.3222262	40	6.989353379	8.779493644
599.5621391	40	6.976285348	8.78923904
601.806315	40	6.963265683	8.798948061
604.0547537	40	6.950294116	8.808620909
606.3074555	40	6.937370384	8.818257785
608.5644201	40	6.924494226	8.827858889
610.8256477	40	6.911665381	8.837424418
613.0911383	40	6.898883591	8.846954568
615.3608917	40	6.8861486	8.856449535

617.6349082	40	6.873460153	8.865909511
619.9131875	40	6.860817998	8.875334689
622.1957298	40	6.848221885	8.884725258
624.4825351	40	6.835671563	8.89408141
626.7736033	40	6.823166787	8.903403331
629.0689344	40	6.81070731	8.912691207
631.3685284	40	6.79829289	8.921945224
633.6723854	40	6.785923283	8.931165567
635.9805054	40	6.77359825	8.940352416
638.2928883	40	6.761317552	8.949505955
640.6095341	40	6.749080952	8.958626361
642.9304429	40	6.736888215	8.967713815
645.2556146	40	6.724739108	8.976768493
647.5850492	40	6.712633399	8.985790571
649.9187468	40	6.700570857	8.994780225
652.2567073	40	6.688551254	9.003737627
654.5989308	40	6.676574363	9.012662951
656.9454172	40	6.664639958	9.021556367
659.2961665	40	6.652747815	9.030418045
661.6511788	40	6.640897712	9.039248155
664.010454	40	6.629089429	9.048046862
666.3739922	40	6.617322745	9.056814335
668.7417933	40	6.605597444	9.065550738
671.1138573	40	6.593913309	9.074256235
673.4901843	40	6.582270125	9.082930989
675.8707742	40	6.570667679	9.091575161
678.2556271	40	6.559105759	9.100188913
680.6447429	40	6.547584155	9.108772404
683.0381216	40	6.536102658	9.117325792
685.4357633	40	6.52466106	9.125849235
687.8376679	40	6.513259155	9.134342888
690.2438355	40	6.50189674	9.142806908
692.654266	40	6.490573609	9.151241447
695.0689594	40	6.479289563	9.15964666
697.4879158	40	6.468044399	9.168022697
699.9111351	40	6.456837919	9.176369711
702.3386174	40	6.445669926	9.18468785
704.7703626	40	6.434540222	9.192977263
707.2063708	40	6.423448613	9.201238099
709.6466418	40	6.412394904	9.209470504
712.0911759	40	6.401378903	9.217674625
714.5399728	40	6.39040042	9.225850605
716.9930327	40	6.379459263	9.233998589
719.4503556	40	6.368555245	9.24211872
721.9119413	40	6.357688177	9.250211139
724.3777901	40	6.346857874	9.258275987
726.8479017	40	6.336064151	9.266313406
729.3222763	40	6.325306824	9.274323532
731.8009139	40	6.314585711	9.282306506
734.2838144	40	6.30390063	9.290262463

736.7709778	40	6.293251401	9.298191541
739.2624041	40	6.282637846	9.306093874
741.7580934	40	6.272059786	9.313969597
744.2580457	40	6.261517045	9.321818844
746.7622609	40	6.251009448	9.329641747
749.270739	40	6.240536821	9.337438438
751.7834801	40	6.23009899	9.345209048
754.3004841	40	6.219695783	9.352953708
756.821751	40	6.20932703	9.360672545
759.3472809	40	6.198992561	9.368365689
761.8770737	40	6.188692208	9.376033268
764.4111295	40	6.178425802	9.383675407
766.9494482	40	6.168193177	9.391292233
769.4920298	40	6.157994169	9.39888387
772.0388744	40	6.147828612	9.406450444
774.5899819	40	6.137696344	9.413992077
777.1453524	40	6.127597203	9.421508891
779.7049858	40	6.117531026	9.429001009
782.2688821	40	6.107497655	9.436468552
784.8370414	40	6.09749693	9.443911639
787.4094636	40	6.087528693	9.451330391
789.9861488	40	6.077592787	9.458724926
792.5670969	40	6.067689056	9.466095361
795.1523079	40	6.057817345	9.473441814
797.7417819	40	6.0479775	9.480764402
800.3355188	40	6.038169368	9.488063239
802.9335187	40	6.028392797	9.495338441
805.5357815	40	6.018647636	9.502590122
808.1423072	40	6.008933734	9.509818395
810.7530959	40	5.999250943	9.517023373
813.3681475	40	5.989599113	9.524205168
815.9874621	40	5.979978099	9.531363892
818.6110396	40	5.970387752	9.538499654
821.2388801	40	5.960827929	9.545612564
823.8709834	40	5.951298484	9.552702733
826.5073498	40	5.941799273	9.559770267
829.147979	40	5.932330155	9.566815275
831.7928712	40	5.922890986	9.573837865
834.4420264	40	5.913481626	9.580838142
837.0954444	40	5.904101935	9.587816212
839.7531255	40	5.894751774	9.59477218
842.4150694	40	5.885431004	9.601706151
845.0812763	40	5.876139487	9.608618229
847.7517462	40	5.866877088	9.615508516
850.426479	40	5.85764367	9.622377115
853.1054747	40	5.848439098	9.629224127
855.7887333	40	5.839263238	9.636049655
858.4762549	40	5.830115957	9.642853799
861.1680395	40	5.820997122	9.649636658
863.864087	40	5.811906601	9.656398332

866.5643974	40	5.802844264	9.66313892
869.2689708	40	5.793809981	9.66985852
871.9778071	40	5.784803622	9.676557228
874.6909063	40	5.775825058	9.683235143
877.4082685	40	5.766874163	9.68989236
880.1298936	40	5.757950808	9.696528976
882.8557817	40	5.749054869	9.703145085
885.5859327	40	5.740186218	9.709740781
888.3203466	40	5.731344733	9.716316159
891.0590235	40	5.722530289	9.722871313
893.8019633	40	5.713742762	9.729406334
896.5491661	40	5.70498203	9.735921315
899.3006318	40	5.696247973	9.742416349
902.0563604	40	5.687540468	9.748891525
904.816352	40	5.678859395	9.755346936
907.5806065	40	5.670204635	9.761782669
910.349124	40	5.66157607	9.768198816
913.1219044	40	5.652973581	9.774595466
915.8989477	40	5.644397051	9.780972705
918.680254	40	5.635846362	9.787330623
921.4658232	40	5.6273214	9.793669307
924.2556554	40	5.618822049	9.799988844
927.0497505	40	5.610348194	9.806289319
929.8481085	40	5.601899721	9.812570819
932.6507295	40	5.593476517	9.818833429
935.4576134	40	5.58507847	9.825077234
938.2687603	40	5.576705467	9.831302318
941.0841701	40	5.568357398	9.837508765
943.9038428	40	5.560034152	9.843696658
946.7277785	40	5.551735618	9.849866079
949.5559772	40	5.543461688	9.856017112
952.3884387	40	5.535212252	9.862149838
955.2251632	40	5.526987203	9.868264338
958.0661507	40	5.518786434	9.874360694
960.911401	40	5.510609837	9.880438985
963.7609144	40	5.502457307	9.886499291
966.6146906	40	5.494328738	9.892541692
969.4727298	40	5.486224024	9.898566267
972.335032	40	5.478143062	9.904573094
975.2015971	40	5.470085749	9.910562251
978.0724251	40	5.46205198	9.916533817
980.947516	40	5.454041653	9.922487867
983.8268699	40	5.446054667	9.928424479
986.7104868	40	5.43809092	9.934343729
989.5983666	40	5.430150311	9.940245693
992.4905093	40	5.42223274	9.946130446
995.3869149	40	5.414338108	9.951998063
998.2875836	40	5.406466316	9.957848618
1001.192515	40	5.398617264	9.963682186
1004.10171	40	5.390790856	9.96949884

1007.015167	40	5.382986993	9.975298654
1009.932887	40	5.37520558	9.9810817
1012.854871	40	5.367446519	9.98684805
1015.781117	40	5.359709715	9.992597777
1018.711626	40	5.351995073	9.998330952

Section B	Section C	Change in yaw rate Total	Yaw Rate Change (CP=(Rad/sec-1
8.07214779	0	8.07214779	0
8.034386827	0	8.102470899	0.030323109
7.99695466	0	8.132488591	0.060340801
7.959847348	0	8.162205369	0.090057578
7.923061008	0	8.191625647	0.119477857
7.886591811	0	8.22075376	0.148605969
7.850435981	0	8.249593956	0.177446165
7.814589798	0	8.278150405	0.206002614
7.779049592	0	8.306427199	0.234279408
7.743811748	0	8.334428352	0.262280562
7.708872699	0	8.362157805	0.290010015
7.674228931	0	8.389619424	0.317471633
7.639876978	0	8.416817003	0.344669213
7.605813424	0	8.443754269	0.371606478
7.5720349	0	8.470434877	0.398287087
7.538538086	0	8.496862419	0.424714628
7.505319707	0	8.523040418	0.450892627
7.472376536	0	8.548972335	0.476824545
7.439705389	0	8.574661569	0.502513778
7.40730313	0	8.600111456	0.527963665
7.375166664	0	8.625325274	0.553177484
7.343292939	0	8.650306242	0.578158451
7.31167895	0	8.675057521	0.60290973
7.280321728	0	8.699582216	0.627434426
7.249218351	0	8.72388338	0.65173559
7.218365933	0	8.747964009	0.675816218
7.187761632	0	8.771827047	0.699679257
7.157402642	0	8.795475389	0.723327599
7.1272862	0	8.818911878	0.746764088
7.097409577	0	8.842139308	0.769991517
7.067770084	0	8.865160425	0.793012634
7.03836507	0	8.887977927	0.815830137
7.009191919	0	8.910594468	0.838446678
6.98024805	0	8.933012655	0.860864865
6.951530921	0	8.955235052	0.883087262
6.923038021	0	8.977264179	0.905116388
6.894766876	0	8.999102513	0.926954722
6.866715044	0	9.02075249	0.9486047
6.838880119	0	9.042216507	0.970068716
6.811259725	0	9.063496918	0.991349127
6.783851519	0	9.08459604	1.012448249
6.756653191	0	9.105516151	1.033368361
6.72966246	0	9.126259493	1.054111703
6.70287708	0	9.146828269	1.074680479
6.67629483	0	9.167224648	1.095076857
6.649913522	0	9.187450762	1.115302971

6.623730998	0	9.207508709	1.135360918
6.597745128	0	9.227400554	1.155252764
6.571953809	0	9.247128329	1.174980538
6.546354969	0	9.266694031	1.19454624
6.520946561	0	9.286099628	1.213951837
6.495726567	0	9.305347054	1.233199264
6.470692996	0	9.324438216	1.252290425
6.445843881	0	9.343374987	1.271227196
6.421177285	0	9.362159212	1.290011422
6.396691292	0	9.380792709	1.308644918
6.372384014	0	9.399277264	1.327129474
6.348253589	0	9.417614638	1.345466848
6.324298176	0	9.435806564	1.363658773
6.300515961	0	9.453854747	1.381706957
6.276905151	0	9.471760868	1.399613077
6.25346398	0	9.48952658	1.417378789
6.230190702	0	9.507153511	1.435005721
6.207083594	0	9.524643267	1.452495477
6.184140957	0	9.541997426	1.469849636
6.161361112	0	9.559217544	1.487069754
6.138742404	0	9.576305154	1.504157363
6.116283196	0	9.593261763	1.521113973
6.093981875	0	9.61008886	1.537941069
6.071836848	0	9.626787908	1.554640117
6.04984654	0	9.64336035	1.57121256
6.0280094	0	9.659807607	1.587659817
6.006323894	0	9.67613108	1.60398329
5.984788508	0	9.692332149	1.620184358
5.963401748	0	9.708412172	1.636264381
5.942162137	0	9.72437249	1.652224699
5.92106822	0	9.740214422	1.668066632
5.900118557	0	9.75593927	1.68379148
5.879311727	0	9.771548316	1.699400525
5.858646328	0	9.787042823	1.714895033
5.838120974	0	9.802424038	1.730276247
5.817734297	0	9.817693187	1.745545396
5.797484947	0	9.832851481	1.760703691
5.777371588	0	9.847900113	1.775752323
5.757392903	0	9.86284026	1.790692469
5.737547592	0	9.87767308	1.80552529
5.717834367	0	9.892399717	1.820251927
5.698251961	0	9.907021298	1.834873508
5.678799118	0	9.921538935	1.849391145
5.6594746	0	9.935953723	1.863805933
5.640277184	0	9.950266743	1.878118953
5.62120566	0	9.964479061	1.892331271
5.602258836	0	9.978591728	1.906443938
5.583435532	0	9.992605781	1.92045799
5.564734581	0	10.00652224	1.934374451
5.546154834	0	10.02034212	1.948194327

5.527695154	0	10.03406641	1.961918615
5.509354416	0	10.04769609	1.975548295
5.49113151	0	10.06123212	1.989084334
5.47302534	0	10.07467548	2.002527689
5.455034822	0	10.08802709	2.015879301
5.437158886	0	10.10128789	2.029140099
5.419396472	0	10.11445879	2.042311
5.401746536	0	10.1275407	2.05539291
5.384208045	0	10.14053451	2.06838672
5.366779977	0	10.1534411	2.081293313
5.349461323	0	10.16626135	2.094113556
5.332251087	0	10.1789961	2.106848309
5.315148282	0	10.19164621	2.119498417
5.298151936	0	10.20421251	2.132064716
5.281261085	0	10.21669582	2.144548032
5.264474778	0	10.22909697	2.156949178
5.247792074	0	10.24141675	2.169268957
5.231212045	0	10.25365595	2.181508163
5.214733772	0	10.26581537	2.193667579
5.198356345	0	10.27789577	2.205747977
5.182078869	0	10.28989791	2.217750121
5.165900454	0	10.30182255	2.229674763
5.149820225	0	10.31367044	2.241522648
5.133837314	0	10.3254423	2.253294509
5.117950863	0	10.33713886	2.264991072
5.102160025	0	10.34876084	2.276613053
5.086463961	0	10.36030895	2.288161158
5.070861845	0	10.37178388	2.299636085
5.055352855	0	10.38318631	2.311038524
5.039936183	0	10.39451695	2.322369156
5.024611027	0	10.40577644	2.333628653
5.009376596	0	10.41696547	2.344817679
4.994232107	0	10.42808468	2.355936889
4.979176784	0	10.43913472	2.366986932
4.964209864	0	10.45011624	2.377968447
4.949330587	0	10.46102986	2.388882066
4.934538207	0	10.4718762	2.399728414
4.919831981	0	10.4826559	2.410508106
4.905211179	0	10.49336954	2.421221754
4.890675075	0	10.50401775	2.431869958
4.876222953	0	10.5146011	2.442453312
4.861854104	0	10.5251202	2.452972405
4.847567829	0	10.53557561	2.463427817
4.833363433	0	10.54596791	2.473820122
4.819240232	0	10.55629768	2.484149886
4.805197547	0	10.56656546	2.494417668
4.791234707	0	10.57677181	2.504624024
4.777351048	0	10.58691729	2.514769498
4.763545915	0	10.59700242	2.524854632
4.749818658	0	10.60702775	2.53487996

4.736168635	0	10.6169938	2.544846009
4.722595209	0	10.62690109	2.554753302
4.709097752	0	10.63675014	2.564602353
4.695675643	0	10.64654146	2.574393672
4.682328266	0	10.65627555	2.584127764
4.669055011	0	10.66595292	2.593805125
4.655855277	0	10.67557404	2.603426248
4.642728467	0	10.68513941	2.61299162
4.629673991	0	10.69464951	2.62250172
4.616691266	0	10.70410482	2.631957026
4.603779715	0	10.7135058	2.641358007
4.590938765	0	10.72285292	2.650705127
4.578167851	0	10.73214664	2.659998846
4.565466414	0	10.74138741	2.669239619
4.5528339	0	10.75057568	2.678427894
4.540269761	0	10.75971191	2.687564115
4.527773454	0	10.76879651	2.696648723
4.515344442	0	10.77782994	2.70568215
4.502982195	0	10.78681262	2.714664826
4.490686186	0	10.79574497	2.723597176
4.478455895	0	10.80462741	2.73247962
4.466290806	0	10.81346036	2.741312573
4.454190411	0	10.82224424	2.750096446
4.442154204	0	10.83097944	2.758831646
4.430181685	0	10.83966636	2.767518573
4.418272361	0	10.84830542	2.776157625
4.406425742	0	10.85689699	2.784749195
4.394641342	0	10.86544146	2.793293672
4.382918684	0	10.87393923	2.801791441
4.37125729	0	10.88239067	2.810242882
4.359656692	0	10.89079616	2.818648371
4.348116425	0	10.89915607	2.827008281
4.336636027	0	10.90747077	2.835322979
4.325215042	0	10.91574062	2.843592831
4.313853018	0	10.92396599	2.851818196
4.302549509	0	10.93214722	2.859999431
4.291304071	0	10.94028468	2.868136889
4.280116267	0	10.94837871	2.876230919
4.268985662	0	10.95642966	2.884281866
4.257911827	0	10.96443786	2.892290072
4.246894335	0	10.97240367	2.900255876
4.235932766	0	10.9803274	2.908179612
4.225026702	0	10.9882094	2.91606161
4.214175729	0	10.99604999	2.9239022
4.20337944	0	11.00384949	2.931701704
4.192637428	0	11.01160823	2.939460444
4.181949292	0	11.01932653	2.947178738
4.171314634	0	11.02700469	2.954856899
4.160733062	0	11.03464303	2.96249524
4.150204185	0	11.04224186	2.970094066

4.139727616	0	11.04980148	2.977653685
4.129302975	0	11.05732219	2.985174396
4.118929881	0	11.06480429	2.992656499
4.10860796	0	11.07224808	3.000100289
4.098336841	0	11.07965385	3.007506058
4.088116154	0	11.08702189	3.014874097
4.077945536	0	11.09435248	3.022204691
4.067824625	0	11.10164592	3.029498125
4.057753065	0	11.10890247	3.036754679
4.047730499	0	11.11612242	3.043974631
4.037756578	0	11.12330605	3.051158257
4.027830953	0	11.13045362	3.05830583
4.017953281	0	11.13756541	3.065417618
4.008123219	0	11.14464168	3.07249389
3.99834043	0	11.1516827	3.079534909
3.988604579	0	11.15868873	3.086540939
3.978915333	0	11.16566003	3.093512237
3.969272365	0	11.17259685	3.100449061
3.959675349	0	11.17949946	3.107351665
3.950123961	0	11.18636809	3.114220301
3.940617882	0	11.19320301	3.121055218
3.931156795	0	11.20000445	3.127856664
3.921740386	0	11.20677267	3.134624881
3.912368344	0	11.2135079	3.141360114
3.903040361	0	11.22021039	3.148062601
3.893756131	0	11.22688037	3.15473258
3.884515352	0	11.23351808	3.161370287
3.875317724	0	11.24012374	3.167975953
3.866162949	0	11.2466976	3.174549811
3.857050734	0	11.25323988	3.181092088
3.847980786	0	11.2597508	3.18760301
3.838952815	0	11.26623059	3.194082803
3.829966536	0	11.27267948	3.200531687
3.821021665	0	11.27909767	3.206949884
3.812117918	0	11.2854854	3.21333761
3.803255019	0	11.29184287	3.219695082
3.794432689	0	11.2981703	3.226022514
3.785650656	0	11.30446791	3.232320117
3.776908647	0	11.31073589	3.238588101
3.768206392	0	11.31697446	3.244826673
3.759543626	0	11.32318383	3.251036041
3.750920083	0	11.3293642	3.257216408
3.742335502	0	11.33551577	3.263367976
3.733789622	0	11.34163874	3.269490945
3.725282186	0	11.3477333	3.275585514
3.716812937	0	11.35379967	3.281651879
3.708381625	0	11.35983803	3.287690236
3.699987996	0	11.36584857	3.293700776
3.691631802	0	11.37183148	3.299683692
3.683312798	0	11.37778696	3.305639173

3.675030737	0	11.3837152	3.311567406
3.666785378	0	11.38961637	3.317468578
3.658576481	0	11.39549066	3.323342873
3.650403807	0	11.40133826	3.329190474
3.64226712	0	11.40715935	3.335011561
3.634166186	0	11.41295411	3.340806315
3.626100772	0	11.4187227	3.346574913
3.618070649	0	11.42446532	3.352317532
3.610075589	0	11.43018214	3.358034345
3.602115364	0	11.43587332	3.363725526
3.59418975	0	11.44153904	3.369391247
3.586298526	0	11.44717947	3.375031678
3.57844147	0	11.45279478	3.380646987
3.570618364	0	11.45838513	3.386237341
3.56282899	0	11.4639507	3.391802906
3.555073134	0	11.46949164	3.397343846
3.547350583	0	11.47500811	3.402860323
3.539661124	0	11.48050029	3.408352499
3.532004548	0	11.48596832	3.413820534
3.524380648	0	11.49141238	3.419264586
3.516789216	0	11.4968326	3.424684812
3.509230049	0	11.50222916	3.430081368
3.501702943	0	11.5076022	3.435454408
3.494207698	0	11.51295188	3.440804085
3.486744113	0	11.51827834	3.446130551
3.479311991	0	11.52358175	3.451433956
3.471911135	0	11.52886224	3.456714449
3.464541352	0	11.53411997	3.461972179
3.457202447	0	11.53935508	3.467207291
3.44989423	0	11.54456772	3.472419931
3.44261651	0	11.54975803	3.477610243
3.435369099	0	11.55492616	3.48277837
3.428151811	0	11.56007224	3.487924454
3.420964459	0	11.56519642	3.493048634
3.413806861	0	11.57029884	3.49815105
3.406678833	0	11.57537963	3.50323184
3.399580196	0	11.58043893	3.508291141
3.392510768	0	11.58547688	3.513329089
3.385470373	0	11.59049361	3.518345819
3.378458835	0	11.59548925	3.523341463
3.371475977	0	11.60046394	3.528316154
3.364521626	0	11.60541781	3.533270024
3.357595609	0	11.61035099	3.538203202
3.350697757	0	11.61526361	3.543115818
3.343827898	0	11.62015579	3.548007999
3.336985866	0	11.62502766	3.552879873
3.330171492	0	11.62987936	3.557731566
3.323384612	0	11.63471099	3.562563202
3.31662506	0	11.6395227	3.567374905
3.309892674	0	11.64431459	3.572166799

3.303187293	0	11.64908679	3.576939004
3.296508755	0	11.65383943	3.581691642
3.289856901	0	11.65857262	3.586424832
3.283231574	0	11.66328648	3.591138694
3.276632617	0	11.66798114	3.595833346
3.270059873	0	11.67265669	3.600508904
3.26351319	0	11.67731327	3.605165484
3.256992413	0	11.68195099	3.609803201
3.250497391	0	11.68656996	3.61442217
3.244027973	0	11.69117029	3.619022504
3.237584009	0	11.69575211	3.623604315
3.231165351	0	11.7003155	3.628167714
3.224771852	0	11.7048606	3.632712813
3.218403365	0	11.70938751	3.63723972
3.212059745	0	11.71389633	3.641748544
3.205740849	0	11.71838718	3.646239394
3.199446533	0	11.72286017	3.650712377
3.193176656	0	11.72731539	3.655167598
3.186931077	0	11.73175295	3.659605163
3.180709656	0	11.73617297	3.664025177
3.174512255	0	11.74057553	3.668427743
3.168338736	0	11.74496075	3.672812964
3.162188964	0	11.74932873	3.677180943
3.156062801	0	11.75367957	3.68153178
3.149960114	0	11.75801337	3.685865576
3.14388077	0	11.76233022	3.690182431
3.137824636	0	11.76663023	3.694482444
3.131791581	0	11.7709135	3.698765713
3.125781473	0	11.77518013	3.703032336
3.119794184	0	11.7794302	3.707282408
3.113829586	0	11.78366382	3.711516027
3.10788755	0	11.78788108	3.715733287
3.101967949	0	11.79208207	3.719934282
3.096070659	0	11.7962669	3.724119107
3.090195555	0	11.80043564	3.728287854
3.084342512	0	11.80458841	3.732440617
3.078511407	0	11.80872528	3.736577485
3.07270212	0	11.81284634	3.740698551
3.066914527	0	11.81695169	3.744803904
3.061148511	0	11.82104142	3.748893634
3.05540395	0	11.82511562	3.75296783
3.049680726	0	11.82917437	3.75702658
3.043978722	0	11.83321776	3.761069972
3.038297821	0	11.83724588	3.765098092
3.032637908	0	11.84125882	3.769111026
3.026998866	0	11.84525665	3.773108861
3.021380582	0	11.84923947	3.777091681
3.015782942	0	11.85320736	3.78105957
3.010205834	0	11.8571604	3.785012612
3.004649146	0	11.86109868	3.78895089

2.999112767	0	11.86502228	3.792874487
2.993596586	0	11.86893127	3.796783484
2.988100495	0	11.87282575	3.800677963
2.982624384	0	11.87670579	3.804558003
2.977168146	0	11.88057148	3.808423686
2.971731674	0	11.88442288	3.81227509
2.966314861	0	11.88826009	3.816112295
2.960917602	0	11.89208317	3.819935378
2.955539792	0	11.89589221	3.823744417
2.950181326	0	11.89968728	3.82753949
2.944842102	0	11.90346846	3.831320673
2.939522017	0	11.90723583	3.835088042
2.934220969	0	11.91098946	3.838841672
2.928938857	0	11.91472943	3.842581638
2.923675581	0	11.91845581	3.846308015
2.918431039	0	11.92216867	3.850020876
2.913205135	0	11.92586809	3.853720295
2.907997768	0	11.92955414	3.857406345
2.902808842	0	11.93322689	3.861079097
2.897638259	0	11.93688641	3.864738623
2.892485924	0	11.94053279	3.868384996
2.887351739	0	11.94416607	3.872018284
2.882235612	0	11.94778635	3.875638559
2.877137446	0	11.95139368	3.87924589
2.872057148	0	11.95498814	3.882840346
2.866994626	0	11.95856979	3.886421997
2.861949787	0	11.9621387	3.88999091
2.856922539	0	11.96569494	3.893547152
2.851912791	0	11.96923858	3.897090792
2.846920452	0	11.97276969	3.900621896
2.841945432	0	11.97628832	3.90414053
2.836987643	0	11.97979455	3.907646761
2.832046996	0	11.98328844	3.911140653
2.827123401	0	11.98677006	3.914622271
2.822216773	0	11.99023947	3.91809168
2.817327024	0	11.99369673	3.921548944
2.812454068	0	11.99714192	3.924994127
2.807597818	0	12.00057508	3.928427291
2.802758191	0	12.00399629	3.931848499
2.7979351	0	12.0074056	3.935257814
2.793128463	0	12.01080309	3.938655298
2.788338196	0	12.0141888	3.942041011
2.783564216	0	12.0175628	3.945415014
2.77880644	0	12.02092516	3.948777369
2.774064788	0	12.02427593	3.952128136
2.769339177	0	12.02761516	3.955467374
2.764629526	0	12.03094293	3.958795142
2.759935757	0	12.03425929	3.962111499
2.755257789	0	12.03756429	3.965416504
2.750595543	0	12.04085801	3.968710216

2.74594894	0	12.04414048	3.97199269
2.741317903	0	12.04741178	3.975263986
2.736702354	0	12.05067195	3.97852416
2.732102215	0	12.05392106	3.981773269
2.727517411	0	12.05715916	3.985011368
2.722947865	0	12.0603863	3.988238513
2.718393502	0	12.06360255	3.99145476
2.713854247	0	12.06680795	3.994660164
2.709330025	0	12.07000257	3.99785478
2.704820763	0	12.07318645	4.001038661
2.700326385	0	12.07635965	4.004211863
2.695846821	0	12.07952223	4.007374437
2.691381996	0	12.08267423	4.010526439
2.686931839	0	12.08581571	4.013667919
2.682496278	0	12.08894672	4.016798932
2.678075242	0	12.09206732	4.019919528
2.673668661	0	12.09517755	4.023029761
2.669276462	0	12.09827747	4.026129681
2.664898578	0	12.10136713	4.02921934
2.660534939	0	12.10444658	4.032298788
2.656185475	0	12.10751587	4.035368076
2.651850118	0	12.11057504	4.038427253
2.6475288	0	12.11362416	4.041476371
2.643221454	0	12.11666327	4.044515478
2.638928012	0	12.11969241	4.047544623
2.634648407	0	12.12271165	4.050563855
2.630382573	0	12.12572101	4.053573223
2.626130444	0	12.12872057	4.056572776
2.621891955	0	12.13171035	4.05956256
2.61766704	0	12.13469041	4.062542623
2.613455635	0	12.1376608	4.065513013
2.609257675	0	12.14062157	4.068473777
2.605073097	0	12.14357275	4.071424961
2.600901838	0	12.1465144	4.074366611
2.596743833	0	12.14944657	4.077298775
2.59259902	0	12.15236929	4.080221497
2.588467338	0	12.15528261	4.083134823
2.584348724	0	12.15818659	4.086038798
2.580243116	0	12.16108126	4.088933467
2.576150454	0	12.16396667	4.091818875
2.572070676	0	12.16684286	4.094695066
2.568003723	0	12.16970987	4.097562084
2.563949534	0	12.17256776	4.100419972
2.55990805	0	12.17541657	4.103268775
2.555879211	0	12.17825633	4.106108535
2.551862959	0	12.18108709	4.108939296
2.547859235	0	12.18390889	4.1117611
2.54386798	0	12.18672178	4.114573989
2.539889138	0	12.1895258	4.117378006
2.53592265	0	12.19232098	4.120173192

2.53196846	0	12.19510738	4.122959589
2.52802651	0	12.19788503	4.125737239
2.524096744	0	12.20065397	4.128506182
2.520179107	0	12.20341425	4.13126646
2.516273542	0	12.2061659	4.134018112
2.512379994	0	12.20890897	4.13676118
2.508498408	0	12.21164349	4.139495702
2.50462873	0	12.21436951	4.14222172
2.500770904	0	12.21708706	4.144939273
2.496924877	0	12.21979619	4.147648399
2.493090595	0	12.22249693	4.150349139
2.489268005	0	12.22518932	4.15304153
2.485457053	0	12.2278734	4.155725612
2.481657688	0	12.23054921	4.158401422
2.477869855	0	12.23321679	4.161069
2.474093504	0	12.23587617	4.163728383
2.470328582	0	12.2385274	4.166379608
2.466575038	0	12.2411705	4.169022713
2.462832821	0	12.24380553	4.171657735
2.459101879	0	12.2464325	4.174284712
2.455382162	0	12.24905147	4.176903679
2.451673621	0	12.25166246	4.179514674
2.447976204	0	12.25426552	4.182117733
2.444289862	0	12.25686068	4.184712891
2.440614546	0	12.25944798	4.187300185
2.436950207	0	12.26202744	4.189879651
2.433296796	0	12.26459911	4.192451323
2.429654263	0	12.26716303	4.195015237
2.426022562	0	12.26971922	4.197571429
2.422401643	0	12.27226772	4.200119932
2.41879146	0	12.27480857	4.202660782
2.415191965	0	12.2773418	4.205194013
2.41160311	0	12.27986745	4.207719658
2.40802485	0	12.28238554	4.210237753
2.404457136	0	12.28489612	4.21274833
2.400899924	0	12.28739921	4.215251424
2.397353166	0	12.28989486	4.217747068
2.393816818	0	12.29238308	4.220235294
2.390290833	0	12.29486393	4.222716137
2.386775167	0	12.29733742	4.225189628
2.383269774	0	12.29980359	4.2276558
2.37977461	0	12.30226248	4.230114686
2.37628963	0	12.30471411	4.232566318
2.372814789	0	12.30715852	4.235010728
2.369350045	0	12.30959574	4.237447948
2.365895353	0	12.3120258	4.239878009
2.36245067	0	12.31444873	4.242300942
2.359015953	0	12.31686457	4.24471678
2.355591158	0	12.31927334	4.247125554
2.352176243	0	12.32167508	4.249527293

2.348771166	0	12.32406982	4.251922029
2.345375883	0	12.32645758	4.254309793
2.341990354	0	12.3288384	4.256690614
2.338614537	0	12.33121231	4.259064524
2.33524839	0	12.33357934	4.261431551

Steering Angle Change			Steering Angle
Section A	Section B	Section C	Radians
0	-161.4429558	-100	1.53370808
0.068084072	-161.4429558	-100	1.532724008
0.135533931	-161.4429558	-100	1.531749333
0.20235802	-161.4429558	-100	1.530783924
0.268564639	-161.4429558	-100	1.529827655
0.334161949	-161.4429558	-100	1.528880401
0.399157975	-161.4429558	-100	1.527942039
0.463560607	-161.4429558	-100	1.527012448
0.527377607	-161.4429558	-100	1.52609151
0.590616605	-161.4429558	-100	1.525179109
0.653285106	-161.4429558	-100	1.524275129
0.715390493	-161.4429558	-100	1.523379459
0.776940025	-161.4429558	-100	1.522491988
0.837940845	-161.4429558	-100	1.521612607
0.898399977	-161.4429558	-100	1.52074121
0.958324333	-161.4429558	-100	1.519877691
1.017720711	-161.4429558	-100	1.519021947
1.076595799	-161.4429558	-100	1.518173877
1.134956179	-161.4429558	-100	1.517333381
1.192808326	-161.4429558	-100	1.51650036
1.25015861	-161.4429558	-100	1.515674719
1.307013302	-161.4429558	-100	1.514856363
1.363378571	-161.4429558	-100	1.514045197
1.419260488	-161.4429558	-100	1.513241131
1.474665029	-161.4429558	-100	1.512444074
1.529598076	-161.4429558	-100	1.511653937
1.584065416	-161.4429558	-100	1.510870633
1.638072747	-161.4429558	-100	1.510094077
1.691625678	-161.4429558	-100	1.509324183
1.744729731	-161.4429558	-100	1.508560868
1.79739034	-161.4429558	-100	1.50780405
1.849612857	-161.4429558	-100	1.50705365
1.901402549	-161.4429558	-100	1.506309588
1.952764605	-161.4429558	-100	1.505571785
2.003704132	-161.4429558	-100	1.504840166
2.054226158	-161.4429558	-100	1.504114655
2.104335637	-161.4429558	-100	1.503395177
2.154037446	-161.4429558	-100	1.502681659
2.203336388	-161.4429558	-100	1.501974029
2.252237193	-161.4429558	-100	1.501272217
2.300744521	-161.4429558	-100	1.500576152
2.348862961	-161.4429558	-100	1.499885767
2.396597033	-161.4429558	-100	1.499200993
2.44395119	-161.4429558	-100	1.498521764
2.490929818	-161.4429558	-100	1.497848013
2.537537239	-161.4429558	-100	1.497179678

2.583777711	-161.4429558	-100	1.496516694
2.629655427	-161.4429558	-100	1.495858998
2.67517452	-161.4429558	-100	1.49520653
2.720339062	-161.4429558	-100	1.494559227
2.765153067	-161.4429558	-100	1.493917031
2.809620487	-161.4429558	-100	1.493279883
2.85374522	-161.4429558	-100	1.492647724
2.897531106	-161.4429558	-100	1.492020497
2.940981928	-161.4429558	-100	1.491398147
2.984101417	-161.4429558	-100	1.490780617
3.02689325	-161.4429558	-100	1.490167853
3.069361049	-161.4429558	-100	1.489559801
3.111508388	-161.4429558	-100	1.488956409
3.153338786	-161.4429558	-100	1.488357623
3.194855716	-161.4429558	-100	1.487763392
3.2360626	-161.4429558	-100	1.487173666
3.27696281	-161.4429558	-100	1.486588395
3.317559673	-161.4429558	-100	1.486007529
3.357856469	-161.4429558	-100	1.485431019
3.397856432	-161.4429558	-100	1.484858818
3.43756275	-161.4429558	-100	1.484290879
3.476978567	-161.4429558	-100	1.483727155
3.516106985	-161.4429558	-100	1.4831676
3.55495106	-161.4429558	-100	1.482612168
3.59351381	-161.4429558	-100	1.482060816
3.631798207	-161.4429558	-100	1.4815135
3.669807186	-161.4429558	-100	1.480970175
3.707543641	-161.4429558	-100	1.4804308
3.745010424	-161.4429558	-100	1.479895332
3.782210352	-161.4429558	-100	1.47936373
3.819146202	-161.4429558	-100	1.478835952
3.855820713	-161.4429558	-100	1.478311958
3.892236589	-161.4429558	-100	1.477791709
3.928396495	-161.4429558	-100	1.477275165
3.964303064	-161.4429558	-100	1.476762287
3.99995889	-161.4429558	-100	1.476253037
4.035366535	-161.4429558	-100	1.475747378
4.070528525	-161.4429558	-100	1.475245272
4.105447356	-161.4429558	-100	1.474746682
4.140125488	-161.4429558	-100	1.474251572
4.17456535	-161.4429558	-100	1.473759907
4.208769338	-161.4429558	-100	1.473271652
4.242739817	-161.4429558	-100	1.472786771
4.276479123	-161.4429558	-100	1.47230523
4.30998956	-161.4429558	-100	1.471826995
4.343273401	-161.4429558	-100	1.471352033
4.376332892	-161.4429558	-100	1.470880312
4.409170249	-161.4429558	-100	1.470411798
4.44178766	-161.4429558	-100	1.469946459
4.474187283	-161.4429558	-100	1.469484264

4.506371252	-161.4429558	-100	1.469025182
4.538341669	-161.4429558	-100	1.468569181
4.570100615	-161.4429558	-100	1.468116231
4.60165014	-161.4429558	-100	1.467666302
4.632992269	-161.4429558	-100	1.467219364
4.664129004	-161.4429558	-100	1.466775389
4.695062319	-161.4429558	-100	1.466334347
4.725794164	-161.4429558	-100	1.465896209
4.756326466	-161.4429558	-100	1.465460948
4.786661126	-161.4429558	-100	1.465028536
4.816800023	-161.4429558	-100	1.464598944
4.846745012	-161.4429558	-100	1.464172147
4.876497925	-161.4429558	-100	1.463748117
4.906060571	-161.4429558	-100	1.463326827
4.935434738	-161.4429558	-100	1.462908252
4.964622191	-161.4429558	-100	1.462492367
4.993624673	-161.4429558	-100	1.462079144
5.022443909	-161.4429558	-100	1.461668559
5.051081598	-161.4429558	-100	1.461260588
5.079539422	-161.4429558	-100	1.460855206
5.107819043	-161.4429558	-100	1.460452389
5.135922099	-161.4429558	-100	1.460052112
5.163850213	-161.4429558	-100	1.459654352
5.191604986	-161.4429558	-100	1.459259085
5.219188	-161.4429558	-100	1.458866289
5.246600819	-161.4429558	-100	1.458475941
5.273844987	-161.4429558	-100	1.458088019
5.300922031	-161.4429558	-100	1.457702499
5.32783346	-161.4429558	-100	1.45731936
5.354580764	-161.4429558	-100	1.456938581
5.381165416	-161.4429558	-100	1.456560139
5.407588873	-161.4429558	-100	1.456184015
5.433852573	-161.4429558	-100	1.455810186
5.459957938	-161.4429558	-100	1.455438631
5.485906374	-161.4429558	-100	1.455069332
5.511699269	-161.4429558	-100	1.454702267
5.537337997	-161.4429558	-100	1.454337416
5.562823916	-161.4429558	-100	1.45397476
5.588158366	-161.4429558	-100	1.453614279
5.613342673	-161.4429558	-100	1.453255954
5.63837815	-161.4429558	-100	1.452899766
5.663266091	-161.4429558	-100	1.452545695
5.688007779	-161.4429558	-100	1.452193724
5.712604479	-161.4429558	-100	1.451843834
5.737057444	-161.4429558	-100	1.451496007
5.761367912	-161.4429558	-100	1.451150224
5.785537107	-161.4429558	-100	1.450806469
5.80956624	-161.4429558	-100	1.450464723
5.833456507	-161.4429558	-100	1.450124969
5.857209092	-161.4429558	-100	1.44978719

5.880825165	-161.4429558	-100	1.449451368
5.904305883	-161.4429558	-100	1.449117488
5.927652391	-161.4429558	-100	1.448785533
5.95086582	-161.4429558	-100	1.448455485
5.973947289	-161.4429558	-100	1.44812733
5.996897904	-161.4429558	-100	1.44780105
6.019718762	-161.4429558	-100	1.44747663
6.042410943	-161.4429558	-100	1.447154055
6.06497552	-161.4429558	-100	1.446833308
6.087413551	-161.4429558	-100	1.446514374
6.109726083	-161.4429558	-100	1.446197239
6.131914153	-161.4429558	-100	1.445881887
6.153978786	-161.4429558	-100	1.445568304
6.175920995	-161.4429558	-100	1.445256474
6.197741784	-161.4429558	-100	1.444946383
6.219442145	-161.4429558	-100	1.444638018
6.241023059	-161.4429558	-100	1.444331362
6.262485498	-161.4429558	-100	1.444026404
6.283830422	-161.4429558	-100	1.443723128
6.305058781	-161.4429558	-100	1.443421521
6.326171516	-161.4429558	-100	1.443121569
6.347169557	-161.4429558	-100	1.442823259
6.368053826	-161.4429558	-100	1.442526577
6.388825232	-161.4429558	-100	1.442231511
6.409484678	-161.4429558	-100	1.441938048
6.430033054	-161.4429558	-100	1.441646173
6.450471244	-161.4429558	-100	1.441355876
6.47080012	-161.4429558	-100	1.441067142
6.491020548	-161.4429558	-100	1.44077996
6.511133382	-161.4429558	-100	1.440494318
6.531139469	-161.4429558	-100	1.440210202
6.551039647	-161.4429558	-100	1.439927601
6.570834743	-161.4429558	-100	1.439646503
6.59052558	-161.4429558	-100	1.439366896
6.610112968	-161.4429558	-100	1.439088769
6.629597712	-161.4429558	-100	1.438812109
6.648980608	-161.4429558	-100	1.438536905
6.668262442	-161.4429558	-100	1.438263147
6.687443994	-161.4429558	-100	1.437990822
6.706526036	-161.4429558	-100	1.437719919
6.725509332	-161.4429558	-100	1.437450428
6.744394637	-161.4429558	-100	1.437182338
6.763182699	-161.4429558	-100	1.436915637
6.781874261	-161.4429558	-100	1.436650316
6.800470055	-161.4429558	-100	1.436386363
6.818970807	-161.4429558	-100	1.436123768
6.837377237	-161.4429558	-100	1.43586252
6.855690056	-161.4429558	-100	1.435602611
6.873909968	-161.4429558	-100	1.435344028
6.892037672	-161.4429558	-100	1.435086763

6.910073859	-161.4429558	-100	1.434830805
6.928019212	-161.4429558	-100	1.434576144
6.945874408	-161.4429558	-100	1.434322771
6.963640119	-161.4429558	-100	1.434070676
6.981317008	-161.4429558	-100	1.43381985
6.998905733	-161.4429558	-100	1.433570282
7.016406945	-161.4429558	-100	1.433321964
7.03382129	-161.4429558	-100	1.433074886
7.051149405	-161.4429558	-100	1.432829039
7.068391923	-161.4429558	-100	1.432584415
7.08554947	-161.4429558	-100	1.432341003
7.102622667	-161.4429558	-100	1.432098795
7.119612128	-161.4429558	-100	1.431857783
7.136518462	-161.4429558	-100	1.431617957
7.15334227	-161.4429558	-100	1.431379308
7.17008415	-161.4429558	-100	1.431141829
7.186744694	-161.4429558	-100	1.430905511
7.203324486	-161.4429558	-100	1.430670345
7.219824107	-161.4429558	-100	1.430436322
7.236244131	-161.4429558	-100	1.430203436
7.252585127	-161.4429558	-100	1.429971677
7.26884766	-161.4429558	-100	1.429741037
7.285032286	-161.4429558	-100	1.429511509
7.301139561	-161.4429558	-100	1.429283083
7.317170031	-161.4429558	-100	1.429055754
7.33312424	-161.4429558	-100	1.428829512
7.349002725	-161.4429558	-100	1.42860435
7.36480602	-161.4429558	-100	1.42838026
7.380534652	-161.4429558	-100	1.428157236
7.396189144	-161.4429558	-100	1.427935268
7.411770015	-161.4429558	-100	1.42771435
7.427277778	-161.4429558	-100	1.427494474
7.442712941	-161.4429558	-100	1.427275634
7.45807601	-161.4429558	-100	1.427057821
7.473367482	-161.4429558	-100	1.426841029
7.488587854	-161.4429558	-100	1.426625251
7.503737615	-161.4429558	-100	1.426410479
7.518817251	-161.4429558	-100	1.426196707
7.533827244	-161.4429558	-100	1.425983927
7.548768072	-161.4429558	-100	1.425772133
7.563640206	-161.4429558	-100	1.425561318
7.578444115	-161.4429558	-100	1.425351475
7.593180264	-161.4429558	-100	1.425142598
7.607849114	-161.4429558	-100	1.42493468
7.622451119	-161.4429558	-100	1.424727714
7.636986732	-161.4429558	-100	1.424521694
7.651456401	-161.4429558	-100	1.424316614
7.665860571	-161.4429558	-100	1.424112467
7.68019968	-161.4429558	-100	1.423909246
7.694474165	-161.4429558	-100	1.423706947

7.708684459	-161.4429558	-100	1.423505562
7.72283099	-161.4429558	-100	1.423305085
7.736914182	-161.4429558	-100	1.42310551
7.750934457	-161.4429558	-100	1.422906831
7.764892232	-161.4429558	-100	1.422709042
7.77878792	-161.4429558	-100	1.422512138
7.792621931	-161.4429558	-100	1.422316112
7.806394673	-161.4429558	-100	1.422120958
7.820106547	-161.4429558	-100	1.421926671
7.833757953	-161.4429558	-100	1.421733245
7.847349287	-161.4429558	-100	1.421540675
7.860880942	-161.4429558	-100	1.421348954
7.874353307	-161.4429558	-100	1.421158077
7.887766768	-161.4429558	-100	1.420968039
7.901121706	-161.4429558	-100	1.420778834
7.914418502	-161.4429558	-100	1.420590457
7.927657531	-161.4429558	-100	1.420402902
7.940839166	-161.4429558	-100	1.420216164
7.953963776	-161.4429558	-100	1.420030237
7.967031728	-161.4429558	-100	1.419845117
7.980043386	-161.4429558	-100	1.419660798
7.992999109	-161.4429558	-100	1.419477275
8.005899255	-161.4429558	-100	1.419294544
8.018744177	-161.4429558	-100	1.419112598
8.031534228	-161.4429558	-100	1.418931432
8.044269756	-161.4429558	-100	1.418751043
8.056951104	-161.4429558	-100	1.418571425
8.069578618	-161.4429558	-100	1.418392572
8.082152634	-161.4429558	-100	1.418214481
8.094673492	-161.4429558	-100	1.418037146
8.107141524	-161.4429558	-100	1.417860563
8.119557061	-161.4429558	-100	1.417684726
8.131920433	-161.4429558	-100	1.417509631
8.144231965	-161.4429558	-100	1.417335274
8.156491979	-161.4429558	-100	1.41716165
8.168700797	-161.4429558	-100	1.416988754
8.180858736	-161.4429558	-100	1.416816581
8.192966112	-161.4429558	-100	1.416645128
8.205023236	-161.4429558	-100	1.41647439
8.217030419	-161.4429558	-100	1.416304361
8.228987968	-161.4429558	-100	1.416135039
8.240896188	-161.4429558	-100	1.415966418
8.252755383	-161.4429558	-100	1.415798494
8.264565851	-161.4429558	-100	1.415631264
8.276327891	-161.4429558	-100	1.415464721
8.288041798	-161.4429558	-100	1.415298863
8.299707864	-161.4429558	-100	1.415133686
8.311326381	-161.4429558	-100	1.414969184
8.322897636	-161.4429558	-100	1.414805355
8.334421915	-161.4429558	-100	1.414642193

8.345899502	-161.4429558	-100	1.414479695
8.357330678	-161.4429558	-100	1.414317857
8.368715722	-161.4429558	-100	1.414156675
8.380054911	-161.4429558	-100	1.413996144
8.39134852	-161.4429558	-100	1.413836262
8.402596821	-161.4429558	-100	1.413677023
8.413800084	-161.4429558	-100	1.413518425
8.424958579	-161.4429558	-100	1.413360462
8.43607257	-161.4429558	-100	1.413203133
8.447142322	-161.4429558	-100	1.413046432
8.458168096	-161.4429558	-100	1.412890356
8.469150154	-161.4429558	-100	1.412734902
8.480088751	-161.4429558	-100	1.412580065
8.490984146	-161.4429558	-100	1.412425842
8.50183659	-161.4429558	-100	1.412272229
8.512646336	-161.4429558	-100	1.412119223
8.523413634	-161.4429558	-100	1.41196682
8.534138733	-161.4429558	-100	1.411815017
8.544821877	-161.4429558	-100	1.41166381
8.555463311	-161.4429558	-100	1.411513195
8.566063278	-161.4429558	-100	1.41136317
8.576622018	-161.4429558	-100	1.41121373
8.58713977	-161.4429558	-100	1.411064873
8.597616769	-161.4429558	-100	1.410916595
8.608053252	-161.4429558	-100	1.410768892
8.618449452	-161.4429558	-100	1.410621761
8.628805599	-161.4429558	-100	1.4104752
8.639121923	-161.4429558	-100	1.410329204
8.649398653	-161.4429558	-100	1.41018377
8.659636014	-161.4429558	-100	1.410038896
8.669834232	-161.4429558	-100	1.409894578
8.679993528	-161.4429558	-100	1.409750812
8.690114123	-161.4429558	-100	1.409607596
8.700196238	-161.4429558	-100	1.409464927
8.71024009	-161.4429558	-100	1.409322801
8.720245895	-161.4429558	-100	1.409181215
8.730213868	-161.4429558	-100	1.409040167
8.740144222	-161.4429558	-100	1.408899652
8.750037167	-161.4429558	-100	1.408759669
8.759892914	-161.4429558	-100	1.408620215
8.769711671	-161.4429558	-100	1.408481285
8.779493644	-161.4429558	-100	1.408342878
8.78923904	-161.4429558	-100	1.40820499
8.798948061	-161.4429558	-100	1.408067619
8.808620909	-161.4429558	-100	1.407930761
8.818257785	-161.4429558	-100	1.407794414
8.827858889	-161.4429558	-100	1.407658574
8.837424418	-161.4429558	-100	1.40752324
8.846954568	-161.4429558	-100	1.407388408
8.856449535	-161.4429558	-100	1.407254076

8.865909511	-161.4429558	-100	1.40712024
8.875334689	-161.4429558	-100	1.406986898
8.884725258	-161.4429558	-100	1.406854048
8.89408141	-161.4429558	-100	1.406721686
8.903403331	-161.4429558	-100	1.40658981
8.912691207	-161.4429558	-100	1.406458417
8.921945224	-161.4429558	-100	1.406327505
8.931165567	-161.4429558	-100	1.406197071
8.940352416	-161.4429558	-100	1.406067112
8.949505955	-161.4429558	-100	1.405937626
8.958626361	-161.4429558	-100	1.40580861
8.967713815	-161.4429558	-100	1.405680062
8.976768493	-161.4429558	-100	1.405551979
8.985790571	-161.4429558	-100	1.405424358
8.994780225	-161.4429558	-100	1.405297198
9.003737627	-161.4429558	-100	1.405170495
9.012662951	-161.4429558	-100	1.405044248
9.021556367	-161.4429558	-100	1.404918453
9.030418045	-161.4429558	-100	1.404793109
9.039248155	-161.4429558	-100	1.404668212
9.048046862	-161.4429558	-100	1.404543762
9.056814335	-161.4429558	-100	1.404419754
9.065550738	-161.4429558	-100	1.404296187
9.074256235	-161.4429558	-100	1.404173059
9.082930989	-161.4429558	-100	1.404050367
9.091575161	-161.4429558	-100	1.403928109
9.100188913	-161.4429558	-100	1.403806282
9.108772404	-161.4429558	-100	1.403684885
9.117325792	-161.4429558	-100	1.403563914
9.125849235	-161.4429558	-100	1.403443369
9.134342888	-161.4429558	-100	1.403323246
9.142806908	-161.4429558	-100	1.403203544
9.151241447	-161.4429558	-100	1.403084259
9.15964666	-161.4429558	-100	1.402965391
9.168022697	-161.4429558	-100	1.402846936
9.176369711	-161.4429558	-100	1.402728894
9.18468785	-161.4429558	-100	1.40261126
9.192977263	-161.4429558	-100	1.402494035
9.201238099	-161.4429558	-100	1.402377214
9.209470504	-161.4429558	-100	1.402260797
9.217674625	-161.4429558	-100	1.402144781
9.225850605	-161.4429558	-100	1.402029164
9.233998589	-161.4429558	-100	1.401913944
9.24211872	-161.4429558	-100	1.401799119
9.250211139	-161.4429558	-100	1.401684687
9.258275987	-161.4429558	-100	1.401570647
9.266313406	-161.4429558	-100	1.401456995
9.274323532	-161.4429558	-100	1.40134373
9.282306506	-161.4429558	-100	1.40123085
9.290262463	-161.4429558	-100	1.401118353

9.298191541	-161.4429558	-100	1.401006238
9.306093874	-161.4429558	-100	1.400894502
9.313969597	-161.4429558	-100	1.400783143
9.321818844	-161.4429558	-100	1.400672159
9.329641747	-161.4429558	-100	1.400561549
9.337438438	-161.4429558	-100	1.400451311
9.345209048	-161.4429558	-100	1.400341442
9.352953708	-161.4429558	-100	1.400231941
9.360672545	-161.4429558	-100	1.400122807
9.368365689	-161.4429558	-100	1.400014037
9.376033268	-161.4429558	-100	1.399905629
9.383675407	-161.4429558	-100	1.399797582
9.391292233	-161.4429558	-100	1.399689893
9.39888387	-161.4429558	-100	1.399582562
9.406450444	-161.4429558	-100	1.399475586
9.413992077	-161.4429558	-100	1.399368964
9.421508891	-161.4429558	-100	1.399262694
9.429001009	-161.4429558	-100	1.399156773
9.436468552	-161.4429558	-100	1.399051201
9.443911639	-161.4429558	-100	1.398945976
9.451330391	-161.4429558	-100	1.398841096
9.458724926	-161.4429558	-100	1.398736558
9.466095361	-161.4429558	-100	1.398632363
9.473441814	-161.4429558	-100	1.398528507
9.480764402	-161.4429558	-100	1.39842499
9.488063239	-161.4429558	-100	1.398321809
9.495338441	-161.4429558	-100	1.398218964
9.502590122	-161.4429558	-100	1.398116451
9.509818395	-161.4429558	-100	1.398014271
9.517023373	-161.4429558	-100	1.39791242
9.524205168	-161.4429558	-100	1.397810898
9.531363892	-161.4429558	-100	1.397709704
9.538499654	-161.4429558	-100	1.397608834
9.545612564	-161.4429558	-100	1.397508288
9.552702733	-161.4429558	-100	1.397408065
9.559770267	-161.4429558	-100	1.397308163
9.566815275	-161.4429558	-100	1.397208579
9.573837865	-161.4429558	-100	1.397109314
9.580838142	-161.4429558	-100	1.397010364
9.587816212	-161.4429558	-100	1.396911729
9.59477218	-161.4429558	-100	1.396813408
9.601706151	-161.4429558	-100	1.396715398
9.608618229	-161.4429558	-100	1.396617698
9.615508516	-161.4429558	-100	1.396520307
9.622377115	-161.4429558	-100	1.396423224
9.629224127	-161.4429558	-100	1.396326446
9.636049655	-161.4429558	-100	1.396229973
9.642853799	-161.4429558	-100	1.396133802
9.649636658	-161.4429558	-100	1.396037934
9.656398332	-161.4429558	-100	1.395942365

9.66313892	-161.4429558	-100	1.395847095
9.66985852	-161.4429558	-100	1.395752123
9.676557228	-161.4429558	-100	1.395657446
9.683235143	-161.4429558	-100	1.395563064
9.68989236	-161.4429558	-100	1.395468975
9.696528976	-161.4429558	-100	1.395375179
9.703145085	-161.4429558	-100	1.395281672
9.709740781	-161.4429558	-100	1.395188455
9.716316159	-161.4429558	-100	1.395095526
9.722871313	-161.4429558	-100	1.395002883
9.729406334	-161.4429558	-100	1.394910525
9.735921315	-161.4429558	-100	1.394818452
9.742416349	-161.4429558	-100	1.394726661
9.748891525	-161.4429558	-100	1.394635151
9.755346936	-161.4429558	-100	1.394543921
9.761782669	-161.4429558	-100	1.39445297
9.768198816	-161.4429558	-100	1.394362296
9.774595466	-161.4429558	-100	1.394271898
9.780972705	-161.4429558	-100	1.394181776
9.787330623	-161.4429558	-100	1.394091927
9.793669307	-161.4429558	-100	1.39400235
9.799988844	-161.4429558	-100	1.393913045
9.806289319	-161.4429558	-100	1.39382401
9.812570819	-161.4429558	-100	1.393735243
9.818833429	-161.4429558	-100	1.393646744
9.825077234	-161.4429558	-100	1.393558511
9.831302318	-161.4429558	-100	1.393470544
9.837508765	-161.4429558	-100	1.39338284
9.843696658	-161.4429558	-100	1.393295399
9.849866079	-161.4429558	-100	1.39320822
9.856017112	-161.4429558	-100	1.393121301
9.862149838	-161.4429558	-100	1.393034642
9.868264338	-161.4429558	-100	1.39294824
9.874360694	-161.4429558	-100	1.392862096
9.880438985	-161.4429558	-100	1.392776207
9.886499291	-161.4429558	-100	1.392690573
9.892541692	-161.4429558	-100	1.392605193
9.898566267	-161.4429558	-100	1.392520065
9.904573094	-161.4429558	-100	1.392435188
9.910562251	-161.4429558	-100	1.392350561
9.916533817	-161.4429558	-100	1.392266184
9.922487867	-161.4429558	-100	1.392182055
9.928424479	-161.4429558	-100	1.392098172
9.934343729	-161.4429558	-100	1.392014536
9.940245693	-161.4429558	-100	1.391931144
9.946130446	-161.4429558	-100	1.391847996
9.951998063	-161.4429558	-100	1.39176509
9.957848618	-161.4429558	-100	1.391682426
9.963682186	-161.4429558	-100	1.391600003
9.96949884	-161.4429558	-100	1.391517819

9.975298654	-161.4429558	-100	1.391435873
9.9810817	-161.4429558	-100	1.391354165
9.98684805	-161.4429558	-100	1.391272694
9.992597777	-161.4429558	-100	1.391191457
9.998330952	-161.4429558	-100	1.391110455

Steering Angle Degrees	Steering Angle Difference (CP=CG
87.875	0
87.81861684	0.056383161
87.76277205	0.112227955
87.7074582	0.167541796
87.65266803	0.222331973
87.59839436	0.276605642
87.54463016	0.330369837
87.49136853	0.383631467
87.43860268	0.436397324
87.38632592	0.48867408
87.33453171	0.540468292
87.28321359	0.591786406
87.23236524	0.642634756
87.18198043	0.693019567
87.13205304	0.742946961
87.08257705	0.792422954
87.03354654	0.84145346
86.9849557	0.890044295
86.93679882	0.938201177
86.88907027	0.985929726
86.84176453	1.033235472
86.79487615	1.080123851
86.74839979	1.12660021
86.70233019	1.172669805
86.65666219	1.21833781
86.61139069	1.263609311
86.56651069	1.308489312
86.52201726	1.352982736
86.47790558	1.397094424
86.43417086	1.440829142
86.39080842	1.484191577
86.34781366	1.527186341
86.30518203	1.569817972
86.26290906	1.612090937
86.22099037	1.654009632
86.17942162	1.69557838
86.13819856	1.736801441
86.097317	1.777683003
86.05677281	1.818227191
86.01656193	1.858438066
85.97668038	1.898319625
85.9371242	1.937875801
85.89788953	1.977110469
85.85897256	2.016027443
85.82036952	2.054630478
85.78207673	2.092923273

85.74409053	2.130909469
85.70640735	2.168592651
85.66902365	2.205976353
85.63193595	2.243064051
85.59514083	2.279859172
85.55863491	2.316365091
85.52241487	2.35258513
85.48647743	2.388522565
85.45081938	2.424180621
85.41543752	2.459562475
85.38032874	2.494671259
85.34548994	2.529510058
85.31091809	2.564081909
85.27661019	2.59838981
85.24256329	2.63243671
85.20877448	2.666225518
85.1752409	2.6997591
85.14195972	2.733040281
85.10892815	2.766071845
85.07614346	2.798856537
85.04360294	2.83139706
85.01130392	2.863696082
84.97924377	2.89575623
84.9474199	2.927580095
84.91582977	2.959170233
84.88447084	2.990529161
84.85334064	3.021659363
84.82243671	3.052563287
84.79175665	3.083243348
84.76129808	3.113701925
84.73105863	3.143941367
84.70103601	3.173963988
84.67122793	3.203772072
84.64163213	3.233367871
84.61224639	3.262753606
84.58306853	3.291931468
84.55409638	3.320903617
84.52532782	3.349672185
84.49676073	3.378239274
84.46839304	3.40660696
84.44022271	3.434777289
84.41224772	3.462752279
84.38446608	3.490533924
84.35687581	3.518124187
84.32947499	3.545525009
84.3022617	3.572738304
84.27523404	3.59976596
84.24839016	3.62660984
84.22172822	3.653271784
84.19524639	3.679753607

84.1689429	3.7060571
84.14281597	3.732184032
84.11686385	3.758136146
84.09108483	3.783915167
84.06547721	3.809522795
84.04003929	3.834960707
84.01476944	3.860230562
83.98966601	3.885333994
83.96472738	3.91027262
83.93995197	3.935048032
83.91533819	3.959661807
83.8908845	3.984115497
83.86658936	4.008410639
83.84245125	4.032548746
83.81846868	4.056531317
83.79464017	4.080359829
83.77096426	4.104035741
83.7474395	4.127560495
83.72406449	4.150935515
83.70083779	4.174162205
83.67775804	4.197241956
83.65482386	4.220176138
83.63203389	4.242966106
83.6093868	4.2656132
83.58688126	4.288118739
83.56451597	4.310484032
83.54228963	4.332710367
83.52020098	4.35479902
83.49824875	4.376751249
83.4764317	4.3985683
83.4547486	4.4202514
83.43319824	4.441801765
83.41177941	4.463220595
83.39049092	4.484509075
83.36933162	4.505668378
83.34830034	4.526699662
83.32739593	4.547604071
83.30661726	4.568382735
83.28596323	4.589036774
83.26543271	4.60956729
83.24502462	4.629975377
83.22473789	4.650262114
83.20457143	4.670428566
83.18452421	4.690475789
83.16459518	4.710404825
83.1447833	4.730216703
83.12508756	4.749912443
83.10550695	4.76949305
83.08604048	4.788959521
83.06668716	4.80831284

83.04744602	4.827553979
83.0283161	4.8466839
83.00929645	4.865703554
82.99038612	4.884613881
82.97158419	4.903415812
82.95288973	4.922110266
82.93430185	4.940698152
82.91581963	4.959180368
82.8974422	4.977557805
82.87916866	4.995831341
82.86099815	5.014001845
82.84292982	5.032070178
82.82496281	5.050037191
82.80709628	5.067903723
82.78932939	5.085670608
82.77166133	5.103338668
82.75409128	5.120908718
82.73661844	5.138381562
82.719242	5.155757997
82.70196119	5.17303881
82.68477522	5.190224782
82.66768332	5.207316683
82.65068472	5.224315276
82.63377868	5.241221315
82.61696445	5.258035548
82.60024129	5.274758713
82.58360846	5.29139154
82.56706525	5.307934753
82.55061093	5.324389068
82.53424481	5.340755192
82.51796617	5.357033826
82.50177434	5.373225663
82.48566861	5.389331389
82.46964832	5.405351683
82.45371278	5.421287217
82.43786134	5.437138656
82.42209334	5.452906657
82.40640813	5.468591872
82.39080506	5.484194944
82.37528349	5.499716513
82.35984279	5.51515721
82.34448234	5.530517659
82.32920152	5.545798478
82.31399972	5.561000281
82.29887633	5.576123673
82.28383075	5.591169254
82.26886238	5.606137618
82.25397065	5.621029352
82.23915496	5.63584504
82.22441474	5.650585256

82.20974943	5.665250572
82.19515845	5.679841552
82.18064124	5.694358755
82.16619726	5.708802735
82.15182596	5.72317404
82.13752679	5.737473212
82.12329921	5.751700789
82.1091427	5.765857303
82.09505672	5.779943281
82.08104076	5.793959244
82.06709429	5.807905709
82.05321681	5.821783188
82.03940781	5.835592187
82.02566679	5.849333207
82.01199325	5.863006747
81.9983867	5.876613297
81.98484666	5.890153344
81.97137263	5.903627373
81.95796414	5.91703586
81.94462072	5.93037928
81.9313419	5.9436581
81.91812721	5.956872786
81.9049762	5.970023797
81.89188841	5.983111589
81.87886339	5.996136615
81.86590068	6.009099319
81.85299985	6.022000147
81.84016046	6.034839536
81.82738208	6.047617921
81.81466427	6.060335733
81.8020066	6.072993398
81.78940866	6.08559134
81.77687002	6.098129976
81.76439028	6.110609721
81.75196901	6.123030987
81.73960582	6.135394181
81.72730029	6.147699706
81.71505204	6.159947961
81.70286066	6.172139344
81.69072575	6.184274247
81.67864694	6.196353058
81.66662384	6.208376162
81.65465606	6.220343943
81.64274322	6.232256777
81.63088496	6.24411504
81.6190809	6.255919105
81.60733066	6.267669338
81.5956339	6.279366105
81.58399023	6.291009768
81.57239932	6.302600684

81.56086079	6.31413921
81.5493743	6.325625698
81.5379395	6.337060496
81.52655605	6.34844395
81.5152236	6.359776403
81.5039418	6.371058196
81.49271034	6.382289664
81.48152886	6.393471141
81.47039704	6.404602959
81.45931455	6.415685445
81.44828107	6.426718925
81.43729628	6.437703721
81.42635985	6.448640153
81.41547146	6.459528536
81.40463081	6.470369186
81.39383759	6.481162414
81.38309147	6.491908527
81.37239217	6.502607833
81.36173937	6.513260634
81.35113277	6.523867231
81.34057208	6.534427922
81.330057	6.544943003
81.31958723	6.555412768
81.30916249	6.565837505
81.2987825	6.576217505
81.28844695	6.586553052
81.27815557	6.59684443
81.26790808	6.607091919
81.2577042	6.617295798
81.24754366	6.627456344
81.23742617	6.63757383
81.22735147	6.647648527
81.21731929	6.657680706
81.20732937	6.667670633
81.19738143	6.677618573
81.18747521	6.687524789
81.17761046	6.697389541
81.16778691	6.707213088
81.15800432	6.716995685
81.14826241	6.726737587
81.13856095	6.736439046
81.12889969	6.746100312
81.11927837	6.755721633
81.10969675	6.765303255
81.10015458	6.774845421
81.09065163	6.784348373
81.08118765	6.793812352
81.07176241	6.803237595
81.06237566	6.812624338
81.05302718	6.821972817

81.04371674	6.831283262
81.0344441	6.840555904
81.02520903	6.849790972
81.01601131	6.858988693
81.00685071	6.868149291
80.99772701	6.87727299
80.98863999	6.886360012
80.97958943	6.895410574
80.9705751	6.904424896
80.96159681	6.913403194
80.95265432	6.922345682
80.94374743	6.931252572
80.93487592	6.940124077
80.9260396	6.948960405
80.91723824	6.957761763
80.90847164	6.966528359
80.8997396	6.975260397
80.89104192	6.983958079
80.88237839	6.992621608
80.87374882	7.001251182
80.865153	7.009847
80.85659074	7.018409259
80.84806185	7.026938154
80.83956612	7.035433879
80.83110337	7.043896625
80.82267342	7.052326585
80.81427605	7.060723946
80.8059111	7.069088897
80.79757838	7.077421624
80.78927769	7.085722312
80.78100886	7.093991145
80.7727717	7.102228305
80.76456603	7.110433972
80.75639167	7.118608326
80.74824845	7.126751546
80.74013619	7.134863807
80.73205471	7.142945286
80.72400384	7.150996156
80.71598341	7.15901659
80.70799324	7.16700676
80.70003316	7.174966836
80.69210301	7.182896986
80.68420262	7.190797379
80.67633182	7.198668181
80.66849044	7.206509557
80.66067833	7.214321671
80.65289531	7.222104686
80.64514124	7.229858764
80.63741594	7.237584064
80.62971925	7.245280746

80.62205103	7.252948969
80.61441111	7.260588888
80.60679934	7.26820066
80.59921556	7.275784439
80.59165962	7.28334038
80.58413137	7.290868633
80.57663065	7.298369351
80.56915732	7.305842683
80.56171122	7.313288779
80.55429221	7.320707786
80.54690015	7.328099852
80.53953488	7.335465123
80.53219626	7.342803743
80.52488414	7.350115856
80.5175984	7.357401605
80.51033887	7.364661131
80.50310542	7.371894576
80.49589792	7.379102079
80.48871622	7.386283778
80.48156019	7.393439813
80.47442968	7.400570318
80.46732457	7.407675431
80.46024471	7.414755286
80.45318998	7.421810017
80.44616024	7.428839756
80.43915536	7.435844637
80.43217521	7.44282479
80.42521966	7.449780345
80.41828857	7.456711431
80.41138182	7.463618178
80.40449929	7.470500712
80.39764084	7.477359159
80.39080635	7.484193647
80.3839957	7.4910043
80.37720876	7.49779124
80.37044541	7.504554593
80.36370552	7.51129448
80.35698898	7.518011022
80.35029566	7.524704341
80.34362544	7.531374555
80.33697822	7.538021784
80.33035385	7.544646147
80.32375224	7.551247759
80.31717326	7.557826739
80.3106168	7.564383201
80.30408274	7.570917262
80.29757097	7.577429034
80.29108137	7.583918631
80.28461383	7.590386166
80.27816825	7.596831752

80.2717445	7.603255498
80.26534248	7.609657516
80.25896209	7.616037915
80.2526032	7.622396804
80.24626571	7.628734291
80.23994952	7.635050484
80.23365451	7.64134549
80.22738059	7.647619414
80.22112764	7.653872362
80.21489556	7.660104439
80.20868425	7.666315748
80.20249361	7.672506393
80.19632352	7.678676477
80.1901739	7.6848261
80.18404463	7.690955366
80.17793563	7.697064373
80.17184678	7.703153223
80.16577799	7.709222014
80.15972916	7.715270844
80.15370019	7.721299813
80.14769098	7.727309017
80.14170145	7.733298553
80.13573148	7.739268517
80.129781	7.745219005
80.12384989	7.751150111
80.11793807	7.757061929
80.11204545	7.762954554
80.10617192	7.768828078
80.10031741	7.774682593
80.09448181	7.780518192
80.08866503	7.786334966
80.082867	7.792133005
80.0770876	7.797912399
80.07132676	7.803673238
80.06558439	7.809415611
80.05986039	7.815139607
80.05415469	7.820845312
80.04846719	7.826532815
80.0427978	7.832202201
80.03714644	7.837853557
80.03151303	7.84348697
80.02589748	7.849102523
80.0202997	7.854700301
80.01471961	7.860280388
80.00915713	7.865842868
80.00361218	7.871387824
79.99808466	7.876915338
79.99257451	7.882425492
79.98708163	7.887918368
79.98160595	7.893394045

79.97614739	7.898852606
79.97070587	7.904294128
79.96528131	7.909718693
79.95987362	7.915126379
79.95448274	7.920517264
79.94910857	7.925891427
79.94375106	7.931248944
79.93841011	7.936589893
79.93308565	7.94191435
79.92777761	7.947222391
79.92248591	7.952514092
79.91721047	7.957789529
79.91195123	7.963048774
79.9067081	7.968291904
79.90148101	7.973518991
79.89626989	7.978730109
79.89107467	7.98392533
79.88589527	7.989104728
79.88073163	7.994268373
79.87558366	7.999416339
79.87045131	8.004548695
79.86533449	8.009665512
79.86023314	8.014766862
79.85514719	8.019852812
79.85007657	8.024923434
79.8450212	8.029978796
79.83998103	8.035018966
79.83495599	8.040044012
79.829946	8.045054004
79.82495099	8.050049007
79.81997091	8.055029089
79.81500568	8.059994316
79.81005524	8.064944755
79.80511953	8.069880471
79.80019847	8.07480153
79.795292	8.079707997
79.79040006	8.084599936
79.78552259	8.089477412
79.78065951	8.094340489
79.77581077	8.099189229
79.7709763	8.104023697
79.76615605	8.108843954
79.76134994	8.113650064
79.75655791	8.118442088
79.75177991	8.123220088
79.74701587	8.127984126
79.74226574	8.132734261
79.73752944	8.137470556
79.73280693	8.14219307
79.72809814	8.146901862

79.72340301	8.151596993
79.71872148	8.156278522
79.71405349	8.160946508
79.70939899	8.165601009
79.70475792	8.170242083

43 Degrees Notch on Lynne Turner Model

Raw Data

0% fin deployment @ 10degrees yaw	Value	Units
Roll Moment	0.141469955	Nm
Pitch Moment	-0.80548501	Nm
Drag Force	7.484310627	N
Drag Force Coefficient	0.50119704	No units
Lift Force	3.192112207	N
Lift Force Coefficient	0.213764131	No units
Yaw Moment	-1.110024929	Nm
Pitch Moment Coefficient	-0.0539404	No units
Roll Moment Coefficient	0.009473728	No units
Side Force	-4.803866863	N
Side Force Coefficient	-0.321697474	No units
Yaw Moment Coefficient	-0.074334331	No units
Ref. Pressure	3.75E+00	Pa
Frontal Area	2.80E-02	m^2

50% fin deployment @ 10degrees yaw	Value	Units
Roll Moment	0.070055597	Nm
Pitch Moment	0.128688276	Nm
Drag Force	6.965256214	N
Drag Force Coefficient	0.466437846	No units
Lift Force	2.549847364	N
Lift Force Coefficient	0.170754001	No units
Yaw Moment	0.60635215	Nm
Pitch Moment Coefficient	0.008617786	No units
Roll Moment Coefficient	0.004691368	No units
Side Force	-6.813680172	N
Side Force Coefficient	-0.456287354	No units
Yaw Moment Coefficient	0.040605195	No units
Ref. Pressure	4.60E+00	Pa
Frontal Area	2.80E-02	m^2

100% fin deployment @ 10degrees yaw	Value	Units
Roll Moment	0.084969543	Nm
Pitch Moment	0.109098323	Nm
Drag Force	7.049565315	N
Drag Force Coefficient	0.472083718	No units
Lift Force	2.573182106	N
Lift Force Coefficient	0.172316641	No units
Yaw Moment	0.590891182	Nm
Pitch Moment Coefficient	0.007305917	No units
Roll Moment Coefficient	0.005690101	No units

Side Force	-7.149894714	N
Side Force Coefficient	-0.478802413	No units
Yaw Moment Coefficient	0.039569832	No units
Ref. Pressure	4.66E+00	Pa
Frontal Area	2.80E-02	m^2

Overall Results

0% Deployment		
Force, Moments & Coefficients	0	10
Drag Force (N)	5.076	7.484
Drag Force Coefficient	0.340	0.501
Lift Force (N)	0.943	3.192
Lift Force Coefficient	0.063	0.214
Side Force (N)	-0.897	4.804
Side Force Coefficient	-0.060	0.322
Roll Moment (Nm)	-0.033	0.141
Roll Moment Coefficient	-0.002	0.009
Pitch Moment (Nm)	-0.208	-0.805
Pitch Moment Coefficient	-0.014	-0.054
Yaw Moment (Nm)	0.034	-1.110
Yaw Moment Coefficient	0.002	-0.074
Reference Pressure (Pa)	3.33271	3.74525
Frontal Area (m^2)	0.02802	0.02802

50% Deployment		
Force, Moments & Coefficients	0	10
Drag Force (N)	N/A	6.965
Drag Force Coefficient	N/A	0.466
Lift Force (N)	N/A	2.550
Lift Force Coefficient	N/A	0.171
Side Force (N)	N/A	6.814
Side Force Coefficient	N/A	0.456
Roll Moment (Nm)	N/A	0.070
Roll Moment Coefficient	N/A	0.005
Pitch Moment (Nm)	N/A	0.129
Pitch Moment Coefficient	N/A	0.009
Yaw Moment (Nm)	N/A	0.606
Yaw Moment Coefficient	N/A	0.041
Reference Pressure (Pa)	N/A	4.59961
Frontal Area (m^2)	0.02802	0.02802

100% Deployment		
Force, Moments & Coefficients	0	10
Drag Force (N)	N/A	7.050
Drag Force Coefficient	N/A	0.472
Lift Force (N)	N/A	2.573
Lift Force Coefficient	N/A	0.172

Side Force (N)	N/A	7.150
Side Force Coefficient	N/A	0.479
Roll Moment (Nm)	N/A	0.085
Roll Moment Coefficient	N/A	0.006
Pitch Moment (Nm)	N/A	0.109
Pitch Moment Coefficient	N/A	0.007
Yaw Moment (Nm)	N/A	0.591
Yaw Moment Coefficient	N/A	0.040
Reference Pressure (Pa)	N/A	4.659
Frontal Area (m^2)	0.028	0.028

Comparison @ 10° Yaw	Fin Deployment Stag	
Force, Moments & Coefficients	0	50
Drag Force (N)	7.484	6.965
Drag Force Coefficient	0.501	0.466
Lift Force (N)	3.192	2.550
Lift Force Coefficient	0.214	0.171
Side Force (N)	4.804	6.814
Side Force Coefficient	0.322	0.456
Roll Moment (Nm)	0.141	0.070
Roll Moment Coefficient	0.009	0.005
Pitch Moment (Nm)	-0.805	0.129
Pitch Moment Coefficient	-0.054	0.009
Yaw Moment (Nm)	-1.110	0.606
Yaw Moment Coefficient	-0.074	0.041
Reference Pressure (Pa)	3.745	4.600
Frontal Area (m^2)	0.028	0.028

Comparison @ 30° Yaw	Fin Deployment Stag	
Force, Moments & Coefficients	0	50
Drag Force (N)	14.308	15.214
Drag Force Coefficient	0.958	1.019
Lift Force (N)	12.923	12.142
Lift Force Coefficient	0.865	0.813
Side Force (N)	12.881	17.054
Side Force Coefficient	0.863	1.142
Roll Moment (Nm)	1.923	0.054
Roll Moment Coefficient	0.129	0.004
Pitch Moment (Nm)	-2.598	0.997
Pitch Moment Coefficient	-0.174	0.067
Yaw Moment (Nm)	-4.124	1.151
Yaw Moment Coefficient	-0.276	0.077
Reference Pressure (Pa)	6.568	10.134
Frontal Area (m^2)	0.028	0.028

Comparison @ 60° Yaw	Fin Deployment Stag	
Force, Moments & Coefficients	0	50
Drag Force (N)	20.886	21.622

Drag Force Coefficient	1.399	1.448
Lift Force (N)	23.940	21.067
Lift Force Coefficient	1.603	1.411
Side Force (N)	9.680	10.704
Side Force Coefficient	0.648	0.717
Roll Moment (Nm)	6.371	-0.330
Roll Moment Coefficient	0.427	-0.022
Pitch Moment (Nm)	-2.721	1.142
Pitch Moment Coefficient	-0.182	0.076
Yaw Moment (Nm)	-6.027	0.965
Yaw Moment Coefficient	-0.404	0.065
Reference Pressure (Pa)	10.858	14.846
Frontal Area (m^2)	0.028	0.028

Comparison @ 90° Yaw	Fin Deployment Stag	
Force, Moments & Coefficients	0	50
Drag Force (N)	15.242	16.788
Drag Force Coefficient	1.021	1.124
Lift Force (N)	25.420	21.830
Lift Force Coefficient	1.702	1.462
Side Force (N)	2.125	3.149
Side Force Coefficient	0.142	0.211
Roll Moment (Nm)	8.152	-0.100
Roll Moment Coefficient	0.546	-0.007
Pitch Moment (Nm)	1.572	1.572
Pitch Moment Coefficient	0.105	0.105
Yaw Moment (Nm)	-5.090	-0.576
Yaw Moment Coefficient	-0.341	-0.039
Reference Pressure (Pa)	7.502	11.322
Frontal Area (m^2)	0.028	0.028

0% fin deployment @ 30degrees yaw	Value
Roll Moment	1.923430562
Pitch Moment	-2.598447084
Drag Force	14.30772877
Drag Force Coefficient	0.958136499
Lift Force	12.92325115
Lift Force Coefficient	0.865423083
Yaw Moment	-4.123958111
Pitch Moment Coefficient	-0.174008548
Roll Moment Coefficient	0.128805146
Side Force	-12.88124943
Side Force Coefficient	-0.8626104
Yaw Moment Coefficient	-0.276166469
Ref. Pressure	6.57E+00
Frontal Area	2.80E-02

50% fin deployment @ 30degrees yaw	Value
Roll Moment	0.053531371
Pitch Moment	0.996965647
Drag Force	15.21417904
Drag Force Coefficient	1.018838167
Lift Force	12.14207554
Lift Force Coefficient	0.81311059
Yaw Moment	1.151279449
Pitch Moment Coefficient	0.066763163
Roll Moment Coefficient	0.003584801
Side Force	-17.05401421
Side Force Coefficient	-1.142045259
Yaw Moment Coefficient	0.077096991
Ref. Pressure	1.01E+01
Frontal Area	2.80E-02

100% fin deployment @ 30degrees yaw	Value
Roll Moment	0.043213777
Pitch Moment	1.071302652
Drag Force	15.85255623
Drag Force Coefficient	1.06158793
Lift Force	11.39568138
Lift Force Coefficient	0.763127267
Yaw Moment	0.984828174
Pitch Moment Coefficient	0.071741238
Roll Moment Coefficient	0.002893869

Side Force	-18.33766556
Side Force Coefficient	-1.228006721
Yaw Moment Coefficient	0.065950356
Ref. Pressure	1.08E+01
Frontal Area	2.80E-02

Yaw		
30	60	90
14.308	20.886	15.242
0.958	1.399	1.021
12.923	23.940	25.420
0.865	1.603	1.702
12.881	9.680	2.125
0.863	0.648	0.142
1.923	6.371	8.152
0.129	0.427	0.546
-2.598	-2.721	1.572
-0.174	-0.182	0.105
-4.124	-6.027	-5.090
-0.276	-0.404	-0.341
6.56809	10.85789	7.50184
0.02802	0.02802	0.02802

Drag Force (N)

Yaw		
30	60	90
15.214	21.622	16.788
1.019	1.448	1.124
12.142	21.067	21.830
0.813	1.411	1.462
17.054	10.704	3.149
1.142	0.717	0.211
0.054	-0.330	-0.100
0.004	-0.022	-0.007
0.997	1.142	1.572
0.067	0.076	0.105
1.151	0.965	-0.576
0.077	0.065	-0.039
10.13401	14.84611	11.32190
0.02802	0.02802	0.02802

Lift Coefficient

Yaw		
30	60	90
15.853	24.715	20.338
1.062	1.655	1.362
11.396	16.293	14.737
0.763	1.091	0.987

18.338	14.458	4.183
1.228	0.968	0.280
0.043	-0.686	-0.786
0.003	-0.019	-0.053
1.071	1.545	1.659
0.072	-0.046	0.111
0.985	0.598	-1.012
0.066	0.040	-0.068
10.805	16.707	14.035
0.028	0.028	0.028

Roll Moment (Nm)

e
100
7.050
0.472
2.573
0.172
7.150
0.479
0.085
0.006
0.109
0.007
0.591
0.040
4.659
0.028

e
100
15.853
1.062
11.396
0.763
18.338
1.228
0.043
0.003
1.071
0.072
0.985
0.066
10.805
0.028

e
100
24.715

1.655
16.293
1.091
14.458
0.968
-0.686
-0.019
1.545
-0.046
0.598
0.040
16.707
0.028

e
100
20.338
1.362
14.737
0.987
4.183
0.280
-0.786
-0.053
1.659
0.111
-1.012
-0.068
14.035
0.028

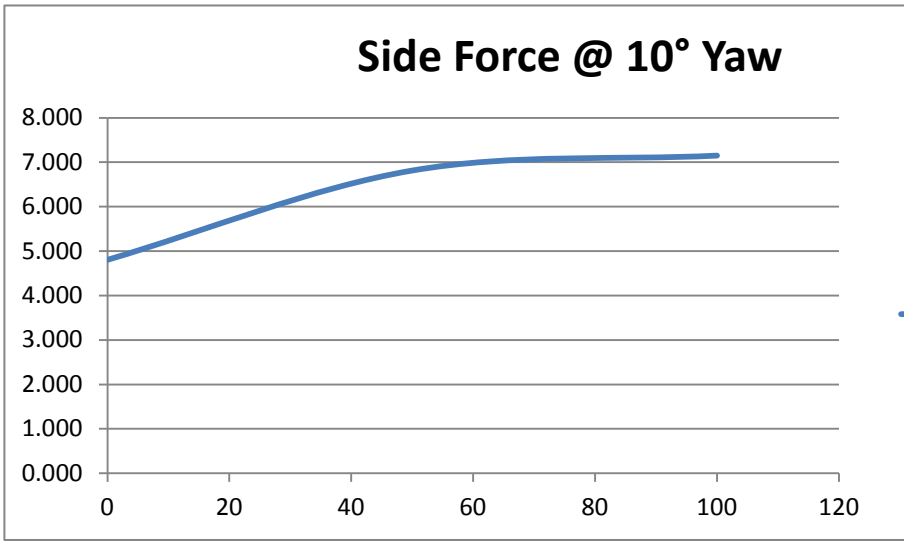

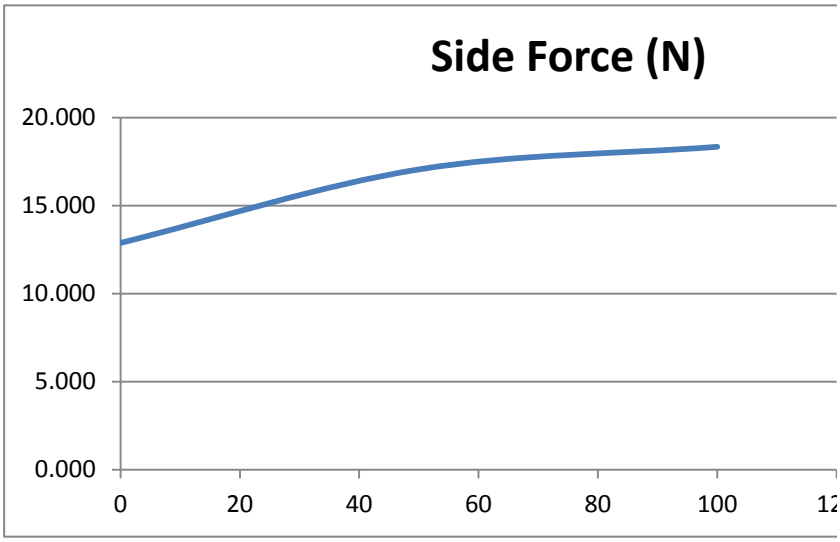

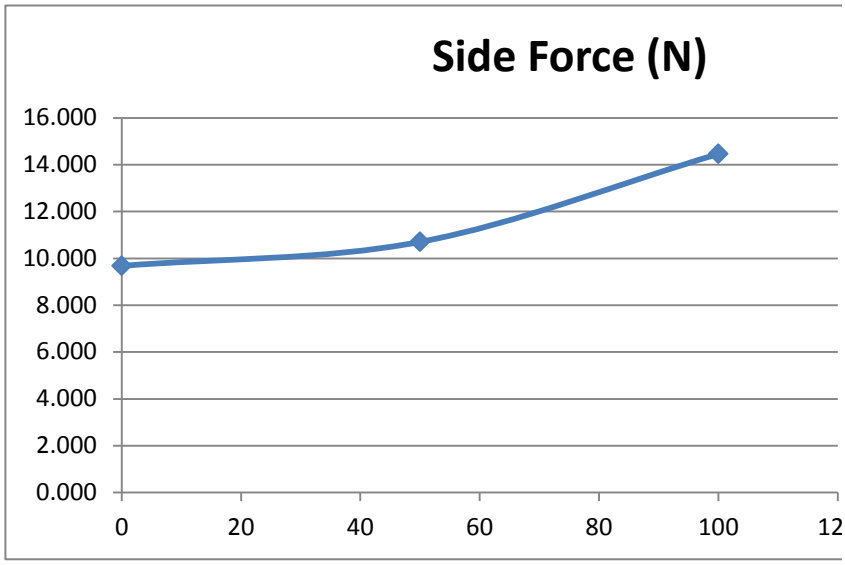

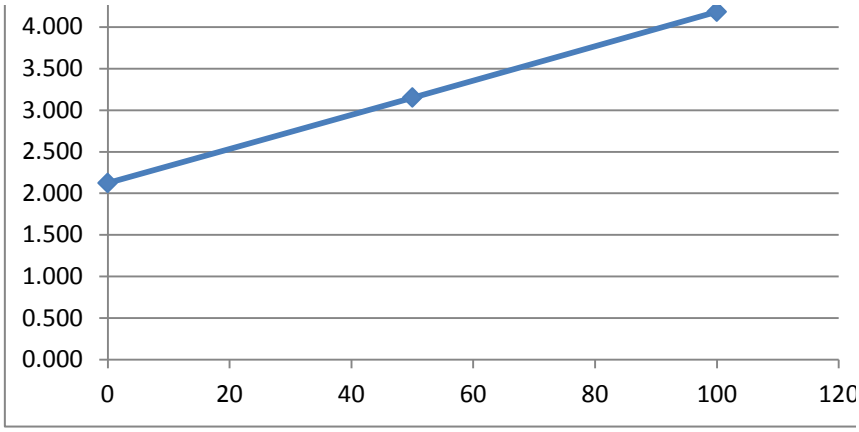
4.000
3.500
3.000
2.500
2.000
1.500
1.000
0.500
0.000
0
20
40
60
80
100
120

Units	0% fin deployment @ 60degrees yaw	Value
Nm	Roll Moment	6.371008396
Nm	Pitch Moment	-2.720584393
N	Drag Force	20.88595009
No units	Drag Force Coefficient	1.398656011
N	Lift Force	23.93993759
No units	Lift Force Coefficient	1.603170514
Nm	Yaw Moment	-6.026785851
No units	Pitch Moment Coefficient	-0.182187632
No units	Roll Moment Coefficient	0.426643252
N	Side Force	-9.679766655
No units	Side Force Coefficient	-0.648218751
No units	Yaw Moment Coefficient	-0.403591901
Pa	Ref. Pressure	1.09E+01
m^2	Frontal Area	2.80E-02

Units	50% fin deployment @ 60degrees yaw	Value
Nm	Roll Moment	-0.329891145
Nm	Pitch Moment	1.141638875
N	Drag Force	21.62191963
No units	Drag Force Coefficient	1.447941303
N	Lift Force	21.06679535
No units	Lift Force Coefficient	1.410766602
Nm	Yaw Moment	0.965242088
No units	Pitch Moment Coefficient	0.076451398
No units	Roll Moment Coefficient	-0.022091608
N	Side Force	-10.70365238
No units	Side Force Coefficient	-0.716784656
No units	Yaw Moment Coefficient	0.064638749
Pa	Ref. Pressure	1.48E+01
m^2	Frontal Area	2.80E-02

Units	100% fin deployment @ 60degrees yaw	Value
Nm	Roll Moment	-0.685865164
Nm	Pitch Moment	1.544643998
N	Drag Force	24.71454048
No units	Drag Force Coefficient	1.655042768
N	Lift Force	16.29276848
No units	Lift Force Coefficient	1.091067433
Nm	Yaw Moment	0.598042607
No units	Pitch Moment Coefficient	-0.045929894
No units	Roll Moment Coefficient	-0.018942891

N	
No units	
No units	
Pa	
m^2	

Side Force	-14.45813942
Side Force Coefficient	-0.968208969
Yaw Moment Coefficient	0.040048737
Ref. Pressure	1.67E+01
Frontal Area	2.80E-02

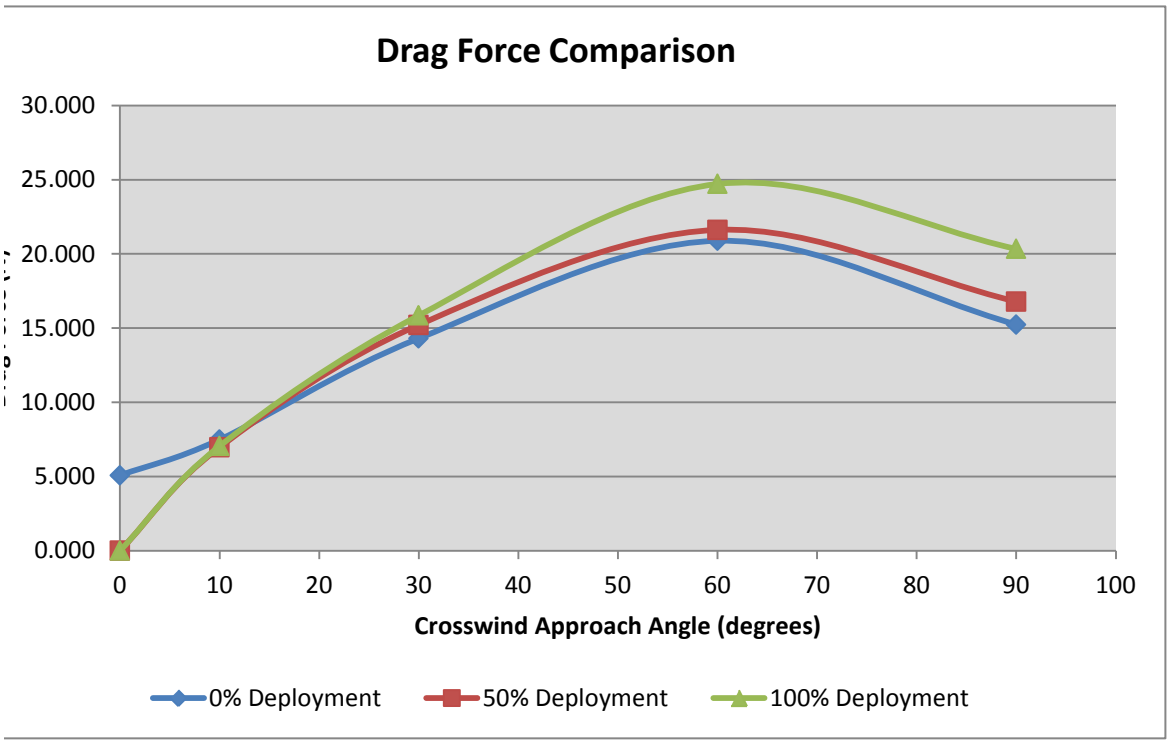

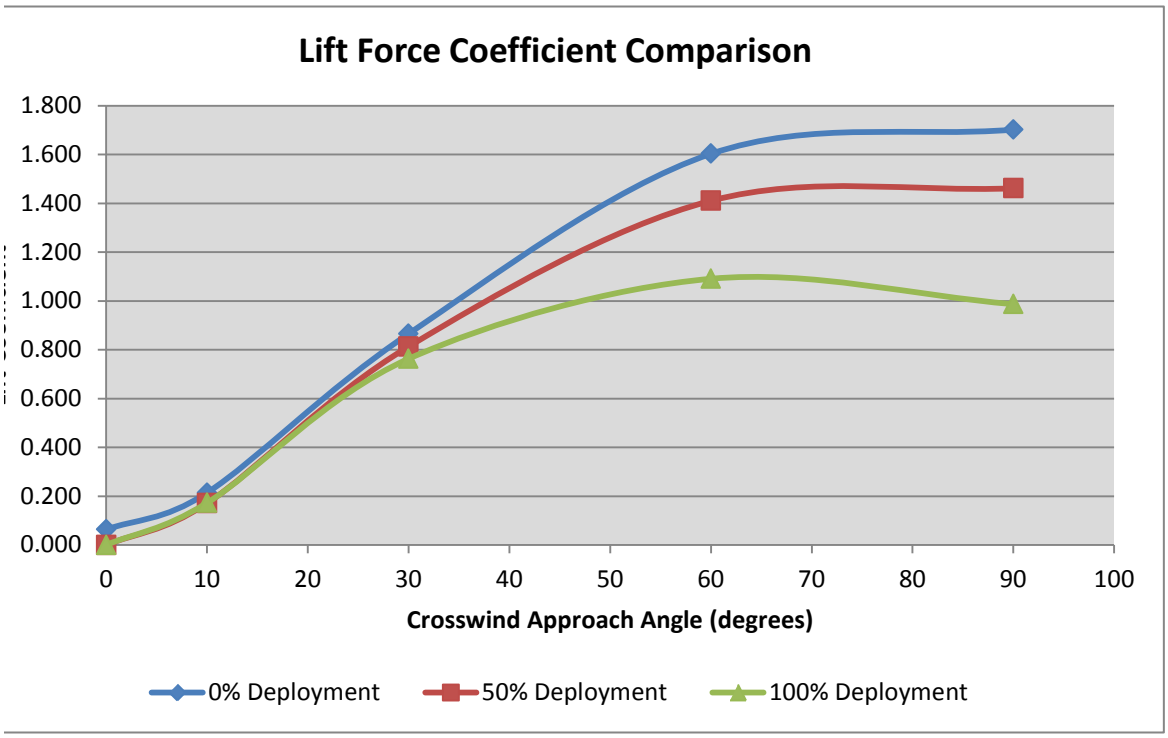

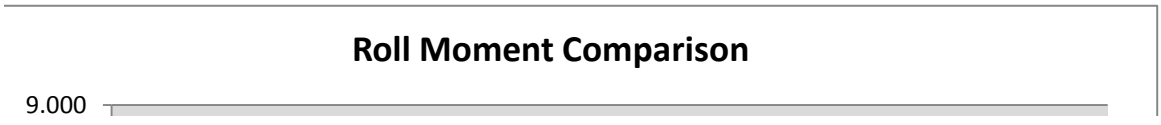

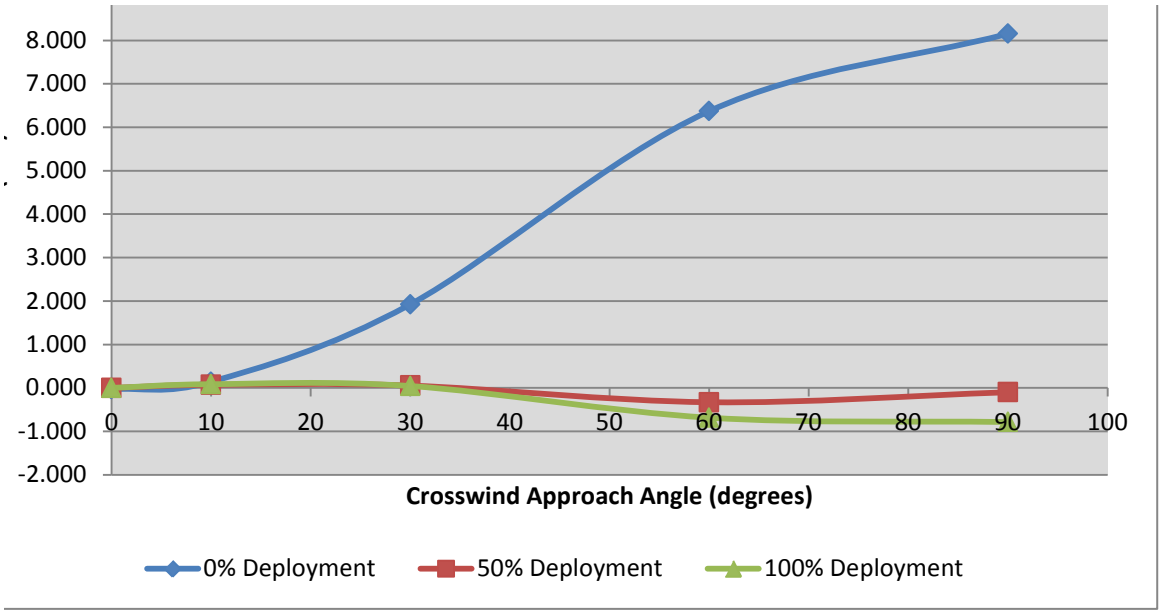
8.000
7.000
6.000
5.000
4.000
3.000
2.000
1.000
0.000
-1.000
-2.000
0
10
20
30
40
50
60
70
80
90
100
Crosswind Approach Angle (degrees)
0% Deployment
50% Deployment
100% Deployment

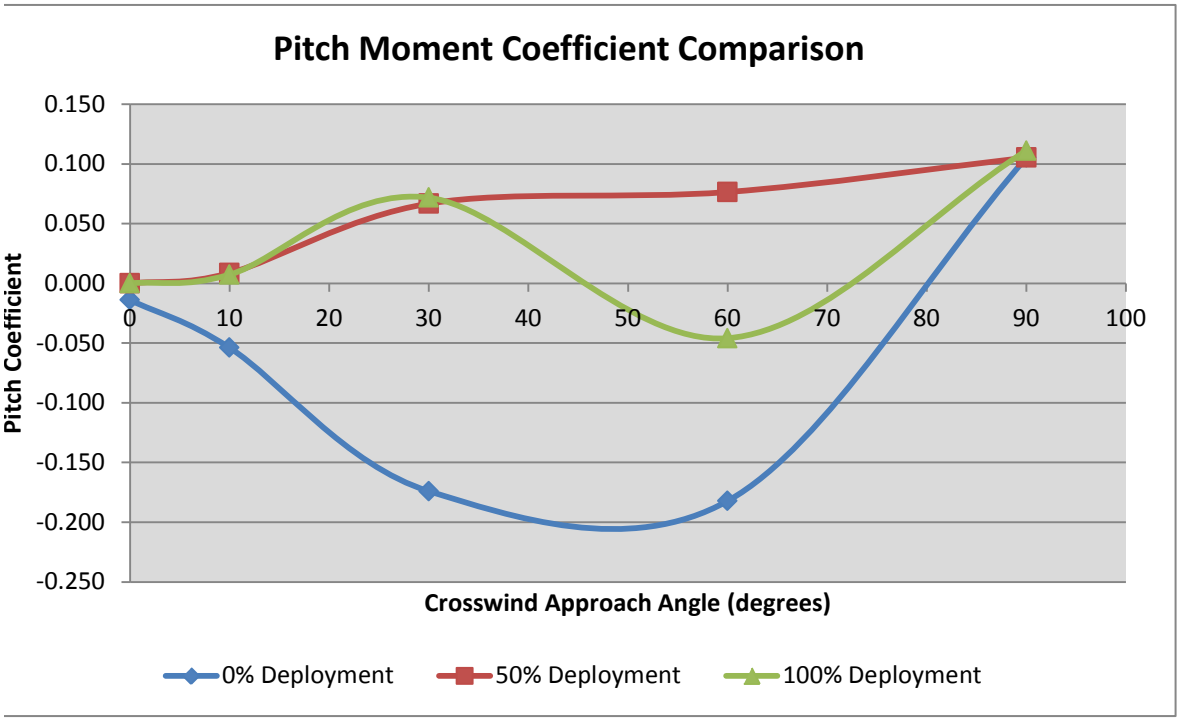
Pitch Moment Coefficient Comparison
0.150
0.100
0.050
0.000
-0.050
-0.100
-0.150
-0.200
-0.250
Pitch Coefficient
0
10
20
30
40
50
60
70
80
90
100
Crosswind Approach Angle (degrees)
0% Deployment
50% Deployment
100% Deployment

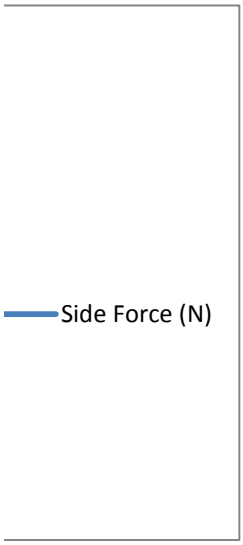
Side Force (N)

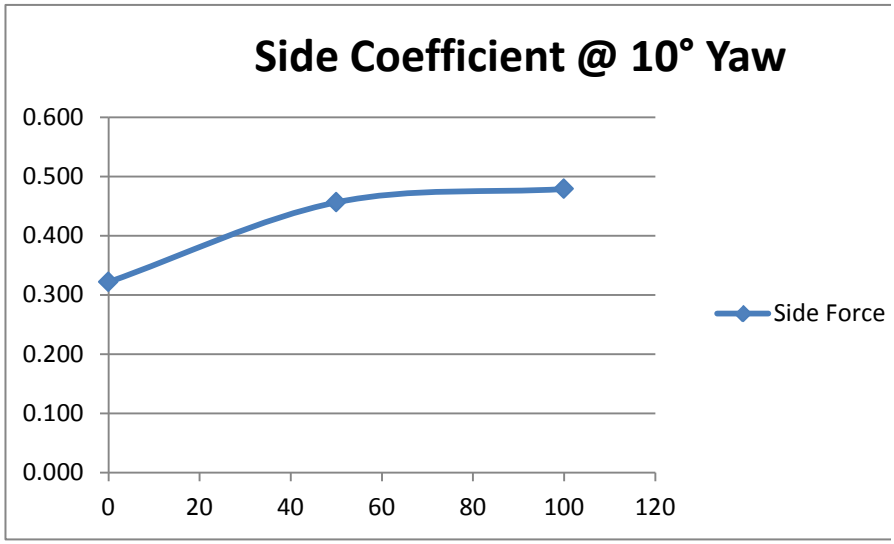
Side Coefficient @ 10° Yaw
0.600
0.500
0.400
0.300
0.200
0.100
0.000
0
20
40
60
80
100
120
Side Force

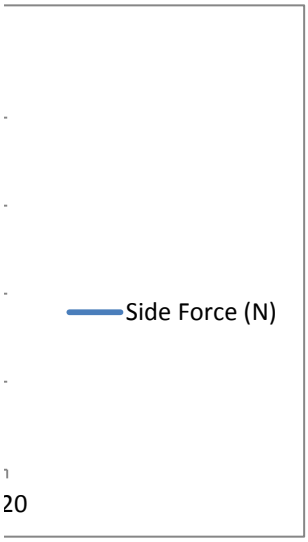
Side Force (N)
20

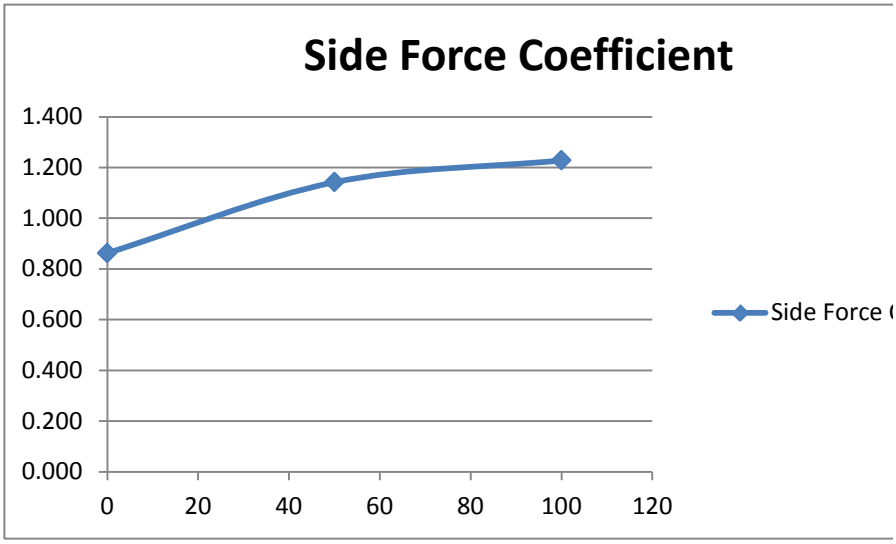
Side Force Coefficient
1.400
1.200
1.000
0.800
0.600
0.400
0.200
0.000
0
20
40
60
80
100
120
Side Force (

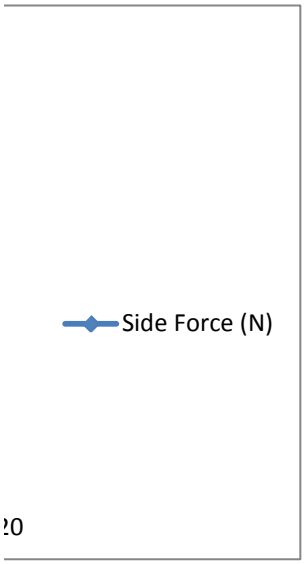
Side Force (N)
20

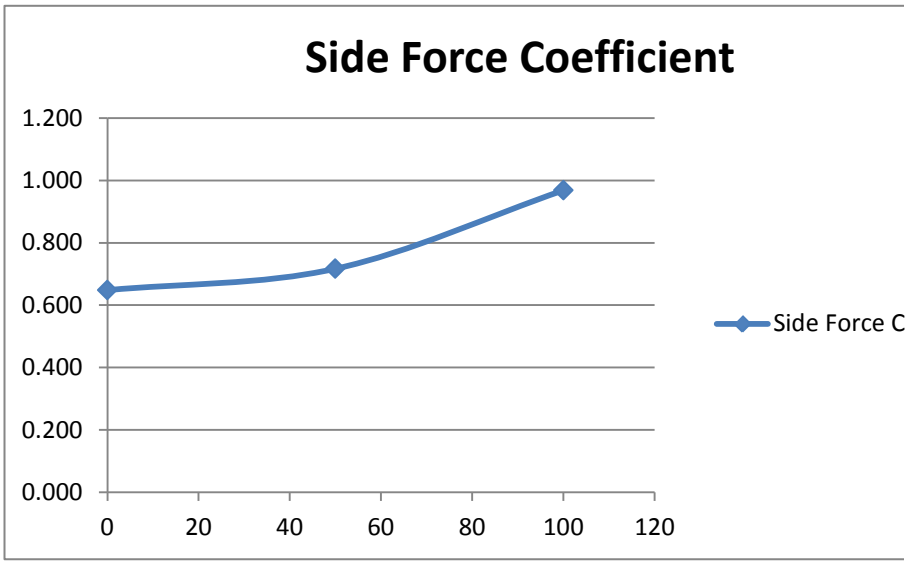
Side Force Coefficient
1.200
1.000
0.800
0.600
0.400
0.200
0.000
0
20
40
60
80
100
120
Side Force C


Side Force Coefficient
0.300

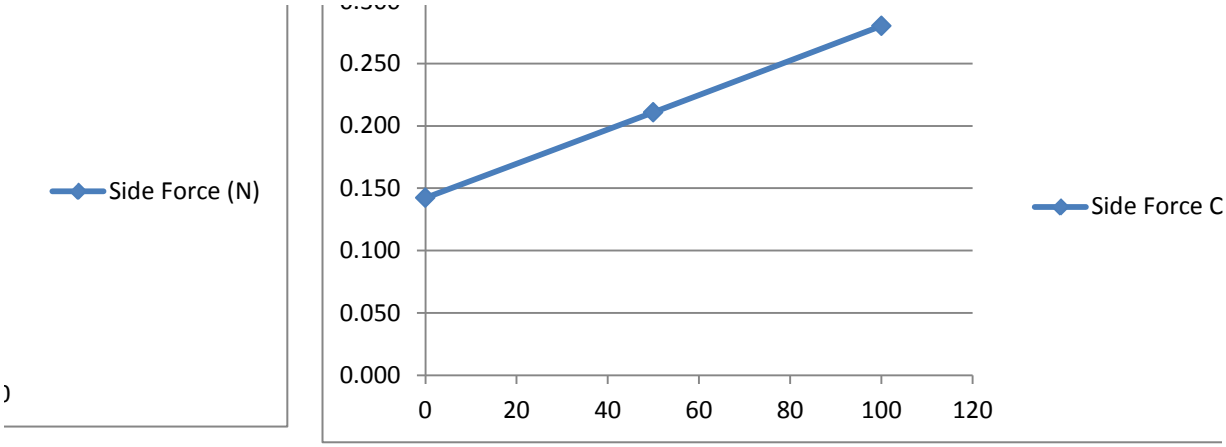
Side Force (N)
0.250
0.200
0.150
0.100
0.050
0.000
0
20
40
60
80
100
120
Side Force C

Units	0% fin deployment @ 90degrees yaw	Value	Units
Nm	Roll Moment	8.152252	Nm
Nm	Pitch Moment	1.571904	Nm
N	Drag Force	15.24222	N
No units	Drag Force Coefficient	1.020716	No units
N	Lift Force	25.41964	N
No units	Lift Force Coefficient	1.702261	No units
Nm	Yaw Moment	-5.08955	Nm
No units	Pitch Moment Coefficient	0.105265	No units
No units	Roll Moment Coefficient	0.545927	No units
N	Side Force	-2.12454	N
No units	Side Force Coefficient	-0.14227	No units
No units	Yaw Moment Coefficient	-0.34083	No units
Pa	Ref. Pressure	7.50E+00	Pa
m^2	Frontal Area	2.80E-02	m^2

Units	50% fin deployment @ 90degrees yaw	Value	Units
Nm	Roll Moment	-0.09987	Nm
Nm	Pitch Moment	1.572261	Nm
N	Drag Force	16.78788	N
No units	Drag Force Coefficient	1.124223	No units
N	Lift Force	21.82979	N
No units	Lift Force Coefficient	1.461862	No units
Nm	Yaw Moment	-0.57596	Nm
No units	Pitch Moment Coefficient	0.105289	No units
No units	Roll Moment Coefficient	-0.00669	No units
N	Side Force	-3.14854	N
No units	Side Force Coefficient	-0.21085	No units
No units	Yaw Moment Coefficient	-0.03857	No units
Pa	Ref. Pressure	1.13E+01	Pa
m^2	Frontal Area	2.80E-02	m^2

Units	100% fin deployment @ 90degrees yaw	Value	Units
Nm	Roll Moment	-0.78613	Nm
Nm	Pitch Moment	1.659322	Nm
N	Drag Force	20.33777	N
No units	Drag Force Coefficient	1.361946	No units
N	Lift Force	14.73709	N
No units	Lift Force Coefficient	0.986889	No units
Nm	Yaw Moment	-1.01215	Nm
No units	Pitch Moment Coefficient	0.111119	No units
No units	Roll Moment Coefficient	-0.05264	No units

	Side Force	-4.18288	N
	Side Force Coefficient	-0.28011	No units
	Yaw Moment Coefficient	-0.0678	No units
	Ref. Pressure	1.40E+01	Pa
	Frontal Area	2.80E-02	m^2

N
No units
No units
Pa
m^2

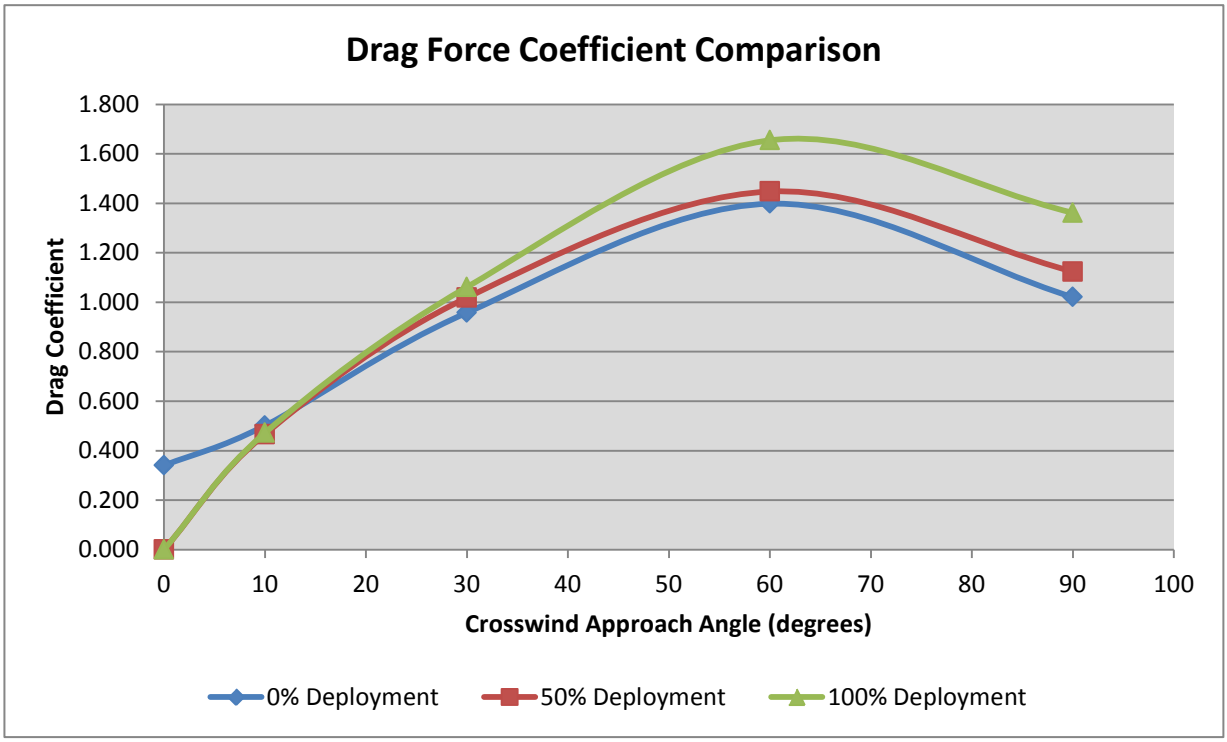

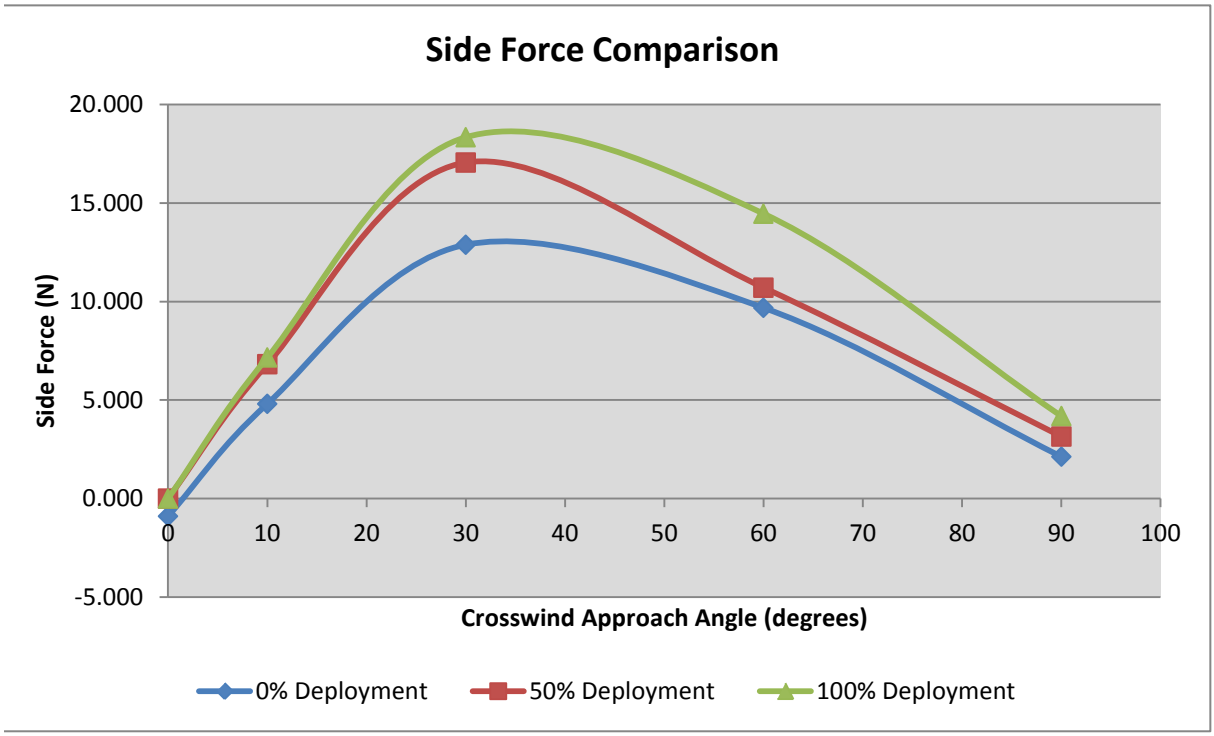

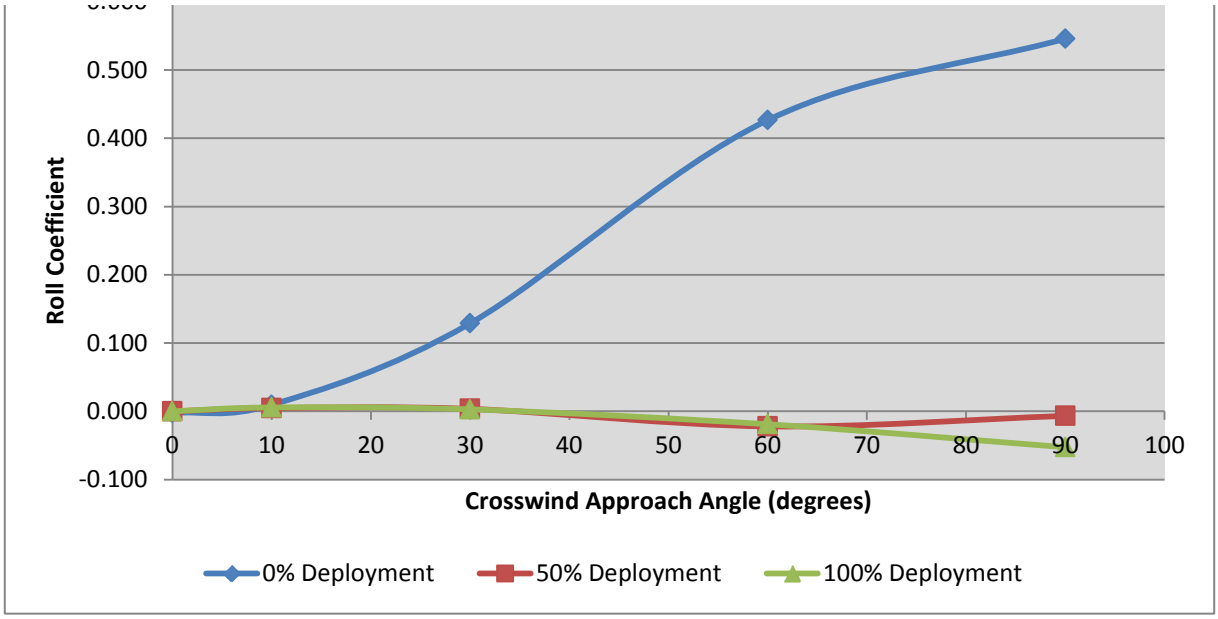
0.500
0.400
0.300
0.200
0.100
0.000
-0.100
Roll Coefficient
0
10
20
30
40
50
60
70
80
90
100
Crosswind Approach Angle (degrees)
0% Deployment
50% Deployment
100% Deployment

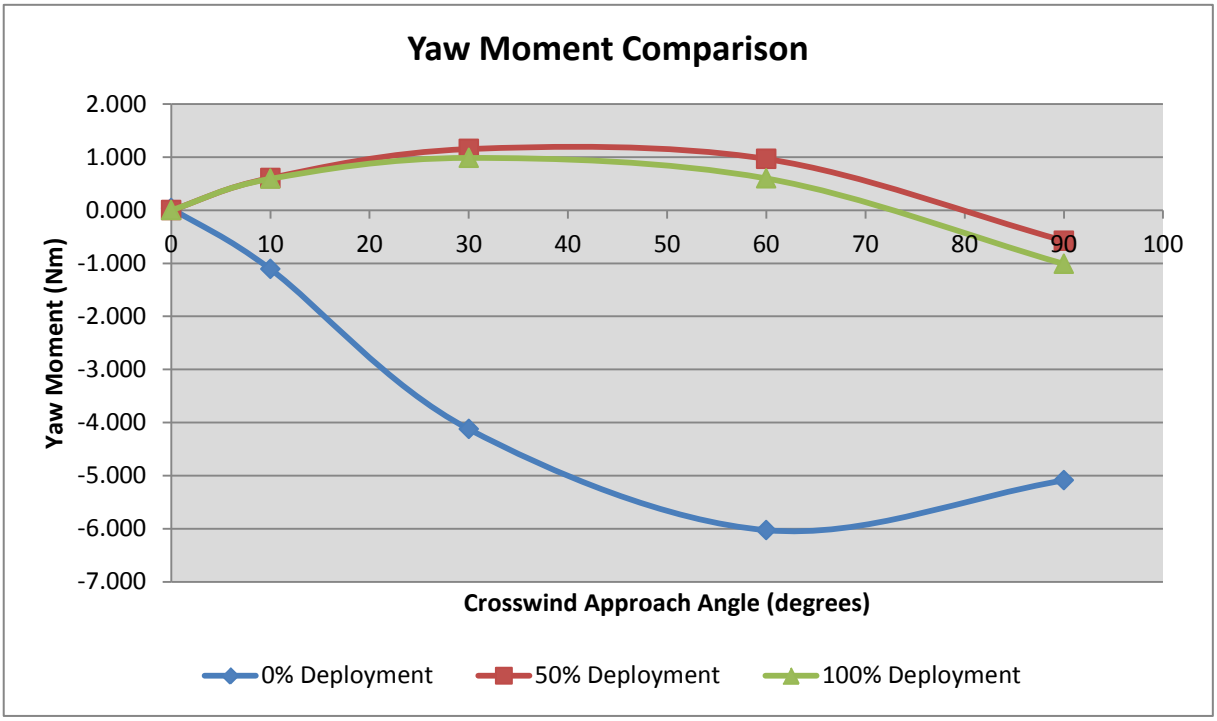
Yaw Moment Comparison
2.000
1.000
0.000
-1.000
-2.000
-3.000
-4.000
-5.000
-6.000
-7.000
Yaw Moment (Nm)
0
10
20
30
40
50
60
70
80
90
100
Crosswind Approach Angle (degrees)
0% Deployment
50% Deployment
100% Deployment

Coefficient

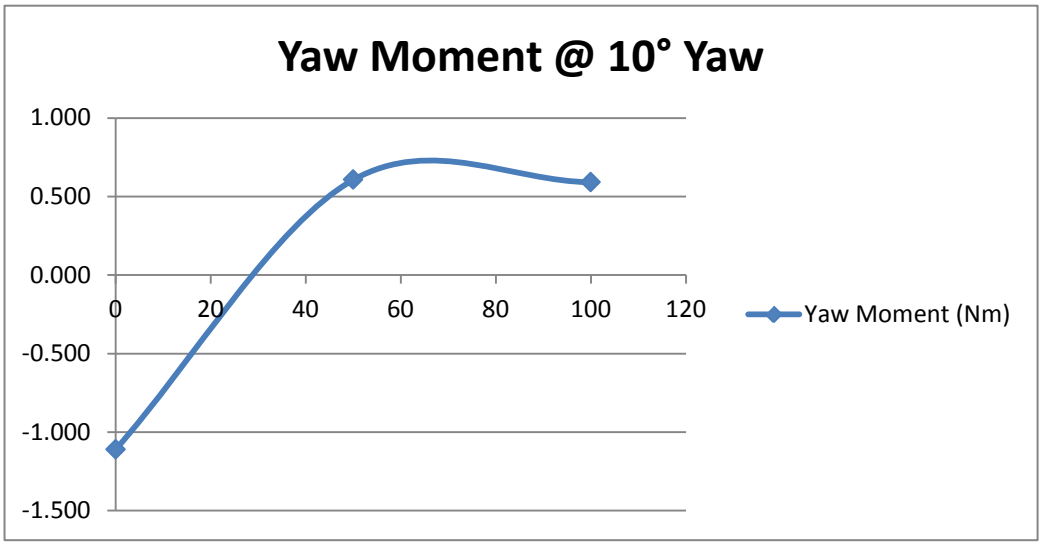

Coefficient

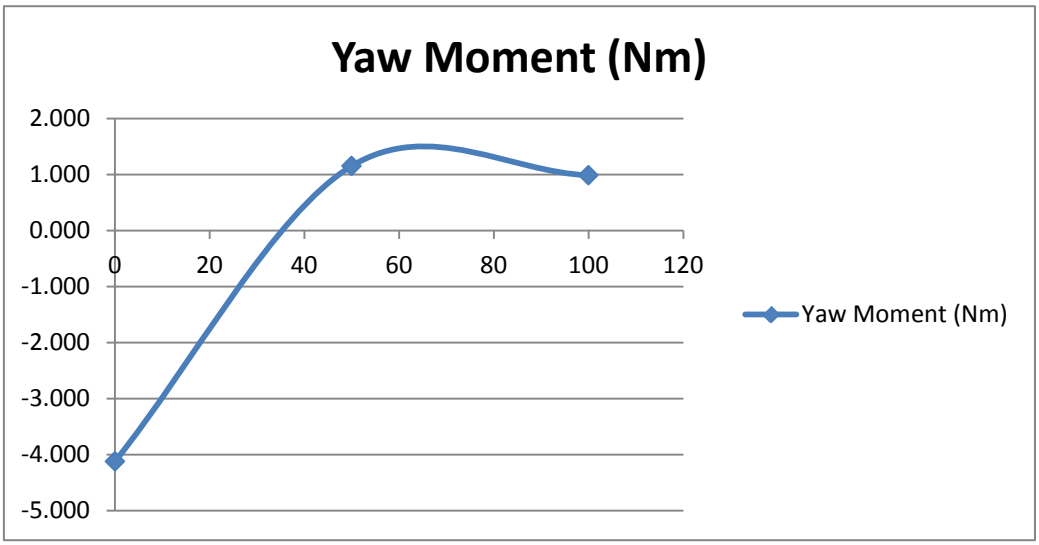

Coefficient

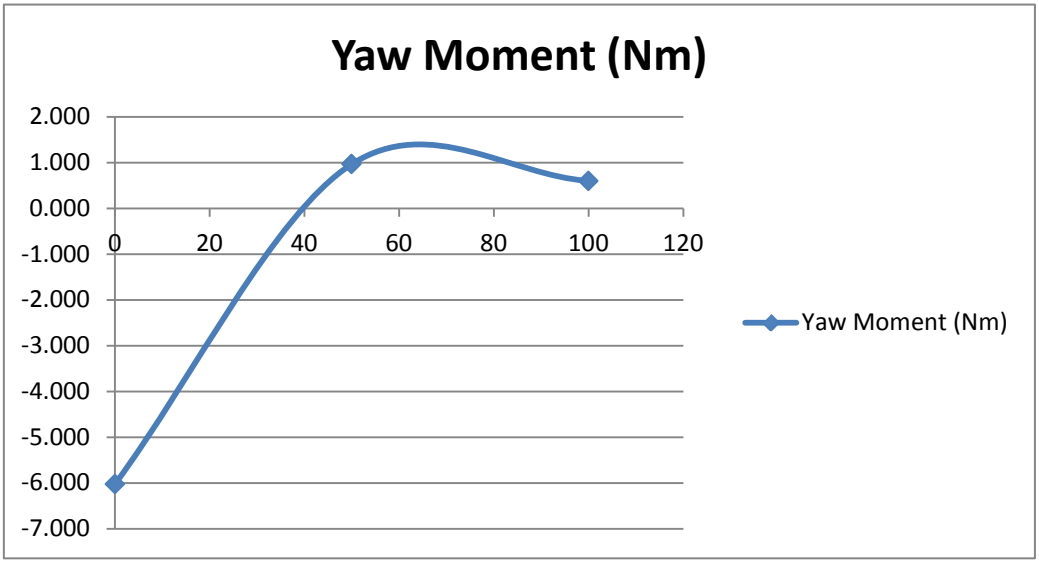

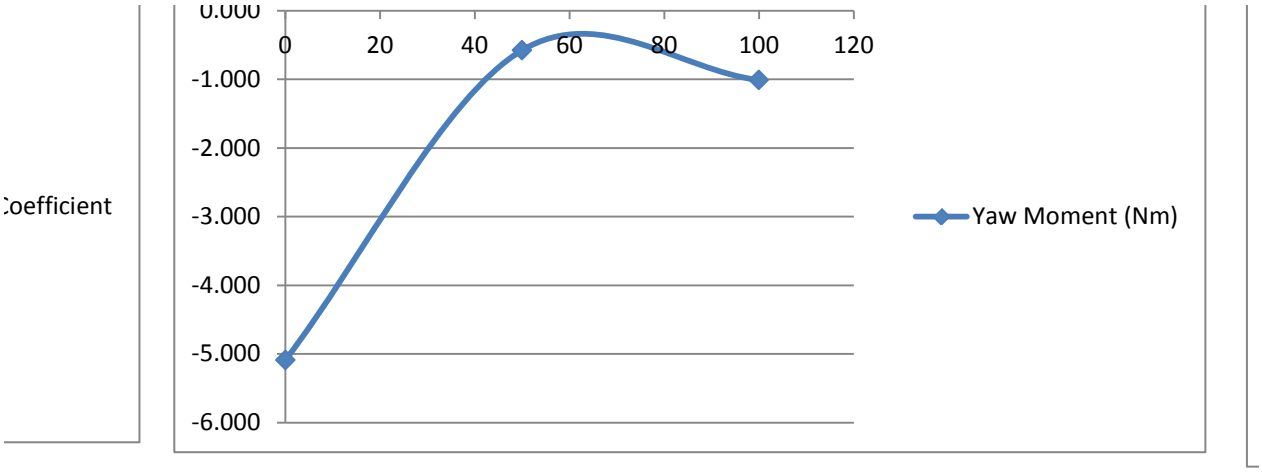
Coefficient
0.000
-1.000
-2.000
-3.000
-4.000
-5.000
-6.000
0
20
40
60
80
100
120
Yaw Moment (Nm)

0% fin deployment @ 0degrees yaw	Value	Units
Roll Moment	-0.03263808	Nm
Pitch Moment	-0.208367541	Nm
Drag Force	5.076488495	N
Drag Force Coefficient	0.339953959	No units
Lift Force	0.943331003	N
Lift Force Coefficient	0.063171446	No units
Yaw Moment	0.034337044	Nm
Pitch Moment Coefficient	-0.013953616	No units
Roll Moment Coefficient	-0.002469465	No units
Side Force	0.89697808	N
Side Force Coefficient	0.060067356	No units
Yaw Moment Coefficient	0.002299427	No units
Ref. Pressure	3.33E+00	Pa
Frontal Area	2.80E-02	m^2

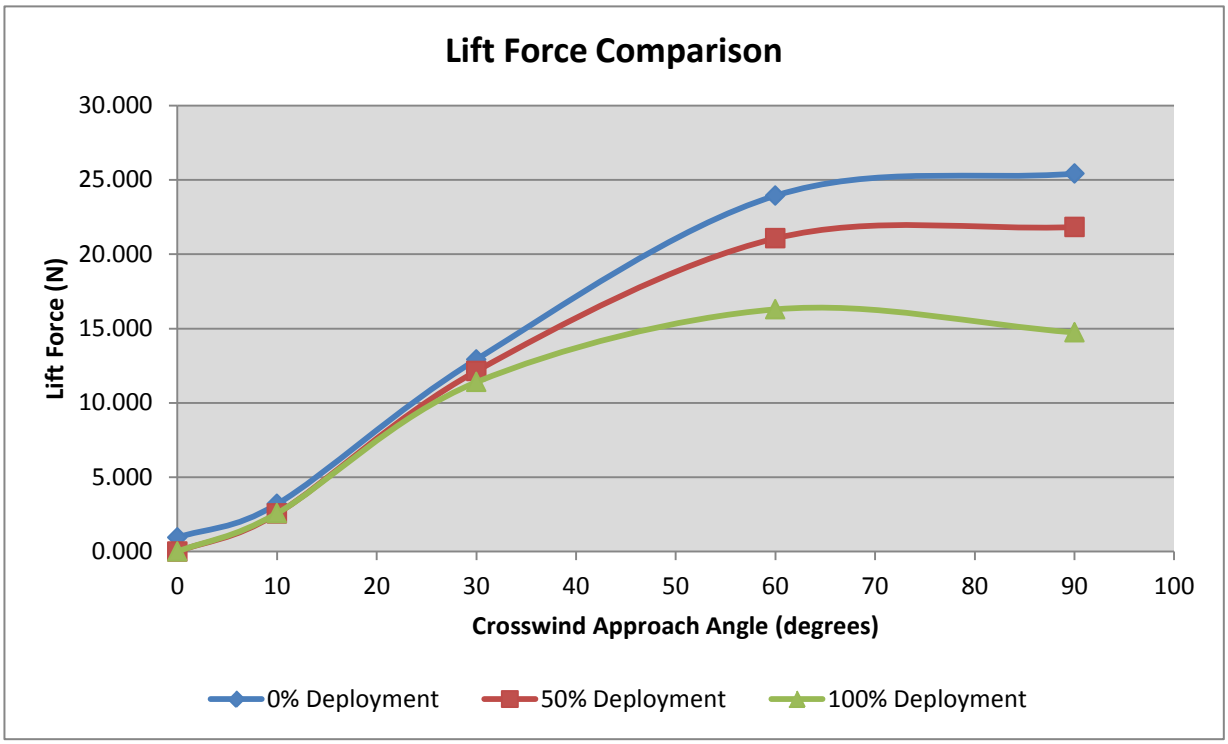
Lift Force Comparison
30.000
25.000
20.000
15.000
10.000
5.000
0.000
Lift Force (N)
0
10
20
30
40
50
60
70
80
90
100
Crosswind Approach Angle (degrees)
0% Deployment
50% Deployment
100% Deployment

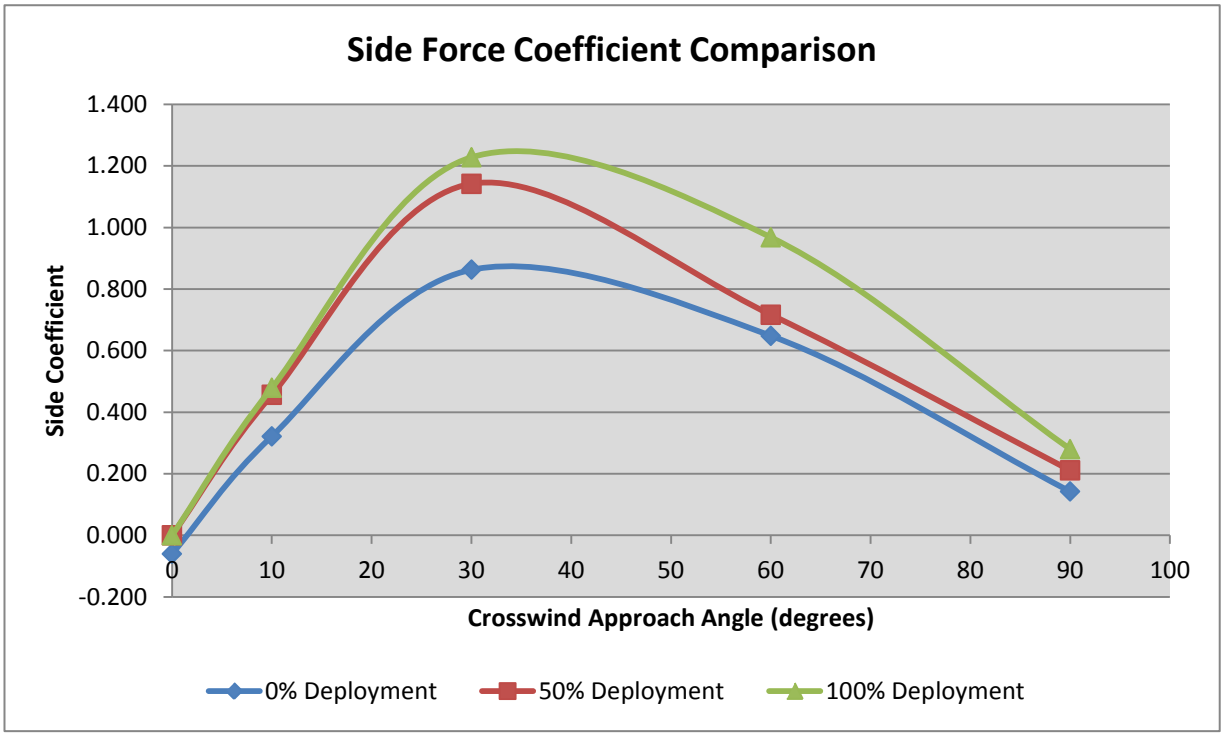
Side Force Coefficient Comparison
1.400
1.200
1.000
0.800
0.600
0.400
0.200
0.000
-0.200
Side Coefficient
0
10
20
30
40
50
60
70
80
90
100
Crosswind Approach Angle (degrees)
0% Deployment
50% Deployment
100% Deployment


Pitch Moment Comparison

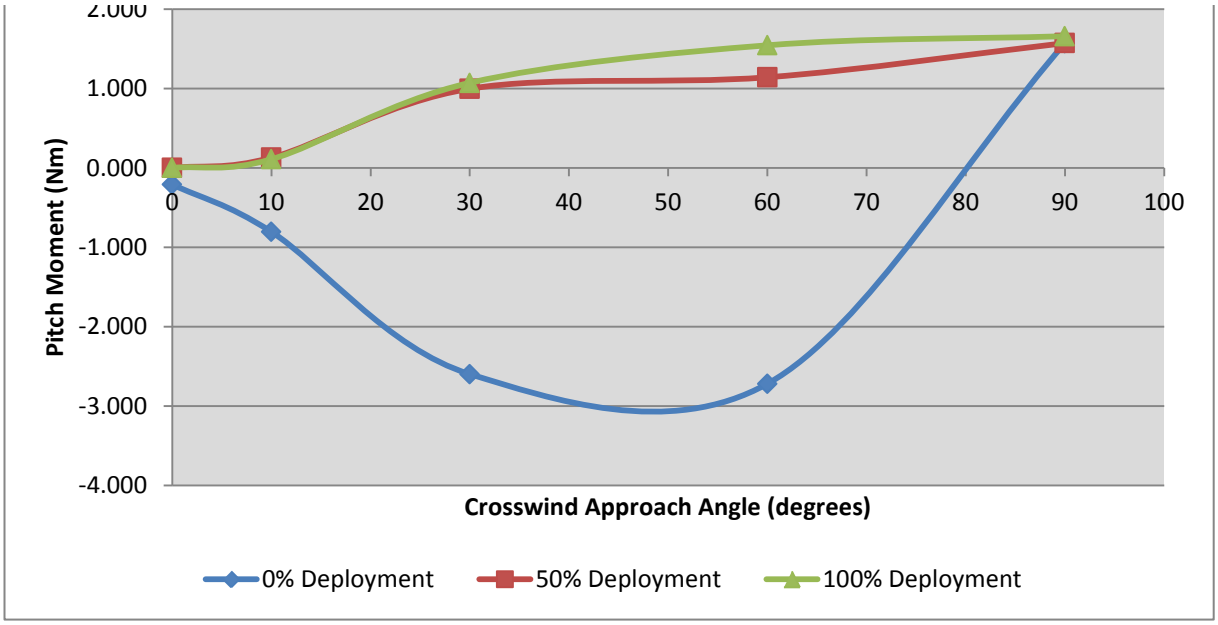
2.000
1.000
0.000
-1.000
-2.000
-3.000
-4.000
Pitch Moment (Nm)
0
10
20
30
40
50
60
70
80
90
100
Crosswind Approach Angle (degrees)
0% Deployment
50% Deployment
100% Deployment

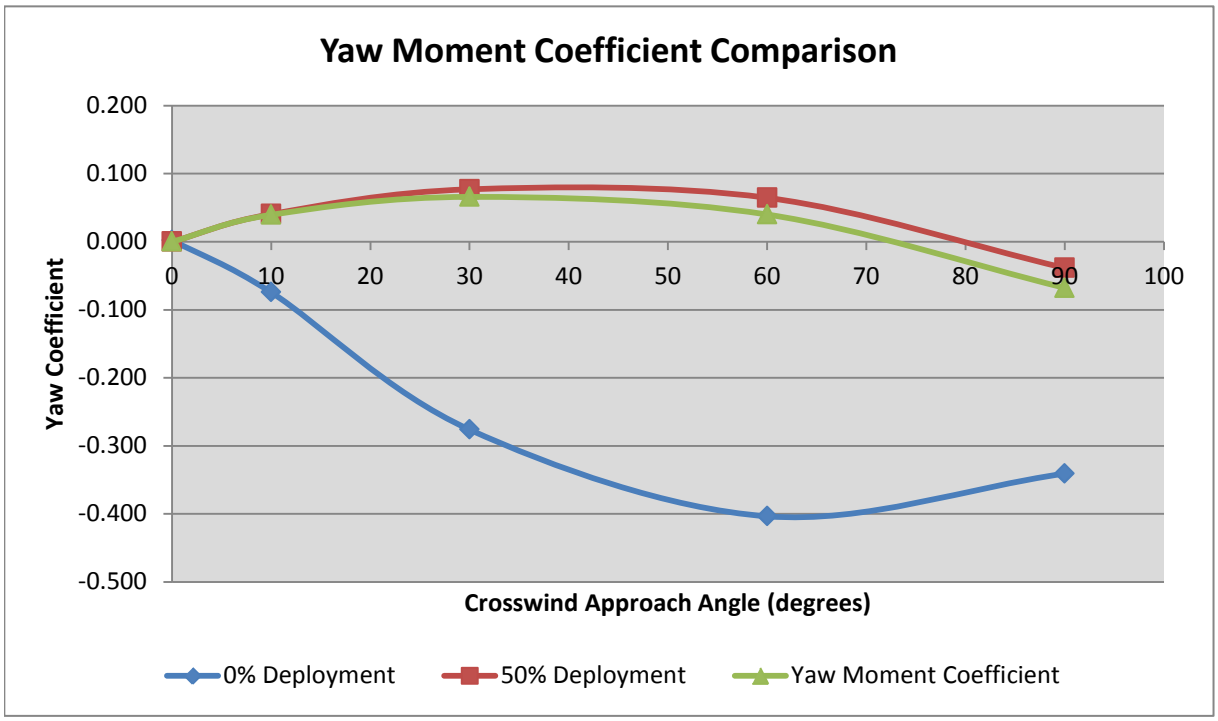
Yaw Moment Coefficient Comparison
0.200
0.100
0.000
-0.100
-0.200
-0.300
-0.400
-0.500
Yaw Coefficient
0
10
20
30
40
50
60
70
80
90
100
Crosswind Approach Angle (degrees)
0% Deployment
50% Deployment
Yaw Moment Coefficient

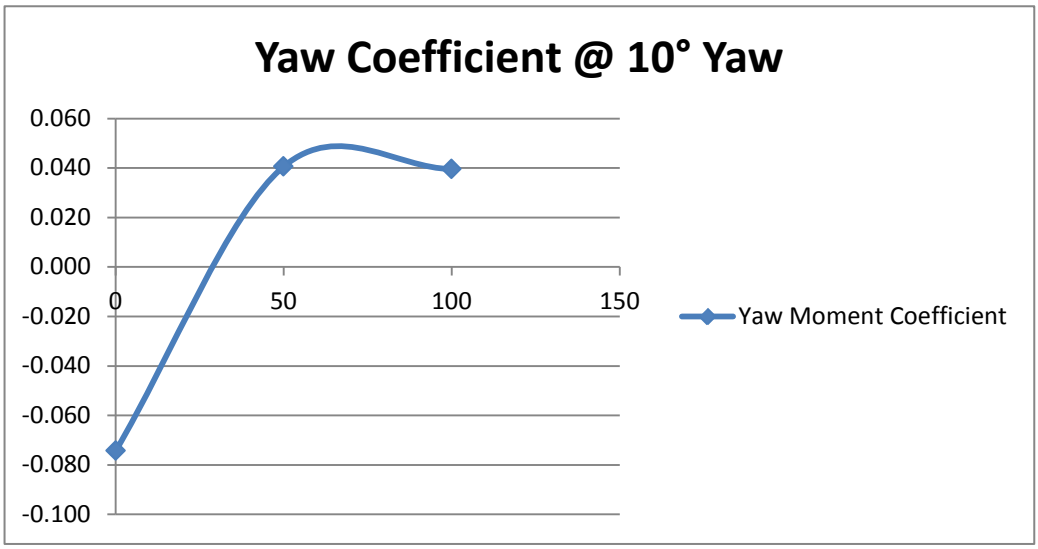
Yaw Coefficient @ 10° Yaw
0.060
0.040
0.020
0.000
-0.020
-0.040
-0.060
-0.080
-0.100
0
50
100
150
Yaw Moment Coefficient

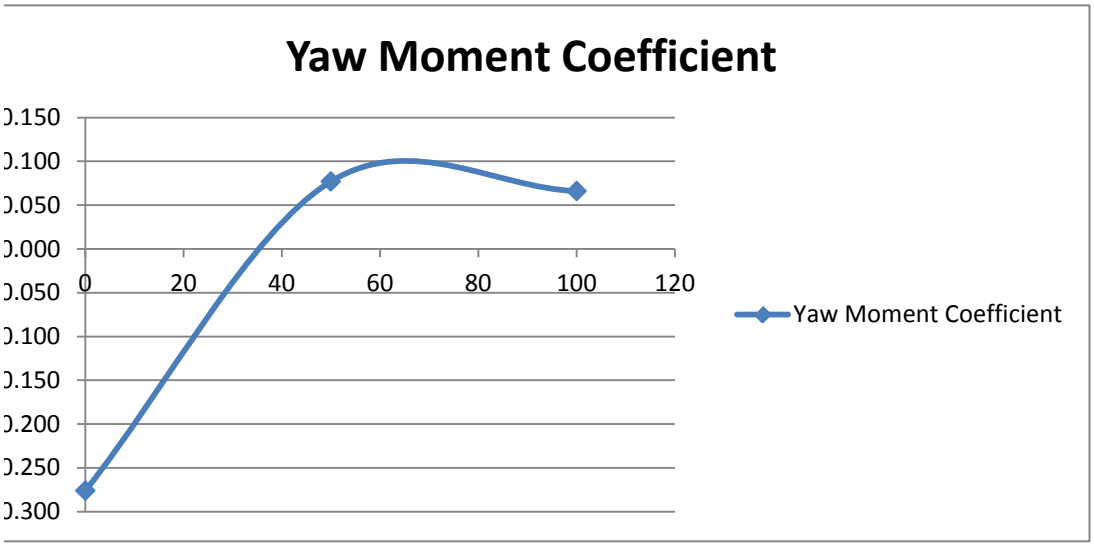
Yaw Moment Coefficient
0.150
0.100
0.050
0.000
0.050
0.100
0.150
0.200
0.250
0.300
0
20
40
60
80
100
120
Yaw Moment Coefficient

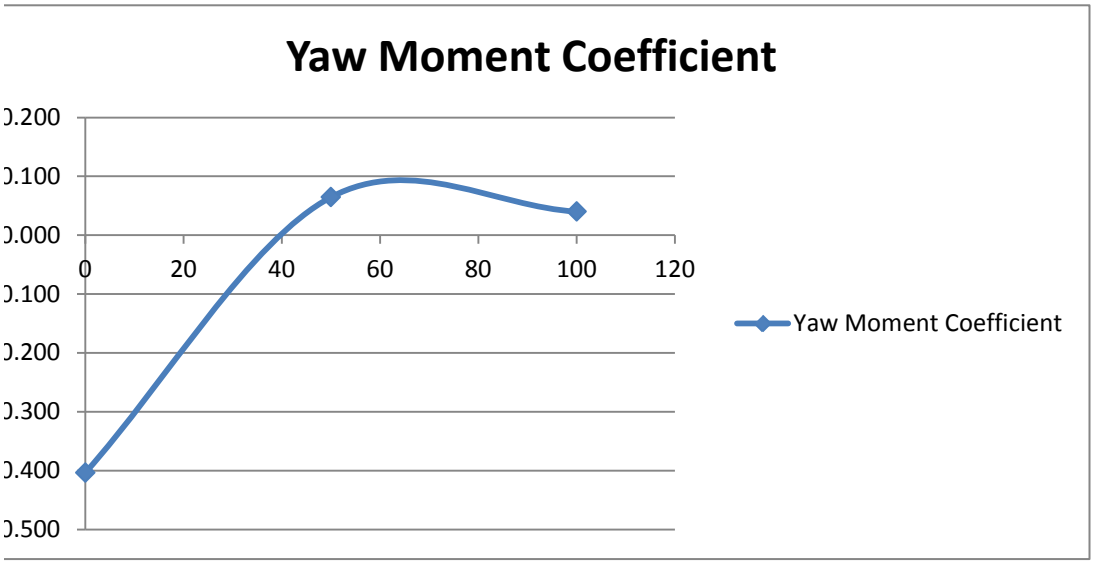
Yaw Moment Coefficient
0.200
0.100
0.000
0.100
0.200
0.300
0.400
0.500
0
20
40
60
80
100
120
Yaw Moment Coefficient


Yaw Moment Coefficient

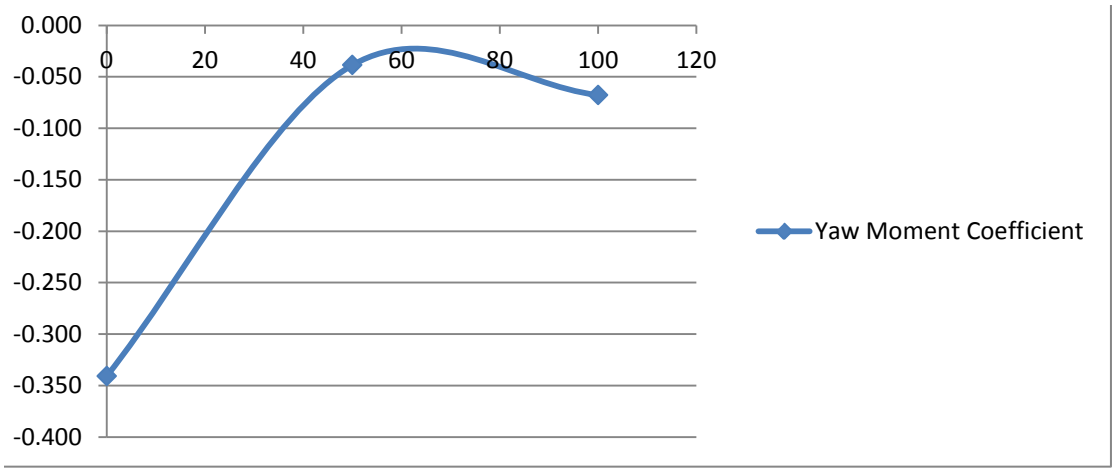
0.000
-0.050
-0.100
-0.150
-0.200
-0.250
-0.300
-0.350
-0.400
0
20
40
60
80
100
120
Yaw Moment Coefficient

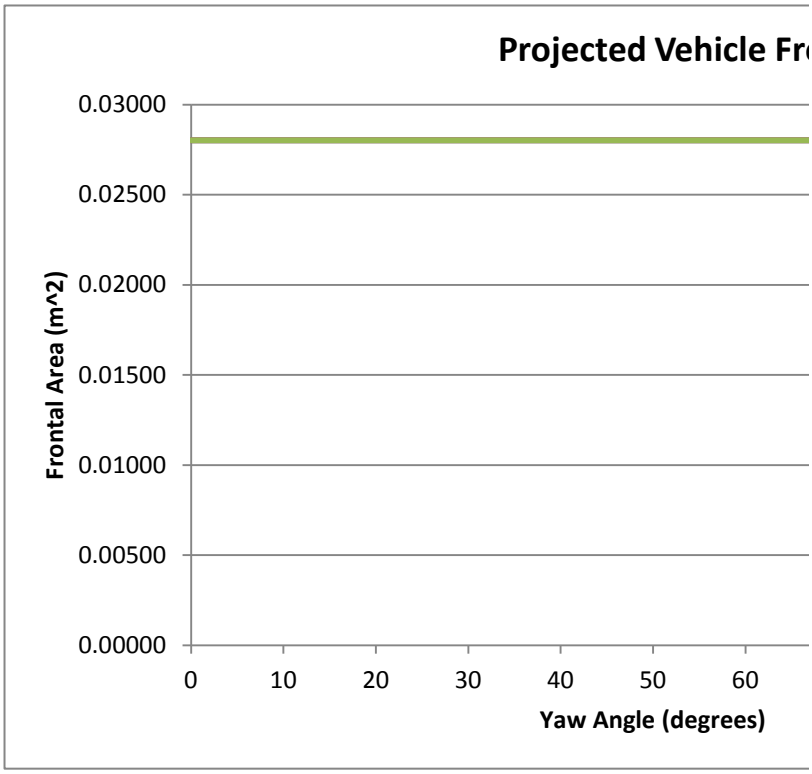
Projected Vehicle Fr
0.03000
0.02500
0.02000
0.01500
0.01000
0.00500
0.00000
Frontal Area (m^2)
0
10
20
30
40
50
60
Yaw Angle (degrees)

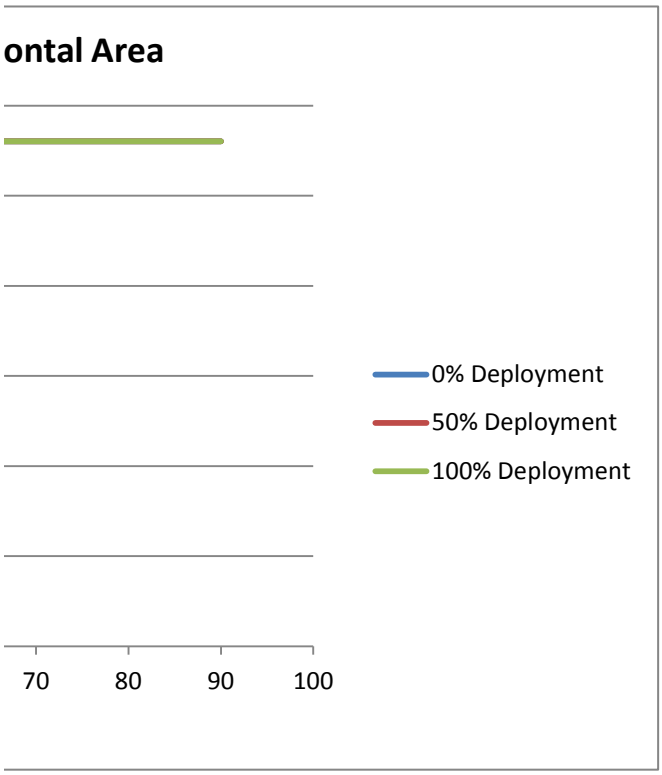
ontal Area
0% Deployment
50% Deployment
100% Deployment
70
80
90
100